ENVIRONMENTAL PERFORMANCE OF BRICK VENEER/STEEL STUD CURTAIN WALLS

THE ENVIRONMENTAL PERFORMANCE OF BRICK VENEER / STEEL STUD CURTAIN WALL SYSTEMS SUBJECT TO AIR PRESSURE, TEMPERATURE AND VAPOUR PRESSURE DIFFERENTIALS

By

ANDREW KLUGE, B.A.Sc.

A Thesis

Submitted to the School of Graduate Studies

in Partial Fulfilment of the Requirements

for the Degree

Master of Engineering

McMaster University

May 1990

MASTER OF ENGINEERING (1990) McMASTER UNIVERSITY
(Civil Engineering) Hamilton, Ontario

TITLE: The Environmental Performance of Brick Veneer / Steel Stud Curtain Wall Systems Subject to Air Pressure, Temperature and Vapour Pressure Differentials

AUTHOR: Andrew Kluge, B.A.Sc. (University of Waterloo)

SUPERVISOR: Professor R.G. Drysdale

NUMBER OF PAGES: xii,228

ABSTRACT

Brick veneer / steel stud curtain wall systems have become a popular alternative in the ever competitive construction market. However, the application of such systems has preceded any formal scientific investigation into its long term serviceability and safety. Of particular interest to many parties is the performance of the wall system under typical winter conditions as would be encountered in cold climate countries such as Canada.

In this study, an experimental investigation of three types of brick veneer / steel stud curtain walls was performed with a specially built apparatus used to impose air pressure, temperature and vapour pressure differentials across test specimens. In all, five wall specimens were tested for air leakage, thermal performance and moisture accumulation.

An analytical investigation was also carried out with a simple, custom made finite difference computer program specially suited to determine temperature profiles in walls with a steel stud framing system. Six types of walls are evaluated with the model.

A significant part of the research involved the design, construction and improvement of the test apparatus. Since the apparatus is unique, a chapter is devoted to its description.

The conclusions presented indicate that certain wall designs perform poorly and that even small construction flaws can lead to serviceability problems. Conversely, care in choice and placement of the air barrier, vapour barrier and thermal insulation in the wall system can lead to a wall system that can sustain a small degree of construction errors and at the same time perform satisfactorily. It is furthermore concluded that the apparatus built for this study has real potential as a cost effective test tool suitable for adaptation for a standard test method to evaluate the environmental performance of wall systems in general.

ACKNOWLEDGEMENTS

Thanks is extended to Professor R.G. Drysdale, the supervisor of this dissertation. Mr Shiping Zhu of the Chemical Engineering Department is acknowledged for the development of Equation 4.4 and is thanked for his and his fellow Chinese students' happy disposition. The present and past members of the McMaster Masonry Group are thanked for their comradeship as are the technicians from Civil, Chemical, Mechanical and Metallurgical Engineering for their advice. Thanks to Ross for his welding skills and patience with his favourite square head. Special thanks to my father who taught me how to labour and to lay brick and to my mother who brought me into the world.

Financial support in the form of scholarships from Canada Mortgage and Housing Corporation in their University Scholarship Program and Lake Ontario Cement in their Stewart Rutter Memorial Award is gratefully acknowledged.

Support in the form of donated materials is acknowledged and thanks are extended to Bailey Metal Products, Blok-Lok, Canada Brick, Durowall, Fibreglas Canada and Westroc Industries.

Meiner lieben Frau, Martina, gebe ich von ganzem Herzen Dank für ihre Geduld und Liebe - auch für unsere Kinder - Greta und Theo.

TABLE OF CONTENTS

CHAPTER 3
EXPERIMENTAL PROGRAM: DESCRIPTION OF TESTS, CONSTRUCTION OF TEST SPECIMENS, AND TEST RESULTS

LIST OF TABLES

LIST OF FIGURES

CHAPTER 1

INTRODUCTION

1.1 INTRODUCTION

The research reported in this thesis is primarily concerned with water vapour condensation problems in brick veneer / steel stud wall systems subjected to cold climate conditions.

The findings of this study are relevant for countries such as Canada where there are periods of cold weather which make it necessary to control a building's interior at an acceptable human comfort level. The net effect of controlling interior conditions is that differing interior and exterior environmental conditions coexist being separated by some sort of physical element. It is this physical element, or wall system, that is the subject of this investigation. More specifically, the wall system of interest consists of a brick veneer tied to a steel stud backup. In this study both experimental and analytical methods are used to investigate how this wall system responds when subjected to differing interior and exterior environmental conditions with special attention paid to the potential for condensation within the wall system.

With regard to building design, the inclusion of condensation considerations in a formal way is relatively new in the engineering profession having been partially spurred on by litigation problems. For this

reason, this first chapter includes some general background information on the causes, effects and control of condensation in wall systems. Of particular interest in this study, however, is the brick veneer / steel stud wall system which is discussed in a separate section. Finally, the purpose and scope of this work is defined.

1.2 BACKGROUND

The problem of condensation is most easily visualized by considering the common condition of frost on the interior surface of windows in dwellings. This problem is not new and even with 'high-tech' windows and modern building techniques it can still occur given the right conditions. In fact, in poorly insulated dwellings this problem of surface condensation is not restricted to windows by any means. For instance, Mr Gordon Hicks of Sudbury, Ontario, tells of how, years ago back on the farm in the north country, he used to awake in the morning in the middle of winter with his hair frosted to the wall[8].

However, with the "advancement of civilization and technology" and the resulting modern construction practices, the condensation problem has, for the most part, been quite literally put out-of-sight. Double and triple pane glass windows, insulated walls, vapour barriers and, more recently, air barriers have all been developed to reduce heat loss and to avoid the possibility of condensation and condensation related problems. Although these techniques work well, for the most part, in eliminating interior surface condensation, the more subtle mechanisms of concealed condensation within the wall system have not been entirely avoided principally because of air exfiltration where the required degree of

perfection in detailing and construction has not been recognized. On the other hand whereas older types of construction leaked badly but dried out easily, newer types of construction have tended to be more air tight and less able to facilitate the drying out of any moisture which may accumulate in the wall.

1.2.1 Causes of Condensation

In 1960, a classic paper on the subject of condensation was published as the first Canadian Building Digest (CBD 1), "Humidity in Buildings". It was written by N.B. Hutcheon of the then Division of Building Research (DBR), National Research Council of Canada (NRCC)[22]. Among other things, this paper describes why the moisture content of interior air is higher than that of the exterior air (under winter conditions); the mechanics of how water vapour enters a wall and is caused to condense (diffusion and air leakage); visible vs concealed condensation; and ways to reduce condensation problems including limits on humidity level, use of insulation and vapour barriers, as well as the use of heat to keep building elements above the temperature at which condensation can form. It will be seen in the course of this work that this last point, the use of heat, can be applied successfully to the case of brick veneer / steel stud (BV/SS) wall systems.

Just how condensation forms can be briefly described as follows. In the presence of a vapour pressure and temperature difference (both decreasing in the outward direction), water vapour can either diffuse through building materials or, in the additional presence of an air pressure difference (decreasing in the outward direction), water vapour can be

carried in the outward direction by exfiltrating air. In either case, under the above conditions, condensation of water vapour will occur at points in the wall at and below the temperature at which water vapour saturation of the air mass is reached.

This process is best illustrated with the aid of a Psychrometric Chart such as reproduced in Figure 1.1. The bottom axis of this chart represents dry air at various temperatures. Moisture content in terms of kg of water per kg of dry air is indicated on the right axis. The left curved border represents saturated air over a range of temperatures. Similarly curved lines in the body of the chart represent various saturation levels in terms of Relative Humidity (%RH).

For purposes of illustration and with reference to Figure 1.1, interior air at state point A has a temperature of T_A, a humidity level of RH_A and a moisture content of MC_A while exterior air has a temperature of T_C, a humidity level of RH_C and a moisture content of MC_C. Cooling of this interior air-vapour mixture occurs as a result of air movement from inside to outside (exfiltration). In the first stage, since no moisture is added or subtracted, the process is represented by A-B which is a horizontal line and represents a constant moisture content condition. When the cooling process reaches point B at 100% RH, the dew point temperature, T_B, has been reached and further cooling to T_C will result in condensation and lowering of the moisture content to MC_C. The difference between MC_A and MC_C represents the mass ratio of condensation moisture to the dry air which has been cooled (kg water / kg dry air). If no air movement occurs, the interpretation is slightly different. In this case, diffusion results in the

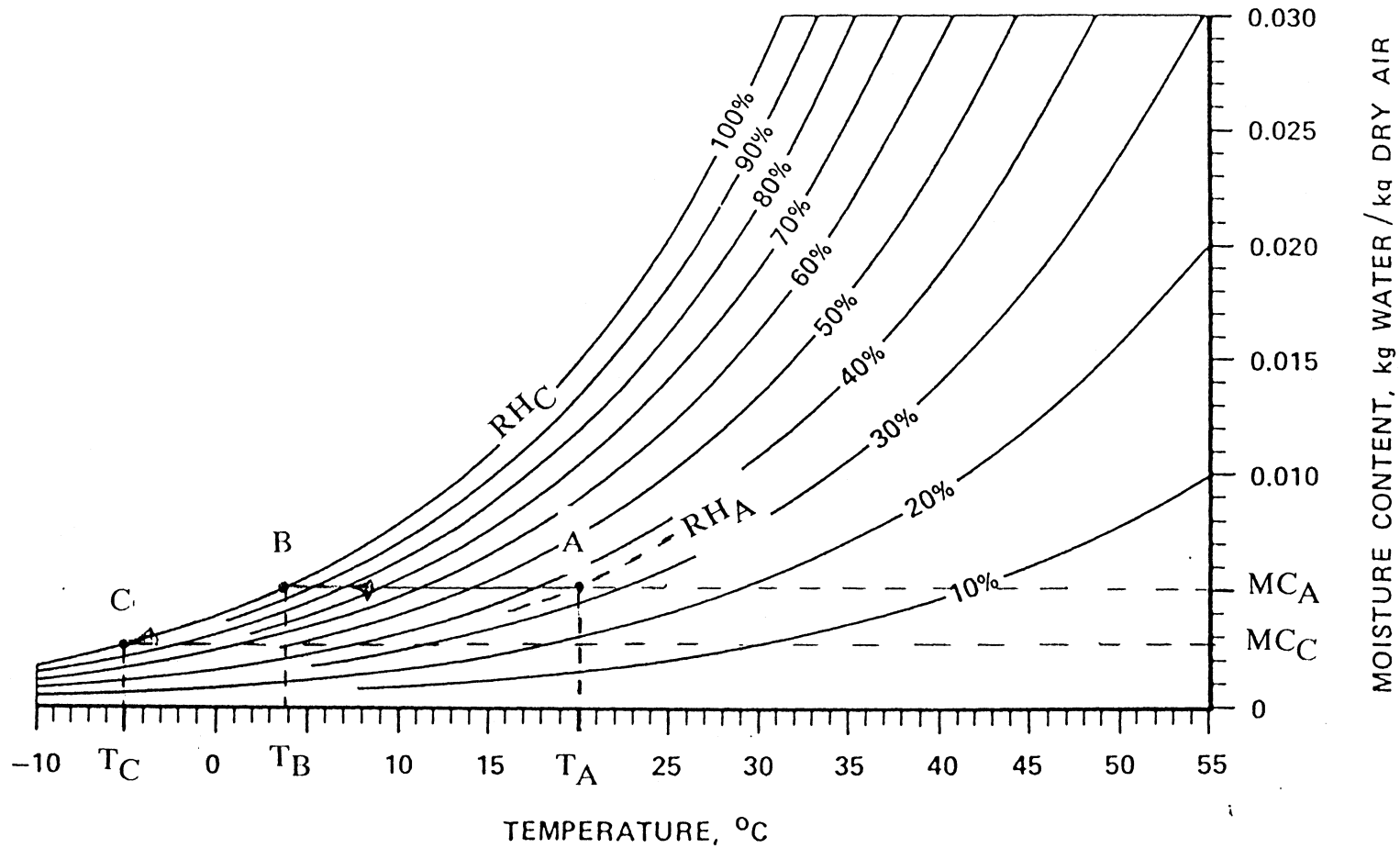

FIGURE 1.1 Simplified Psychrometric Chart (From Rousseau[34])

supply of water vapour to the existing air in the wall system. Water vapour supplied above that required for saturation of the air mass will condense.

In summary, condensation resulting from water vapour diffusion occurs as a result of a vapour pressure difference in the presence of a temperature difference. Similarly, condensation resulting from air flow occurs as a result of a combination of air pressure, vapour pressure and temperature differences.

In the context of this work, these three factors are called **environmental loads - environmental** since they result from the interior and exterior environments - **loads** since the analogy can be drawn with structural loads for which buildings have been traditionally designed. Although in general these three environmental loads occur simultaneously under winter conditions, the causes and effects of each will now be discussed individually.

1.2.1.1 Air Pressure Difference

Imbalances of air pressure result from wind loads, stack effect and mechanical ventilation. The resulting air flow can be inward (infiltration) or outward (exfiltration) and will vary at different points in the building at the same time. Infiltration can cause excessive heating loads but does not cause condensation problems under winter conditions since outside air has a lower moisture content than inside air. Exfiltration can cause both extra heating load and condensation problems. For this reason, the three causes of air pressure differences will be reviewed mainly in terms of exfiltration in the following sections.

Wind • The highest and most variable air pressure differences across walls are caused by wind loads. The actual air pressure difference at any point is affected by a number of factors including the velocity, duration and direction of the wind as well as the air tightness of the building envelope and of interior walls. Generally, on the windward portions, a wind pressure of about 0.5 to 0.9 of the stagnation pressure exists and can cause infiltration. On the leeward portions, a suction pressure of -0.2 to -0.7 of the stagnation pressure exists and can cause exfiltration[46]. In either case, a very air tight building envelope would experience net local pressure differences which approach the actual wind induced pressures whereas a very leaky wall system would experience lower pressure differences as the building itself could be locally pressurized. This effect is further affected by the air tightness of interior walls since equilibrium of air pressure is sought by the movement of air through a building from the windward to the leeward side.

Although wind gusting effects cause the highest pressures, they have little influence on overall air flow through the building envelope since they are of short duration. For this reason, it is suggested that wind speeds that represent maximum average values over a period of several hours be used in air leakage studies. This typically implies values[46] of less than 40 km/h which represents a stagnation pressure for air at -20° C of 86.4 Pa.

Tamura and Wilson[40] report a maximum wind induced pressure difference across walls in two houses at a wind speed of 16 km/h of 6.25 Pa which is equivalent to a pressure coefficient of 0.53. There is little information in the literature about actual sustained wind pressure measurements in tall buildings. Ganguli and Dalgleish[16] report peak wind

loads across a building envelope of between 400 - 475 Pa for wind speeds of between 50 - 58 km/h at the 24th floor of a 27 storey building. These represent 10 minute averages and are thus not considered to be sustained loads. Wind tunnel testing of both fully exposed tall buildings (Shaw and Tamura[38]) as well as tall buildings surrounded by lower structures (Shaw[36]) have been conducted to develop infiltration models. From these tests, pressure coefficients for various vertical and horizontal exterior wall locations as well as for building corners are reported for wind at various angles. What such tests cannot give is the net wind induced pressure difference across the building envelope, which, as discussed earlier, could be lower due to air leakage effects. However, use of such coefficients would result in upper bound pressure values and would thus be conservative.

Stack Effect • The same principle that causes a hot air balloon to rise causes positive interior air pressure. This phenomena occurs under winter conditions and has been termed stack effect in the context of buildings since the analogy can also be drawn with draft operating in chimneys as a result of the difference in air temperature between outside and inside air as well as chimney height. It is operative in all heated buildings and is greatly affected by the air tightness of the building envelope.

In the extreme case of a perfectly air tight building with a single opening at street level, outside and inside absolute air pressure would be equal at this level resulting in no net air pressure difference across the exterior wall. Since the air in the building is heated, it is less dense than the cold exterior air and therefore the change in absolute pressure with height inside the building is less than outside. The difference between absolute

pressures in this case would thus cause positive pressure in the building above street level and would be maximum at the top of the building. This case is shown in Figure 1.2(a) taken from CBD 104[45].

At the opposite extreme, if the opening in the hypothetical air tight building was at the top, the absolute interior and exterior pressures would be equal at this point and every point in the building below the top of the building would have a lower absolute pressure than the outside. As a result, a negative pressure, with respect to the outside, would exist throughout the building - visualize a cup submerged to the brim in the bathtub.

In the real world, building envelopes are not air tight but have holes distributed throughout the building height. Wilson and Tamura[47] suggested that these holes are generally evenly distributed. As a result, a condition of equal absolute pressures between inside and outside occurs in the vicinity of building mid-height. In other words, with an even distribution of leakage paths, air flow out due to positive stack effect in the upper portion of a building must equal air flow in due to a negative stack effect in the lower portion. This situation is illustrated in Figure 1.2(b).

Since buildings have internal vertical separations, i.e. floors, part of the net or theoretical pressure difference occurs across these separations. In the extreme case of complete isolation between storey pressure differences, the net stack effect pressure distribution would be as shown in Figure 1.2(c). However, the real situation lies somewhere between that shown in Figure 1.2(b) and (c) as internal separations offer only partial isolation and vertical shafts such as stair wells and elevator shafts also effect the net pressure distribution.

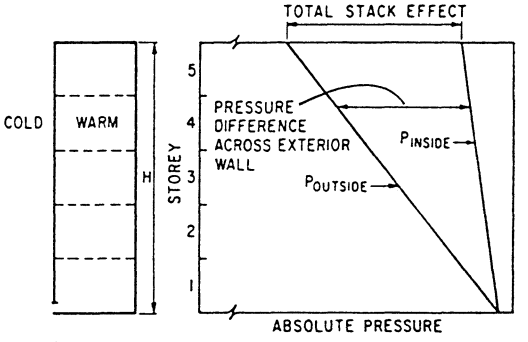

(a) No Internal Partition
Single Opening at Bottom

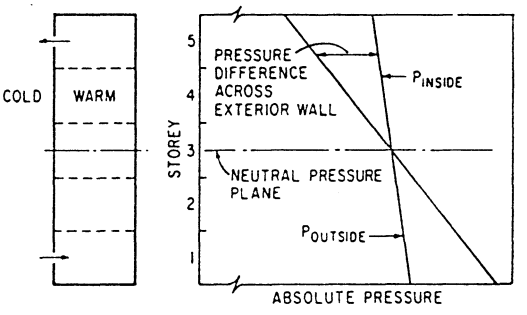

(b) No Internal Partition
Equal Openings at Top and Bottom

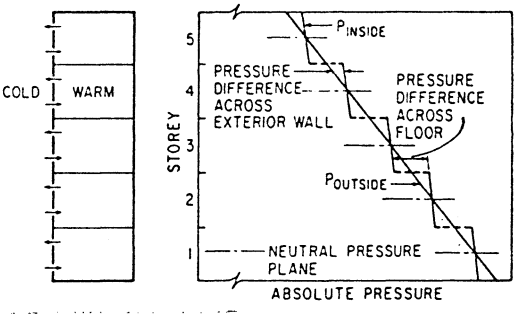

(c) Complete Isolation of Each Storey
Equal Openings at Top and Bottom

FIGURE 1.2 Stack Effect for Simple Enclosures
(From Wilson and Tamura[45])

Hutcheon and Handegord[25], pg 268, presented a numerical formulation to determine theoretical stack effect based on first principles which they used to obtain a graphical presentation. For the case of a 100 m high building with the neutral pressure level at mid height, the resulting theoretical stack effect pressure at the top of the building for an air temperature difference of 40°C would be 90 Pa. This is similar to the sustained wind induced stagnation pressure described earlier. Also, half of this value, 45 Pa, represents the average stack effect pressure over the top half of the building.

Tamura and Wilson[40] presented actual measured stack effect in two - one storey houses where they found the neutral pressure level to be close to the first floor ceiling level. Both houses had chimneys which, being high level openings, would presumably be the main cause of such high neutral pressure levels.

Tamura and Wilson[41] also studied a nine storey building where it was found that the neutral pressure level was above the middle at 0.72 of building height and 0.62 for the case where the vertical air shafts were sealed. Based on this height, the actual measured pressure was found to be about 0.82 of the theoretical draft pressure discussed earlier. In a further study involving 17, 34 and 44 storey buildings[42], they report neutral pressure levels of 0.40, 0.35 and 0.52 of building height with actual to theoretical stack effect pressure ratios of 0.72, 0.82 and 0.77 respectively.

Hutcheon and Handegord[25], pg 272, referred to a paper by Min in which pressure differences across the ground floor entrances of 23 buildings are reported as being between 0.30 to 0.70 of the theoretical stack effect.

They point out that this implies neutral pressure levels of 0.30 to 0.70 of building height assuming a linear variation of interior pressure with height.

Mechanical Ventilation • Ventilation is required in all buildings to maintain air quality by the removal of contaminants and supply of oxygen. Mechanical means are one way of providing this ventilation and primarily involves the use of fans and air ducts for supply and exhaust. The nature of a fan is to move air, which, depending on the ratio between supply and exhaust, can cause pressurization or depressurization of an enclosed space. Wilson[46] pointed out that some buildings are intentionally pressurized by an oversupply of air to prevent drafts and the entrance of contaminants. At the other extreme, buildings can be operated at a slight negative pressure to reduce exfiltration problems. Although there is little information available regarding actual pressures induced by mechanical ventilation systems, the nature of such systems allows the building pressure to be closely controlled.

1.2.1.2 Vapour Pressure Difference

The second environmental force involves vapour pressure which is a measure of the molecular activity of water molecules in air. On the basis that the interaction of air and water molecules can be neglected without serious error, separate calculations of dry air and water vapour pressures can be made according to the gas laws. The total pressure is then found by applying Dalton's Law of Partial Pressures which states that the total pressure is equal to the sum of the individual pressures (Hutcheon and Handegord[25], pg 62).

In the context of this work, consideration of vapour pressure is made at the standard atmospheric pressure of 101.3 kPa. Therefore, for one cubic meter of a given moist air, the only factor affecting vapour pressure is temperature and moisture content. The relationship between vapour pressure, moisture content and temperature is given by a form of the gas law as:

$$pV = wR_gT \qquad \text{[Eq. 1.1}$$

where p = vapour pressure, Pa

V = volume, m^3

w = water vapour mass, kg

R_g = gas constant, J/kg K

T = temperature, K

There is a limit, however, to how much water vapour a volume of air can contain at a given temperature. A volume of air at this limit is said to be saturated with respect to the water vapour content. The water vapour pressure associated with air over a range of temperatures is tabulated in standard tables such as Table 5.1 of Hutcheon and Handegord[25]. At 0°C and 20°C, saturated air has a water vapour pressure component of 0.618 kPa and 2.337 kPa respectively. These pressures are small compared to a total or atmospheric pressure of 101.3 kPa. Moreover, under normal environmental conditions, air at 20°C generally has a lower water vapour or moisture content than that at saturation.

There are several ways of describing conditions below saturation including moisture content (kg of moisture / kg of dry air); actual vapour pressure; and relative humidity - the ratio of actual vapour pressure to saturation vapour pressure, p_V/p_S, at the same temperature. The

Psychrometric Chart, described earlier under section 1.2, can be used to determine the moisture content of a volume of air. For instance, from Figure 1.1, air at 20°C and 40% RH has an estimated moisture content of 0.00575 kg of moisture / kg of dry air. This could also be found from Equation 1.1 by first determining the water vapour pressure from the relative humidity as:

$$p_V/p_S = 0.40$$

therefore $p_V = 0.4 \times p_S = 0.4 \times 2.337 = 0.9348$ kPa

Then, the moisture content for a cubic meter of air is found as:

$$w/V = p_V/(R_g \times T) = 934.8/(461.5 \times (273+20))$$
$$= 0.006913 \text{ kg/m}^3$$

and for a dry air density at 20°C of 205 kg/m^3,

$$w = 0.00574 \text{ kg of moisture / kg dry air}$$

which corresponds closely with the value obtained by using the chart.

In summary, the vapour pressure and moisture content of an air mass can be determined from first principles and/or tabulated values. Knowing the vapour pressure on the interior and exterior allows the calculation of the vapour pressure difference. For instance, air at 20°C and 40% RH was shown to have a vapour pressure of 934.8 Pa. Similarly, air at -20°C and say 100% RH has a water vapour pressure of 103.2 Pa. If such conditions were to exist across an exterior wall it is evident that a net imbalance of water vapour pressure of 934.8 - 103.2 = 831.6 Pa would exist which would result in the tendency for water vapour to flow from the high pressure side to the low pressure side by diffusing through the various wall components.

It is interesting to consider the hypothetical case where there is no moisture source inside a building. In such a situation, since the outside air

is used for ventilation purposes, the moisture content of the inside and outside air would be equivalent. This can be illustrated with the aid of a Psychrometric Chart. By starting at -10°C and 100% RH, air heated to 20°C would have an RH of 11.1% and there would be no vapour pressure difference across the exterior wall. However, buildings are both intentionally and incidentally humidified and therefore water vapour pressure differences causing diffusion exist across exterior walls under winter conditions.

Hutcheon[22] pointed out in 1960 that dwellings at that time had low ventilation rates and high rates of moisture supply resulting in relatively high vapour pressure differences. Conversely, public buildings had high ventilation rates and low rates of moisture supply resulting in low vapour pressure differences. In a later publication, Hutcheon[23] noted that industrial and commercial buildings were starting to be humidified thereby increasing the vapour pressure difference and the potential for diffusion.

The source of moisture in dwellings along with typical values were given by Hansen[20] and include bathing, washing, clothes drying, cooking, human activity and house plants. These can be classified as incidental sources since moisture is a by product of the activity. In industrial / commercial buildings such incidental sources include processes such as textile, paper and food or features such as swimming pools and fountains. Conversely, intentional humidification is a common practice in museums, hospitals and computer installations where RH values of 50% and higher are maintained for protection of artifacts, for comfort and to eliminate static electricity. In most houses intentional humidification is also practiced.

The implications of high humidities were discussed in Section 1.2.1 where the mechanics of moisture condensation were described. Further discussion is given in Section 1.2.2 while current methods of controlling such problems are given in Section 1.2.3.

1.2.1.3 Temperature Difference

The temperature difference across walls is primarily a function of the exterior conditions since human comfort requires interior conditions to be maintained at about 20 ± 2°C for low activity occupancies. Minimum hourly January temperatures having a 2½% chance of exceedance for various centers across Canada are given in the Supplement to the National Building Code of Canada[3] and represent design temperatures typically used to size heating systems. As was the case with peak wind loads, they are somewhat extreme for purposes of condensation studies. For this reason, minimum January temperatures for both a 20% and a 50% chance of exceedance for each provincial and territorial capital were compiled for this study and are presented in Table 1.1. These values were obtained from Environment Canada's "Principal Station Data"[15] which summarizes temperatures for every month and for many centers in Canada over a period of approximately 20 years. Although any percent exceedance value can be obtained from these publications, 20 and 50% were chosen for illustrative purposes. Table 1.1 is divided into four groups representing the West Coast, the Mid West, the East and the North. It is interesting to note that the difference in average temperatures between each group is about 10°C. Excluding the West Coast, it is clear that a temperature of -13°C or lower must be considered for condensation studies for the 20% exceedance case.

The 50% or average January temperature is not much higher at -7°C. In any case, with such values readily available, condensation studies can be conducted for exterior temperatures reasonably representative of most places in Canada. Most of the examples in this study will use -20°C as a convenient exterior temperature as this corresponds closely with the average Canadian January temperature having a 20% chance of exceedance.

TABLE 1.1

Minimum January Temperatures (°C) Having a 20 and 50% Chance of Exceedance for Various Canadian Cities

Region	City	20%	avg.	50%	avg
West Coast	Victoria	0.5		3.6	
Mid West	Edmonton	-26.2		-15.6	
	Regina	-26.1	-26	-17.9	-18
	Winnipeg	-26.7		-19.5	
East	Toronto	-12.3		-6.6	
	Quebec	-18.9		-11.8	
	Fredericton	-16.1	-13	-9.0	-7
	Halifax	-11.8		-5.7	
	Charlottetown	-13.3		-6.8	
	St John's	-8.3		-3.4	
North	Whitehorse	-31.8	-34	-20.3	-25
	Yellowknife	-36.7		-28.9	
	Average	-19		-12	

1.2.1.4 Summary

In section 1.2.1, air pressure, vapour pressure and temperature differences across wall systems were identified as environmental forces which, when combined, can lead to the occurrence of condensation. Typical

values were also presented. The next section contains a review of the effect condensation has had on actual wall systems in Canada.

1.2.2 The Effects of Condensation

An excellent summary of moisture related problems in Canadian residential construction was presented by Rousseau[33]. In this report, various types of observed problems were described including mould and mildew, window condensation, attic condensation, wall cavity problems, siding damage and basement moisture problems. It is noted that "80% of the houses that reported problems were electrically heated and did not have active flues". There is also significant correlation between high interior humidity levels and moisture problems. Although some of the reported problems were attributed to wind driven rain, the majority were a result of condensation during cold weather conditions.

Wilson and Garden[44] gave several examples of condensation related moisture problems in multi-storey buildings. They identified typical leakage paths including unfinished walls above suspended ceilings; cracks in the structural elements; and around the perimeter of windows. They pointed out that moisture tends to accumulate along these leakage paths.

Grimm[18], addressing the issue of the corrosion of brick veneer screw fasteners due to moisture problems, states that "The only structural element holding the masonry on the building is typically the single thread of an abraded steel screw". He then illustrates the dangers with photos of corroded fasteners. Such corrosion could result from rain penetration or condensation.

Many problems have been reported for high humidity buildings such as swimming pool enclosures. These highly humidified warm buildings are especially prone to condensation problems. After describing two pools with wall moisture problems, Burn[12] concluded that the best way to handle such situations is to install an effective air barrier to stop air leakage.

In summary, condensation related problems can lead to both aesthetic, eg. mould, and structural, eg. corrosion, deterioration of the building envelope. Current methods which have been developed to reduce condensation problems are described in the next section.

1.2.3 The Control of Condensation

Control of water vapour condensation in modern wall systems is achieved with basically three subsystems. These are insulation, vapour barrier and air barrier. These subsystem combined with the wall system as a whole can be used to reduce and control condensation. Of the two "barriers" (sometimes called "retarders"), the most important by far is the air barrier. This has been identified and discussed by many researchers and practitioners including Wilson[46] in 1961, Hutcheon[24] in 1963, Garden[17] in 1965, Latta[29] in 1976, Handegord[19] in 1979, M.Z. Rousseau[34] in 1983, Lstiburek[30] in 1984, and Quirouette[32] in 1985. Each of the three subsystems will now be discussed.

1.2.3.1 Insulation

Insulation is primarily used to reduce heat flow. However, when properly placed it can also serve to eliminate surface condensation and to control the location of concealed condensation. Many types of insulation

are available including glass fibre of various densities, polystyrene, and phenolic foam - a relatively new. low conductivity material. Table 1.2 contains typical conductance and resistance values for 25.4 mm thicknesses of the above insulations.

TABLE 1.2

Various Insulation Materials

Material	Density (kg/m^3)	RSI per 25.4 mm ($m^2K/W/25.4$ mm)
Glass fibre	72.1 17.6	0.76 0.67
Expanded Polystyrene	35	0.88
Phenolic foam	40	1.46

Note : Values taken from Sweet's Canadian Construction Catalogue File, Vol 1, 1986, McGraw Hill.

1.2.3.2 Vapour Barrier

By definition, vapour barriers are materials that retard molecular water vapour diffusion. For instance, CAN 2-51.33-M80, "Vapour Barrier Sheet for Use in Building Construction", defines Type I and II vapour barriers as having maximum allowable permeances of 15 and 45 ng/sm^2Pa respectively. Based on these rather arbitrary values, Table 1.3 contains a list of materials that satisfy these requirements.

TABLE 1.3
Permeance Ratings of Various Materials

Material	Specification	Permeance (ng/sm^2Pa)
Polyethylene film	0.05 mm 0.10 mm 0.15 mm	8 4 2
Foamed polystyrene	35 kg/m^3	42
Nylon film	0.025 mm	40
Vinyl film	0.05 mm	19
Waxed building paper	med. weight	9
Plywood, douglas fir, 6.5 mm	ext. glue	40
Paint, semi gloss latex		33

Note : All values taken from Reference 25, Tables 5.5 and 5.6, wet cup method, except Paint taken from Reference 30.

Certainly the most common vapour barrier material is polyethylene film although it is clear from Table 1.3 that other materials perform just as well. Lstiburek[30] argues that the actual permeance rating of the vapour barrier is not the important issue. Instead, because vapour diffusion is only a minor source of vapour, he suggests that a more realistic approach is to supply a vapour barrier having a permeance rating of 1/10th the permeance of the exterior cladding. The reason for this is that it ensures that vapour can escape from within the wall at least 10 times easier than it can get there by diffusion from the inside. Latta[29] goes one step further when he says "**If, therefore, a building can be made tight against air leakage it may not need a vapour barrier**" (to stop vapour diffusion).

When vapour barriers of polyethylene film were first introduced, not only did they retard diffusion but they restricted air flow to some degree as well. Furthermore, the concept alone of a plastic sheet in the wall system has caused many people to think that a polyethylene vapour barrier is also an air barrier. Quirouette[32] differentiates between the function of a vapour barrier in retarding diffusion and the function of an air barrier in limiting air flow. He also noted the requirements of a vapour barrier which include the permeance rating, the location (on the warm side of the insulation), and continuity (it need not be perfectly continuous since small imperfections do not increase the overall moisture diffusion rate).

1.2.3.3 Air Barrier

It has only been in the past 10 years that air barriers have been actively promoted although, as noted earlier, the concept that air leakage could be the prime source of water vapour for condensation has been recognized since 1961. This was illustrated by M.Z. Rousseau[34] with calculations showing air flow causing 100 times more condensation than vapour diffusion. Also, and more importantly, whereas diffusion occurs over large areas, air flow occurs in specific paths. This results in relatively large amounts of moisture accumulating in a very localized fashion.

Quirouette[32] listed air barrier design requirements which can be summarized as follows :

- Continuity
  - eg. from wall to roof
- Strength
  - resist peak wind loads
  - not creep under sustained loads

- minimal displacement of other building materials

• Air Tightness
  - less than 0.1 L/sm^2 at 75 Pa pressure difference

• Durability
  - long service life

Lstiburek[30] added that air barrier materials or systems must be "easy to maintain over the service life of the building".

Although these design requirements are generally agreed upon, there are two issues that are being discussed among professionals. These are air tightness and location of the air barrier.

There is as yet no consensus on how air tight an air barrier system must be. In the US, the National Architectural Metal Manufacturers specify a maximum leakage rate of 0.3 L/sm^2 at a 75 Pa pressure difference (Reference 25, pg 284). Actual leakage rates for 8 multi-storey office buildings[43] led to a tight - average - loose classification of 0.5 - 1.5 - 3.0 L/sm^2 at a 75 Pa pressure difference. Lstiburek[30] suggested a maximum leakage rate of 0.02 L/sm^2 although no indication is given of the pressure difference nor upon what such a number is based. Values for "discussion purposes only" were presented by NRC[10] corresponding to low, average and high humidity levels as 0.15, 0.10 and 0.05 L/sm^2 at a pressure difference of 75 Pa.

Measurement of leakage rates for various air barrier materials have been reported[8,37,11] and it was found that some were essentially air tight. However, a more realistic approach is to test the entire wall system as built. One such test program[9] for 10 wood frame walls incorporating air barrier systems reported leakage rates ranging from 0.488 to less than 0.001 L/sm^2 at a 75 Pa pressure difference. It should be noted that these were

laboratory constructed 2.6m by 2.6m wall panels designed to include air barrier systems. The wide range of results is significant and reflects material and system limitations.

The location of the air barrier is an interesting issue. Some professionals believe that it can be anywhere in the wall system. Others qualify this by saying that the preferred location is on the warm side of the insulation[32] and if it is placed on the cold side of the insulation then it should be 10 to 20, times more permeable to vapour diffusion than the vapour barrier. Others consider that it should be located on the warm side of the insulation because air barrier systems, no matter how well designed, will inevitably have construction flaws and/or flaws formed during the service life of the building. If such a violation of the air barrier occurs on the cold side of the insulation then condensation will likely form there with the potential for condensed moisture being trapped between the warm side vapour barrier and the cold side air barrier. This would not be the case if the air barrier were on the warm side fo the insulation.

In summary, condensation control is attained in modern wall systems by the use of insulation, vapour barriers and air barriers. Of these three, the air barrier is the most recent addition and has not yet been fully defined as to allowable leakage rates and location in the wall system.

1.3 BRICK VENEER / STEEL STUD WALL SYSTEMS

Buildings typically consist of some sort of structural framework to which a non-load bearing cladding is attached. This attachment can be by hanging with connectors, such as with prefabricated panels, or by supporting on slabs and shelf angles, such as with built-in-place masonry.

There are two common methods currently used to provide a brick masonry finish in highrise buildings - both of which include a backup wall. The oldest method involves a concrete block backup while a more recent innovation is the use of steel studding as a backup wall. (Wood studding has been used in housing for many years but the concern for a proper fire rating in highrise construction prohibits the use of wood.) Some of the advantages of using steel studding are the savings incurred in construction, the ability to provide a higher insulating value, the savings in space as compared to concrete block backup, and the reduction in dead load.

However, as noted in a recent publication by Keller[26] in which a survey was reported on current brick veneer / steel stud design and construction practices,

> "During the past 15 years, brick veneer / steel stud (BV/SS) walls have become widely used in Canada as an economical building enclosure system in residential and highrise structures. However, the construction of these walls has preceded the development of adequate design, construction and inspection standards. This situation has led to concern over the longterm safety, serviceability and durability of this form of construction."

There has been a lot of material written and opinions expressed about the brick veneer / steel stud wall system. Some of the players involved include manufacturers, who want to obtain, preserve or increase their share of the market, building owners, who often want to pay as little as possible, and engineers, architects and contractors who want to avoid liability problems.

In view of conflicting ideas presented by such people, this study was undertaken to provide an independent assessment of brick veneer / steel stud wall systems in terms of their response to the environmental loads which were introduced in Section 1.2.

1.4 PURPOSE AND SCOPE OF INVESTIGATION

The purpose of this research is to investigate and document the potential for moisture condensation problems in brick veneer / steel stud type wall systems.

The experimental component consisted of air tightness, thermal and condensation studies. Air tightness studies were conducted with intentional or construction related leakage paths to determine the effect of small flaws in the air barrier system. Thermal profiles were investigated to determine the effect of two dimensional heat flow caused by the presence of the steel stud component. Condensation studies were conducted to examine the extent and effect of water vapour condensation in the wall system. Three types of brick veneer / steel stud wall systems were investigated and included non-insulating and insulating exterior sheathings as well as a non-standard steel stud framing system.

The analytical component of this work was primarily concerned with the development of a simple two dimensional heat flow model capable of determining temperature profiles so that wall systems could be assessed at the design stage for their vulnerability to condensation problems . The model was not developed to include latent heat effects caused by the release of heat associated with condensation. An empirical equation relating interior temperature and humidity level to dew point temperature is also presented and assessed.

A significant portion of this research project was the development of a single test apparatus to conduct the above mentioned tests in an economical fashion suitable for possible standards adoption or adaptation.

The design, construction and operation of this apparatus is described in the next chapter.

CHAPTER 2

DESIGN AND CONSTRUCTION OF THE ENVIRONMENTAL SIMULATION TEST APPARATUS (ESTA)

2.1 INTRODUCTION

Both private industry and government groups have developed test facilities for evaluation of the environmental performance of curtain wall assemblages. As a result, standardization of certain test methods has been possible. In this regard, four applicable ASTM standard test methods for the environmental testing of curtain wall assemblages are listed in Table 2.1 along with the associated test conditions.

The development of such standards is important as it gives a common basis for the specification of minimum standards as well as aiding in the development of building products. The inherent difficulty with the standardization process is the simplification of test conditions required to make the standard method reasonable to implement. This is especially true in thermal performance testing where air infiltration and moisture migration can have a significant effect on heat transfer. This difficulty is acknowledged in ASTM C976[5] with the following note:

> "Air infiltration or moisture migration can significantly alter net heat transfer. Complicated interaction and dependence upon many variables, coupled with only a limited experience in testing under such conditions, make it inadvisable to attempt standardization at this time."

As discussed in Chapter 1, air infiltration and moisture migration not only affect the heat transfer characteristics of a wall but also the serviceability of a wall if water vapour can condense within the construction and provision for removal of moisture is not part of the design. The investigation of this aspect of curtain wall performance is termed moisture accumulation testing in this work and was the prime impetus behind the development of the new test apparatus described in this chapter .

TABLE 2.1

Applicable ASTM Standard Test Methods for the Environmental Performance of Curtain Wall Assemblages

ASTM Designation	Title	Test Condition
C236[4]	Steady State Thermal Performance by Means of a Guarded Hot Box	Temperature Gradient
C976[5]	Thermal Performance of Building Assemblies by Means of a Calibrated Hot Box	Temperature Gradient
E283[6]	Rate of Air Leakage Through Exterior Windows Curtain Walls and Doors	Air Pressure Gradient
E331[7]	Water Penetration of Exterior Windows, Curtain Walls and Doors by Uniform, Static Air Pressure Difference	Water Spray With Air Pressure Gradient

To achieve the goal of developing tests to investigate the combined influences and interactions of environmental loads on curtain walls, it was recognized that with careful planning a single test apparatus could be used.

In addition to providing thermal and vapour pressure differentials across a wall, air leakage tests (to characterize the air tightness of a given wall system), and rain penetration tests (to investigate the effect of wind driven rain on a veneer), would need to be accommodated.

Whereas moisture accumulation tests are non-standard, both air leakage and rain penetration testing can be, respectively, modelled after the test methods described in ASTM E283 and E331, previously noted in Table 2.1.

Details of the development of the Environmental Simulation Test Apparatus (ESTA) are discussed in the following section in terms of:

- establishment of the design parameters,
- construction details,
- measurement and control systems.

2.2 DESIGN PARAMETERS

The design of ESTA was developed to satisfy the need to provide four environmental loading conditions. These are:

1. Temperature differential across the wall assembly.
2. Vapour pressure differential across the wall.
3. Air pressure differential across the wall.
4. Rain over the exterior of the veneer.

It was felt that a test facility designed to provide these four environmental loading conditions and instrumented to measure:

- Temperature profiles through the wall,
- Moisture accumulation in the wall,
- Air leakage rates,

- Rain penetration through the veneer,

would be both versatile and unique.

To achieve this goal, the four types of data required were looked at individually to establish the design parameters for the total system in terms of the two primary tests - Moisture Accumulation and Rain Penetration.

2.2.1 Moisture Accumulation Testing

The potential for the accumulation of moisture within a wall system was discussed in Chapter 1 along with the associated problems. As noted for the Canadian climate, the worst case, (i.e. the environmental condition likely to cause the most moisture accumulation) is that of the simultaneous flow of heat, air and water vapour in the outward direction. To be able to simulate these actions, a test apparatus must be capable of supplying and maintaining with minimal boundary effects:

- a temperature gradient,
- an air pressure gradient, and
- a vapour pressure gradient,

across a curtain wall specimen. Each of these gradients were discussed in terms of Canadian conditions in Chapter 1. Reasonable gradient values for the design of ESTA based on the previous discussions along with a consideration of boundary effects are identified in the following sections.

Temperature Gradient : To establish a reasonable temperature gradient across an exterior wall under winter conditions, a standard interior temperature of $+20^{\circ}C$ was adopted. Exterior conditions vary across Canada; however, it is evident from Table 1.1 that curtain walls in most

parts of Canada may reasonably be expected to experience a cold side temperature of -20°C or colder each winter. An apparatus built to test curtain walls in a laboratory should thus be capable of maintaining a temperature gradient across the wall specimen of at least +20°C to -20°C.

Air Pressure Gradient : Air pressure gradients across exterior walls were discussed in Chapter 1. It was noted that under winter conditions it is possible to have a net outward pressure or a net inward pressure at various locations in the same building and at the same time. Of prime interest, though, is the positive pressure, as this will tend to cause moisture laden air to exfiltrate into the wall system. It was shown in Section 1.2.1.1 that long term pressure differentials could be in the order of 100 - 200 Pa. This is a very low range of pressures and the final design was based on much higher pressures as dictated by the Rain Penetration Test described under Section 2.2.2.

Vapour Pressure Gradient : Vapour pressure differentials exist as a result of temperature and relative humidity differences on each side of the wall. Having established, then, a typical temperature differential of +20°C to -20°C, it remains to specify typical relative humidity values.

Interior R.H. values can vary in the winter from 30-60% depending on the dryness of the exterior air, the amount of incidental moisture evaporated inside the building, and the degree of mechanical humidification. Exterior winter R.H. values are generally 80-100% as air at -20°C is so cold that only a small amount of vapour present causes the air to be close to saturation. It is therefore necessary to be able to control the

humidity on the warm side of the wall specimen, between say 30-60% R.H., whereas the humidity on the cold side will be indirectly controlled by the cold temperature at close to saturation.

Boundary Effects : A further consideration in the design of the apparatus for moisture accumulation testing was boundary effects. Heat loss through the wall specimen boundary must not be so significant that two and three dimensional heat flow effects will extend too far into the specimen. This implies the need to install the specimen with an efficient insulating layer around the perimeter.

Air leakage through the pressurized portion of the apparatus must also be minimal and ideally an order of magnitude smaller than the air leakage rate through the wall specimen in order to minimize experimental error.

2.2.2 Rain Penetration

The Environmental Simulation Test Apparatus was also designed for rain penetration testing. Specific considerations were containment and collection of sprayed water and the air pressure at which water was to be sprayed against a wall specimen. The air pressure was a significant consideration as it set the controlling requirement of 3 kPa pressure for which the load box was to be designed. Such a pressure could be realized in the case of wind driven rain.

2.2.3 Summary of Primary Operational Requirements

In Table 2.2, a summary of the primary operational requirements is presented. These requirements provided the basis for the design and construction of the Environmental Simulation Test Apparatus.

TABLE 2.2

Primary Operational Requirements

1. Air Pressure
   - 3 kPa (rain test)
   - minimal apparatus leakage
2. Temperature
   - +20°C to -20°C or lower
   - minimal boundary heat loss
3. Vapour Pressure (RH)
   - 30-60% RH @ 20°C
   - ~90-100% RH on cold side
4. Rain Spray
   - Facilitate collection of sprayed and penetrated water.

2.3 CONSTRUCTION DETAILS

Over the course of the investigation presented in this report, two versions of ESTA, ESTA 1 and ESTA 2, were constructed and used. Both versions are described in this chapter.

2.3.1 General Description - ESTA 1

ESTA 1[27] consisted of a Load Box, Specimen Box and Cold Box. Figure 2.1 is a schematic drawing of the basic components of ESTA 1 as arranged for moisture accumulation testing. In this set-up the Load Box

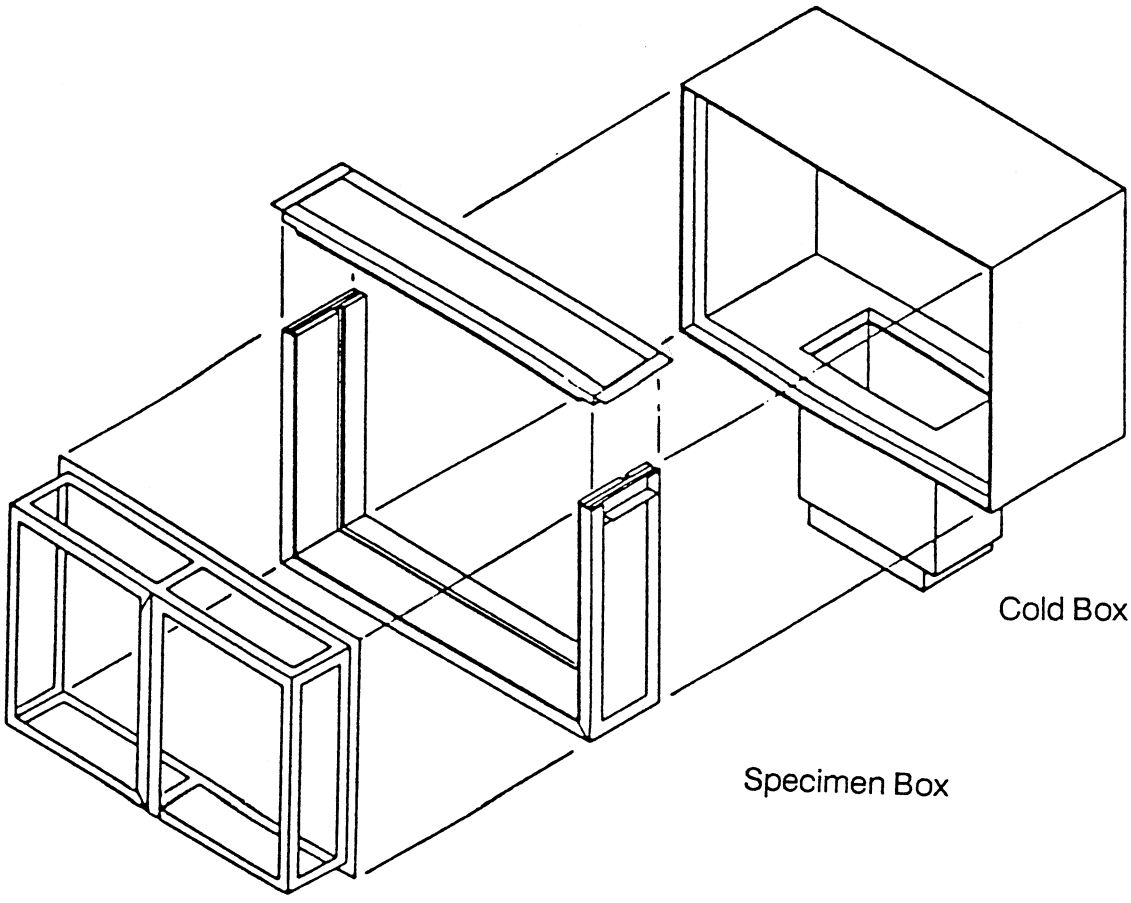

FIGURE 2.1 The Environmental Simulation Test Apparatus

was used to simulate an interior environment while in the Cold Box, exterior winter conditions were simulated.

In the case of rain penetration testing, the Load Box is attached to the other side of the Specimen Box and is used to contain the water spray gear and the run off water. This versatility allows the same wall specimen to be tested for all three types of tests without disturbing its location in the Specimen Box.

Measurement and control systems included air pressure, air flow rate, temperature and humidity in the load box and temperature in the cold box. Data acquisition was achieved by manual means for pressure, humidity and air flow and by a computer automated method for the wall temperature profile. Sizing of the wall specimen and the system components are discussed in detail in the following sections.

2.3.2 Wall Test Area

The first decision that was made in the design of ESTA was the area of wall that was to be tested. Indeed, the subsequent design process revolved around this one decision. In examining the ASTM Standard Test Methods for the single environmental actions as listed in Table 2.1, the key phrase in each case is that the wall area should be representative of the in situ case.

For thermal testing where heat flow is to be determined (eg. ASTM C976), the standard guidelines specify typical full scale sections. The main concern of course is to have representative boundary conditions so that boundary effects due to wall modeling are minimized. NRCC (National Research Council, Canada) and NBS (National Bureau of Standards, USA)

each have such a test facility. Both satisfy the provisions of ASTM 976 and are called Calibrated Hot Boxes. The dimensions of each facility are listed in Table 2.3

TABLE 2.3

Dimensions of Hot Box Test Facilities

Owner	Date Built	Wall Specimen Size Height	Width	Area
NRC[39]	≈1959	2.6m	2.6m	6.9m^2
NBS[1]	≈1985	3m	4.6m	13.8m^2

The NRC facility was built strictly for heat flow testing with no imposed air pressure difference. The NBS facility is unique in that it was designed as a calibrated hot box to meter heat flow as well as being capable of introducing air pressure and vapour pressure differentials. As noted in Table 2.3, the sizes of these test facilities are indeed for full scale walls. In contrast to this it was believed that a smaller test wall area would still give representative results. It must be stressed that the primary intent of ESTA was not to meter heat flow but rather to examine moisture accumulation given a temperature, air pressure and vapour pressure gradient. Therefore, as long as a significant percent of the wall area is unaffected by the boundary heat flow effects then the moisture accumulation patterns within this area are representative of what can happen in the field. Furthermore, although none of the ASTM standards for testing of curtain wall assemblages specifies a minimum wall area, ASTM E514-86 "Water

Penetration and Leakage Through Masonry", does specify a minimum of 1 m^2.

With these considerations in mind, a convenient wall size area of 1 m^2 was chosen for the Environmental Simulation Test Apparatus. It was concluded that representative sections of walls, including joints, thermal bridges and attachments could be included effectively while keeping the cost of specimen fabrication and handling within reason. Lower specimen costs and time saving in fabrication, instrumenting and testing all provided the opportunity to study more variations of construction or influencing factors than would normally be the case for more expensive and time consuming procedures.

2.3.3 Specimen Box

The Specimen Box has three main functions. These are:

1. Act as a frame for wall specimen construction
2. Provide containment of wall specimen
3. Supply the means of attachment and sealing for the Load Box and the Cold Box.

Furthermore, the operational requirements of Table 2.2 specify that the Specimen Box:

- be structurally capable of withstanding a 3 kPa air pressure with minimal air leakage,
- have a low conductance value to minimize heat loss,
- be unaffected by either high vapour or direct water contact, and
- facilitate water collection.

With these functions and requirements in mind, it was decided to construct the Specimen Box with a framework of 51 mm steel angles lined with timber panels. The steel angles in conjunction with the timber panels provide strength and rigidity to contain and to pressurize the wall specimen. The steel angle also provided the means of attachment and sealing for the Load Box and Cold Box. This sealing is an important aspect of the apparatus and is discussed further below.

The first version of the Specimen Box incorporated solid pine timber for the panels. This proved to be a poor choice as the timber was not properly cured and warped badly after planing. Sealing against air leakage was a problem as was poor dimensional accuracy.

The second and present version of ESTA 1 consisted of laminating three layers of 19 mm plywood together. This provided an overall thickness of 57 mm. The panels were designed to rest in the steel framework and can thus be easily removed. Gasketing between panels was achieved with 12.5 mm diameter solid neoprene cord.

An important aspect in terms of construction and removal of the wall specimen was the ability to remove the top of the Specimen Box. By special milling of the steel angles and construction of the laminated tops and side panels, the top was made removeable. Figure 2.2 contains details of this arrangement. Two bolts on each end are used to compress the gaskets and thus hold the assembly together. This results in a controlled amount of gasket compression and a good "air tight" fit.

With the removeable top, construction was especially aided in that the last course of brick could be laid without interference from above. Also, removal of the wall intact was made possible. Alternatively, a wall

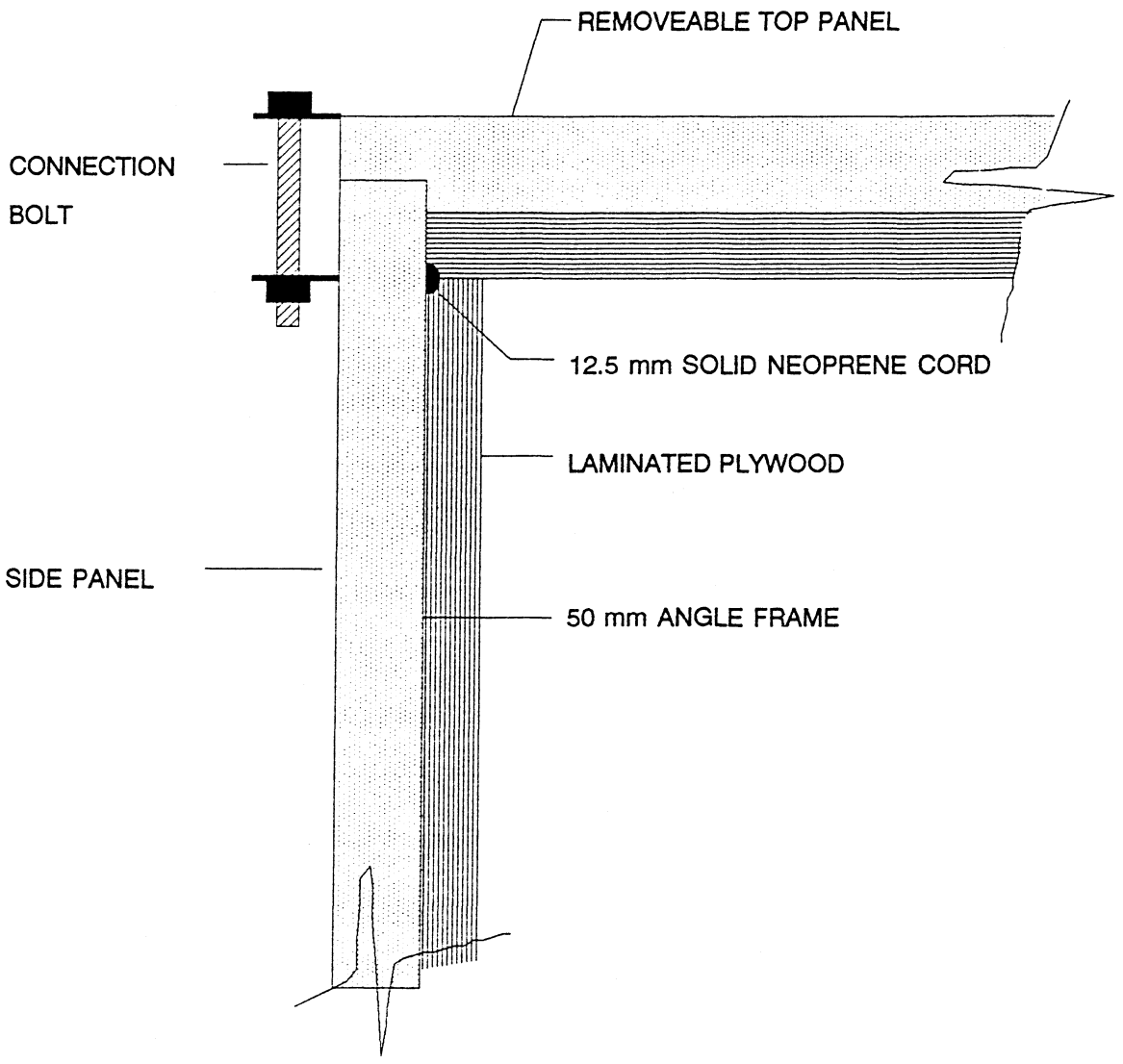

FIGURE 2.2 Top Connection Detail - ESTA 1

built to proper tolerances can be constructed outside the Specimen Box for later installation. The later approach is useful for two reasons. Firstly, a wall system may require a "curing" period of up to one month before testing. By constructing the wall or walls outside the Specimen Box, the apparatus can be used for other tests during this period of time. Secondly, outside help (eg. a brick layer), may be required to build a series of walls for testing. In such cases, it is economically convenient to be able to build several walls together rather than singly upon completion of the previous test.

All wood panels were protected against abrasion, moisture damage and air leakage by three coats of liquid plastic. The steel angles were likewise protected against rust with 2 coats of rust resistant paint.

A 20 mm x 20 mm slot was built into the full inner perimeter of the Specimen Box. This served two purposes. Firstly, the slot was located one standard brick width in from one edge. This slot, with proper end details, serves as a drainage channel for water that has penetrated the brick veneer in the case of water penetration testing. Secondly, for purposes of calibration for extraneous apparatus air leakage, a 19 mm sheet of plywood can be inserted in the slot and sealed in place. Leakage tests can then be performed to characterize leakage of the test apparatus.

The overall mass of the Specimen Box alone is approximately 42 kg. A typical steel stud/brick veneer wall speciment adds about 200-250 kg to this value. Support of the Specimen Box was provided using two wooden rails with inlaid steel runners on top of a laboratory table on wheels (Figure 2.3). This set-up allows the box to be easily manouvered.

Figure 2.3 is a drawing showing the exact inner dimensions of the Specimen Box. The gross inner area is 1.029m^2. The net wall area is

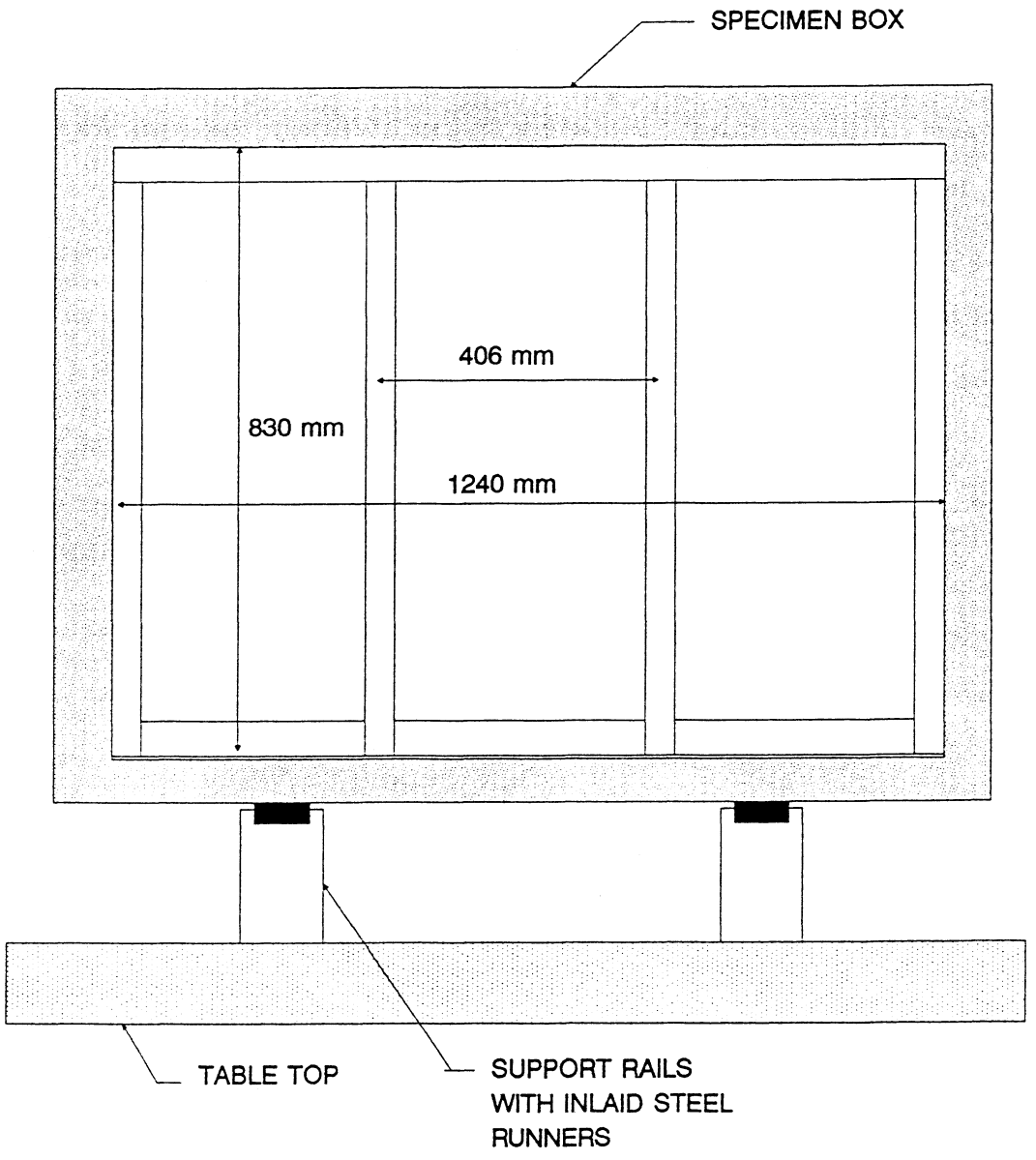

FIGURE 2.3 Specimen Box with Typical Steel Stud Arrangement - ESTA 1

fractionally smaller as a result of perimeter sealing. A net wall area of $1.00m^2$ is attained if wall specimens are built in a 6 mm subframe for easy placement and removal of the wall specimen. The width of 1.24m allows room for four steel studs with 35 mm flanges arranged as depicted in Figure 2.3 with 406 mm between interior stud center lines. The height of 830 mm is very convenient as it allows 12 full courses of brick with a standard 10 mm mortar joint. It is therefore unnecessary to cut bricks lengthwise. The 300 mm depth of the Specimen Box will accommodate most steel stud/brick veneer wall systems.

2.3.4 Load Box

The main function of the Load Box is to provide a means of maintaining a desired environment. For moisture accumulation testing, this implies steady pressure, temperature and humidity levels.

Like the Specimen Box, the Load Box consists of a steel angle framework. Heat loss through the Load Box was not an issue since the temperature within the load box would not be much different from the ambient temperature in the laboratory. Furthermore, for water penetration testing, it is necessary to contain the water spray in a non-corroding environment. On this basis, and for wall viewability during testing, it was decided to line the framework with 6 mm thick acrylic sheet to form a transparent box.

In conjunction with the steel framework, the 6 mm acrylic box was constructed to withstand positive or negative pressures of up to 3 kPa with negligible deflection. The Load Box proved itself by sustaining a 4 kPa positive pressure.

The details of a specially adapted fitting used for an air supply and a pressure tap in the acrylic box are shown in Figure 2.4. The same fitting was further adapted and used to provide access to temperature and humidity controllers located in the box. By removal of the washer sealed bolt and insertion of a small flat screwdriver, the controllers, located inside the Load Box, can be adjusted during a test without having to disconnect the Load Box from the Specimen Box.

Provision was made for the collection of water during rain penetration testing by sloping the bottom plate away from the wall specimen.

Overall dimensions of the Load Box are given in Figure 2.5. Connection details are described below. Similar to moving the Specimen Box, the Load Box can be manouvered into place on rails.

2.3.5 Cold Box

In the case of moisture accumulation testing, condensation would not occur unless the wall specimen was subjected to a significant temperature gradient. For this reason, a means of applying a realistic cold temperature to the exterior of the wall was required. Originally the plan was to place the Specimen Box in an exterior window during the winter months. Although the resulting conditions would be quite realistic, the problems of scheduling and unpredictable winter temperatures led to the adaptation of an open top freezer unit to supply the cold environment. A 0.14m^3 freezer unit capable of attaining approximately -30°C in the chest was fitted with a plywood box insulated with 50 mm of polystyrene. The freezer unit was on wheels and thus the whole assembly was easily manouvered up to the Specimen Box

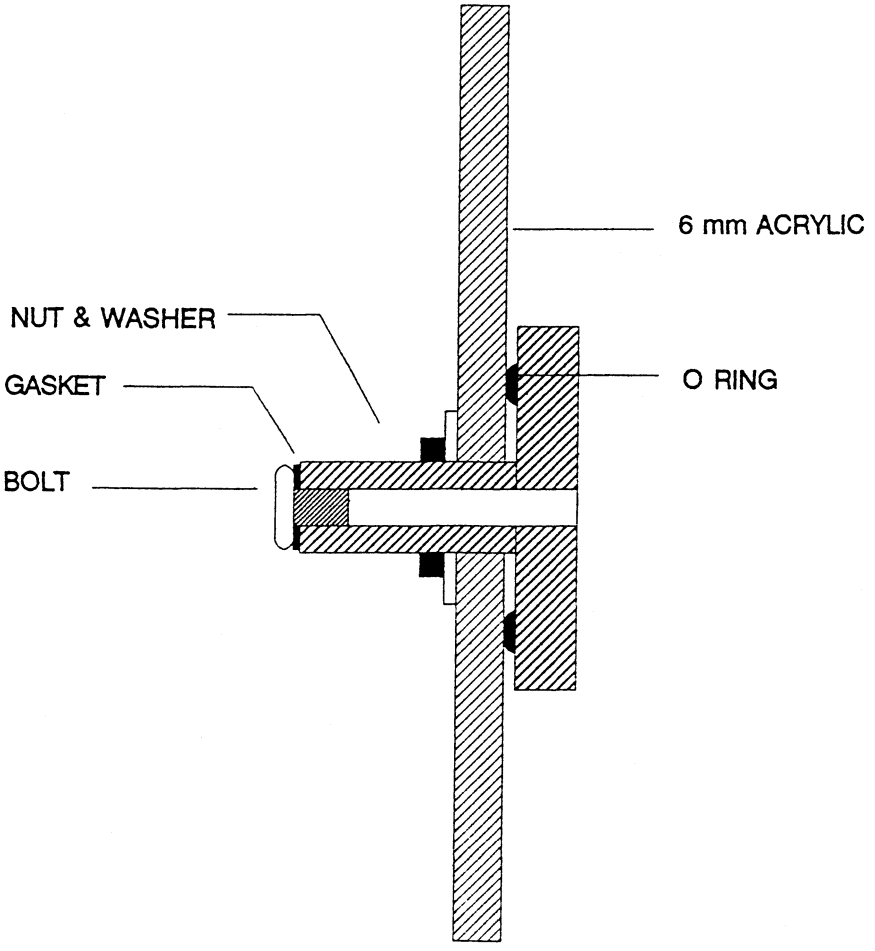

FIGURE 2.4 Access Port Fitting Details

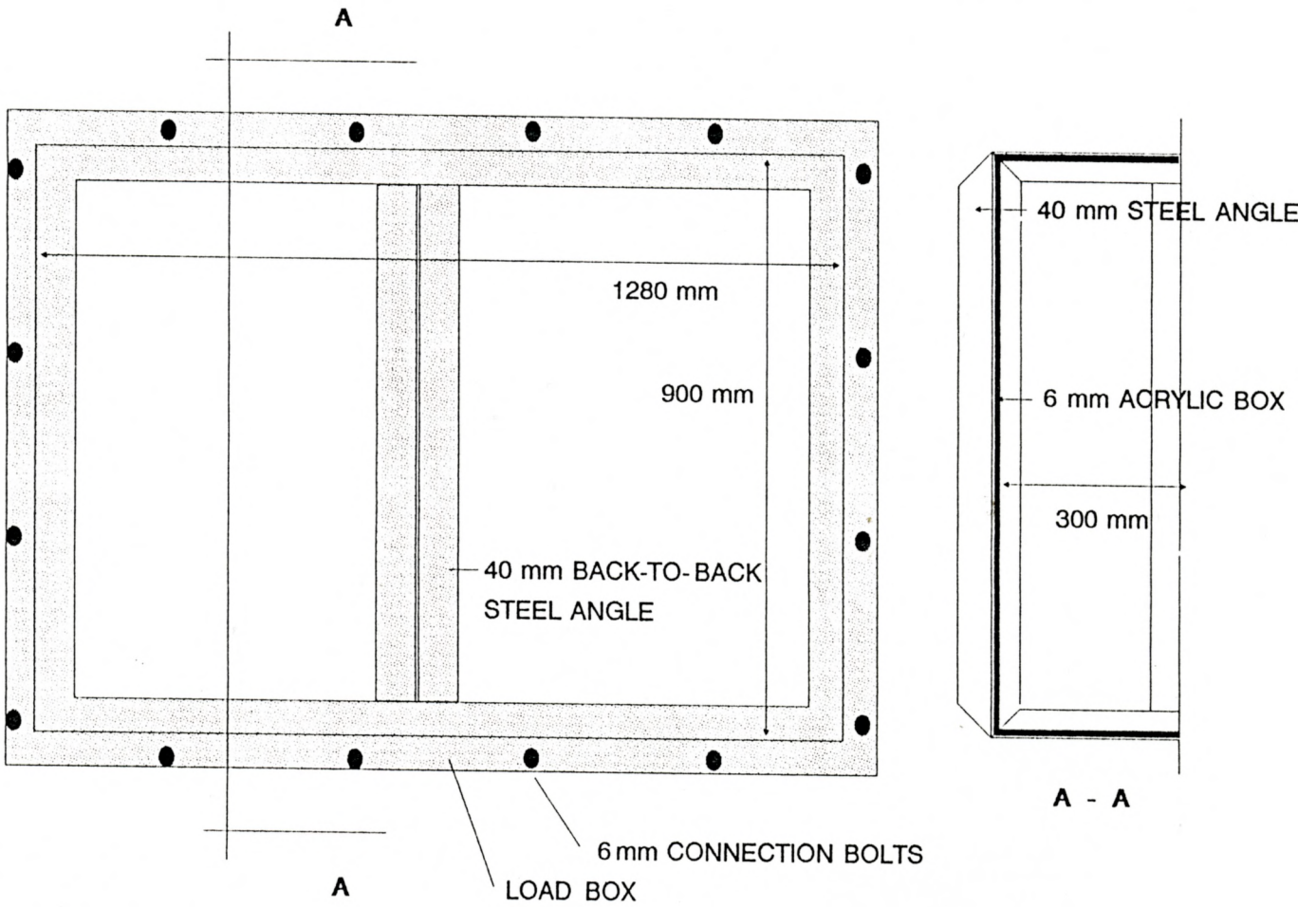

FIGURE 2.5 Load Box - ESTA 1

around which the plywood box fit snugly (Figure 2.6). The inset polystyrene then bore up against the steel frame of the Specimen Box and a reasonable fit was possible. There was no need to make this connection air tight since some loss must be permitted in order that air coming through the wall would not pressurize the Cold Box and thus affect the total pressure differential. On the other hand, too much perimeter leakage would allow warm relatively moist air to enter, cause frost build up, and thus affect the cooling capability of the Cold Box.

Pilot testing with the Cold Box demonstrated the need for a fan to be placed in the freezer chest to push the cold air up into the Cold Box. With this set up, a mid wall temperature of approximately 0° C was attained with a 2° C difference from top to bottom of the wall. To avoid the expense of a new mechanical cooling system, dry ice was used to further lower the temperature. Two 40 lb. blocks of dry ice were placed on either side of the freezer at the base of the wall. In this configuration temperatures reached as low as -16° C. The problem, however, was an inability to maintain a steady temperature. Also, although two fans were placed or hung in the chest, the air was so cold around the fans that they sometimes froze and turned very slowly or not at all. Furthermore, after a week of operation the freezer chest frosted over to the point of becoming ineffective. This configuration was used to test Specimen 1A.

During the course of the test program the cooling system was upgraded with a mechanical system which was able to maintain a temperature of -22° C in the Specimen 2A test series. The system includes a 1/4 hp compressor, a temperature controller with a 2° C switching differential and a defrosting element on the evaporator coil. A

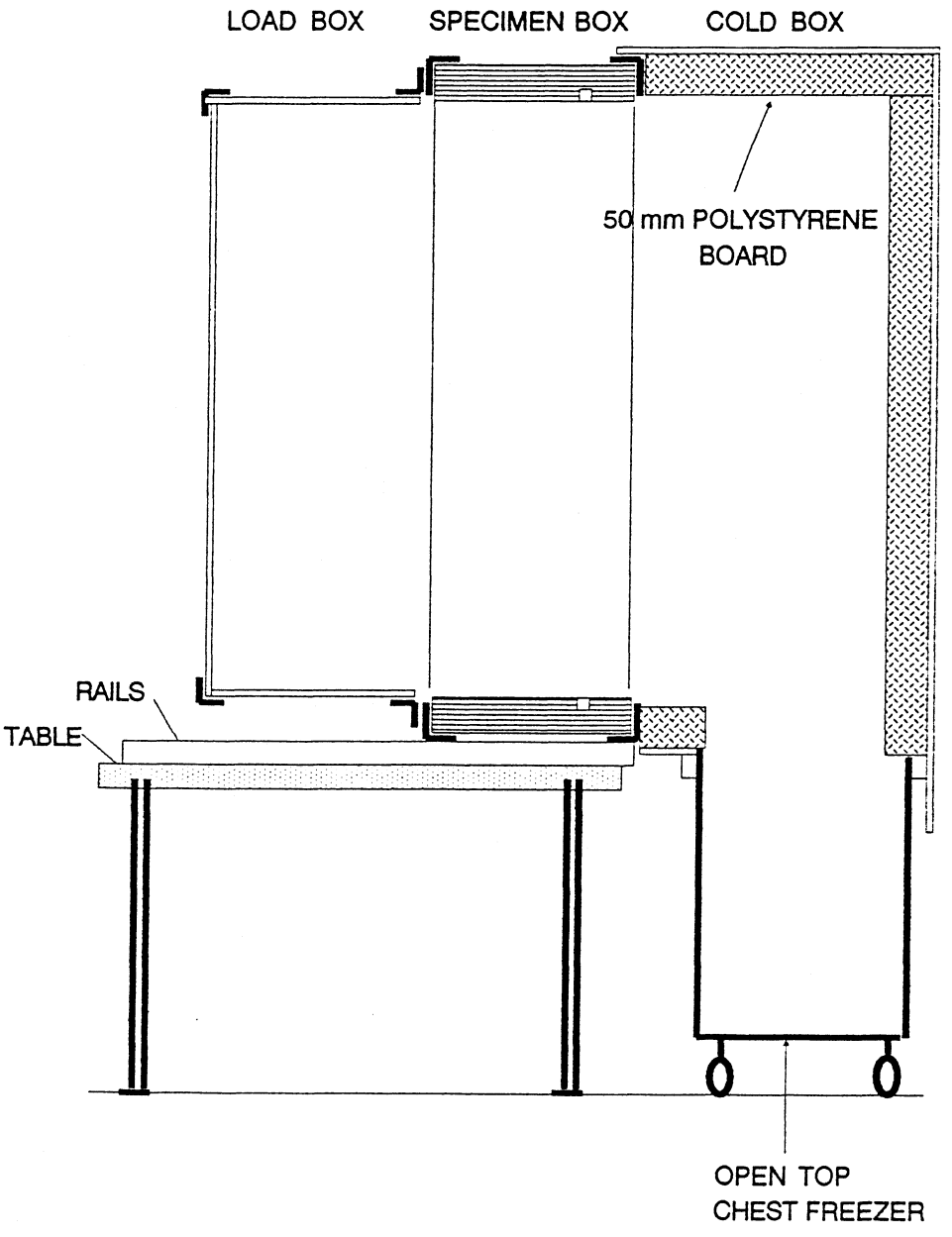

FIGURE 2.6 Vertical Section Through Apparatus - ESTA 1

programmable controller operates the defrosting element for the desired length of defrost time and time between defrost cycles. The previous Cold Box was adapted for the new system and was placed on a laboratory table on wheels.

2.3.6 Connection Details

Much time and energy was spent in obtaining an effective seal between the Specimen Box and the Load Box. Pilot testing with the original neoprene gasket material indicated that incidental equipment air leakage rates were of the same order of magnitude as the leakage rates through the wall. This was undesirable as it tended to give large experimental error. However, not all incidental leakage was through the gasket seal. Initially, a surprising amount of air leakage occurred through pressure tap holes drilled through the plywood side panel. Air entered the holes and escaped through the exposed plywood layers. After sealing these holes completely, a significant improvement in incidental air leakage was obtained.

The primary seal between the Specimen Box and the Load Box was a special problem. This seal must be easily broken when dismantling the setup; it must be easily and repeatably achieved when assembling the setup; and it must be available on both sides of the Specimen Box. The present mode of sealing is shown in Figure 2.7. It consists of a 10 mm outside diameter Tygon tube in which is placed a 1.5 mm polyvinyl tube. The 'hard' inner tube limits the amount of possible compression of the 'soft' outer tube. This tubing is bedded in silicone on the Specimen Box steel frame between two 1.5 mm steel rods 12 mm apart. The joint in the tubing gasket is sealed with silicone. This seal performed satisfactorily.

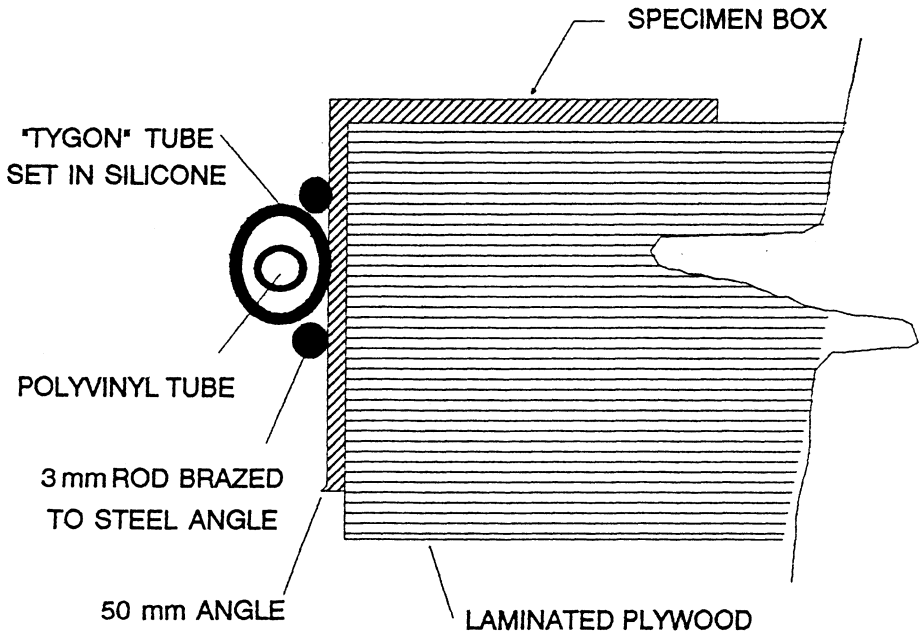

FIGURE 2.7 Primary Seal - ESTA 1

2.3.7 Performance of ESTA 1

The main purpose of this research, that of moisture accumulation testing, was economically accomplished with ESTA 1. The addition to the setup of the mechanical cooling system brought ESTA 1 into the realm of a low cost yet versatile and productive piece of test equipment.

After experience was gained in using the equipment, two problems were identified. The first, as previously mentioned, was the inability to reduce the incidental apparatus leakage to one order of magnitude less than the wall leakage for relatively air tight wall specimens. It was difficult to pin point where this apparatus leakage was occurring. The second problem was associated with attachment and detachment of the Load Box from the Specimen Box. The process was quite time consuming and there was some question as to the repeatability attainable in one detach-attach cycle. For these reasons a second version of ESTA was built and is described in the next section.

2.4 GENERAL DESCRIPTION - ESTA 2

ESTA 2 was built with the same design parameters as outlined for ESTA 1 yet in a simpler fashion. The Load Box and Specimen Box are one unit and consist of a 7 mm thick steel plate box lined with a 75 mm thickness of polystyrene insulation. Seventy-five millimeter steel angles welded to the outer perimeter of the Specimen Box on both sides serve as reaction points for clamping devices as shown Figure 2.8. A frame of 75 mm steel angles matching the dimensions of the steel angles framing the Specimen Box is used to rigidly support a 9 mm thick acrylic sheet which is used to

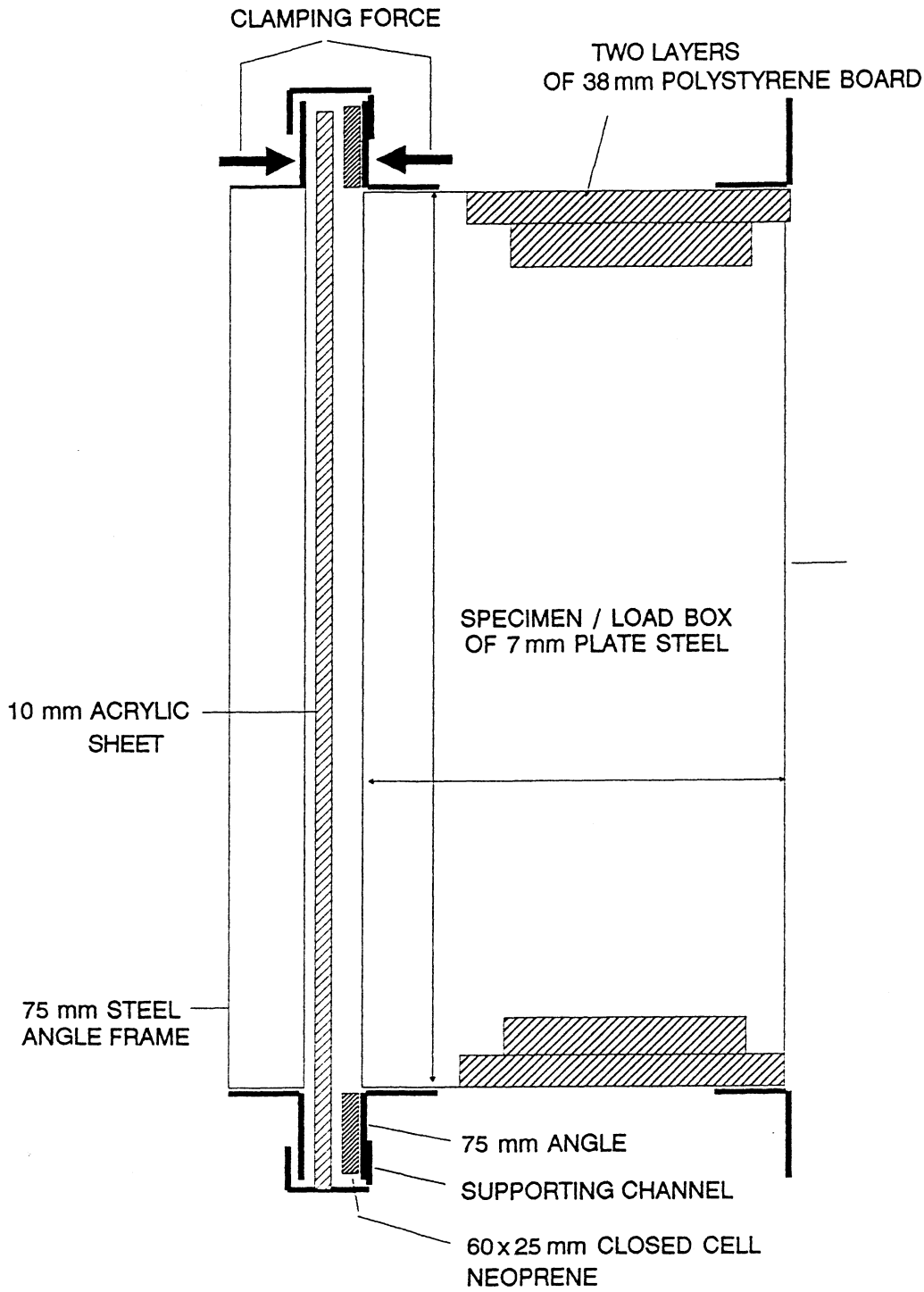

FIGURE 2.8 Vertical Section Through Apparatus - ESTA 2

cover the open area of the Specimen Box. Sealing at the perimeter is accomplished with a 60 x 25 mm closed cell neoprene material as shown in Figure 2.8. Clamps are used as quick connect and disconnect features to compress the neoprene seal. The mechanically cooled Cold Box remained unchanged.

ESTA 2 is a much improved version of the apparatus for both air tightness and ease of use. The acrylic sheet slides in and out for easy access. A maximum of 6 clamping devices are needed to achieve an essentially air tight fit. Repeatability between opening and closing the Specimen Box was found to be excellent. Ports for instrumentation access are easily accommodated in the plate steel as standard bulk head type connectors can be used. The steel stud portion of the specimen can be constructed inside or outside of the box. It is normally necessary, however, to build the brick veneer inside the apparatus. Figure 2.9 and 2.10 are photos showing ESTA 1 and ESTA 2 respectively.

2.5 INSTRUMENTATION

The following section describes the instrumentation used to measure the environmental loads and the performance of the various wall specimens.

2.5.1 Air Pressure

Pressure differentials across the wall are measured with a range of commercially made manometers. These included a U-tube micro-manometer and two inclined manometers.

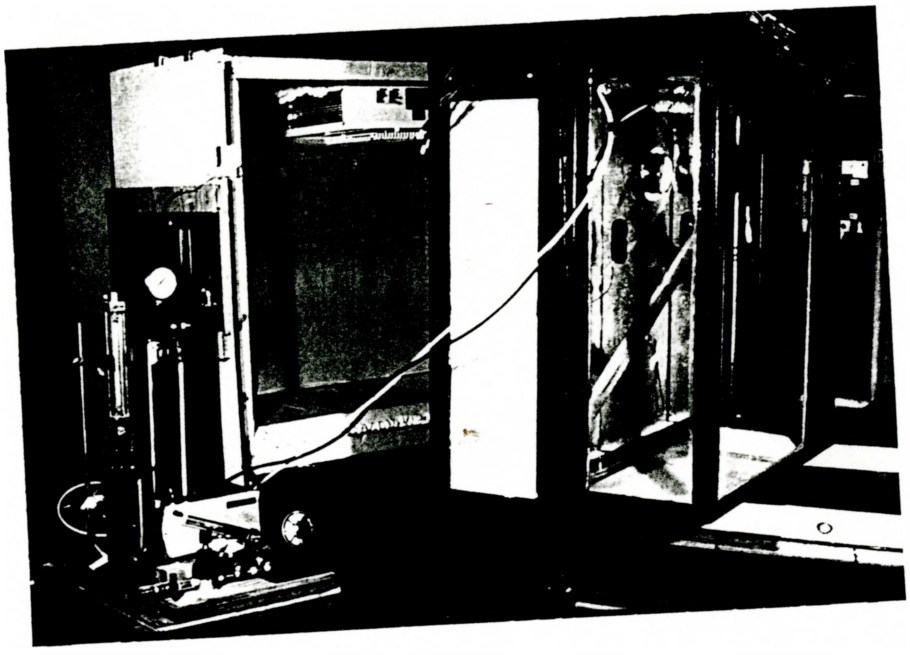

FIGURE 2.9 Photo Showing ESTA 1

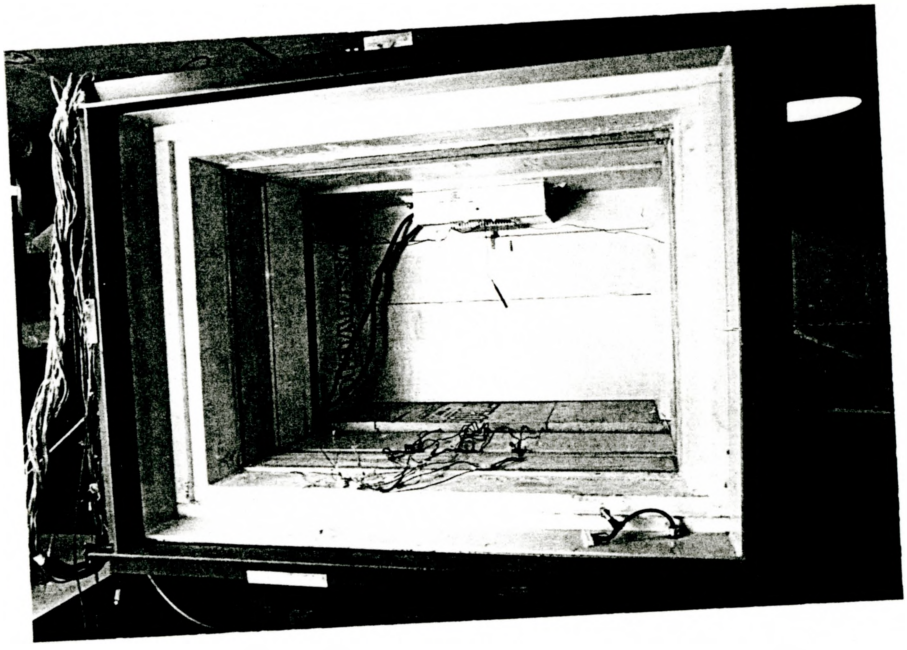

FIGURE 2.10 Photo Showing ESTA 2

The U-tube micromanometer has a scale in 0.001 inch (0.025 mm) increments. Isopropalalcohol having a relative density of 0.782 was used as the manometer fluid. In a U-tube manometer, pressure is determined on a first principles basis by measuring the height of a vertical column of fluid. If both legs of the manometer are read to the nearest 0.005 inch, the accuracy obtained from this instrument was better than 1 Pa as shown below. The instrument had a maximum range of 8 inches or 1560 Pa.

Micromanometer Accuracy

Read each leg to 0.005 inch

Possible error of 0.0025 inch in each reading = 0.005 inch net error

Weight Density of isopropalalcohol = $0.782 \times 9810 = 7671\ N/m^3$

Read error = $0.005\ in \times 0.0254\ m/in \times 7671\ N/m^3$

$= 0.974\ N/m^2 = 0.974\ Pa$

Direct reading inclined manometers manufactured by Air Flow Developments with ranges of 0 - 400 Pa and 0 - 100 Pa are also used.

2.5.2 Air Flow

Air flow rates were measured with rotameters. These instruments consist of a variable area vertical glass tube in which a 'float' assumes a certain level for a given air flow rate. The reported accuracy of such instruments is 5% of full scale when not specially calibrated or 2% of full scale when calibrated. All four rotameters used in this study were calibrated with "Wet Test Meters" and linear regression was used to obtain

the equation relating float elevation (mm) to flow rate (L/s). The rotameters covered the calibrated range of 0.017 L/s to 1.4 L/s. Table 2.4 contains a summary of the rotameter types, ranges and regression equation coefficients. Since the rotameter for the lowest range had a non-linear calibration, the calibration curve was read directly to obtain the flow rate. The other three rotameters all had linear calibration and therefore linear calibration equations were used. Calibration curves for all rotameters are given in Appendix A.

TABLE 2.4

Rotameter Types and Calibration Coefficients

Make	Tube/Model (float type)	Calibrated Range (scale)	Flow Range (L/s)	Equation* Coefficients A	B
Fisher & Porter	06-150/s 5180	5-14 mm	0.017-0.042	non-linear	
Brooks	R6-15A (Sapphire)	20-130 mm	0.031-0.175	0.00273	0.002977
Brooks	R6-15A (Tantalum)	20-120 mm	0.052-0.325	0.00273	0.002997
Fisher & Porter	84-27-10/77	1-3.4 in	0.333-1.4	27.6	-9.3

* Flow in L/s = A x (Scale Reading) + B

2.5.3 Temperature Profiles

Up to fifty Type T thermocouples, made from thermocouple grade wire manufactured to industry standard calibration specifications (eg. NEMA) were used in this study to measure temperature.

Thermocouples work on the principle that two types of metal in mutual contact generate a voltage in proportion to the temperature. In this case the two types of metals are copper and constantan, a copper-nickel alloy where copper is positive with respect to constantan. A third degree

polynomial calibration equation relating voltage output to temperature was used for computation purposes[14]. This equation had the following form:

$$T = a + bV + cV^2 + dV^3 \qquad \text{[Eq. 2.1}$$

where T = temperature, $^{\circ}C$
V = output, millivolts

and regressed equation coefficients are:

$a = -0.0099$
$b = +25.8827$
$c = -0.6964$
$d = +0.02613$

The reported average accuracy of this equation is $0.012^{\circ}C$. In this setup, since a large number of thermocouples were used and since each lead was approximately 7 meters long, it was more economical to use thermocouple grade extension wire for about 3.5 meters and then normal copper wire for the remaining portion. As shown in Figure 2.11, the splices between the thermocouple wires and the copper wires were wrapped in glassfibre batt insulation to form an isothermal block where all the thermocouple wire ends were maintained at the same temperature. This was necessary since the output voltage of a thermocouple is relative to the temperature at the end of the thermocouple wire. To obtain this reference temperature, the temperature within the batt was measured by one of two methods. For the first two specimens tested, a thermocouple placed in an ice bath was used while for the remaining specimens a thermistor was used.

The ice bath arrangement required daily monitoring to ensure that the thermocouple in the bath was at $0^{\circ}C$. This was accomplished by means of a thermometer placed alongside the thermocouple. The ice bath consisted of a two litre plastic container filled with three trays of ice cubes

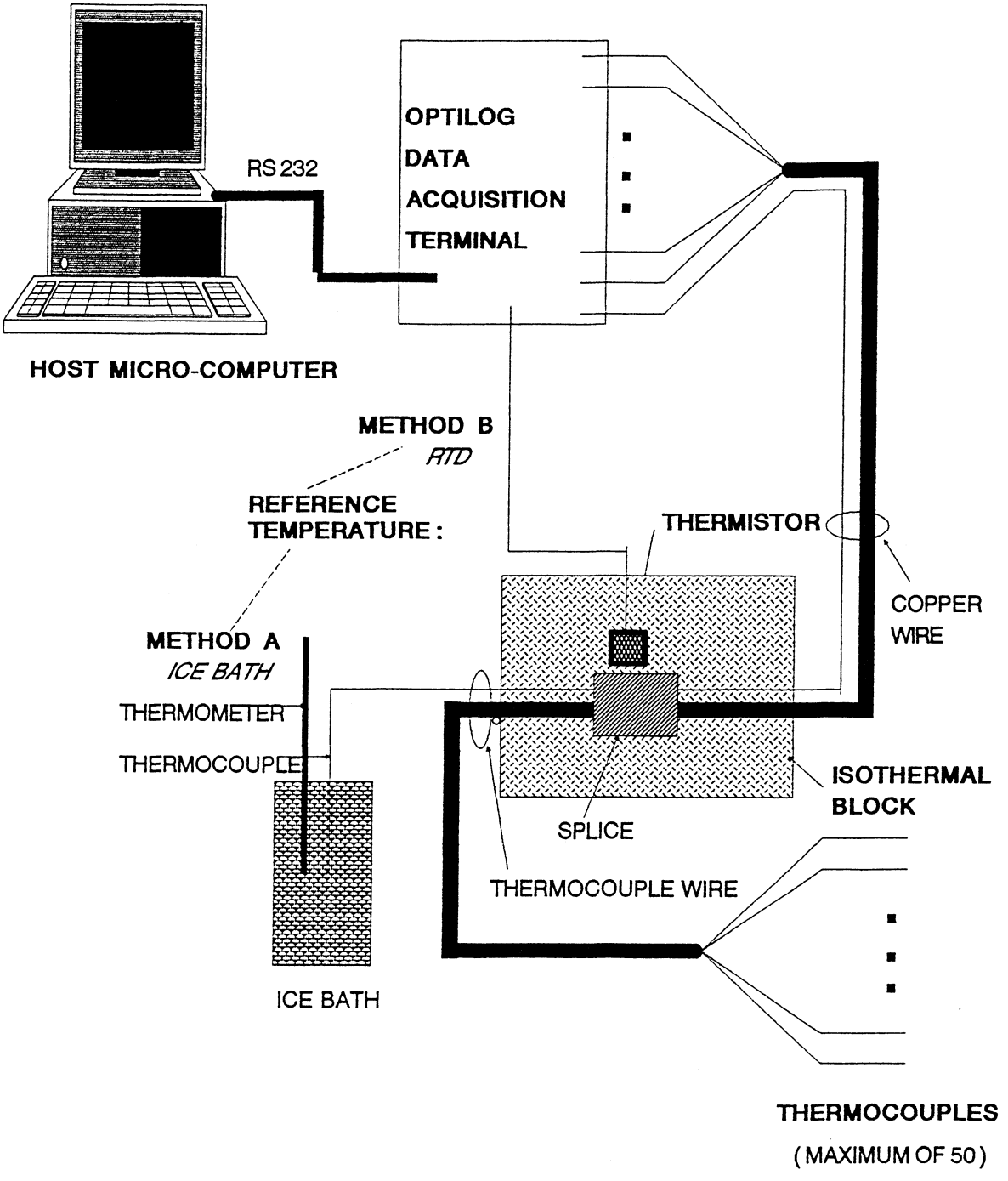

FIGURE 2.11 Schematic Drawing of Temperature Measurement Scheme

and then filled with water. The container was wrapped with a glass fibre batt and placed in a pail. The top and bottom of the pail was insulated with 38 mm of polystyrene. In this way, the ice bath maintained a 0°C temperature for approximately 48 hours. The leads of the thermocouple in the ice bath were terminated in the isothermal block. With this arrangement, the temperature at any point in the wall was obtained by simply adding the voltage generated by the ice bath thermocouple to the voltage generated by each of the thermocouples in the wall. Equation 2.1 was then used to convert voltage to temperature.

In the second arrangement, the temperature at the ends of the thermocouple wires in the isothermal block were measured directly by means of a thermistor. Thermistors, or RTDs, have an absolute correlation between resistance and temperature. By applying a known current through the device and measuring the resulting voltage across it, the resistance is determined by Ohm's law as:

$$R = E/I \qquad \text{[Eq. 2.2}$$

where R = resistance, Ohms
E = voltage, volts
I = current, amperes

The thermistor used was a Yellow Springs Instrument precision thermistor model #44005. For this device, temperature is related to resistance by the following curve fitted equation[14] :

$$T = 1/[\{a + bLn(R) + cLn(R)^2 + dLn(R)^3\} - 273] \qquad \text{[Eq. 2.3}$$

where R = thermistor resistance, Ohms
T = thermistor temperature, °C

and the regressed equation coefficients are :

$a = 1.403 \times 10^{-3}$
$b = 237.5 \times 10^{-6}$
$c = -318.8 \times 10^{-6}$
$d = 10.06 \times 10^{-6}$

This temperature was then converted to the equivalent type T thermocouple voltage output by means of the following equation[14]:

$$V = e + fT + gT^2 + hT^3 \qquad \text{[Eq. 2.4}$$

where T = thermistor temperature, °C
V = equivalent type T thermocouple output voltage referenced to 0 °C, mV

and the regressed equation coefficients are :

$e = 10.00119$
$f = 0.03862$
$g = 43.65 \times 10^{-6}$
$h = -20.67 \times 10^{-9}$

The temperature at any point in the wall was then obtained by adding the equivalent voltage output to the measured output for each thermocouple and Equation 2.4 was used to convert voltage to temperature.

Automation of temperature measurements was made possible by a computer controlled system consisting of a Texas Instruments Professional Computer attached by serial cable to an OPTILOG model 200 data acquisition device. The system was driven by custom made software written in the Basic language.

2.5.4 Moisture/Humidity

The measurement of humidity was for the most part accomplished by a Haener humidity gauge having an accuracy of ±5% RH. Maintenance of a specified humidity level was provided by a wet spray humidifier which was controlled by a Honeywell Humidistat which was in turn calibrated to the

Haener humidity gauge. Although it was necessary to perform most of the tests in this way, the equipment was subsequently upgraded with an electronic humidity gauge manufactured by Omega (model HX91) and having an accuracy of ±3%RH. The previously mentioned data acquisition system was used to monitor humidity levels with this instrument and to control the humidifier by means of a custom made relay circuit. With this new setup the humidistat became obsolete.

Finally, the presence of condensation was determined by observation, and material mass measurement. By observation it was possible in various tests to see frost, water droplets, and the formation of corrosion products. By mass measurements it was possible to determine moisture gain in certain materials.

2.6 CLOSURE

A major component of the research effort and a significant part of research contribution consisted of designing and improving the Environmental Simulation Test Apparatus. The approach taken in its design was to concentrate on the overall response of the wall to the imposed environmental loads. For this reason the apparatus is not suited for the precise scientific measurement of heat flow. It is well suited, however, to investigate air flow rates through wall specimens, thermal profiles and the occurrence of condensation. These features make the facility unique.

Exclusive of the data acquisition equipment and labour, the materials needed to build and instrument ESTA 2 require a fairly modest capital outlay estimated at $3000. This, combined with the test area of 1 m^2, makes the apparatus very attractive to industry as there is an increased awareness

of the need to carry out an assessment of new wall systems to determine their environmental performance. Although full scale tests may be necessary in some cases, ESTA is ideally suited to test different combinations or variations of wall designs to determine the best one or two. Then, if required, a more expensive full scale test can be performed. In many cases the results obtained form ESTA will in themselves be conclusive. In this way, ESTA fulfills a need identified by industry for an economical method to evaluate the performance of wall systems subjected to individual or combined environmental loads.

Another facet to the development of the equipment is the need for a standard test method. The concept and development of a single test apparatus to perform these tests combined with the practical experience gained in testing makes this work a stepping stone to the establishment of a standard test method. Not only is such a standard of value to the construction industry but it is also valuable to building owners and the public in general. By requiring that new wall systems meet certain performance standards, the service life and indeed safety of buildings will be improved.

In the next chapter, details of the experimental program are given. All of the tests described were performed with the Environmental Simulation Test Apparatus.

CHAPTER 3

EXPERIMENTAL PROGRAM: DESCRIPTION OF TESTS, CONSTRUCTION OF TEST SPECIMENS, AND TEST RESULTS

3.1 INTRODUCTION

The primary goal of this research was to subject various wall systems to air pressure, vapour pressure and temperature differentials and to thereby evaluate the potential for and the amount and location of moisture accumulation caused by water vapour condensation within the wall. Two secondary goals were to determine thermal properties and air leakage characteristics as these are the main factors influencing condensation of air borne water vapour.

The test procedures developed to investigate the above characteristics are described in this chapter. In addition, details of the wall test specimens and the test results are presented. The discussion and interpretation of these results are located in Chapter 5 following a consideration of some analytical results presented in Chapter 4.

3.2 TEST PROCEDURES

3.2.1 General

Since temperature distributions and air leakage characteristics are individual factors which play key roles in moisture accumulation, tests were

conducted to document these properties before moisture accumulation tests were performed. The main features of each type of test are briefly described in the following sections.

3.2.2 Air Leakage Test

Air leakage tests were performed to determine the air flow rate through wall systems under a range of pressure differentials. Since air barriers are required by the 1985 edition of the NBC[3], this type of testing in the context of modern wall systems is primarily aimed at quantifying the air tightness of the air barrier, although other components of the wall system can have some effect on restricting air flow.

The two approaches taken in this work were:

1. Introduce a well defined leakage path in a 'perfect' air barrier.
2. Construct the wall system according to specifications and quantitatively determine the effectiveness of the air barrier.

In either case the method involved either applying a known pressure differential across the wall system and measuring the air flow rate, or, conversely, setting the air flow rate and measuring the pressure differential.

3.2.3 Thermal Performance

Two types of thermal profiles were measured. The predominate type was through-the-wall at each material interface. A typical through-the-wall profile consisted of measurements at the following locations:

- interior air
- air/interior gypsum board
- gypsum/insulation or stud

- insulation or stud/exterior sheathing
- exterior sheathing/air cavity
- cavity air
- air cavity/brick
- brick/air
- exterior air

Through-the-wall profiles were normally taken to coincide with the line of the stud or at the lateral center line of the insulation mid way between studs. A second type of profile was taken in-the-plane of the wall at the interface between the stud or stud space insulation and the interior side of the exterior sheathing. A third type of thermal measurement performed involved taking local measurements at points of interest.

Since every measured profile had slightly different interior and exterior temperature conditions, a method similar to that of Sasaki[35] was used to facilitate comparison between results. This involved calculating a non-dimensional coefficient for each thermocouple location as:

$$\alpha_X = 1 - (T_i - T_X)/(T_i - T_e) \qquad \text{[Eq. 3.1}$$

where α_X = non-dimensional coefficient for location X
T_i = interior temperature
T_e = exterior temperature
T_X = temperature at point X

In this way, each measured point has a value ranging from 1 (interior) to 0 (exterior). Then, for the standard interior and exterior temperatures of T_i and T_e, the normalized temperature, T_{NX}, becomes :

$$T_{NX} = (T_i - T_e)(\alpha_X - 1) + T_i \qquad \text{[Eq. 3.2}$$

The thermal results in the following section are presented in this fashion for comparative purposes along with the average α_X values used to

obtain the profiles. For each specimen a number of thermal profiles were experimentally determined over the course of the test. Since the cooling equipment could not maintain a steady temperature indefinitely, it was necessary to determine a set of average α_x values representing equilibrium conditions. This was accomplished by determining a subset of α_x values such that the standard deviation of the product of α_x and $(T_i - T_e) = 40^\circ C$ was less than $1^\circ C$.

3.2.4 Moisture Accumulation Testing

The main purpose of this test was to examine the potential for condensation and to assess vulnerability of various wall systems to condensation and condensation related damage. Testing involved:

- creating a pressure differential across the wall and measuring the resulting air flow rate or alternately setting a desired flow rate and measuring differential pressures,
- maintaining a specified and constant level of humidity on the interior of the wall system
- providing a constant temperature differential across the wall and measuring temperatures at set locations and
- examining the wall during and after the test for evidence of condensation.

The details of exactly how these conditions were accomplished for each test are explained as the test results are presented.

3.3 CONSTRUCTION OF WALL TEST SPECIMENS

3.3.1 General

Three types of brick veneer/steel stud wall systems were investigated. Listing the components from the interior to the exterior, each wall type

consisted of interior gypsum board; a polyethylene vapour barrier; a steel stud framing system with insulation in the space between studs; a sheathing material on the exterior of the studs; an air space between sheathing material and brick veneer (cavity); and a brick veneer tied by brick ties to the steel stud framing system.

The basic differences between the three wall types investigated can be summarized as follows:

- Wall type 1 was built with an exterior grade gypsum board sheathing material which by its nature has negligible insulating value.
- In contrast, Wall Type 2 was built with an insulating polystyrene sheathing material.
- Wall Type 3 was different from Type 1 and 2 in that the steel framing system was non-standard. Furthermore, a range of insulation schemes was investigated to obtain an optimum configuration.

In summary, the three types of wall systems investigated in this work could be classified as having a non-insulating sheathing, an insulating sheathing and a non- standard steel framing system. In total, 5 wall specimens were tested corresponding to two Type 1 and 2 walls (Specimen 1A, 1B, 2A and 2B) and one Type 3 wall (Specimen 3).

Before discussing the various tests performed, the construction details for each wall specimen built will be described.

3.3.2 Type 1 Walls

3.3.2.1 General

The distinguishing feature of Wall Type 1 was the exterior grade gypsum board sheathing on the exterior face of the steel stud. In contrast to friction fit fibreglass insulation, 12.5 mm thick gypsum board has little

insulating value (RSI = 0.080 m^2K/W) and thus this wall type is classified as having a non-insulating sheathing.

Viewing the wall in cross-section as shown in Figure 3.1 (a), the basic components were as listed in Table 3.1. The two Type 1 wall specimens differed on three main points. Firstly, Wall Specimen 1A included a brick veneer tied to the studs with brick ties. Wall Specimen 1B had no brick veneer and thus no brick ties. Secondly, for Wall Specimen 1A, the fibreglass batt insulation used was manufactured to fit in a wood frame system and therefore was not wide enough to fully extend into the stud channel cavity. This allowed use of a fibre optics viewing instrument in the stud channel cavity. Wall Specimen 1B was constructed with fibreglass batt insulation specifically manufactured for steel stud framing systems and was thus wide enough to fit tightly into the stud channel cavity. Thirdly, the 6 mil polyethylene vapour barrier in Wall Specimen 1A had an overlap of 75 mm centered on Stud B (See Figure 3.1 (b)). For Wall Specimen 1B, this overlap was 450 mm and extended over the space between Stud A and Stud B and over both studs.

3.3.2.2 Construction Details

Construction details in the order of construction of the various components are given. In this section reference is made to Part 9 of the National Building Code[3], "Housing and Small Building" and to Part 5, "Wind, Water and Vapour Protection".

TABLE 3.1

Component Details for Wall Type 1

Component	Detail
Interior Finish	two coats latex paint
Interior Wall Board	fully taped 12.5 mm gypsum board
Vapour Barrier	6 mil polyethylene
Framing	20 gauge galvanized steel stud and track
Insulation	RSI 2.1 glass fibre batt
Exterior Sheathing	12.5 mm exterior grade gypsum board
Cavity +	25 mm vented
Brick Tie +	wire loop adjustable wire loop fixed double leg adjustable
Brick +	90 mm clay

+ Wall Specimen 1A only

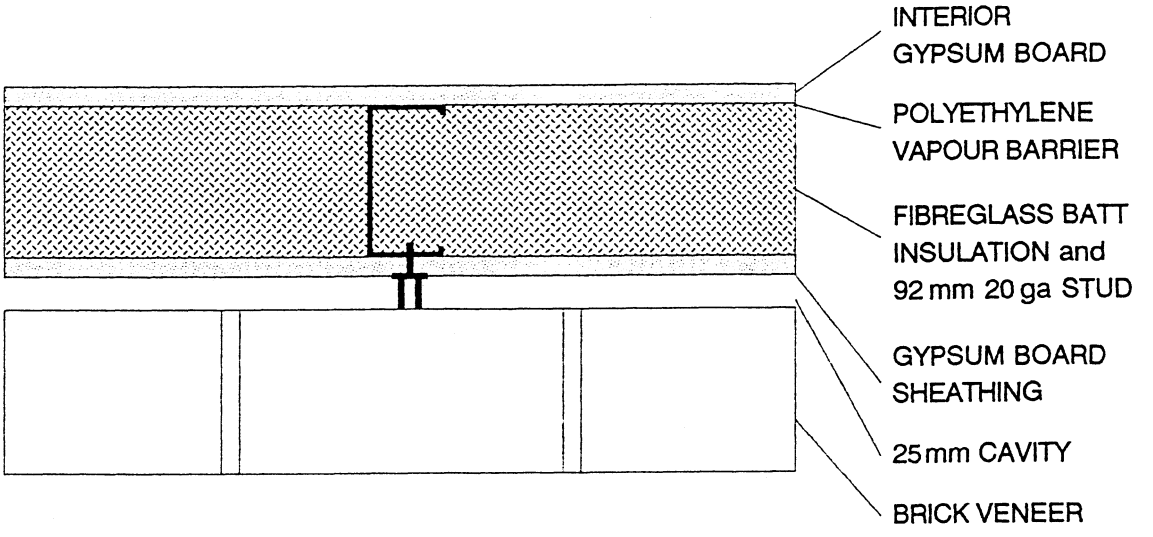

(a) Horizontal Section

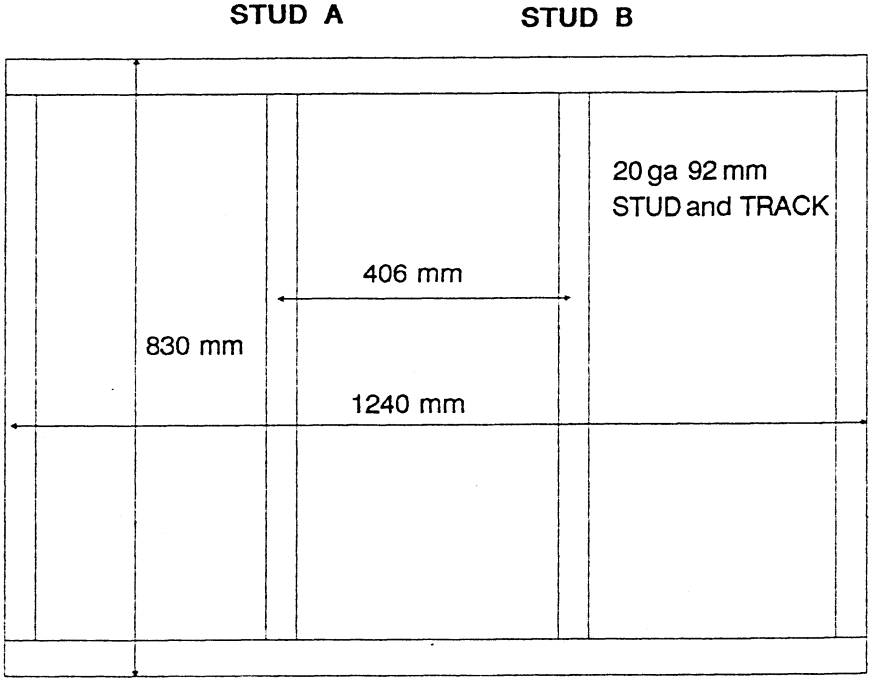

(b) Interior View of Stud Framework

FIGURE 3.1 Wall Type 1 Construction Details

Steel Stud Framing System: Galvanized 20 gauge (0.91 mm thick) steel stud and track were used in both wall specimens. The galvanizing was applied by the hot dip process. The dimensions of the steel stud were 92 mm deep by 35 mm wide. The track matched the 92 mm stud width and was 33 mm in height. Stud framing details are shown in Figure 3.1 (b). The purpose of the top and bottom tracks shown in Figure 3.1 (b) was to align and secure the studs and to serve as backing for the sheathing. The spacing between Stud A and Stud B was 406 mm center-to-center. The stud and track were fastened together with 6-20 x 3/8 pan head self-drilling cadmium plated framing screws.

The two perimeter studs along with the top and bottom track were secured to the Specimen Box of ESTA 1 by wood screws to provide lateral stability. In addition, the interior perimeter of the stud assembly was caulked with a silicone sealant to ensure that no air leakage occurred at the edges.

In the context of this research, all requirements in Section 9.25 of NBC[3], "Sheet Steel Stud Wall Framing", were met.

Thermal Insulation: In Section 9.26, "Thermal Insulation and Vapour Barriers", Article 9.26.2.1. states that "Buildings of residential occupancy shall be provided with sufficient thermal insulation to prevent moisture condensation on the interior surfaces of walls, ceilings and floors during the winter and to ensure comfortable conditions for the occupants". This requirement was met by the use of standard density friction fit fibreglass batt insulation having an RSI value of 2.1 m^2K/W. The glass fibre batt insulation conformed to the requirements of CSA A101-M1983 "Mineral

Fibre Thermal Building Insulation". Two types of batt insulation were used with the only difference being the manufactured batt width.

In Wall Specimen 1A, the batt used was designed to fit in a wood frame system with studs at 406 mm on centre and was thus manufactured with a width of about 370 mm and a depth of about 95 mm. Although the batt fit snugly in its depth the batt width was insufficient to extend into the stud channel. In Specimen 1B, a batt specially manufactured for use with steel stud at 406 mm was used and thus fit snugly in its depth and width. A point to note is the fit of this "steel stud batt" in the stud channel. As illustrated in Figure 3.2, the return on the stud flanges protruded into the batt insulation causing a poor fit of the batt around the returns. This configuration of insulation does not satisfy either Article 9.26.4.1 or 9.26.4.2 of NBC 1985. However, it represents existing practice.

Vapour Barrier: In accordance with Section 9.26, a Type 1 vapour barrier consisting of 6 mil polyethylene sheet was used in the wall construction. It was located on the warm side of the thermal insulation on the interior face of the steel stud. A vertical 75 mm overlap in the vapour barrier was formed over Stud B in Wall Specimen 1A. In Wall Specimen 1A the overlap was extended from Stud A to Stud B and was thus 450 mm wide. The minimum overlap width over framing members required under section 9.26 was 25 mm in the 1980 NBC and is 100 mm in the 1985 NBC. The idea of overlapping the polyethylene over two studs was taken from recommendations in "Guide to Energy Efficiency in Masonry and Concrete Buildings"[31].

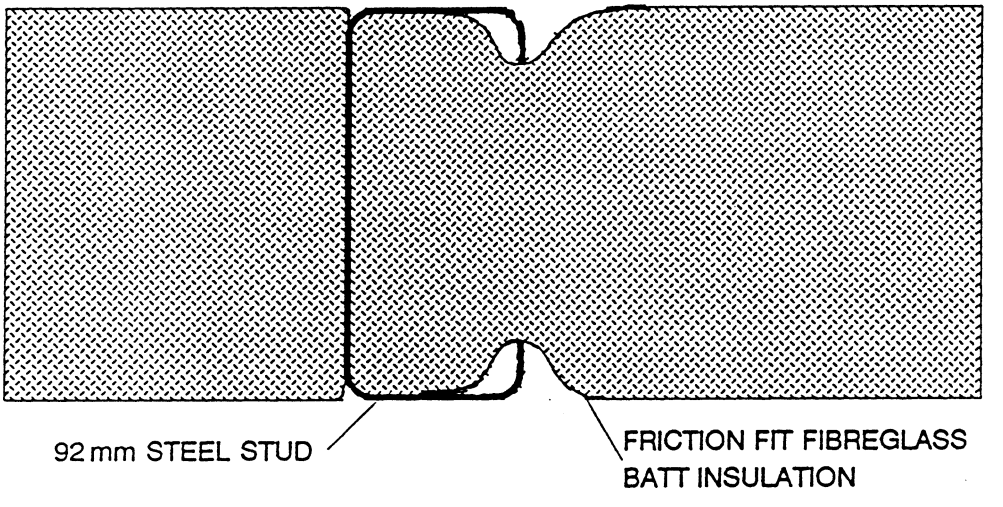

FIGURE 3.2 Section Showing Fit of Batt Insulation Around Return on Stud Flange

Gypsum Board: 12.5 mm gypsum board for interior application conforming to CSA A82.27 - "Gypsum Board Products" was fastened to the interior stud surface. The fasteners used were 25 mm S-12 type self-drilling drywall screws with no special plating. The screws were black and had an oil type finish. The screws were spaced at 200 mm. This is well within NBC minimum code requirements of 300 mm (9.30.6). Furthermore, the 25 mm length satisfied the Section 9.25 requirement of a minimum penetration into the stud of 10 mm (25 mm screw - 12.5 mm gypsum board = 12.5 mm penetration). It is note worthy that the National Building Code makes no statement as to minimum corrosion resistance of fasteners used with steel framing systems where these are not recognized as having structural significance.

An interesting observation is the state of the screw after attaching the gypsum board. That is, in the self drilling operation, the screw tip acts like a drill cutting into the steel stud. The cuttings resulting from this operation are very fine. Whereas some cuttings fall, the magnetic drill bit in the electric drywall screw gun magnetizes the screw causing some cuttings to magnetically adhere to the screw -especially at the screw tip. The net result is fine bits of steel covering the tip. Furthermore, the inner surface of the stud is caused to "bugle out" out as depicted in Figure 3.3 as a result of the drilling force. Both the interior side of the "bugled" steel at the screw hole and the magnetized cuttings are prime breeding grounds for corrosion due to the large surface area of unprotected steel.

The interior gypsum board surface of Wall Specimen 1A was finished by applying two coats of a latex paint. Wall Specimen 1B differed only in that the screw heads were sealed with tape to allow removal of the board

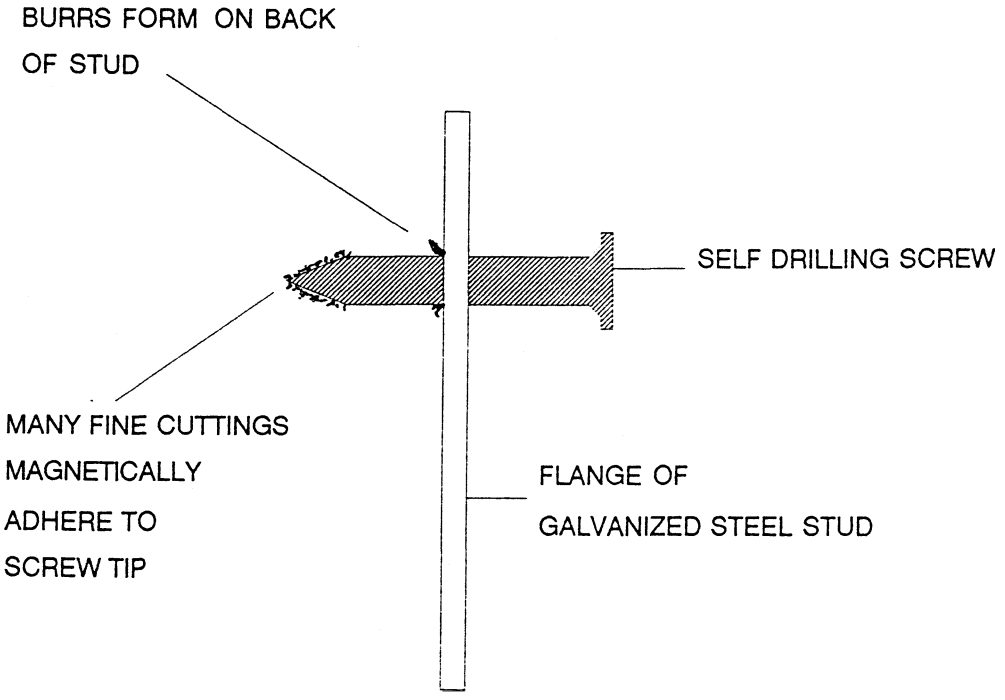

FIGURE 3.3 Condition of Screw and Stud After Self Drilling Operation

during the test. Finally, the perimeter of the gypsum board was sealed with a silicone sealant to seal off any air leakage paths between the specimen and the Specimen Box.

An exterior grade gypsum board was applied to the outside of the studs in Wall Specimen 1A such that a horizontal, unfinished joint existed at mid height. The joint was made by butting two rounded finished edges together. The difference between the interior and exterior gypsum board was the type of paper used on the outside of the board. That is, the exterior board had a water repellant paper to meet the requirements of ASTM C79-84 "Standard Specification for Gypsum Sheathing Board". The same type of screws were used at the same spacing to fasten the board to the stud. Also, the perimeter was sealed with a silicone sealant.

Wall Specimen 1B was constructed without a horizontal joint. In this specimen it was desired to monitor the weight of the exterior gypsum board sheathing during the test. To do this the central portion of the board was cut into three vertical strips, two centered on the studs and one centered on the center of the batt insulation as shown in Figure 3.4. To prevent moisture from entering the board via the cut edges, all edges were sealed with tape. It was further desired to make this the air barrier and therefore, during the test the vertical joints and all screw heads were sealed with tape and the perimeter was sealed with silicone.

Brick Ties: The quantity and type of screw mounting brick ties used in Specimen 1A are listed below :

1 - Wire Loop Adjustable

1 - Wire Loop Fixed

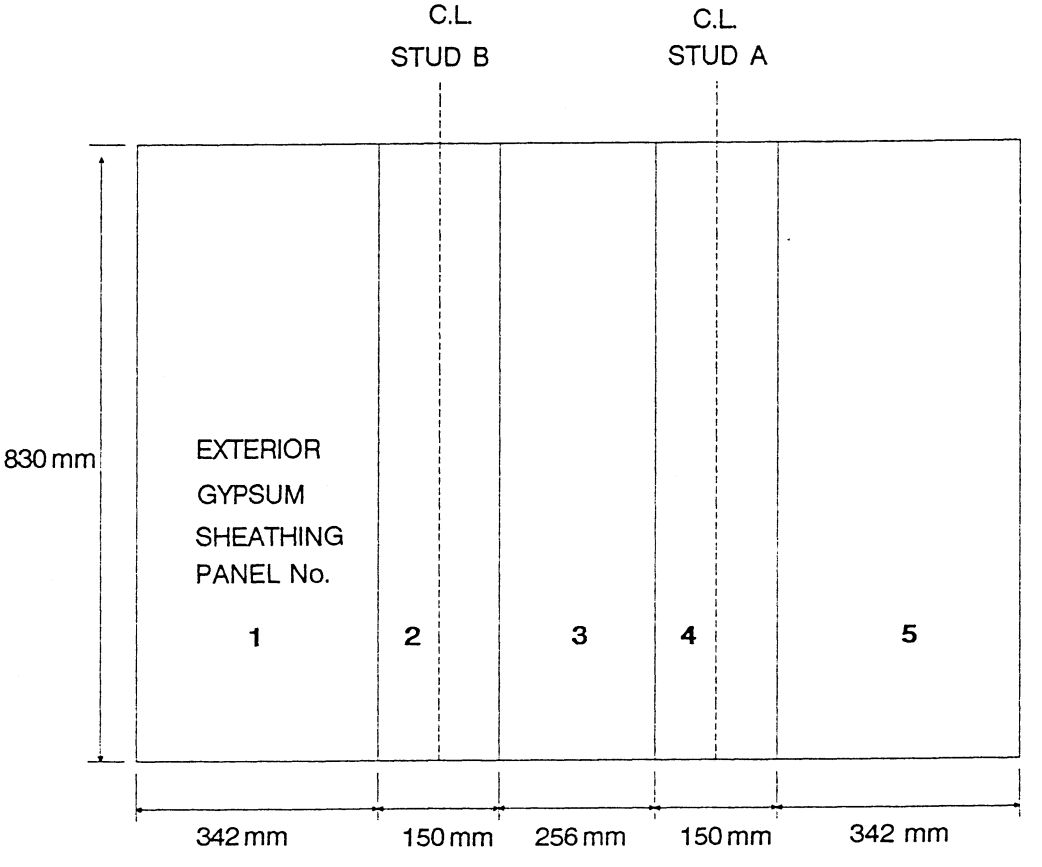

FIGURE 3.4 Exterior View of Gypsum Sheathing Panels in Wall Specimen 1B

2 - Double Leg Adjustable.

The locations of the ties are illustrated in Figure 3.5 (a). The cadmium plated screw fastener used was a 10 -16x30 mm. One screw was used for the Wire Loop Adjustable tie while 2 screws were used for each of the 2 others. The ties are shown in Figure 3.5(b).

Bricks: Clay bricks having an approximate size of 190 mm long by 90 mm wide by 57 mm high were used for Wall Specimen 1A. Full head and bed mortar joints were ensured during construction. Type N mortar was used. In both the top and bottom course, 2 head joints were left empty to simulate vent and weepholes. The perimeter was sealed with a silicone sealant.

Wall Specimen 1B did not have a brick veneer. It was left off to facilitate visual observations and removal of components for weighing.

3.3.3 Type 2 Walls

3.3.3.1 General

In Specimens 2A and 2B, the insulating exterior sheathing used was a 25 mm polystyrene board product having a rated RSI value of 0.88 m^2K/W. The wall cross-section is illustrated in Figure 3.6 and the component details are listed in Table 3.2 in order from the interior to the exterior.

3.3.3.2 Construction Details

Construction details were for the most part the same as for Wall Specimens 1A and 1B. Therefore, only new aspects are described in the following section.

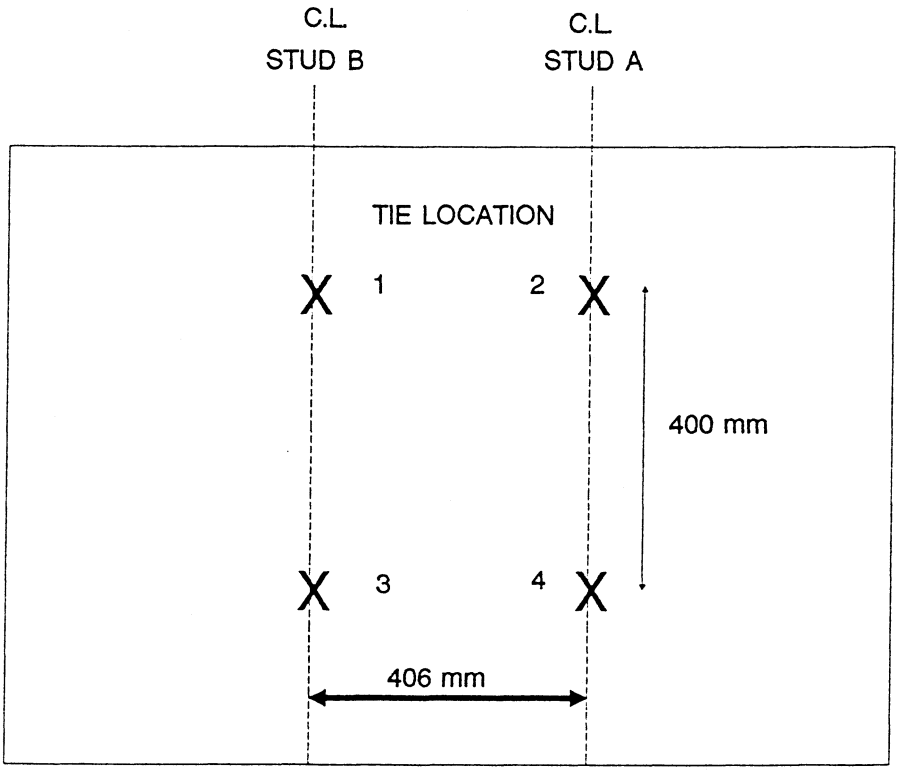

(a) Exterior View of Wall Specimen 1A Showing Location of Brick Ties

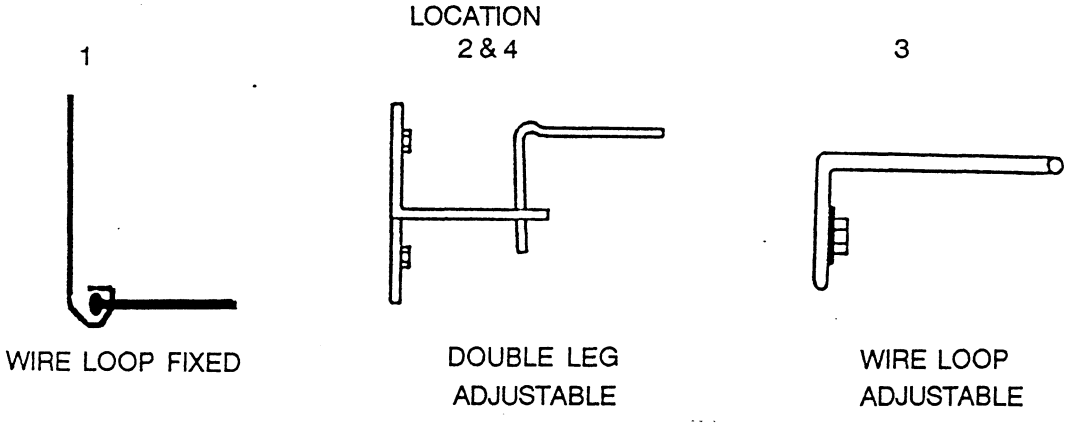

(b) Types of Brick Ties Used

FIGURE 3.5 Specimen 1A Brick Tie Arrangement

TABLE 3.2

Component Details for Wall Type 2

Component	Detail
Interior Finish	unfinished
Interior Wall Board	12.5 mm gypsum board
Vapour Barrier	6 mil polyethylene
Framing	20 gauge galvanized steel stud and track
Insulation	RSI 2.1 glass fibre batt
Exterior Sheathing	25 mm extruded smooth skin polystyrene
Cavity +	25 mm vented
Brick Tie +	wire loop adjustable double leg adjustable
Brick +	90 mm clay

+ Wall Specimen 2A only

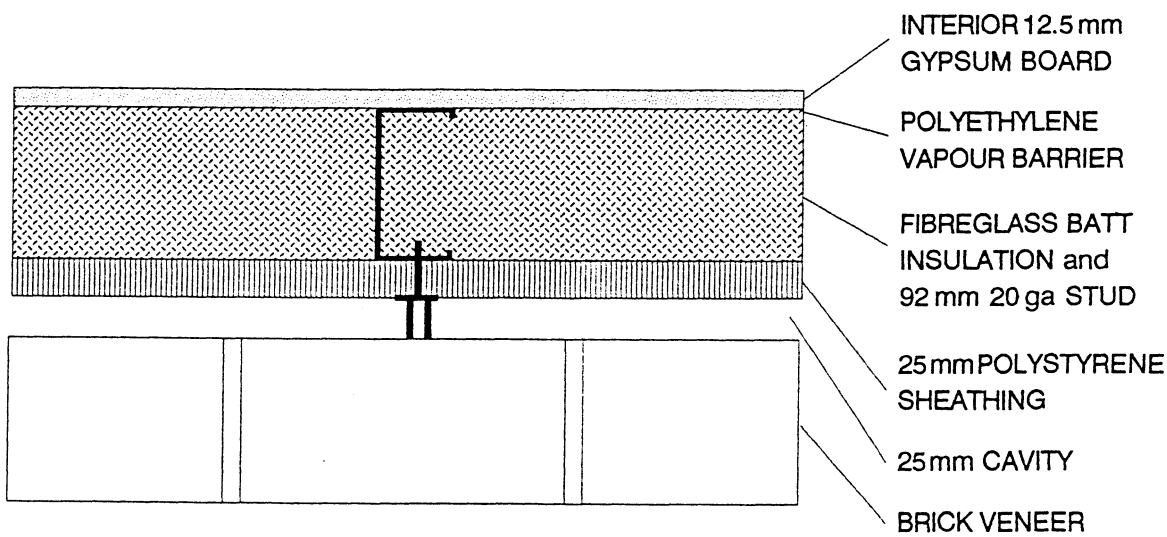

FIGURE 3.6 Horizontal Section Showing Components of Wall Type 2

Stud Wall Framing: The stud framework was identical to that of Wall Specimens 1A and 1B as illustrated in Figure 3.1(b).

Thermal Insulation: The batt insulation used was the same kind as Specimen 1A and 1B. The batt width was the full fit batt specifically designed for steel studs.

Gypsum Board: In Wall Specimen 2A, the interior gypsum board was not painted while for Wall Specimen 2B tests were done with it unpainted, then painted.

Vapour Barrier: The 6 mil polyethylene vapour barrier was identically placed and lapped as in Wall Specimen 1B. That is, it was placed on the interior face of the steel studs and with a 450 mm lap extending from Stud A to Stud B.

Polystyrene: As indicated previously, the exterior sheathing used was a 25 mm thick expanded polystyrene product having an RSI value of 0.88 m^2K/W. This rigid insulation was an extruded board with a smooth skin surface and conformed to CGSB 51-20M (1978) "Thermal Insulation, Expanded Polystyrene". As shown in Figure 3.7(a), the insulation was applied with one horizontal joint at 300 mm from the bottom. In the construction phase, no effort was made either to make the joint overly tight or to introduce a gap .

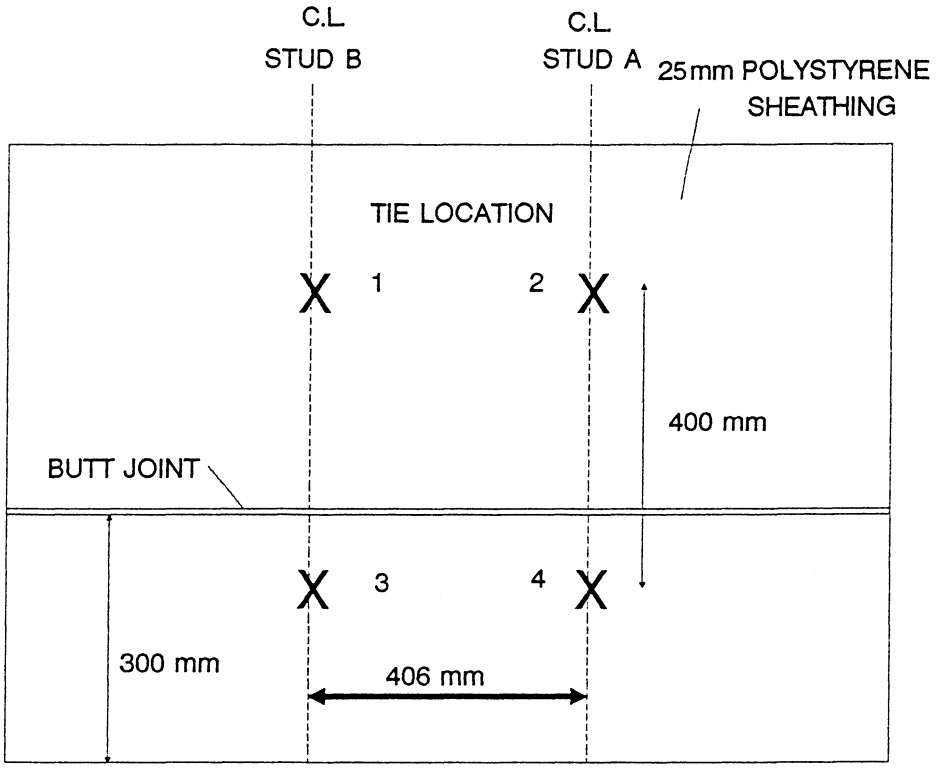

(a) Exterior View Showing Location of Brick Ties and Butt Joint in Sheathing

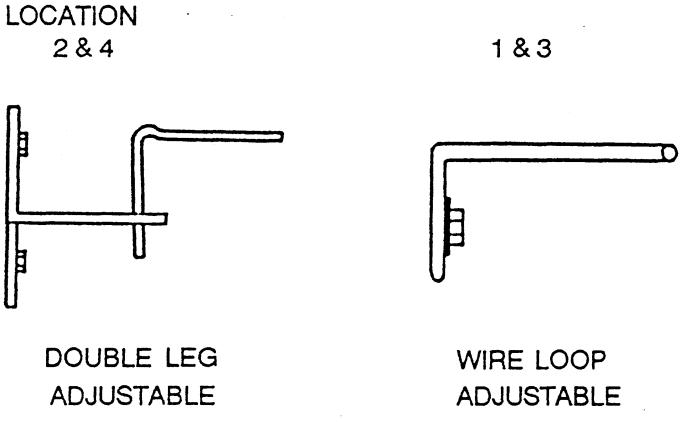

(b) Types of Brick Ties Used

FIGURE 3.7 Specimen 2A Brick Tie and Polystyrene Sheathing Arrangement

Two types of insulation fasteners were used. On Stud B, a pin type fastener designed to minimize thermal bridging effects was used. This fastener had a pin, 1 mm in diameter by 35 mm long, attached at right angles to a 35 mm square base plate of 24 gauge sheet steel. On the back of the face plate, a double sided tape was applied which allowed the fastener to be attached to the stud by adhesion. The rigid polystyrene board was then impaled on the pin and a retaining clipped was forced over the protruding portion of the pin. Figure 3.8 is a sketch of the above attachment. In contrast, mechanical type fasteners consisting of a self drilling screw with a 50 mm square washer of 16 gauge steel, were used on Stud A. A similar arrangement is used on roofing systems to attach polystyrene. It was thought that the large steel screw and washer would provide significantly more potential for thermal bridging than the adhesive pin. The perimeter of the polystyrene was sealed with a silicone type sealant.

Brick Ties: In Specimen 2A, two types of ties were used both of which were screw mounting. On Stud B, 2 Wire Loop Adjustable ties were used. This single screw tie is relatively light and therefore is a "minimal" conductor. It was used on Stud B in conjunction with the light pin type sheathing fastener. On Stud A, 2 Double Leg Adjustable ties were used.(Figure 3.7(b)) These double screw ties are heavier and were used on the same stud as the heavier sheathing fasteners described earlier. The net result was that Stud A had more thermal bridging potential then did Stud B.

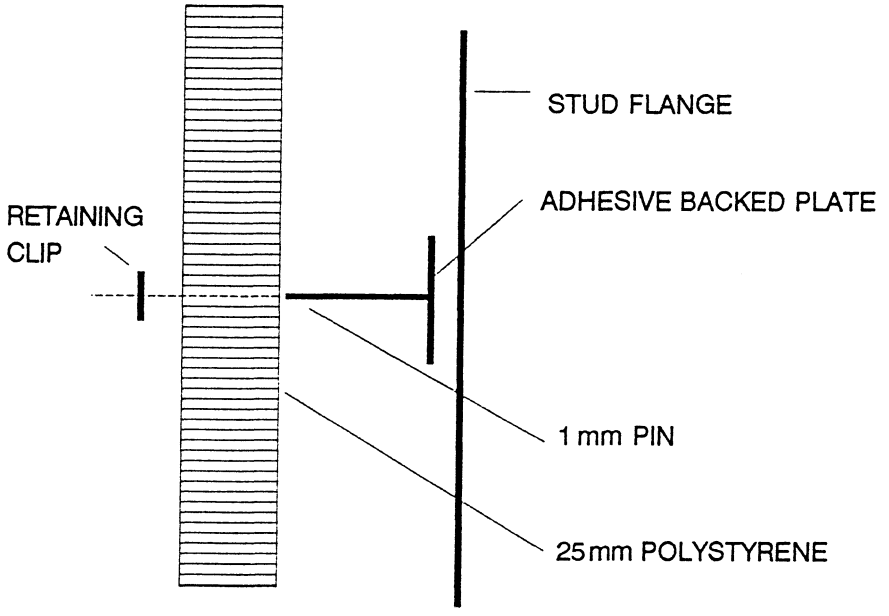

FIGURE 3.8 Light Weight Pin Connector for Application of Polystyrene Sheathing

Brick: The brick veneer used for Wall Specimen 2A was constructed in the same way as in Wall Specimen 1A. Specimen 2B did not have a brick veneer attached.

3.3.4 Type 3 Wall

3.3.4.1 General

As mentioned previously, Wall Specimen 3 incorporated a non-standard steel framing system. It was developed in an attempt to improve some of the structural and building science features of brick veneer/steel stud wall construction. Since the steel framing system was so different from the simple arrangement used in Wall Types 1 and 2, in the context of this work, this wall system is classified as having a non-standard framing system. The basic wall section consisted of two layers of gypsum board separated by a 25 mm air gap; back to back steel stud with insulation in the stud space; brick tie/cavity; and brick veneer. The component details for Wall Specimen 3 are listed in Table 3.3 and can best be understood with the aid of the sections shown in Figure 3.9.

3.3.4.2 Construction Details

Steel Stud Wall Framing: In this system, studs are placed back-to-back at 813 mm centers. Since the test apparatus was only 1200 mm wide, a single set of back-to-back studs was placed in the middle of the specimen. Single studs were then placed at the sides to provide lateral stability. Galvanized 18 gauge 92 mm studs were used. The middle set of studs were set into the base shoe prescribed for the system, while the top was simply blocked in place. The stud arrangement for Wall Specimen 3 is shown in Figure 3.10.

TABLE 3.3

Component Details for Wall Type 3

Component	Detail
Interior Finish	two coats latex paint
Interior Wall Board	12.5 mm gypsum board supported on horizontally placed steel hat and J sections
Air Barrier	12.5 mm exterior grade gypsum board
Vapour Barrier	6 mil polyethylene
Framing	back-to-back 18 gauge galvanized steel stud
Insulation	75 mm glass fibre board, RSI 2.2
Exterior Sheathing	none
Cavity +	-
Brick Tie +	bayonette style
Brick +	-

+ Wall Specimen 3 did not have a brick veneer

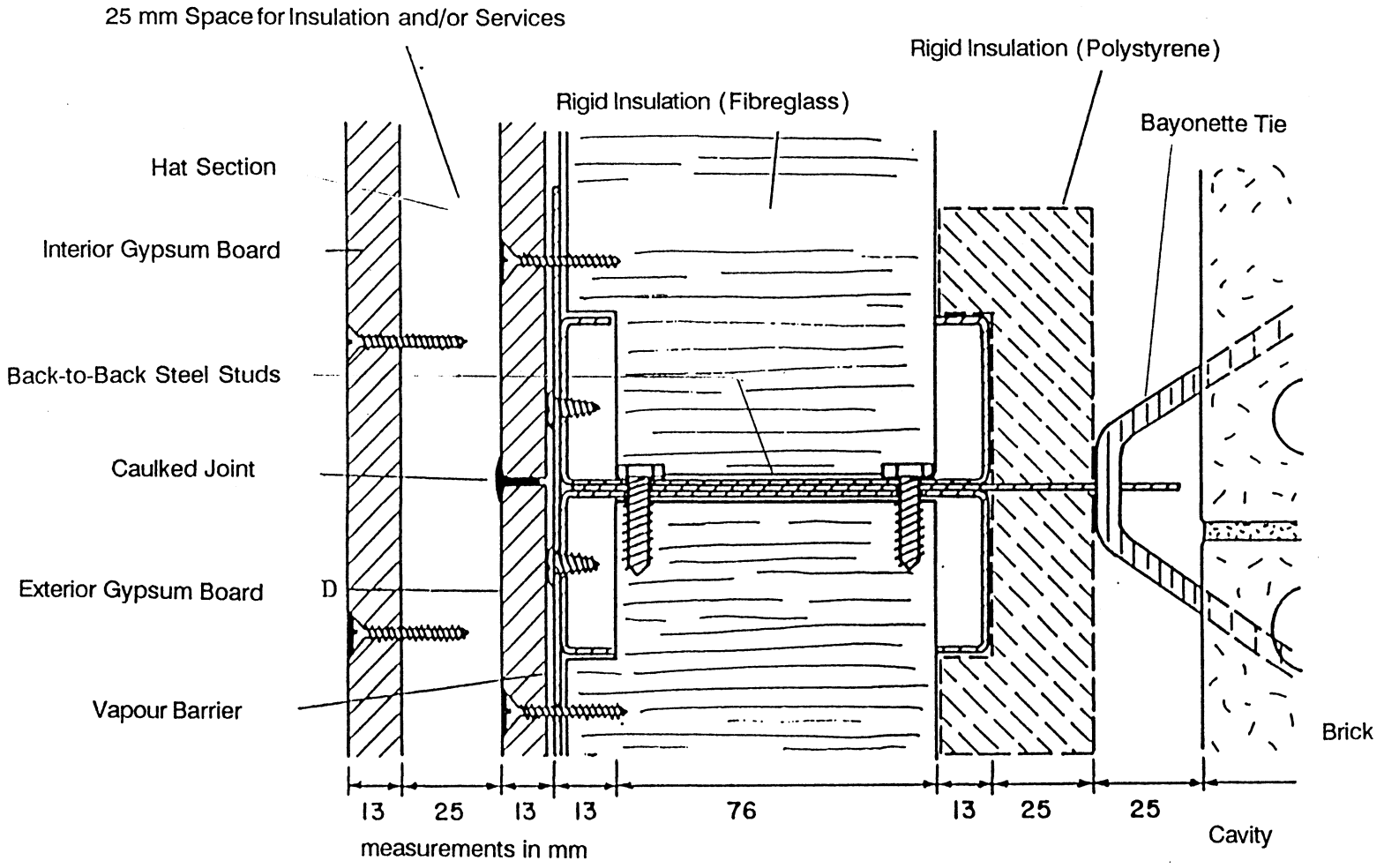

FIGURE 3.9 Horizontal Section Showing Tie and Thermal Insulation Features of Wall Type 3

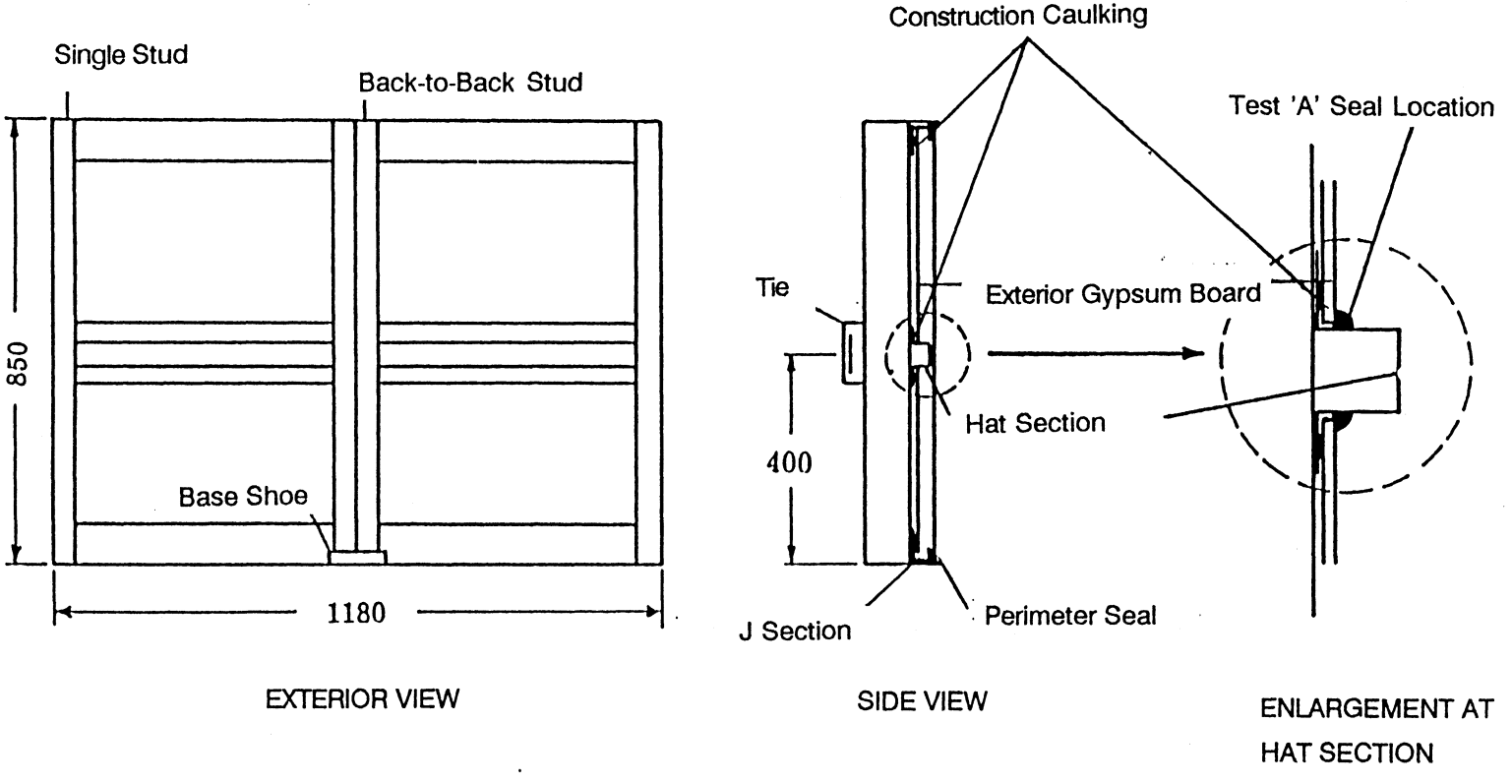

FIGURE 3.10 Specimen 3 Framing and Construction Details

Thermal Insulation: A semi-rigid type of glass fibre insulation having a density of 48.1 kg/m^3 was prescribed for the space between the studs. To avoid the possibility of convection currents between the insulation and the gypsum board, the insulation was notched as per Figure 3.9 to fit around the return on the flange of the steel stud. In this way the insulation fit tightly against the gypsum board as well as on the edges against the stud web.

Air Barrier: In this test specimen, the air barrier was provided by a 12.5 mm layer of exterior grade gypsum board on the interior face of the stud, spanning 425 mm vertically from hat section to J section. Caulking at the gypsum board/hat section interface was used to ensure an air tight construction. For testing purposes, Wall Specimen 3 was built with a horizontal hat section in the middle of the wall along with J sections top and bottom to provide support and sealable joints. Thus, two pieces of exterior grade gypsum were installed and sealed in place with a silicone caulking as shown in Figure 3.10. The perimeter was also caulked.

Vapour Barrier: The vapour barrier of Wall Specimen 3 was provided by a continuous 6 mil polyethylene sheet which spanned vertically from J section to hat section to J section.

Interior Gypsum Board: The interior of Wall Specimen 3 was finished in the usual way with a 12.5 mm layer of gypsum board and two coats of latex paint.

3.4 TEST RESULTS

3.4.1 Wall Specimen 1A

3.4.1.1 Air Leakage Test

Air leakage testing of this Type 1 wall was conducted with version 1 of the Environmental Simulation Test Apparatus. In Specimen 1A, the interior gypsum board was the intended air barrier. In the laboratory it would have been a simple task to demonstrate that a 1 square meter area of wall with a gypsum board air barrier could be constructed in an air tight fashion. However, the main purpose of the test program was to study the effects of unintentional air leakage. To this end, the gypsum board air barrier of Specimen 1A was violated with various size openings and the air leakage through these openings was measured for various pressure differences applied across the wall. In this series of tests the openings were cracks formed by leaving the horizontal joint in the gypsum board at mid wall height untaped over various lengths (see Figure 3.11). Crack lengths of 0, 12, 120 and 1200 mm were investigated. The average crack height was measured with a feeler gauge to be 0.3 mm. Table 3.4 contains a summary of the results for the four crack lengths. The ambient conditions on the day of test were 21°C and 40% RH.

The results were plotted in Figure 3.12 (a). Air leakage for the 0 mm crack length represents apparatus leakage. By graphically subtracting this leakage from the other sets of data, Figure 3.12 (b) was plotted and represents the air leakage rate for each crack length. The method used to record data was to set an air flow rate on the rotameter and then to read the resulting pressure when a steady state was reached. In this fashion, two sets of data were taken for each of the 12, 120 and 1200 mm crack lengths. It was

TABLE 3.4

Specimen 1A Air Leakage Characteristics

Crack Length (mm)	Pressure Difference (Pa)	Flow Rate (L/sm^2)
0	19.5	0.0047
	42.9	0.0092
	62.4	0.014
	105.3	0.019
	140.4	0.025
	185.3	0.030
	247.6	0.037
12 +	11.7	0.0047
	31.2	0.014
	60.5	0.025
	97.5	0.037
120 +	25.4	0.020
	59.5	0.047
	90.7	0.073
	124.8	0.098
1200 +	10.7	0.020
	22.4	0.047
	31.2	0.074
	38.0	0.100
	43.9	0.127
	57.5	0.152

+ average of two sets of readings

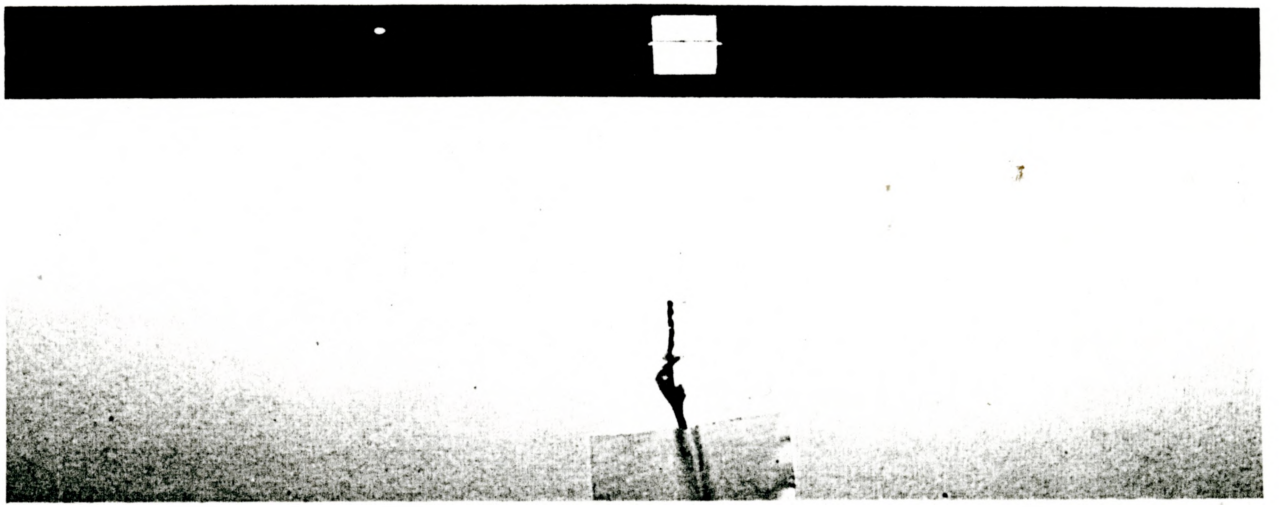

FIGURE 3.11 Photo Showing Taped Butt Joint in Interior Drywall and 12mm Crack Opening for Air Leakage Testing of Specimen 1A

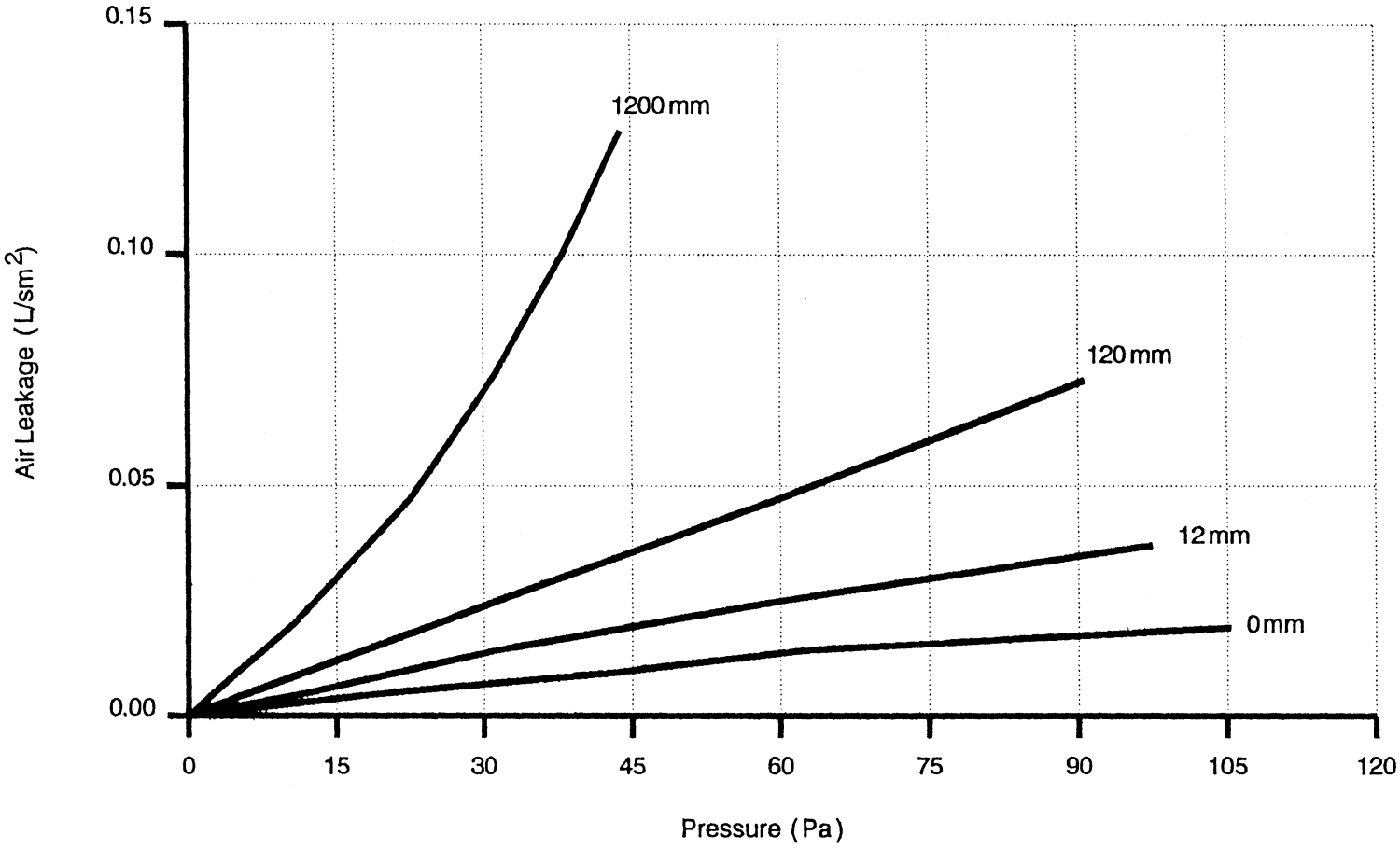

FIGURE 3.12(a) Specimen 1A Air Leakage Characteristics for Various Crack Lengths - Including Apparatus Leakage

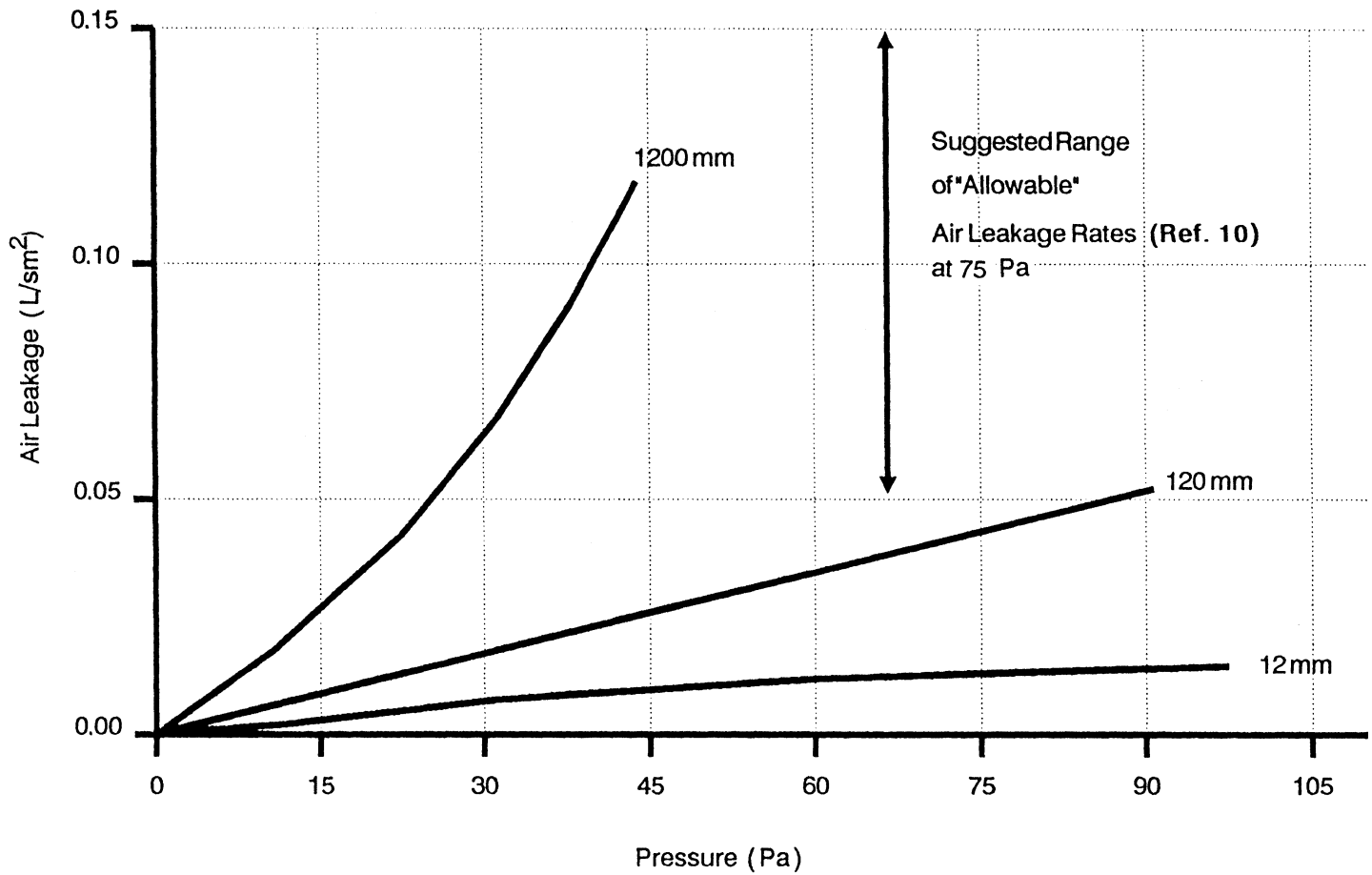

FIGURE 3.12(b) Specimen 1A Air Leakage Characteristics for Various Crack Lengths - Excluding Apparatus Leakage

found that an average repeatability of 1.5 Pa was achieved between sets of readings.

3.4.1.2 Thermal Performance Test

Although performed simultaneously with the moisture accumulation test, the thermal performance of Wall Specimen 1A will be reported separately in this section. In this test, 48 thermocouples were used to measure thermal profiles at the 6 locations illustrated in Figure 3.13. A limitation on the number of available data logging channels required that the thermocouples used to monitor air temperatures be limited to two at the top (T) and bottom (B) locations. The two air temperatures obtained were then averaged and recorded as the air temperature at each of the three thermal profile locations.

Temperature profiles were measured over a period of one week. After examining the data, 6 sets of readings were chosen as representative of steady-state conditions and as meeting the criteria that the standard deviation of the calculated temperature was less than $1^{\circ}C$ (see Section 3.2.3). Table B1 of Appendix B contains a listing of the six sets of measured temperature profiles for each of the six locations. Average α_X values obtained from these measured temperatures are listed in Table 3.5. Figures 3.14(a), (b) and (c) represent the calculated temperature profiles AT and AB; BT and BB; and IT and IB respectively. The values shown were standardized by the method described in Section 3.2.3.

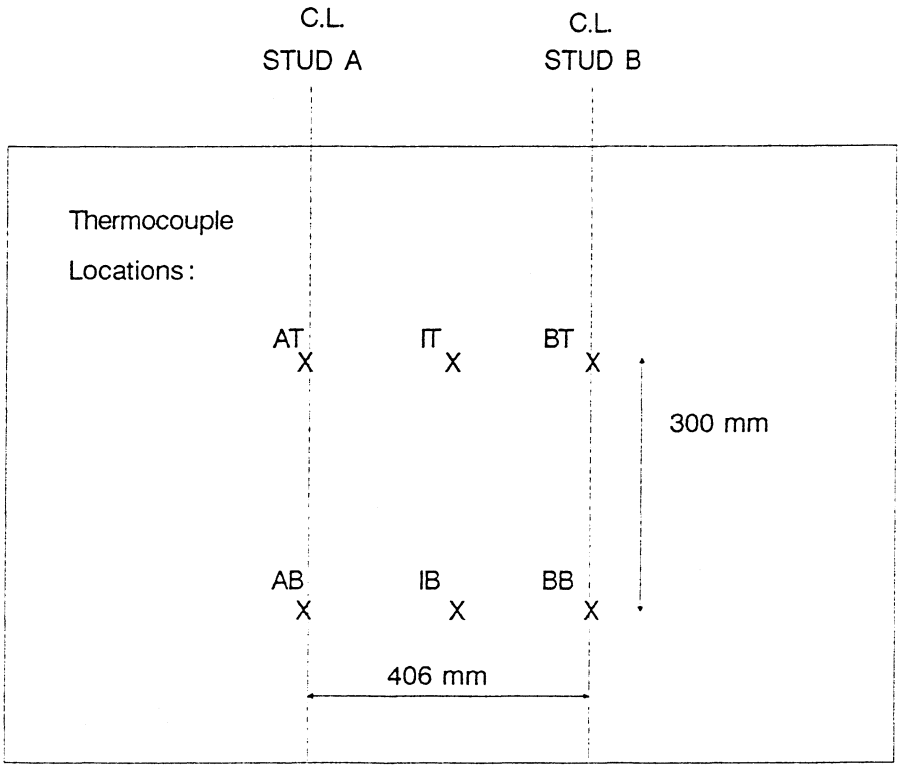

FIGURE 3.13 Interior View Showing Thermocouple Locations for Specimens 1A and 2A

TABLE 3.5

α_x Values for Specimen 1A[1]

Name	Location[2] I A	A/G	G/S,I	S,I/G	G/A	C A	A/B	B/A	E A
AT	1	0.926	0.700	0.482	0.381	0.204	0.193	0.013	0
BT	1	0.916	0.717	0.455	0.281	0.204	0.204	0.025	0
IT	1	1.000	0.972	0.229	0.195	0.204	0.129	0.008	0
AB	1	0.874	0.646	0.430	0.274	0.135	0.131	0.008	0
BB	1	0.872	0.655	0.430	0.257	0.135	0.151	0.015	0
IB	1	1.000	1.000	0.173	0.116	0.141	0.086	0.008	0

1 average of six samples

2
I A : Interior Air
A/G : interior Air / Gypsum board
G/S,I : Gypsum board / Stud or Insulation
S,I/G : Stud or Insulation / Gypsum board
G/A : Gypsum board / cavity Air
A/B : cavity Air / Brick
B/A : Brick / exterior Air
E A : Exterior Air

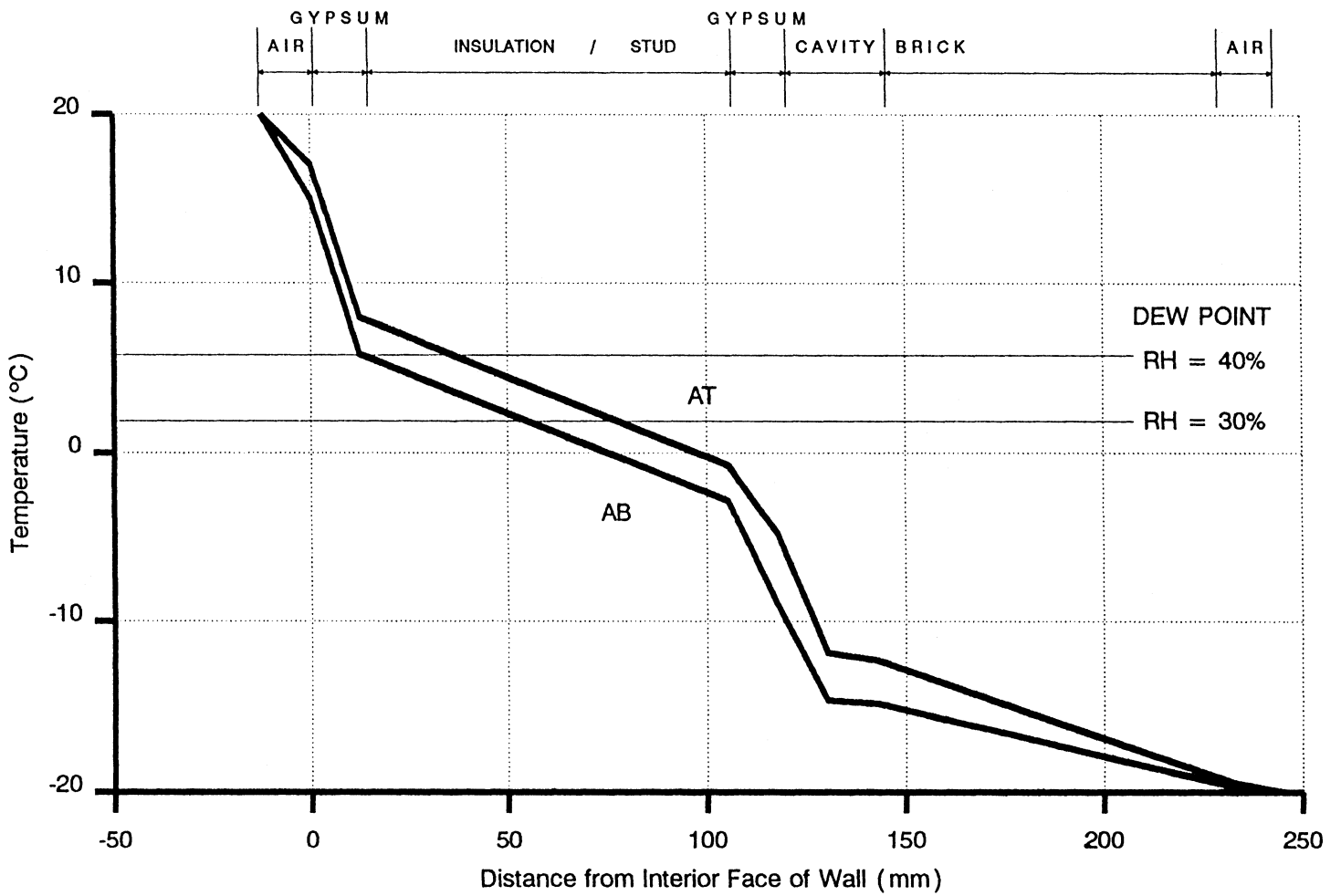

FIGURE 3.14(a) Through-the-Wall Thermal Profiles at Stud A of Specimen 1A

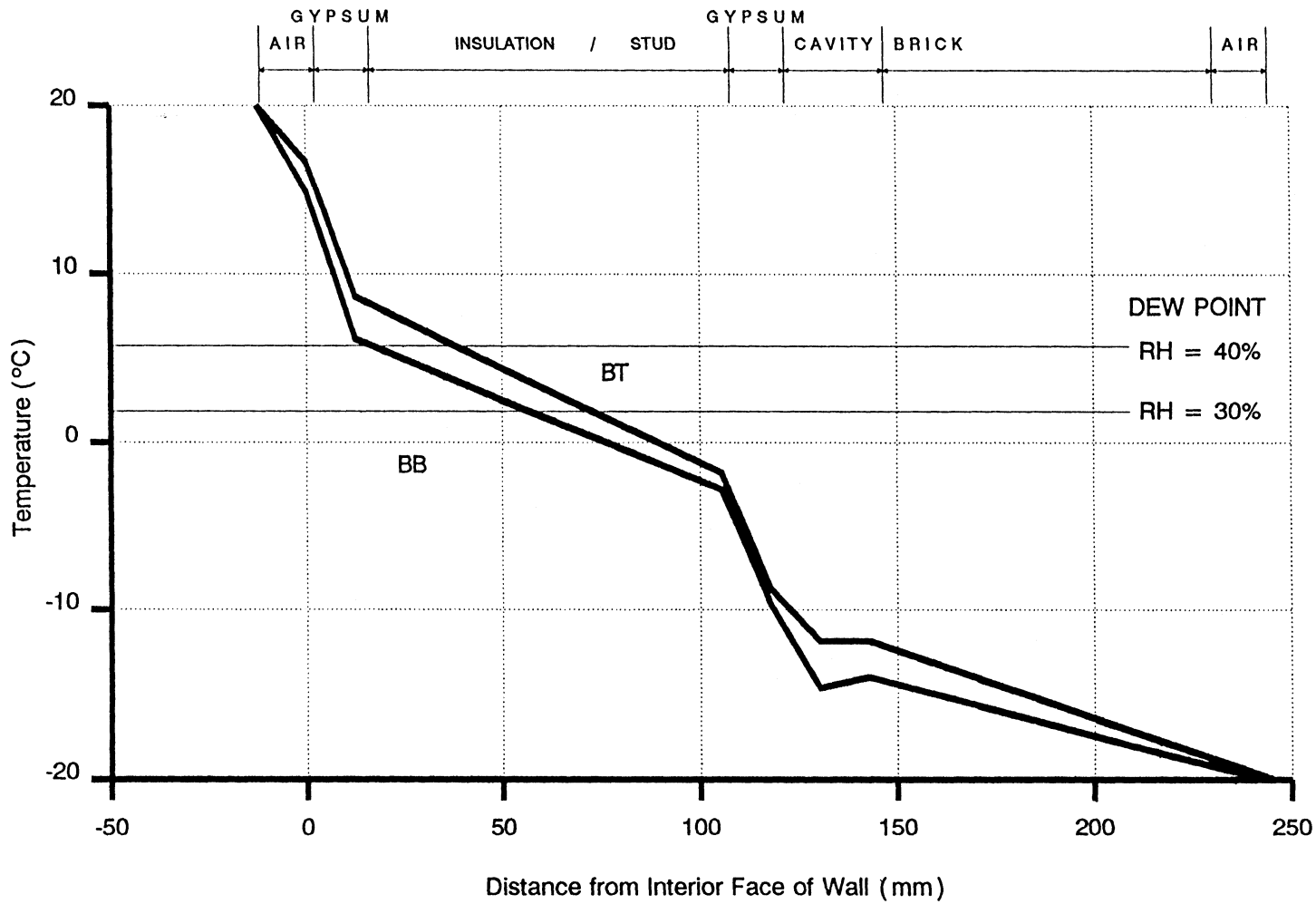

FIGURE 3.14(b) Through-the-Wall Thermal Profiles at Stud B of Specimen 1A

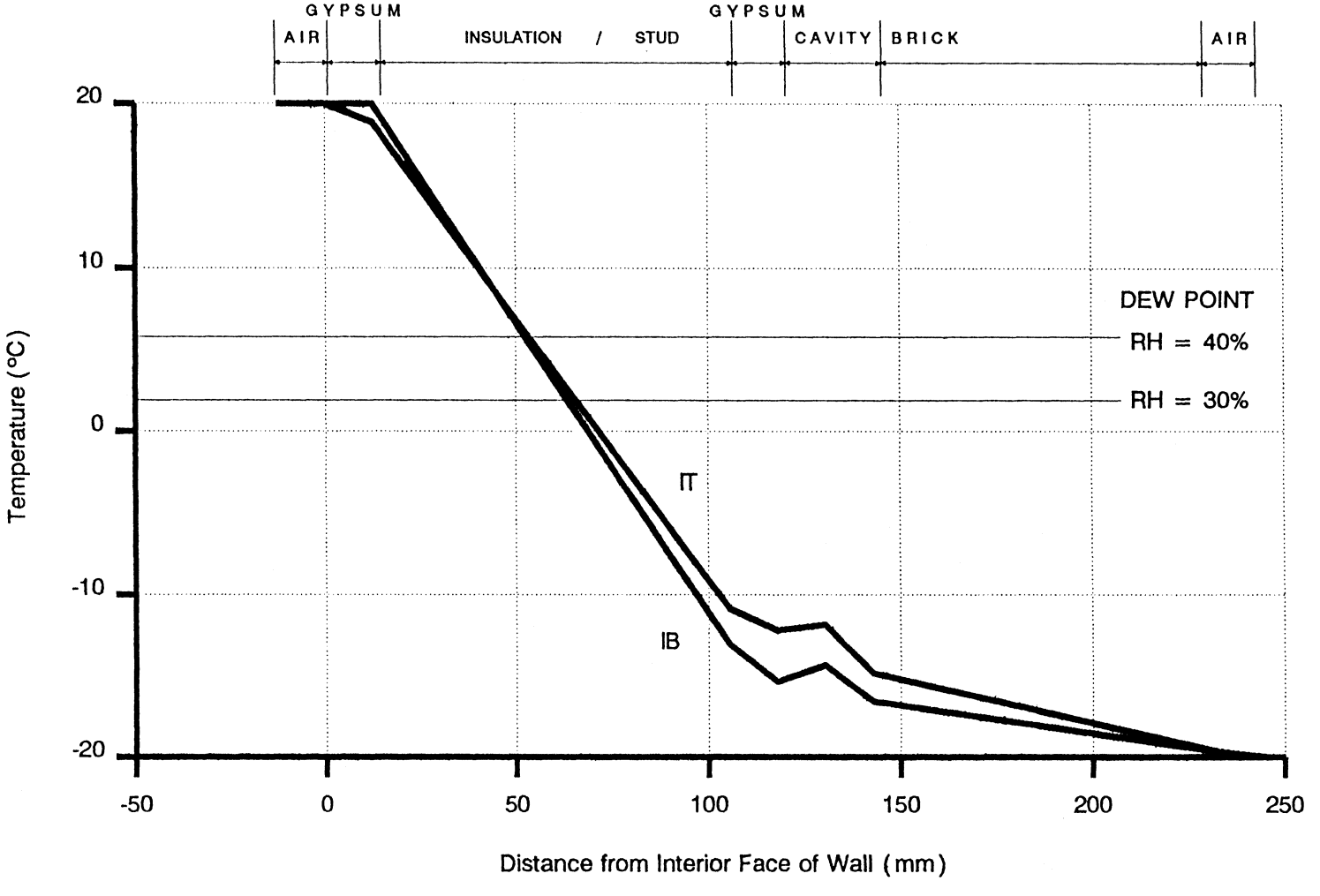

FIGURE 3.14(c) Through-the-Wall Thermal Profiles at Centre Line of Insulation of Specimen 1A

3.4.1.3 Moisture Accumulation Test

In this test, an air pressure difference, a vapour pressure difference and a temperature gradient were maintained across the wall to simulate winter conditions. A net outward pressure of 75 Pa was chosen as the air pressure difference since such a pressure can occur from the action of stack effect alone in the upper floors of high rise buildings and since this represents an industry standard benchmark. A relative humidity of 35 - 40%, considered representative for dwellings, was maintained.

With the 75 Pa pressure difference, air flowed through the wall at a rate of 0.015 L/sm^2. This leakage rate can be seen in Figure 3.12 (b) for a 12 mm gap in the gypsum board joint. Maintaining the temperature gradient proved to be a problem. At this stage the cooling was provided by an open top freezer in conjunction with dry ice. It was difficult to maintain the temperature at a steady condition. Thus, over the 1 week test duration, the cold side varied between a minimum of -17°0C and a maximum of -0°C, while the warm side was kept at 21 ± 2°C. Figure 3.15 is a plot of the temperature regimes for the Load Box and Cold Box over the 7 day test period.

After 7 days, the cooling system could not maintain a temperature below 0°C and the wall was dismantled. Upon dismantling there were no signs of moisture on the stud, on the fasteners or in the batt insulation. There was, however, evidence that moisture had formed at some point in the test as corrosion was present in four distinct locations.

Figure 3.16 is a sectional view showing a non-plated normal drywall screw fastener used to attach the exterior 12.5 mm gypsum board to the steel studs. Corrosion was evident along the length of the portion

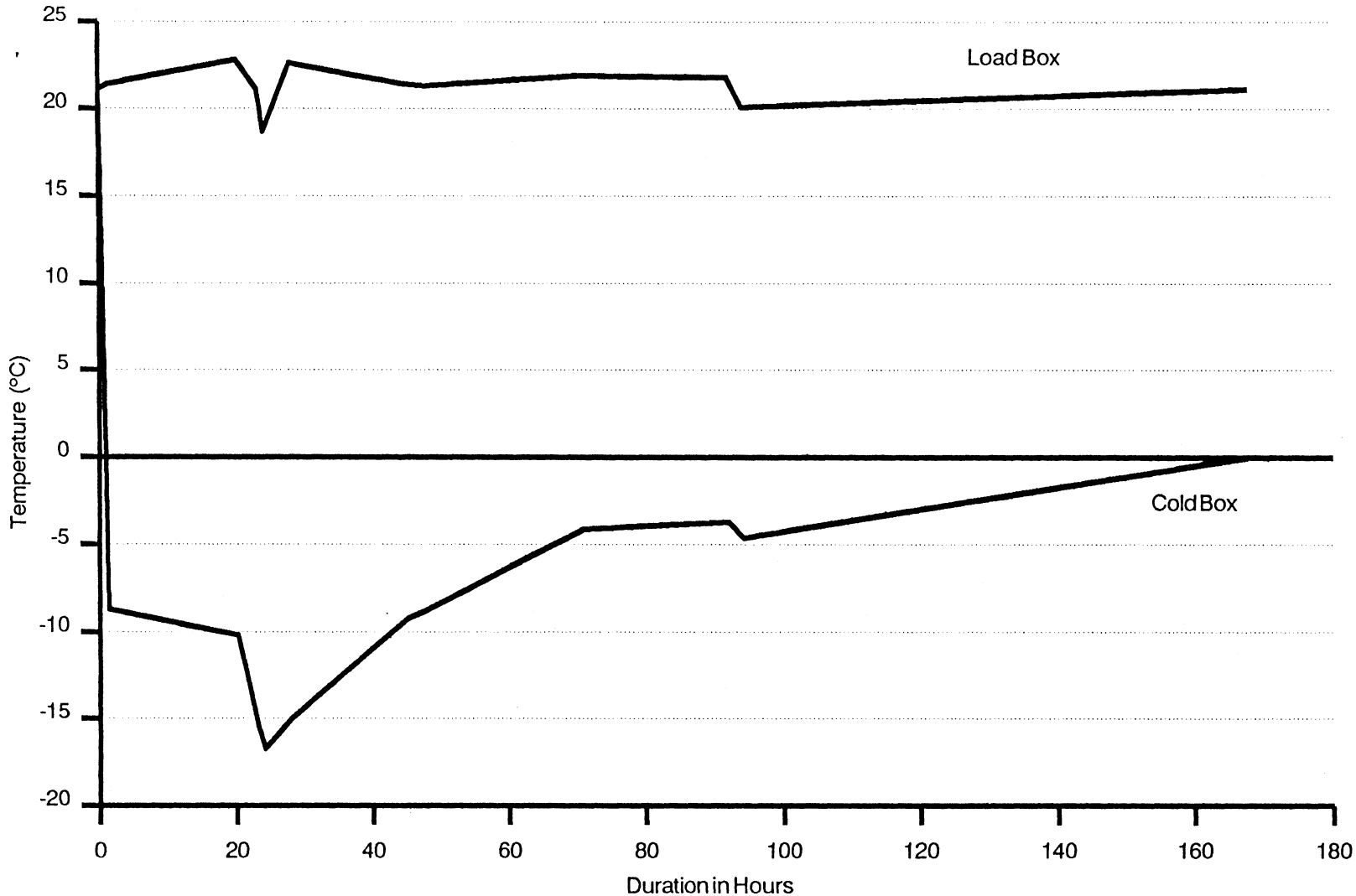

FIGURE 3.15 Temperatures Recorded in Load Box and Cold Box Over Duration of Test - Specimen 1A

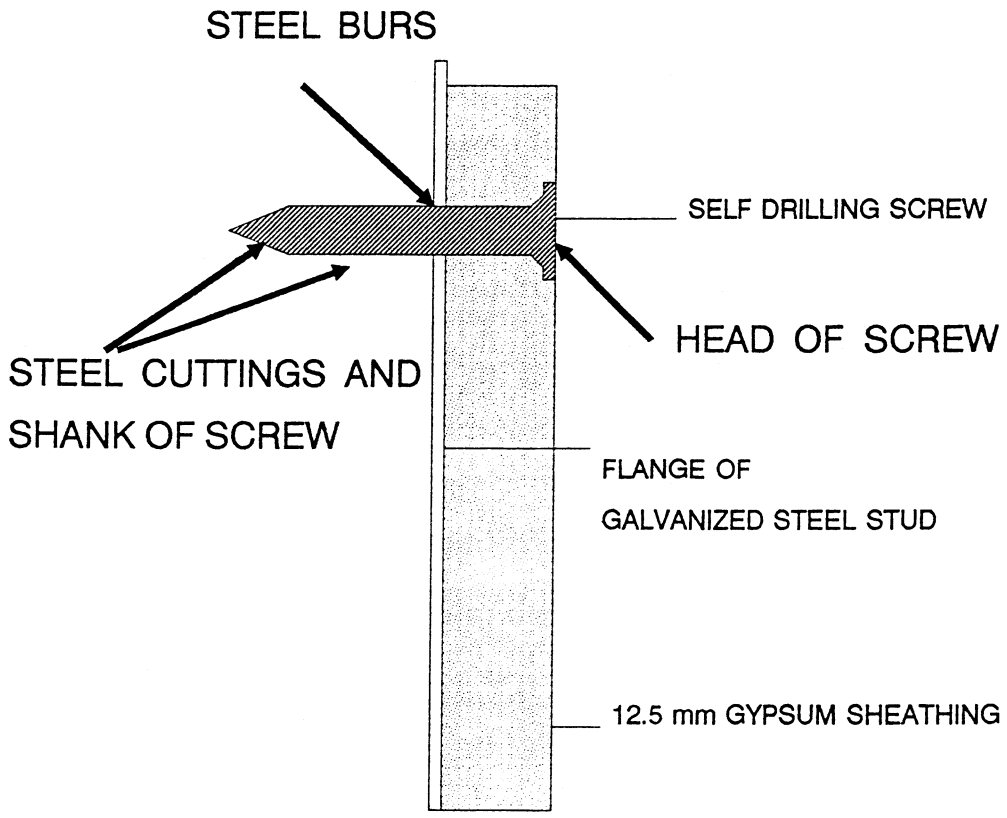

Note: Highlighted Areas Refer to Location of Corrosion

FIGURE 3.16 Schematic Showing Location of Noted Corrosion Products

of the fastener which protruded into the stud channel; on cuttings at the fastener tip; and also on the head of the fastener exposed to the cavity. Corrosion was also present on the "bugled" steel burs formed during self-drilling by the screw fastener.

3.4.2 Wall Specimen 1B

3.4.2.1 Thermal Performance Test

The thermal behaviour of Wall Specimen 1B was obtained over a period of 11 days. The data obtained was divided into 8 sequential groups representing 8 days. From each group, 10 sets of steady state temperature profiles were chosen and are listed in Appendix B, Table B2, for each of the thermal profiles monitored. Three of the profiles, Stud A, INS and Stud B, were in the standard configuration at each material interface at mid wall height (Figure 3.17 (a)). The fourth profile, AIB was in the plane of the wall at the interior face of the exterior gypsum board sheathing (Figure 3.17 (b)). The three through-the-wall profiles were measured with six thermocouples while the in plane profile was measured with nine thermocouples, three of which were common with the three perpendicular profiles. Average α_X values for the entire set of data is presented in Table 3.6. Figure 3.18 and 3.19 represent the calculated temperature profiles for each of the four profiles as obtained from the overall average α_X values.

3.4.2.2 Moisture Accumulation Test

The test for moisture accumulation in Wall Specimen 1B was performed over a period of 11 days. The conditions under which the test was run were as follows:

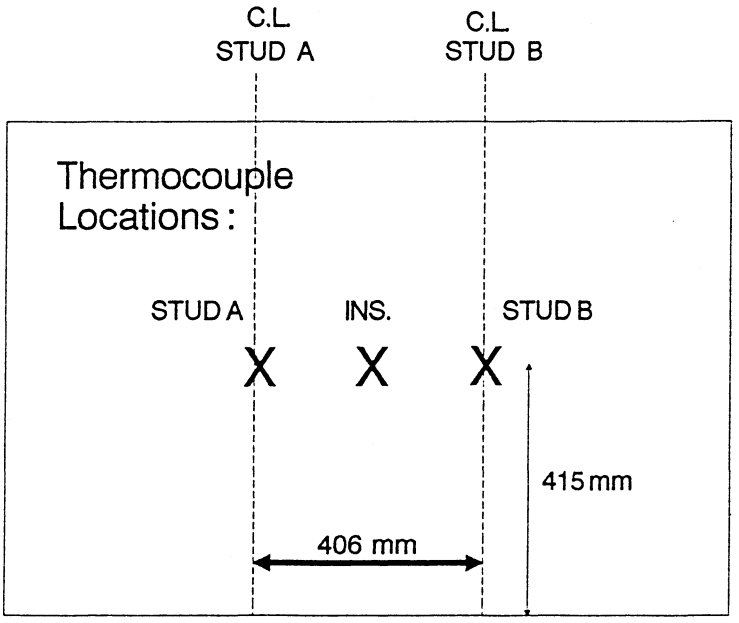

(a) Elevation Showing Thermocouple Locations for Through-the-Wall Profiles

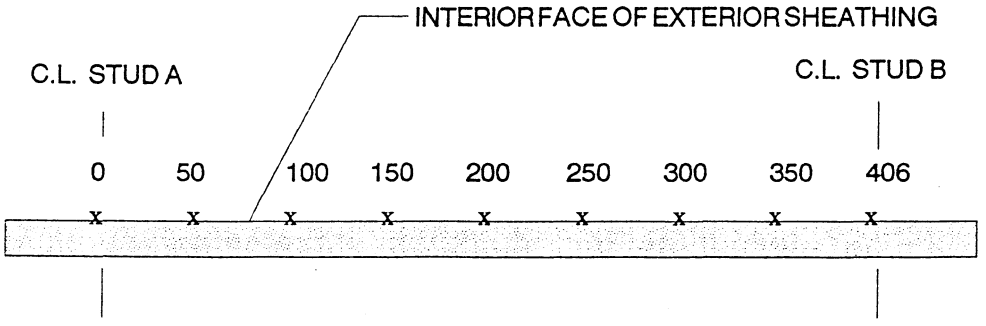

(b) Horizontal Section Showing Locations of Thermocouples for Lateral Profile

FIGURE 3.17 Thermocouple Locations - Specimen 1B

TABLE 3.6

α_x Values for Specimen 1B[1]

	Location[2] for through-the-wall profiles					
Name	I A	A/G	G/S,I	S,I/G	G/A	E A
STUD A	1	0.904	0.718	0.460	0.089	0
STUD B	1	0.899	0.647	0.426	0.127	0
INS	1	0.982	0.939	0.093	0.030	0

	mm From Stud A[3] for in plane profile								
Name	0	50	100	150	203	250	300	350	406
AIB	0.443	0.128	0.114	0.094	0.094	0.098	0.098	0.159	0.426

[1] average of eighty samples

[2] I A : Interior Air
A/G : interior Air / Gypsum board
G/S,I : Gypsum board / Stud or Insulation
S,I/G : Stud or Insulation / Gypsum board
G/A : Gypsum board / exterior Air
E A : Exterior Air

[3] at interior face of exterior sheathing

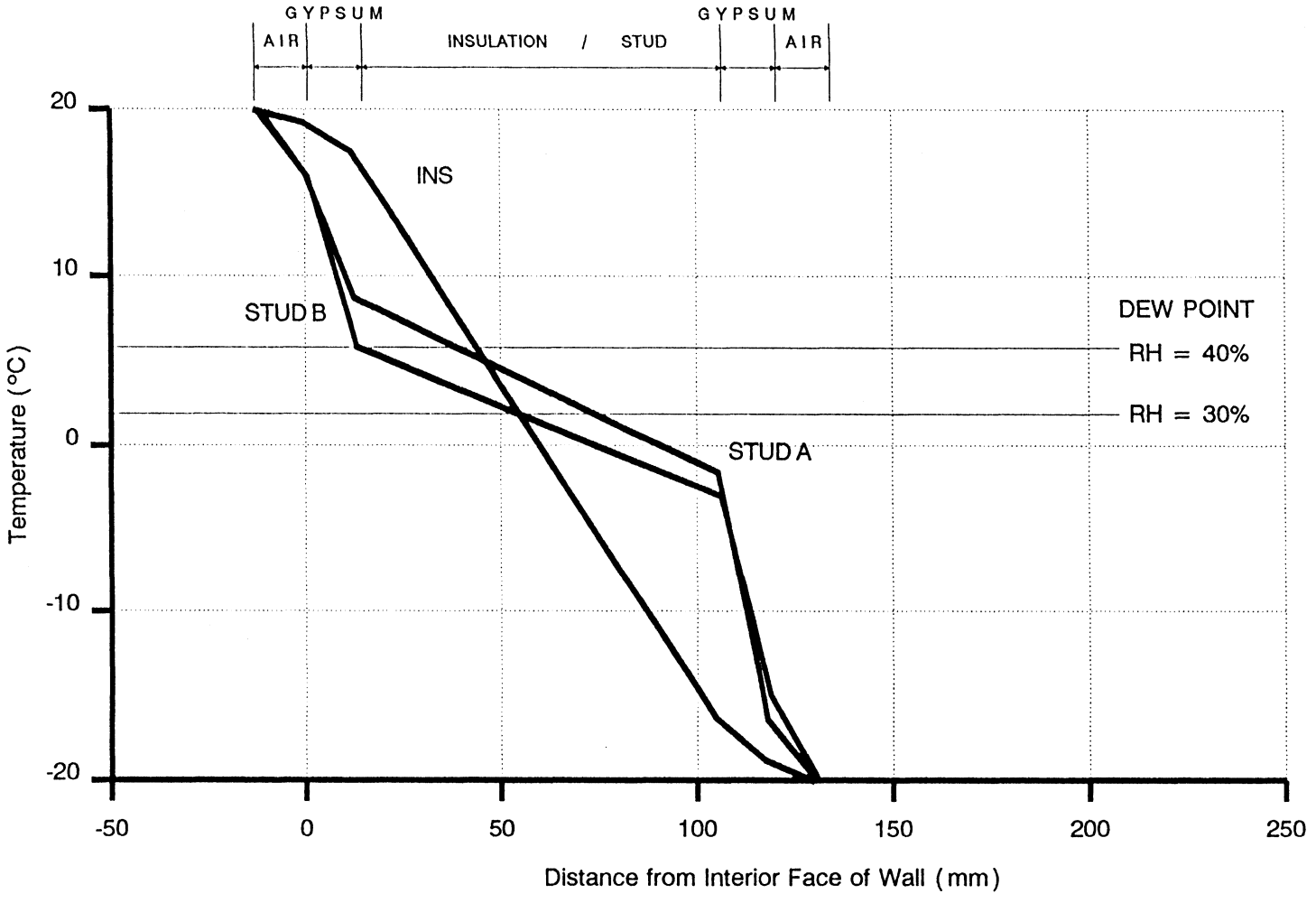

FIGURE 3.18 Through-the-Wall Thermal Profiles at Stud A, Stud B and Ins for Specimen 1B

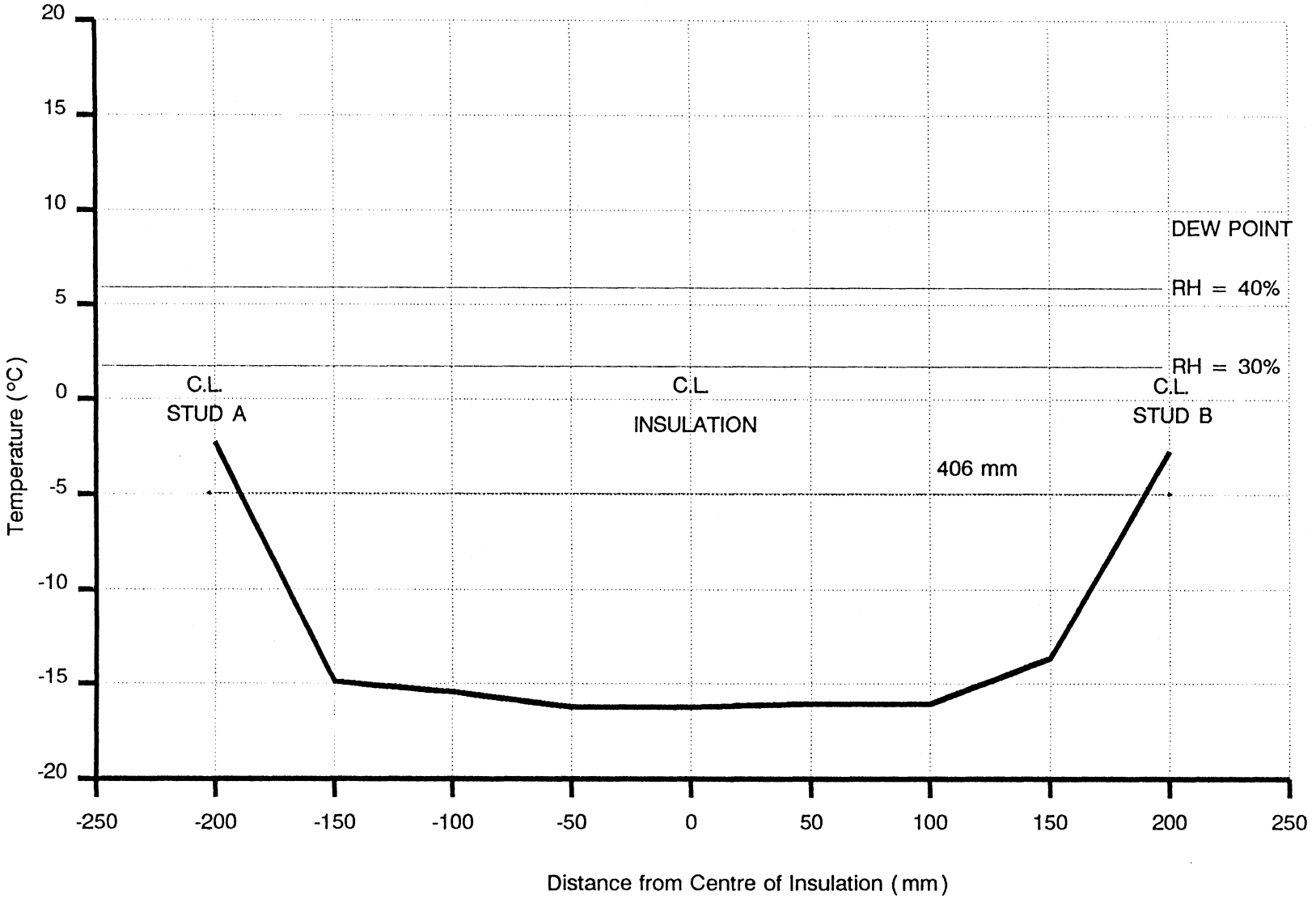

FIGURE 3.19 In-Plane Thermal Profile at Interior Face of Exterior Sheathing for Specimen 1B

- air flow through the wall at a rate of 0.15 L/s.m^2
- temperature gradient of +21 to -20° C
- interior humidity level of 40% RH

The intended air barrier in this specimen was the exterior gypsum board. To this end, the perimeter and all joints were sealed with silicone and/or tape. As noted in Section 3.3.2, the exterior gypsum board was constructed with three panels spanning from Stud A to Stud B as well as two side panels.

Since the exterior gypsum board was the intended air barrier, a rather large leakage path on the vertical perimeter of the interior gypsum board closest to Stud A was permitted by not applying sealant. The resulting opening was about 800 mm long (full height) and 2 mm wide. After running the test for 11 days under the above conditions, weight gain in the gypsum panels was recorded as 6, 16, 41 and 109 grams for panel number 2 to 5 respectively (see Figure 3.4). This gain in weight was a result of moisture gain from condensation. Figure 3.20 is a sketch which displays the pattern of moisture accumulation on the interior face of panel 5. At the top of the panel, moisture condensation was observed right across the board. Going down from the top, the condensation pattern is funnel shaped and becomes a vertical line which tapers out before reaching the bottom. This vertical line corresponds exactly with a vertical fold or crease in the outer layers of the batt insulation.

There was no noticeable weight gain in the batt insulation. However, as was the case with Wall Specimen 1A, corrosion was present on the fasteners attaching the exterior gypsum board to the steel stud as well as on the burs around the fastener hole in the stud.

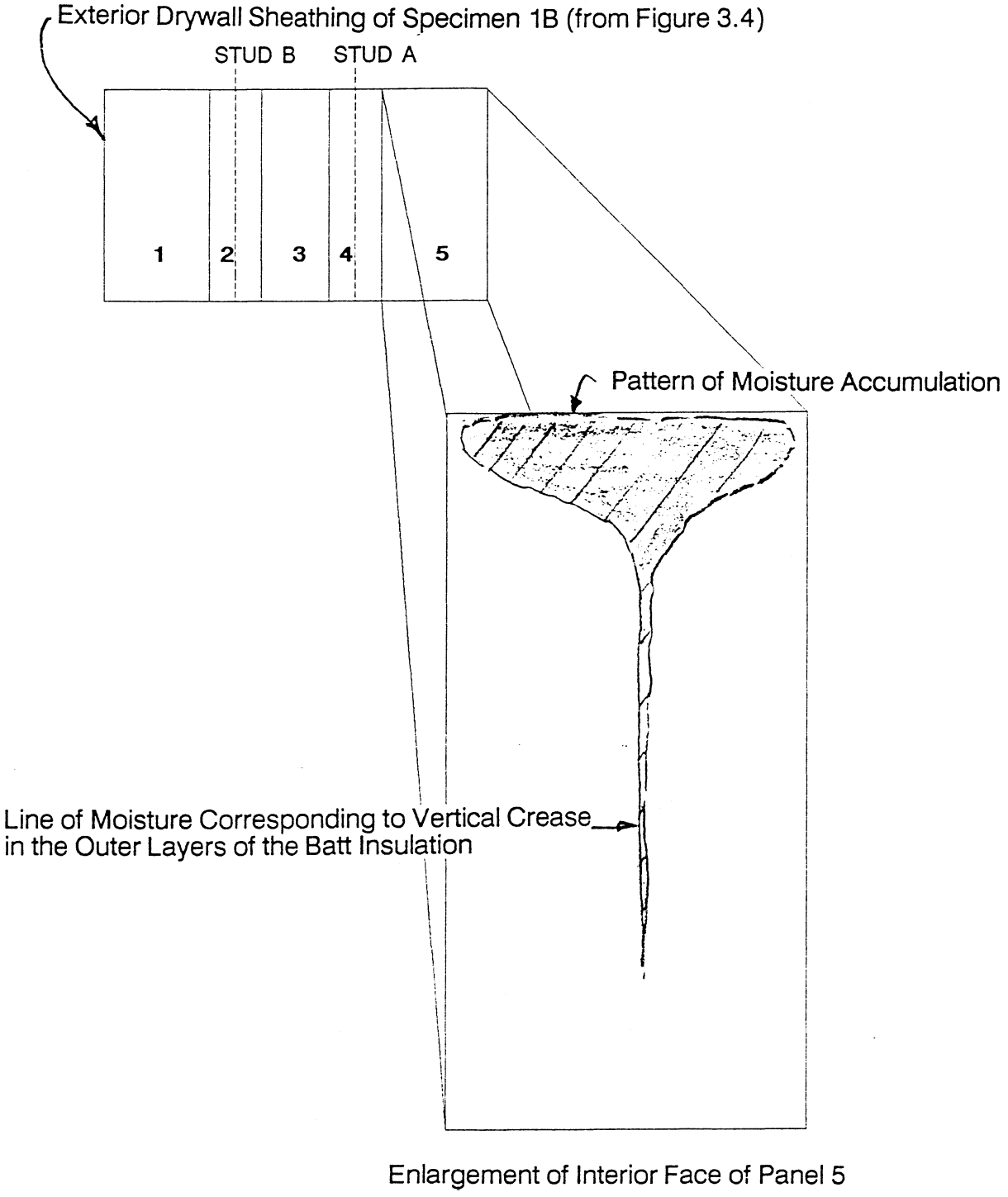

FIGURE 3.20 Pattern of Moisture Accumulation on Panel 5 - Specimen 1B

3.4.3 Wall Specimen 2A

3.4.3.1 Thermal Test

Two types of thermal tests were performed on Wall Specimen 2A as follows:

- general thermal performance
- localized thermal bridging effects.

General Thermal Performance: The locations of thermocouples in Specimen 2A were identical to the system used in Wall Specimen 1A shown in Figure 3.13. With this arrangement, six thermal profiles were monitored. After analyzing the data in a manner similar to that described under Section 3.2.3, average α_X values were obtained for each profile location from six sets of values representing steady state conditions. The measured temperatures are listed in Table B3 of Appendix B. Average α_X values are given in Table 3.7.

The thermal profiles obtained from these average α_X values are provided for comparison purposes in Figures 3.21(a), (b) and (c) representing the profiles at the centerline of Stud A, Stud B and INS,the batt insulation, respectively.

Localized Thermal Bridging Effects:

In an additional test, by rearranging some of the thermocouples, bridging effects in the vicinity of brick ties were studied primarily at the exterior flange of the steel studs. In this test, Stud A and Stud B were monitored at two locations, both of which corresponded with a brick tie (See Figure 3.22). The polystyrene was attached to Stud A with heavy gauge

TABLE 3.7

α_x Values for Specimen 2A[1]

Name	Location[2] I A	A/G	G/S,I	S,I/P	P/A	C A	A/B	B/A	E A
AT	1	0.944	0.824	0.646	0.317	0.163	0.117	0.017	0
BT	1	0.940	0.847	0.703	0.216	0.163	0.129	0.041	0
IT	1	1.000	0.970	0.432	0.168	0.163	0.105	0.030	
AB	1	0.916	0.805	0.628	0.299	0.123	0.099	0.012	0
BB	1	0.937	0.860	0.684	0.172	0.123	0.084	0.019	0
IB	1	1.000	0.996	0.431	0.133	0.123	0.066	0.008	0

[1] average of six samples

[2] I A : Interior Air
A/G : interior Air / Gypsum board
G/S,I : Gypsum board / Stud or Insulation
S,I/P : Stud or Insulation / Polystyrene board
P/A : Polystyrene board / cavity Air
A/B : cavity Air / Brick
B/A : Brick / exterior Air
E A : Exterior Air

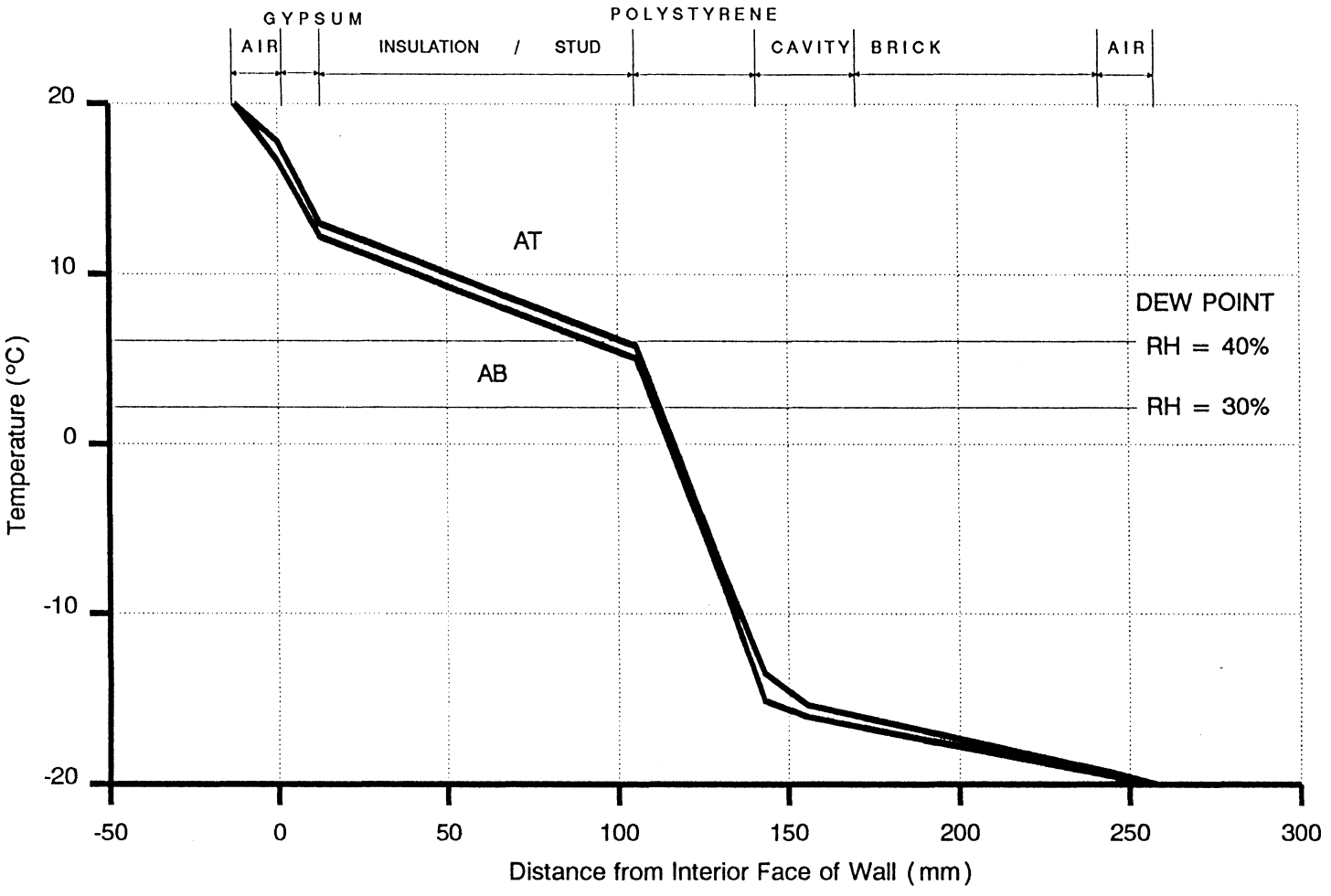

FIGURE 3.21(a) Through-the-Wall Thermal Profiles at Stud A of Specimen 2A

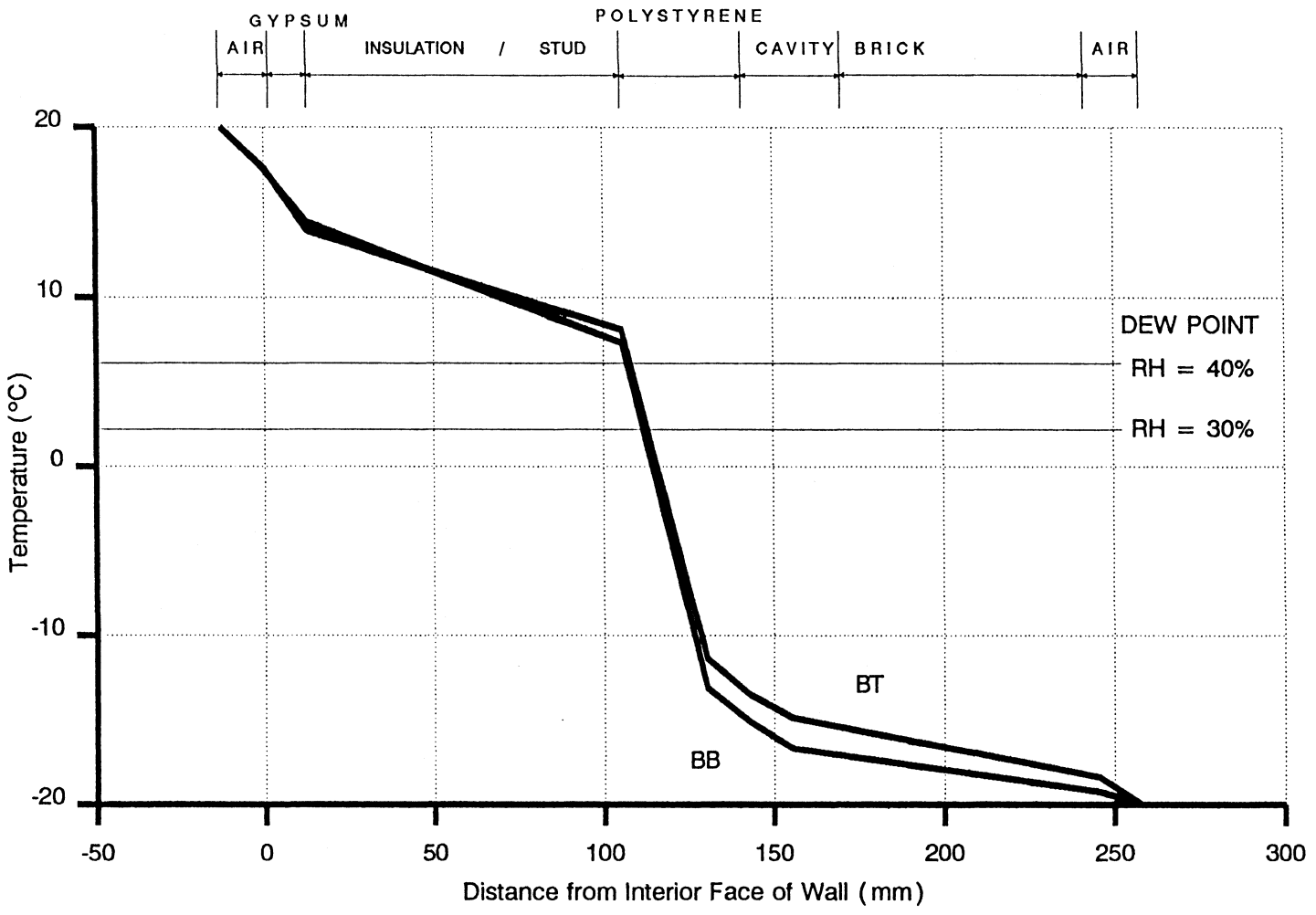

FIGURE 3.21(b) Through-the-Wall Thermal Profiles at Stud B of Specimen 2A

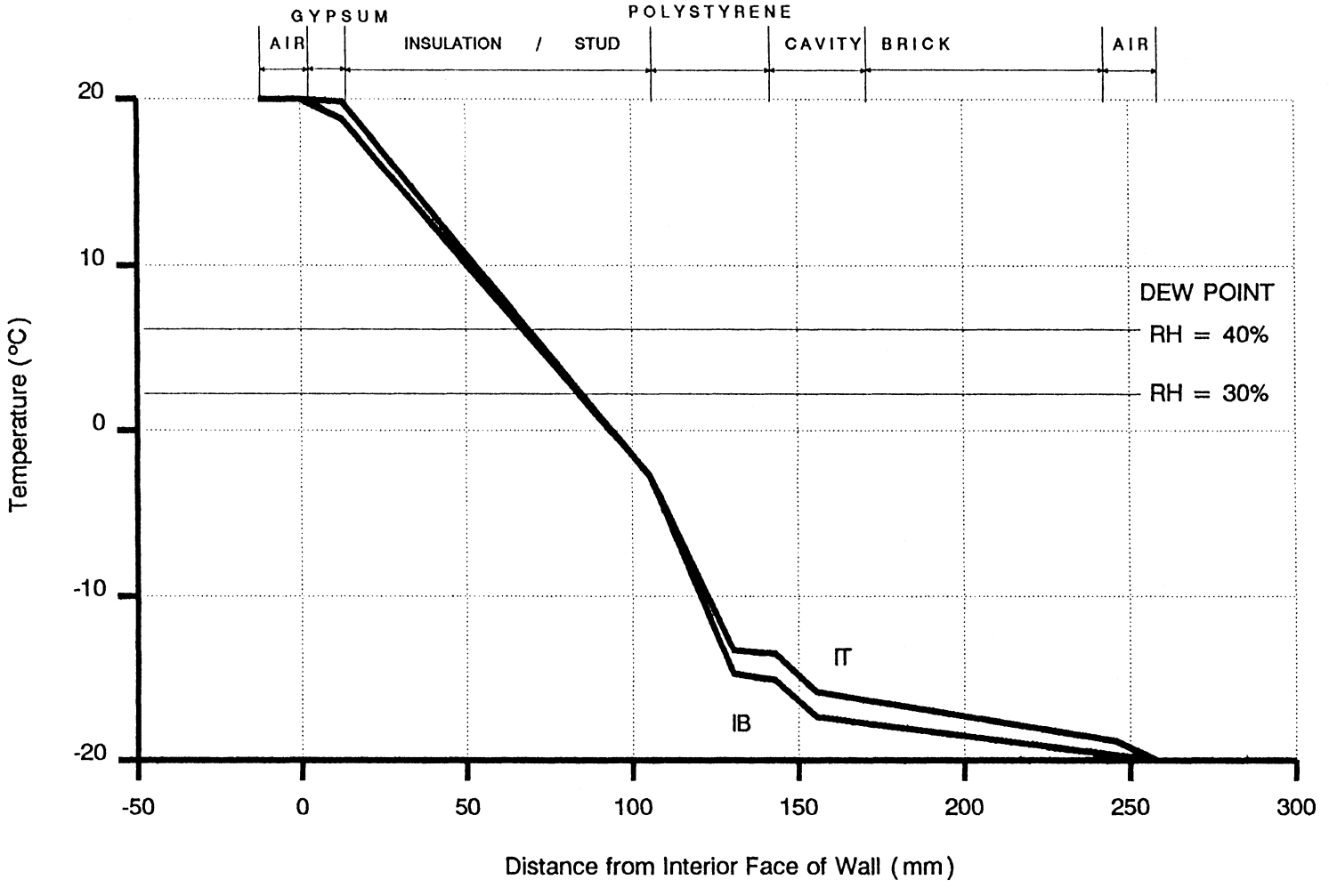

FIGURE 3.21(c) Through-the-Wall Thermal Profiles at Insulation Centre Line of Specimen 2A

screws and large, heavy gauge washers. In contrast, Stud B had less steel bridging through the polystyrene. In this case stick or pin connectors and lighter brick ties were used. Stud B was altered for this test by attachment of a 14 gauge Bailey tie at the lower tie location. This 'heavy' tie was used as a contrast to the almost minimum amount of steel at the upper tie location on Stud B.

Extra thermal measurements were taken on Stud A at the lower tie location shown in Figure 3.22. The upper tie location and the two Stud B tie locations were monitored as described earlier.

Table 3.8 contains a summary of the average α_x values obtained for this test while the actual measured results are listed in Table B5 of Appendix B. Figure 3.23(a) and 3.23(b) provide data for comparing the thermal response of the two monitored locations on Studs A and B respectively. In Figure 3.23(a), a range of temperatures is indicated which represents the range of localized thermal bridging on the exterior face of the stud. In this test, a maximum difference of $4^{\circ}C$ occurred between the measured points indicated in Figure 3.22.

3.4.3.2 Moisture Accumulation

Part 1: Part 1 of the moisture accumulation test on Wall Specimen 2A covered a period of 13 days. Conditions of the test were essentially the same as for Wall Specimen 1A, Section 3.4.1.3. A net pressure differential of 75 Pa was maintained across the wall which caused an air flow rate of 0.011 L/sm^2 through the wall. In this test the air barrier was the interior gypsum board and the leakage path in the air barrier was a 12 mm crack similar to that of Wall Specimen 1A. The interior relative humidity was

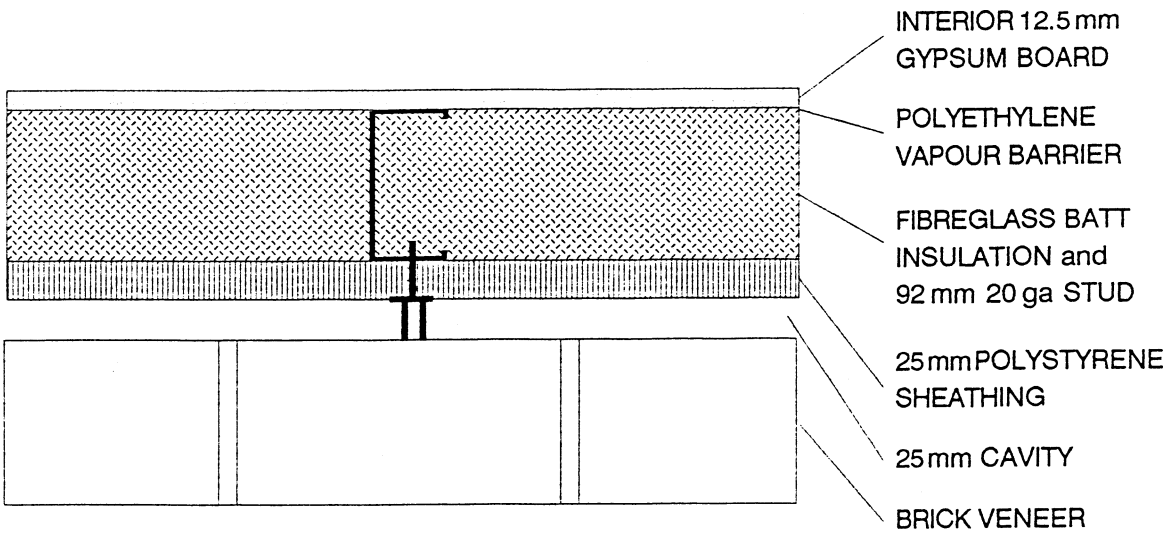

a) Wall Section - Horizontal

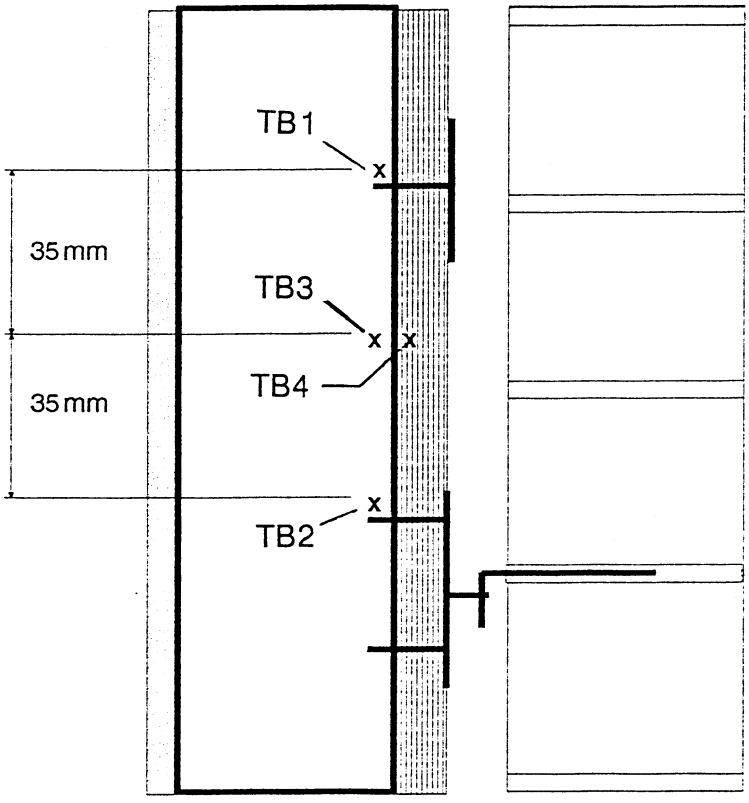

b) Wall Section - Vertical

.FIGURE 3.22 Location of Thermocouples in Thermal Bridging Test of Specimen 2A

TABLE 3.8

α_x Values for Specimen 2A[1], Thermal Bridging

	Location[2] for through-the-wall profiles						
Name	I A	A/G	G/S	S/P	P/A	A/B	B/A	E A
AT	1	0.938	0.825	0.643	0.339	0.153	0.030	0
AB	1	0.932	0.842	0.638	0.326	0.133	0.013	0
BT	1	0.949	0.853	0.702	0.233	0.167	0.036	0
BB	1	0.945	0.828	0.679	0.249	0.171	0.020	0

	Location[3] for thermal bridge measurements			
Name	TB1	TB2	TB3	TB4
TB	0.680	0.743	0.667	0.648

1 average of eleven samples

2
- I A : Interior Air
- A/G : interior Air / Gypsum board
- G/S : Gypsum board / Stud
- S/P : Stud / Polystyrene board
- P/A : Polystyrene board / cavity Air
- A/B : cavity Air / Brick
- B/A : Brick / exterior Air
- E A : Exterior Air

3 see Figure 3.22 for location on stud

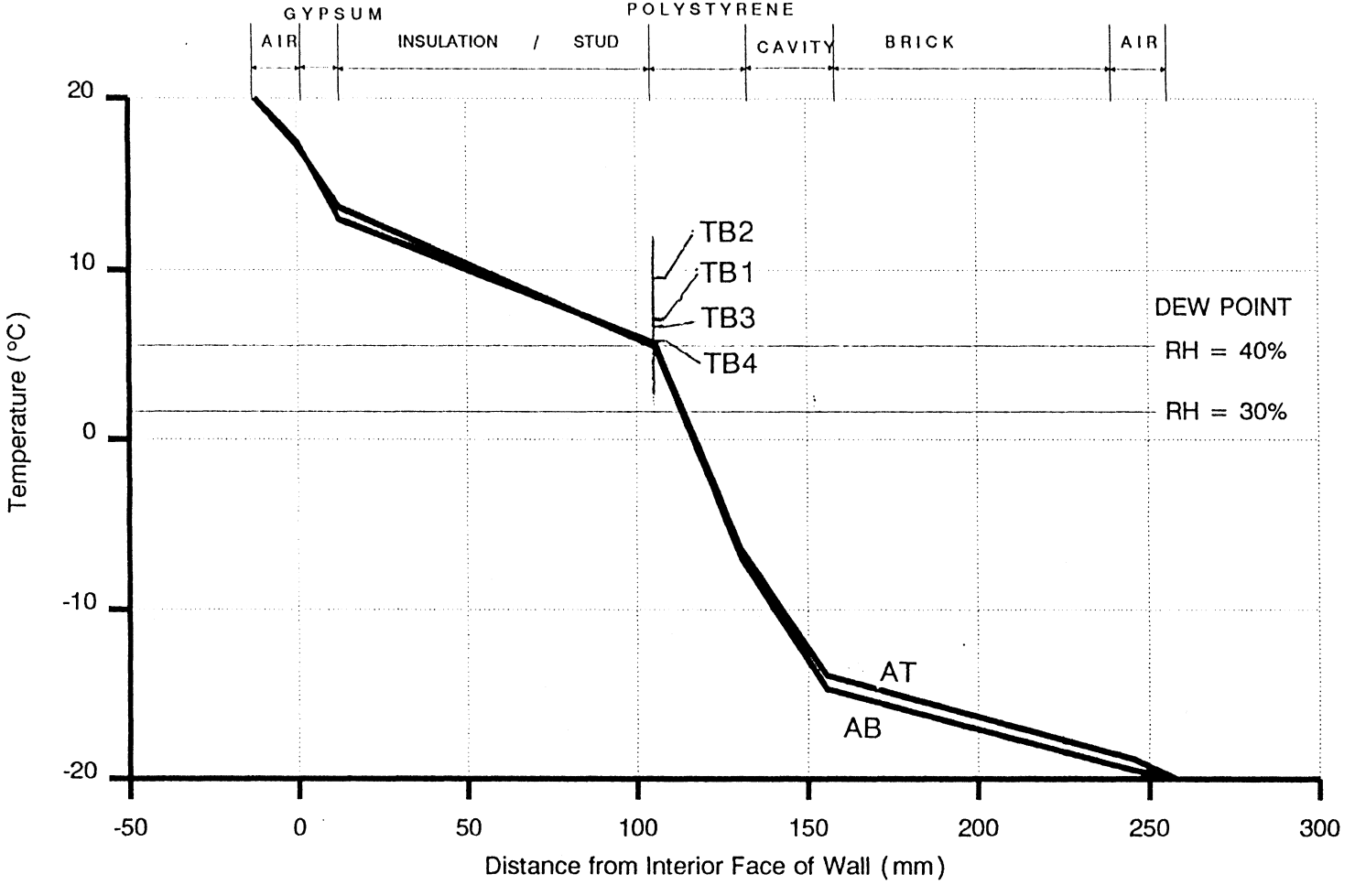

FIGURE 3.23(a) Through-the-Wall Thermal Profiles at Stud A in Thermal Bridging Test of Specimen 2A

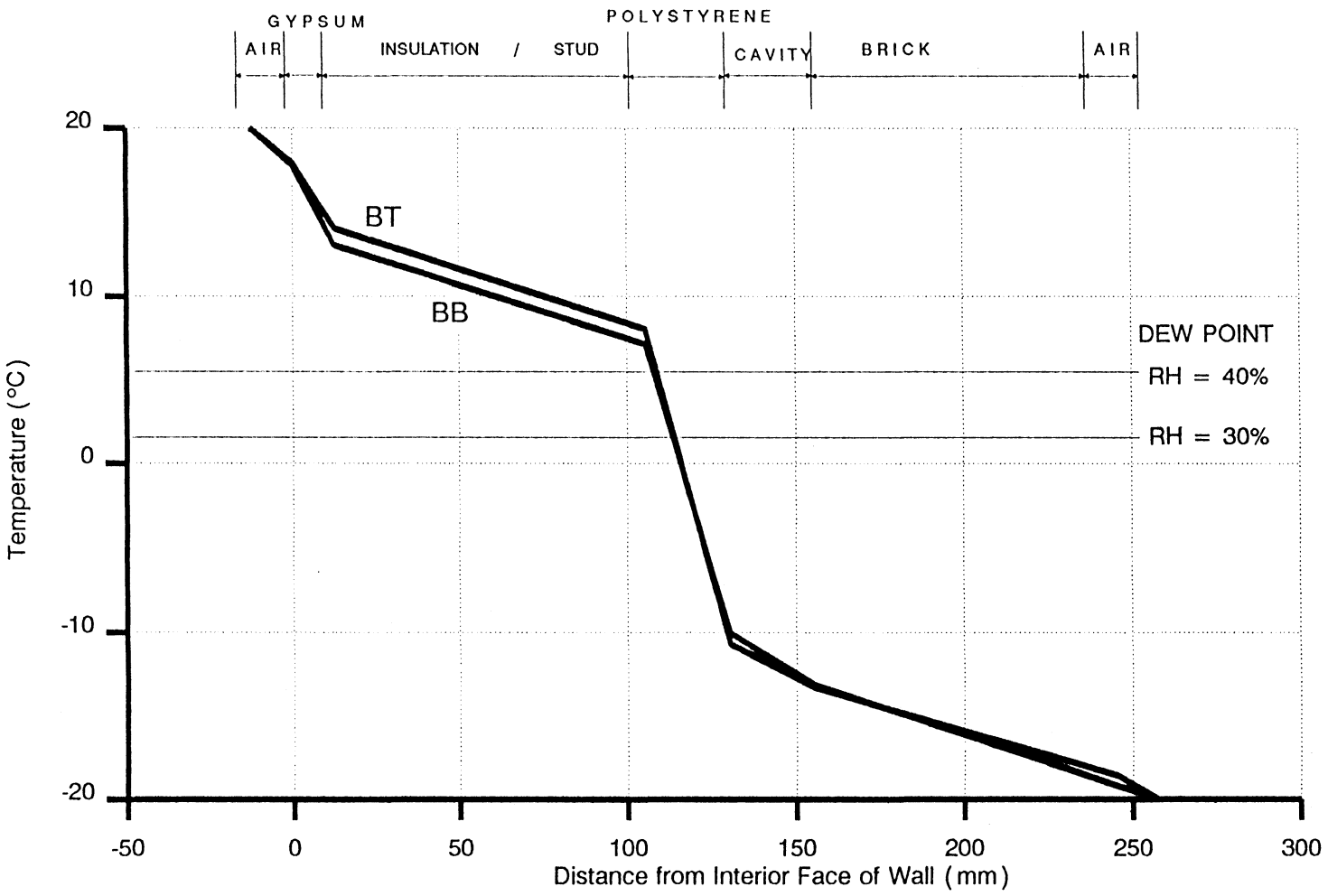

FIGURE 3.23(b) Through-the-Wall Thermal Profiles at Stud B in Thermal Bridging Test of Specimen 2A

maintained at 35 - 40% and the net temperature gradient was 21 ± 2°C to a minimum of -17°C.

The wall was dismantled from the inside after 7 days and again after 13 days. In neither case were there any signs of moisture having accumulated.

Part 2: In Part 2 the method for measuring the flow rate through the wall was changed. In Part 1 the Load Box was pressurized to 75 Pa and the flow through the wall was determined as the flow into the Load Box minus the apparatus leakage. This latter value was determined by sealing off the wall with a plastic sheet and measuring the flow rate with a 75 Pa pressure difference. This gave the net flow through the opening in the drywall into the wall system. Although this method realistically simulated the interior pressure, some difficulty was encountered in obtaining an accurate apparatus leakage value.

To overcome the above problem, a new method was developed. In this method the flow meter was placed inside the Load Box with the inlet open to the Load Box environment and the outlet connected by tubing to a hole in the drywall (Figure 3.24). With all other paths through the wall sealed, the only air flow through the wall had to first go through the flow meter. A direct reading of air flow through the wall was then possible. In Part 2, the Load Box was pressurized to 200 Pa to obtain a flow rate of .007 L/sm^2 through the wall. This value is much less than the 0.05 L/sm^2 discussed in Section 1.2.3.3. A portion of the 200 Pa pressure was required to offset the pressure drop incurred across the flow meter and tubing.

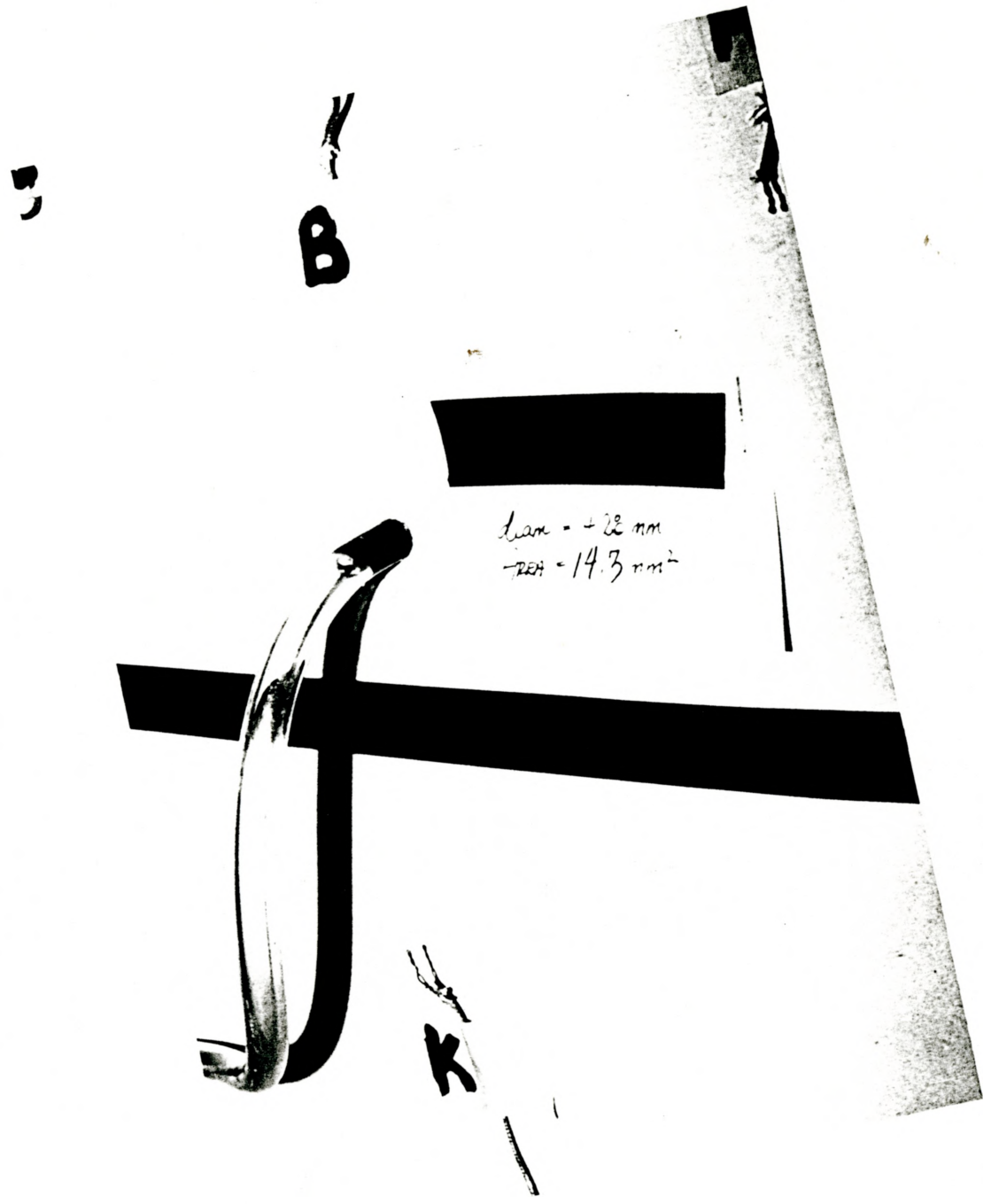

FIGURE 3.24 Photo Showing Tubing Used to Introduce Controlled Air Leakage into the Wall - Specimen 2A

Since the only difference between Part 1 and Part 2 was the air flow rate, accumulation of moisture was not expected to occur. This was indeed the case.

Part 3: Knowing the performance of the wall system under average conditions from Parts 1 and 2, in Part 3 it was decided to subject the wall to a more severe environment. For this reason, the RH in Part 3 was increased to 50-55% from 35 -40%. All other environmental factors were kept the same with a net pressure differential sufficient to cause a flow of 0.007 L/sm^2 through the flow meter and thus through the wall and a temperature difference of $+21^{\circ}C$ on the interior to a minimum of $-17^{\circ}C$ in the Cold Box.

After the test was run for 7 days, the wall was dismantled again from the inside by removing the interior drywall, vapour barrier and batt insulation. In Figure 3.25, the photograph of the interior face of the exterior rigid insulation sheathing shows a dashed line which outlines the boundary of the zone of moisture accumulation which occurred at this plane in the wall system during Part 3 of the test. Within the dashed outline, condensation had formed and the board was essentially covered with water droplets like dew. There was no evidence of any moisture accumulation on the steel stud.

Part 4: At this point in the test program the chest freezer/dry ice cooling combination was replaced with a new mechanical cooling system. This new system was capable of maintaining $-20^{\circ}C$ and incorporated programmable evaporator coil defrost cycles.

FIGURE 3.25 Photo Showing Pattern of Moisture Accumulation (Moisture Formed inside Dashed Line away from Studs) - Specimen 2A

Part 4 was performed with this new cooling system. For this test the main concern was to investigate the effect of workmanship in the installation of the rigid insulation by simulating a 3 mm gap at a joint between insulation boards. This was accomplished by simply cutting a 3 mm wide slot, extending horizontally from Stud A to Stud B at the joint between boards.

The test was run under the same conditions as Part 3 except that the exterior temperature was maintained continuously at about -21°C save for 20 minute defrost cycles every 6 hours. After 4 days the wall was dismantled. At this time the batt insulation was frozen to the polystyrene board in the same area that was found moist in Part 3. After the batt was allowed to warm up a little, it was noted that moisture could be felt on the exterior batt face to a depth of approximately 12 mm. The slot cut into the polystyrene was frosted shut (Figure 3.26) along with the two upper vent holes in the brick veneer (Figure 3.27). The two lower weep holes in the veneer had no signs of frost.

As was the case in Part 3, there was no sign of moisture accumulation on the studs. However, upon melting of the frost, water flowed down the interior face of the polystyrene board to the bottom track. In this test, the track lip was not in contact with the polystyrene (manufactured with an inward bend) and the moisture ran between the track and the board.

3.4.4 Wall Specimen 2B

3.4.4.1 Air Leakage Test

Air leakage testing of Specimen 2B was performed without the exterior polystyrene sheathing and without any batt insulation in the stud

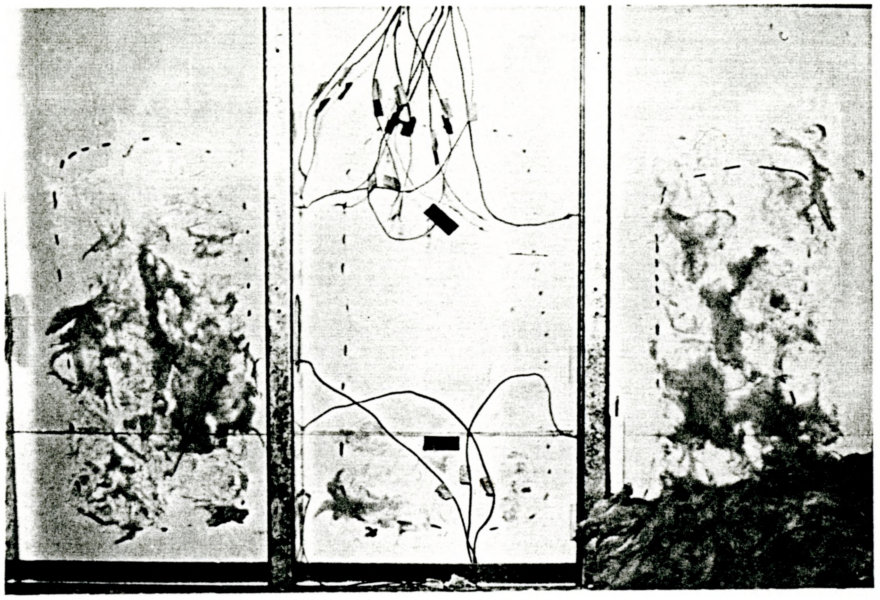

FIGURE 3.26 Photo Showing Frost Accumulation in Opening in Polystyrene Sheathing

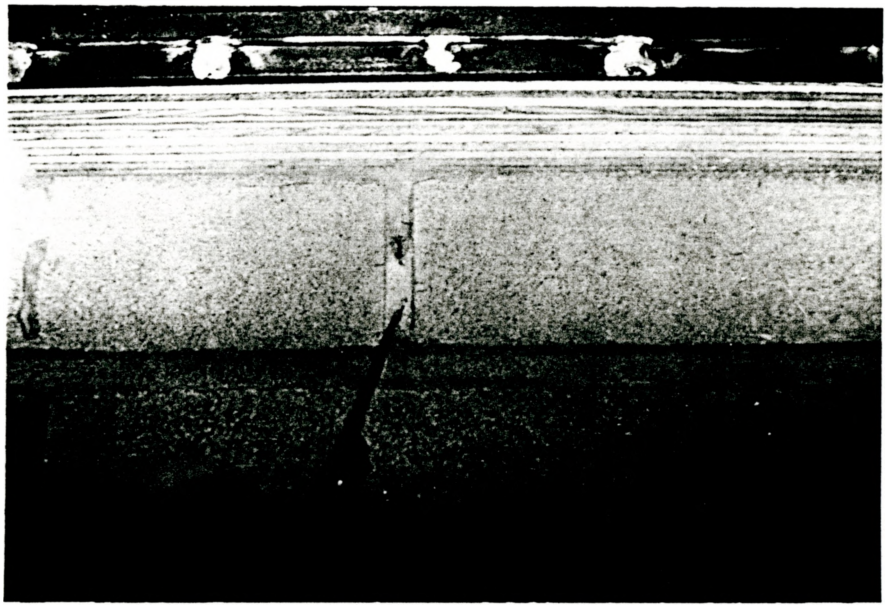

FIGURE 3.27 Photo Showing Frost Accumulation in Veneer Vent Hole

space. Both of these elements were not intended to function as air barriers and were thus omitted for testing convenience.

Twelve different specimen configurations (See Table 3.9) which can be divided into tests on unpainted gypsum board and painted gypsum board with various holes were tested. The results obtained are listed in Table 3.10. In all of these tests the interior gypsum board was the intended air barrier. Testing was conducted up to about 100 Pa pressure difference across the specimen. Figures 3.28(a), (b) and (c) contain the plotted test results.

In Figure 3.28(a), the results from Tests 1 and 6 are plotted. Test 1 was intended as a calibration test and as such an extra sheet of polyethylene was taped over the unpainted drywall interior to prevent flow through the wall. Test 6 represents the results after the drywall was painted but with the extra polyethylene sheet and the polyethylene vapour barrier removed. The resulting leakage rates for the two tests were essentially the same indicating that proper sealing and painting of the drywall produces a very good air barrier. A regression curve obtained from these two sets of data is also plotted in Figure 3.28(a). The equation for this curve was used to remove apparatus leakage from the remaining results.

In Figure 3.28(b), the results from Tests 2 to 5 are plotted - all of which were conducted with unpainted gypsum board. In tests 2 and 3, the air flow rate was plotted for the case of unsealed and sealed gypsum board screw heads. Test 4 was conducted to investigate the effect of a 12.5 mm slit in the polyethylene vapour barrier since it was noticed that the polyethylene billowed out between studs in tests 2 and 3 and was thus acting as an air

TABLE 3.9

Air Leakage Test Configurations, Specimen 2B

Test No	Gypsum Board	Polyethylene
1	sealed; unpainted	intact
2	screw heads exposed; unpainted	intact
3	screw heads sealed; unpainted	intact
4	screw heads sealed; unpainted	12.5 mm slit
5	screw heads sealed; unpainted	removed
6	screw heads sealed; painted	removed
7	8 mm dia. hole; painted	intact
8	8 mm dia. hole; painted	8 mm dia. hole
9	sealed electrical box; painted	intact
10	sealed electrical box w/cable; painted	intact
11	"Vapour Proof" electrical box; painted	clipped to box
12	electrical box foamed-in-place; painted	intact

TABLE 3.10
Air Leakage Characteristics, Specimen 2B

Test	Pressure (Pa)	Flow (L/sm^2)
1	0	0
	28	0.0047
	48	0.0068
	61	0.0092
	79	0.0115
	98	0.0140
2	0	0.000
	11	0.003
	17	0.007
	26	0.010
	40	0.013
	54	0.017
	74	0.020
	93	0.023
3	0	0.000
	9	0.003
	17	0.007
	26	0.010
	41	0.013
	59	0.016
	75	0.020
	95	0.023
4	0	0.000
	17	0.007
	31	0.015
	41	0.019
	55	0.022
	76	0.026
5	0	0.000
	13	0.007
	19	0.011
	26	0.015
	33	0.020
	42	0.024
	50	0.029
	64	0.038
	84	0.049
	101	0.059
6	0	0
	33	0.005
	63	0.009
	98	0.014
7	0	0.000
	30	0.007
	60	0.009
	90	0.012
8	0	0.000
	6	0.044
	12	0.068
	20	0.090
	31	0.111
	44	0.132
	61	0.152
	76	0.163
	95	0.185
9	0	0.000
	16	0.050
	31	0.070
	56	0.088
	89	0.105
10	0	0.000
	19	0.075
	47	0.091
	67	0.111
	109	0.126
11	0	0.000
	4	0.083
	7	0.108
	20	0.157
	38	0.204
	63	0.249
	84	0.297
12	0	0.000
	32	-0.001
	42	0.000
	55	0.001
	73	0.000
	90	-0.001
	93	0.000

Note : Test 1 and 6 - gross flow ; all other tests net flow (i.e. apparatus leakage removed)

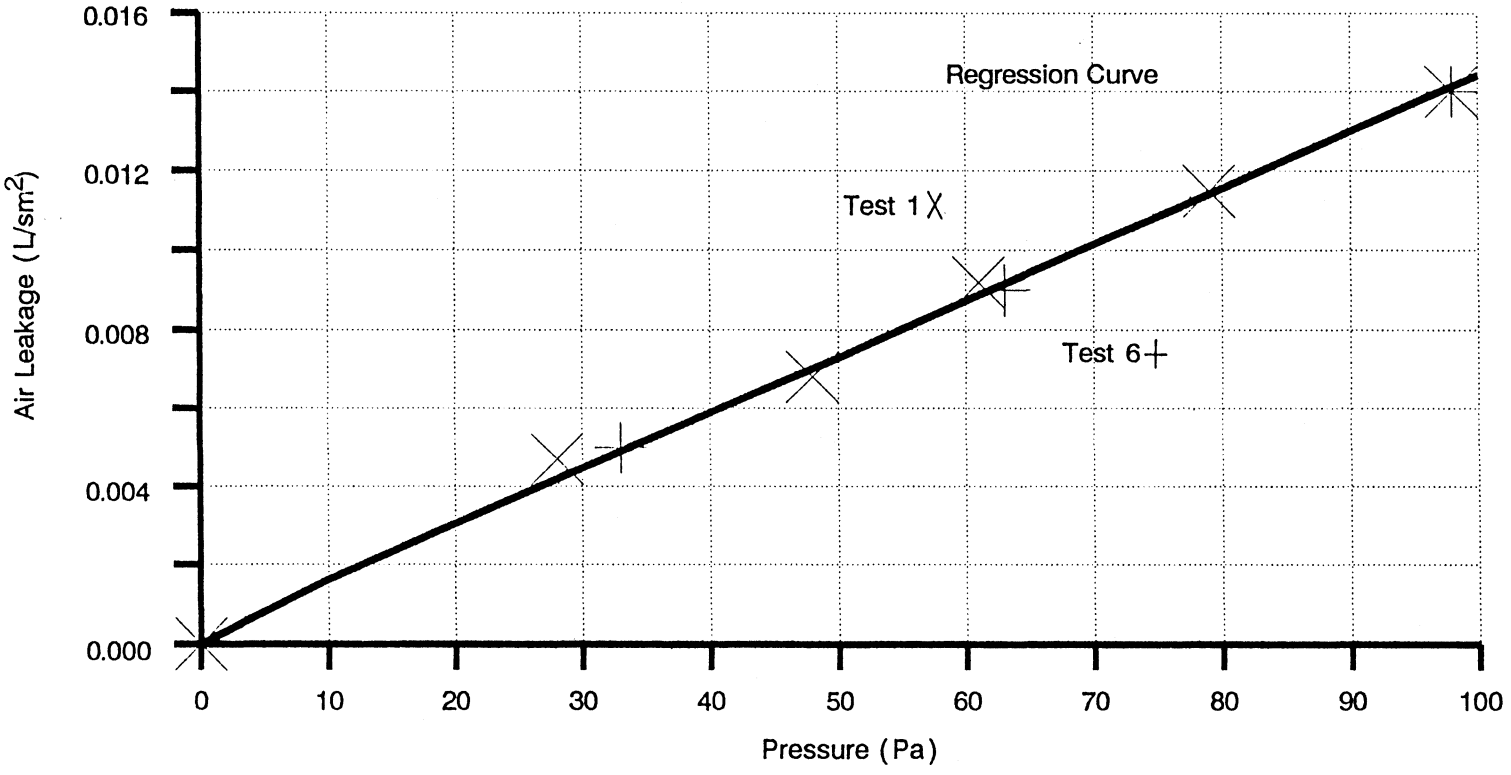

FIGURE 3.28(a) Specimen 2B Air Leakage Characteristics - Tests 1 and 6

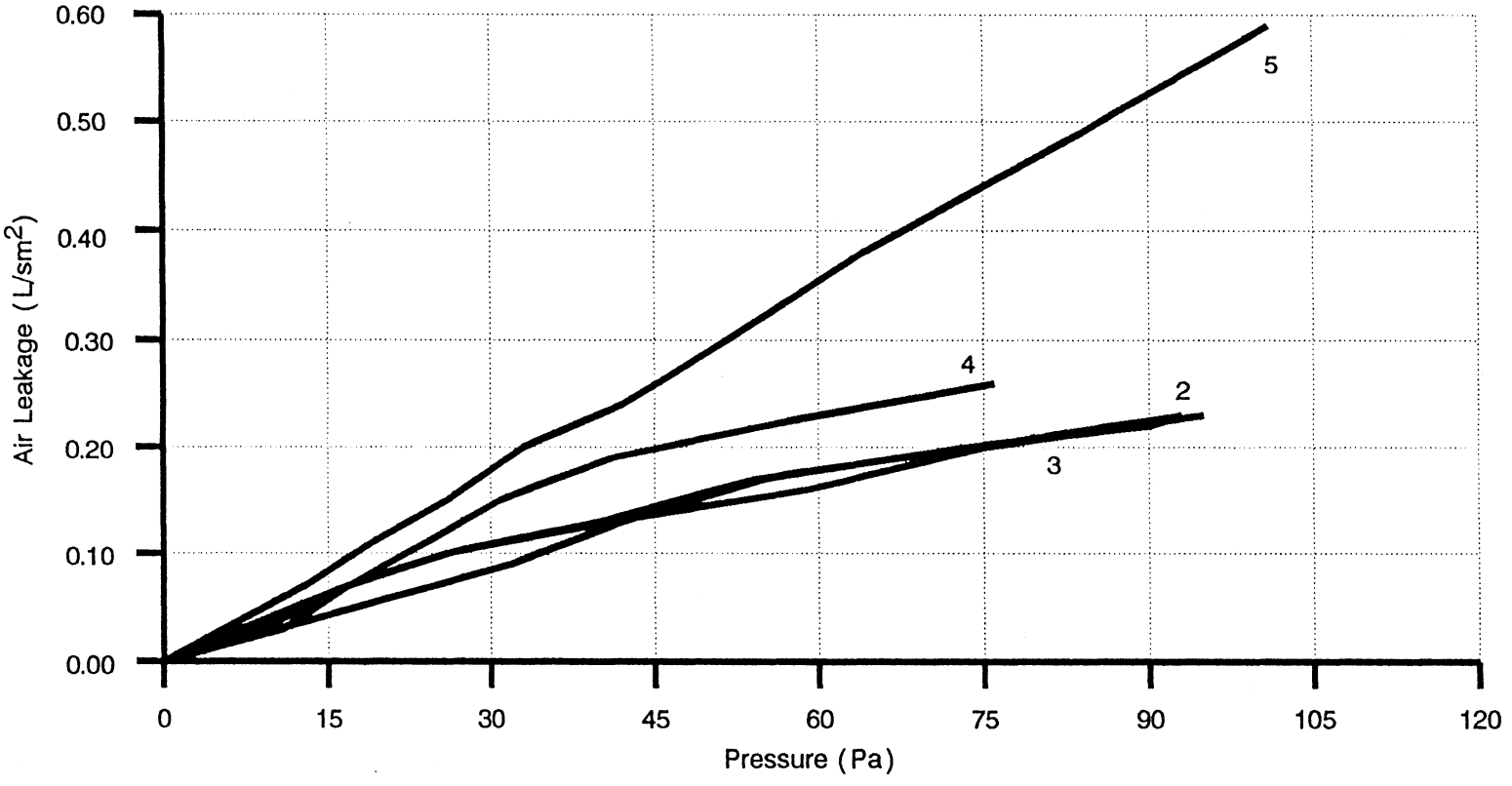

FIGURE 3.28(b) Specimen 2B Air Leakage Characteristics - Tests 2 to 5
(minus apparatus leakage)

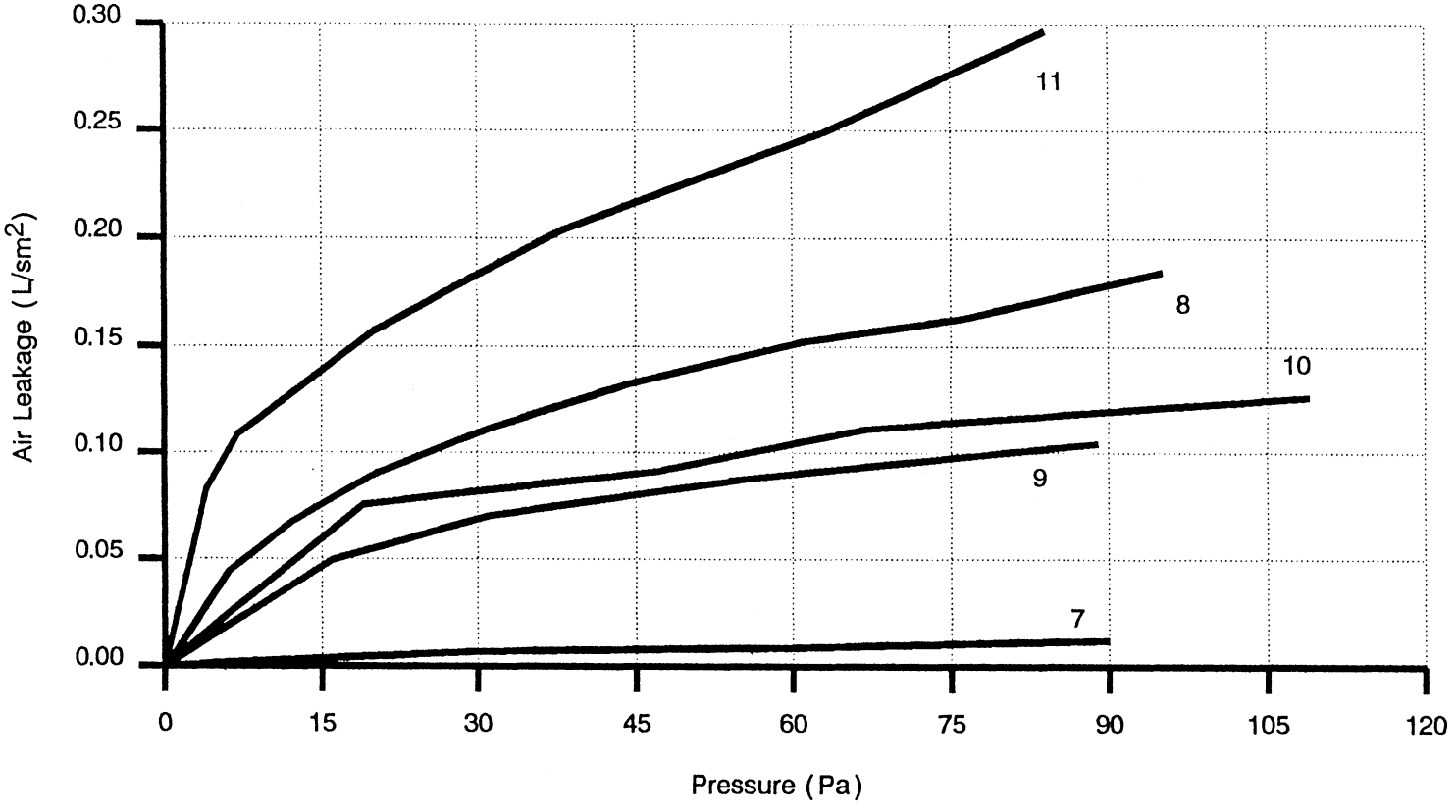

FIGURE 3.28(c) Specimen 2B Air Leakage Characteristics - Tests 7 to 11

(minus apparatus leakage)

barrier to some extent. The next test, test 5, was then performed to determine the permeability to air flow of unpainted gypsum board (screw heads sealed). In this test, the polyethylene vapour barrier was removed. It can be seen that the vapour barrier was also a partial air barrier.

The next set of tests, Tests 7 to 12, demonstrated the effect of an electrical service box in the plane of the painted gypsum board air barrier. The results were plotted in Figure 3.28 (c).

For comparative purposes, Tests 7 and 8 were run with an 8 mm diameter hole in the gypsum board (Test 7), and with the same hole plus a corresponding hole in the vapour barrier (Test 8).

In Test 9 the gypsum board was cut to fit a standard size single unit electrical box. Care was taken to wrap the box with polyethylene and to seal the wrapping to the vapour barrier. This was all done from the exterior side of the specimen and therefore this standard of sealing could not be standard practice for a job site. At 75 Pa the resulting flow was about 0.10 L/s. By introducing a small hole in the wrap (Test 10) and inserting an electrical cable the flow rate went up to about 0.12 L/s.

The next test, Test 11, was conducted on a commercially available plastic unit for electrical boxes which is said to provide a vapour tight assemblage. It consists of a standard electrical box inside a plastic box with a special frame clip on the front. After installing the box, and the polyethylene vapour barrier, the frame clip is forced into the box front causing the polyethylene to be tightly clipped in place around the perimeter of the plastic box. From Figure 3.28 (c) it is clear that the "vapour tight" box is not air tight as at 75 Pa more than 0.30 L/s of air flowed through it.

The final tests involved the same plastic box but with a polyurethane foam sprayed into it and around the perimeter so that the foam was flush with the interior wall surface. The foam expanded and filled the plastic box and the electrical box. After letting the foam set and removing the foam from inside the electrical box, the air tightness of the system was investigated (Test 12) and it was found that there was no discernable air flow through the electrical box. Since the results would have plotted as the 'x' axis they were not included in Figure 3.28(c).

3.4.5. Wall Specimen 3

3.4.5.1 Air Leakage Tests

Specimen 3 was tested with ESTA, version 2. In terms of air leakage testing this was a much improved version of the test apparatus as incidental apparatus leakage was reduced to a negligible amount.

The results from the various air leakage tests performed on Specimen 3 are listed in Table 3.11 and are shown graphically in Figure 3.29. Pressures of up to 75 Pa were applied across the wall and flow through the wall was measured in L/sm^2. Apparatus leakage is shown as curve D which at 75 Pa amounted to less than 0.007 L/sm^2. The first air leakage test performed on the wall as constructed produced very high leakage rates. In an attempt to reduce the leakage, additional sealant was applied around the perimeter. Curve C in Figure 3.29 represents the air leakage characteristics at this stage. At 75 Pa the 0.25 L/sm^2 exceeded a suggested maximum leakage rate[10] of between 0.05 and 0.15 L/sm^2.

For the next test, sealant was applied along the middle hat section (See Figure 3.10). Curve A represents the resulting air leakage rate at this

TABLE 3.11

Air Leakage Characteristics, Specimen 3

Test	Pressure (Pa)	Flow (L/sm^2)
A	0	0
	25	0.079
	50	0.132
	75	0.181
B	25	0.079
	50	0.130
	75	0.178
C	25	0.115
	50	0.189
	75	0.246
D	40	0.0022
	55	0.0033
	75	0.0069

Note - A : as constructed plus extra sealant
B : 30 screw heads sealed
C : secondary seal removed at hat section
D : apparatus leakage

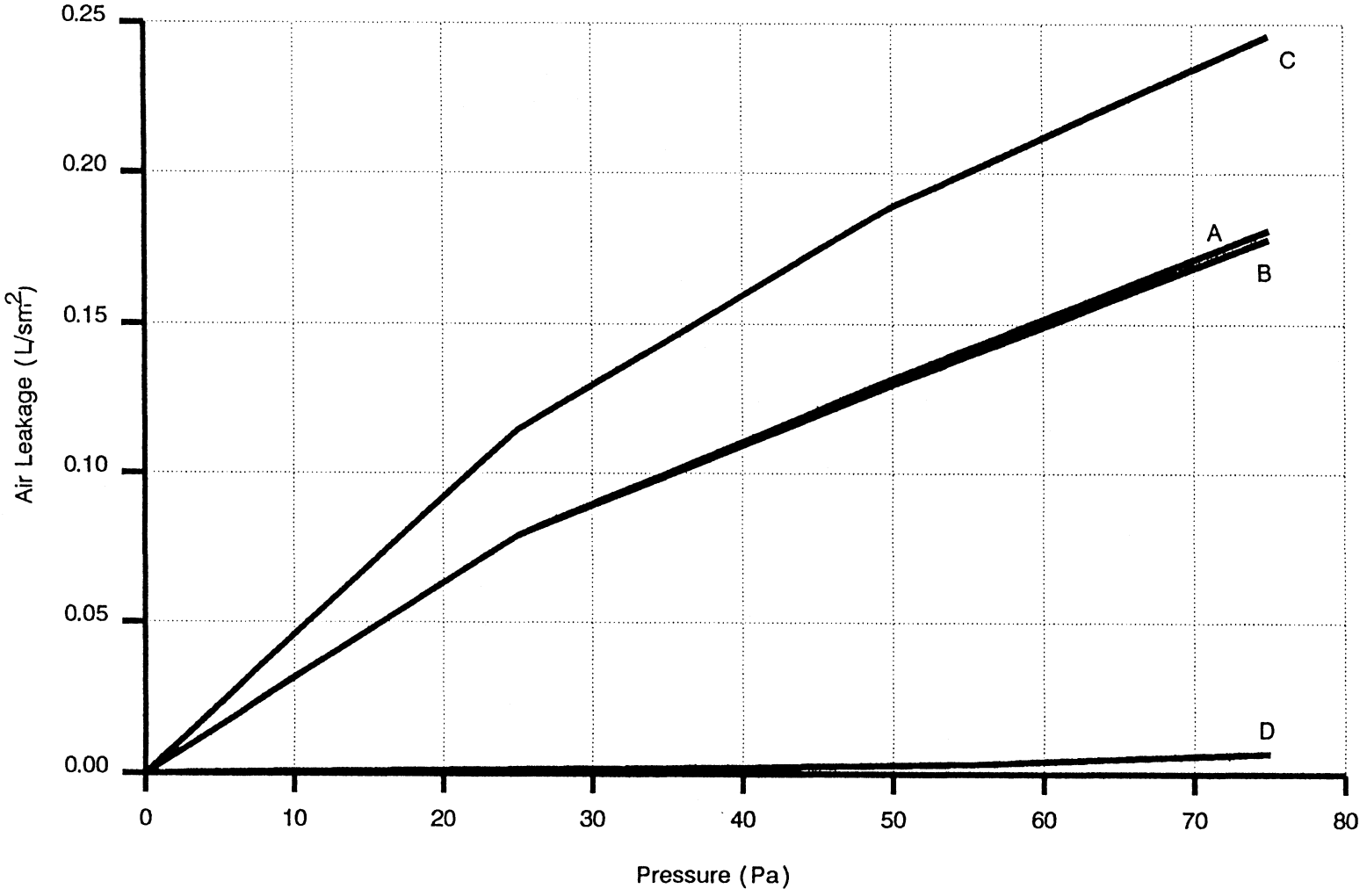

FIGURE 3.29 Specimen 3 Air Leakage Characteristics

stage with the difference between Curves A and C representing the leakage along the hat section. At 75 Pa, this difference was 0.065 L/sm^2 and demonstrated that the caulking between the gypsum board and the hat section had not been an effective seal. A fourth test with sealant applied over the heads of all 30 drywall screws used in the air barrier layer of gypsum board resulted in only a slight decrease in leakage as indicated by Curve B in Figure 3.29.

Review of the construction indicated that the heads of the screws, used to attach the hat sections to the studs, prevented the gypsum board from being sealed up tight to the hat section. Use of smoke as a tracer gas confirmed the presence of holes at these screw locations where smoke flowed through in well defined paths as though from a nozzle. Therefore, although it would have been possible to re-caulk these areas, it was decided to leave these flaws in the wall to serve as accidental leakage paths for the moisture accumulation tests.

3.4.5.2 Thermal Performance

General: This set of tests was performed to evaluate the merits of various configurations for placement of insulation. Starting with a basic 90 mm layer of rigid fibreglass insulation in the spaces between the steel studs, three additional insulation locations were identified. These were:

- the 25 mm space between the layers of gypsum board
- the space inside the hat section
- the exterior face of the steel studs

Five combinations of these insulation locations were tested as shown in Table 3.12.

TABLE 3.12

Insulation Configurations for Specimen 3

Test	90 mm Rigid Fibreglass in Stud Space	25 mm Rigid Fibreglass between Gypsum Boards	Batt Insulation in Hat Section	25 mm Rigid Polystyrene over Steel Studs
A	Yes	No	No	No
B	Yes	Yes	No	No
C	Yes	No	No	Yes
D	Yes	No	Yes	No
E	Yes	No	Yes	Yes

Through-the-wall thermal profiles were recorded at the following 3 different wall locations:

- S1 - This location was at a point where the steel studs, brick tie, and hat section coincided. It represents the maximum possible thermal bridge at any single section.
- S2 - This location was through the back-to-back steel studs but half way between hat sections.
- S3 -This location was mid-way between lines of steel studs and hat sections and is the point furthest from thermal bridging.

The five thermal profiles for each of the locations S1, S2 and S3 are shown in Figures 3.30(a), (b) and (c) respectively. Due to use of slightly differing interior and exterior temperatures, the thermal profiles have been linearly adjusted by the method described in Section 3.2.3 to represent a $+20^{\circ}$C to -20°C temperature gradient . The measured temperature profiles are listed in Table B6 of Appendix B and the average α_x values are listed in Table 3.13.

3.4.5.3 Moisture Accumulation Test

In the previous section, five different insulation configurations were evaluated in terms of thermal performance. The optimum configuration was chosen as configuration E. With this wall system, the environmental performance was examined in terms of the potential for moisture accumulation. The test was run for 120 hrs (5 days). Figure 3.31 is a plot of the temperature cycle on the cold side.

For the first 65 hours, the 20 minute defrost cycle came on every 4 hours. Beyond 65 hours, since the frost build up was relatively light, the 20 minute defrost cycle was programmed to come on once every 6 hours. In

TABLE 3.13

α_x Values for Specimen 3[1]

Name		Location[2] 1	2	3	4	5	6	7	8	9	10
S1	A	1	0.854	0.648	-	0.512	0.338	0.307	0.222	0.184	0
	B	1	0.865	0.539	-	0.408	0.258	0.237	0.168	0.136	0
	C	1	0.895	0.705	-	0.685	0.474	0.471	0.293	0.380	0
	D	1	0.879	0.665	-	0.438	0.372	0.342	0.269	0.200	0
	E	1	0.924	0.790	-	0.669	0.630	0.622	0.571	0.557	0
S2	A	1	0.930	0.816	0.623	0.416	0.280	0.265	0.227	0.113	0
	B	1	0.958	0.875	0.378	0.287	0.210	0.199	0.170	0.077	0
	C	1	0.963	0.845	0.685	0.538	0.424	0.424	0.405	0.398	0
	D	1	0.961	0.829	0.643	0.437	0.310	0.292	0.245	0.124	0
	E	1	0.973	0.864	0.746	0.618	0.531	0.530	0.514	0.481	0
S3	A	1	0.954	0.870	0.802	0.754	-	-	-	0.024	0
	B	1	0.970	0.926	0.677	0.640	-	-	-	0.022	0
	C	1	0.961	0.878	0.801	0.749	-	-	-	0.016	0
	D	1	0.966	0.877	0.806	0.750	-	-	-	0.014	0
	E	1	0.967	0.886	0.821	0.765	-	-	-	0.009	0

1 : average of thirty samples

2 : refer to Figure 3.30(a) to (c) for location

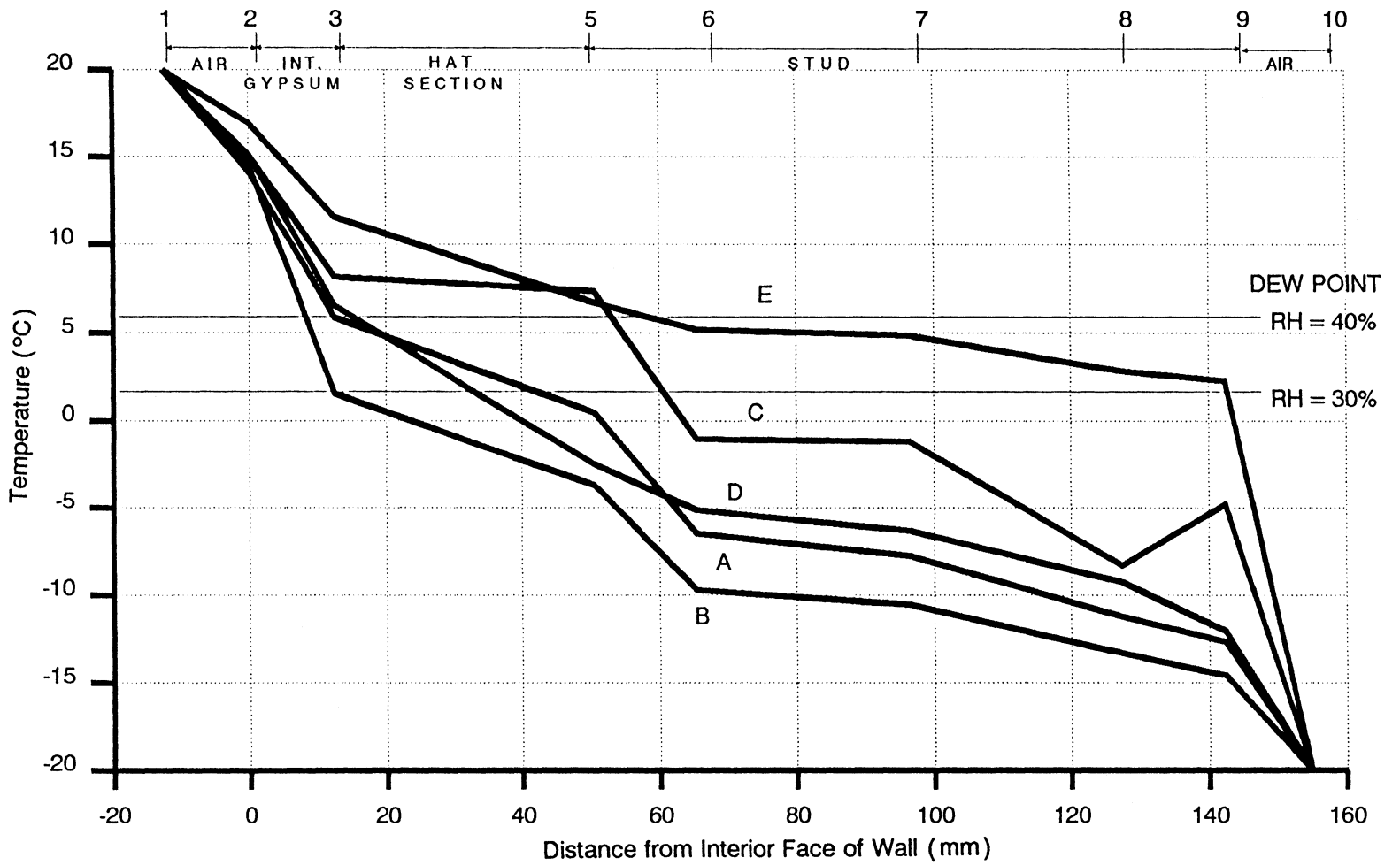

FIGURE 3.30(a) Through-the-Wall Thermal Profiles at Location S1 of Specimen 3

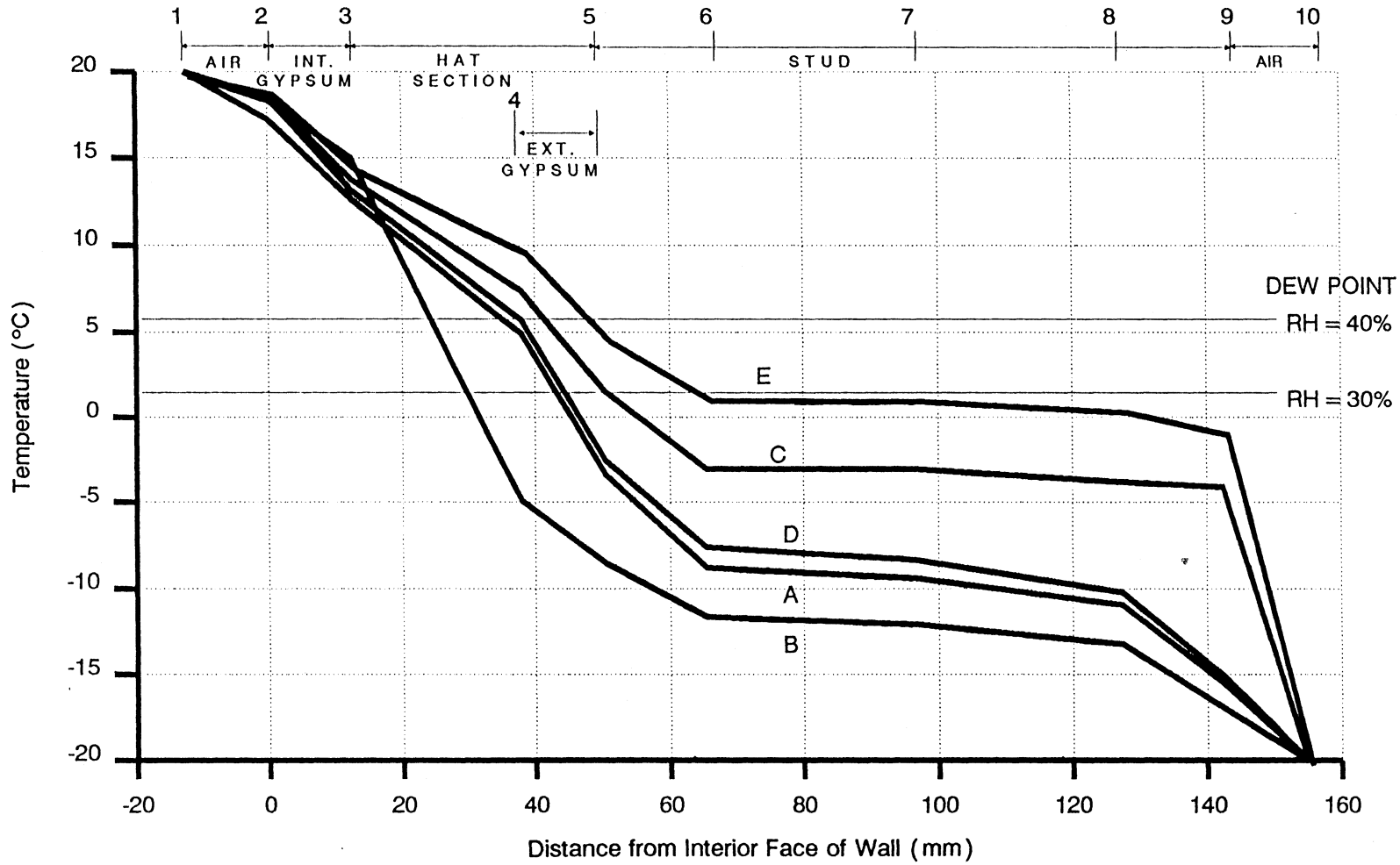

FIGURE 3.30(b) Through-the-Wall Thermal Profiles at Location S2 of Specimen 3

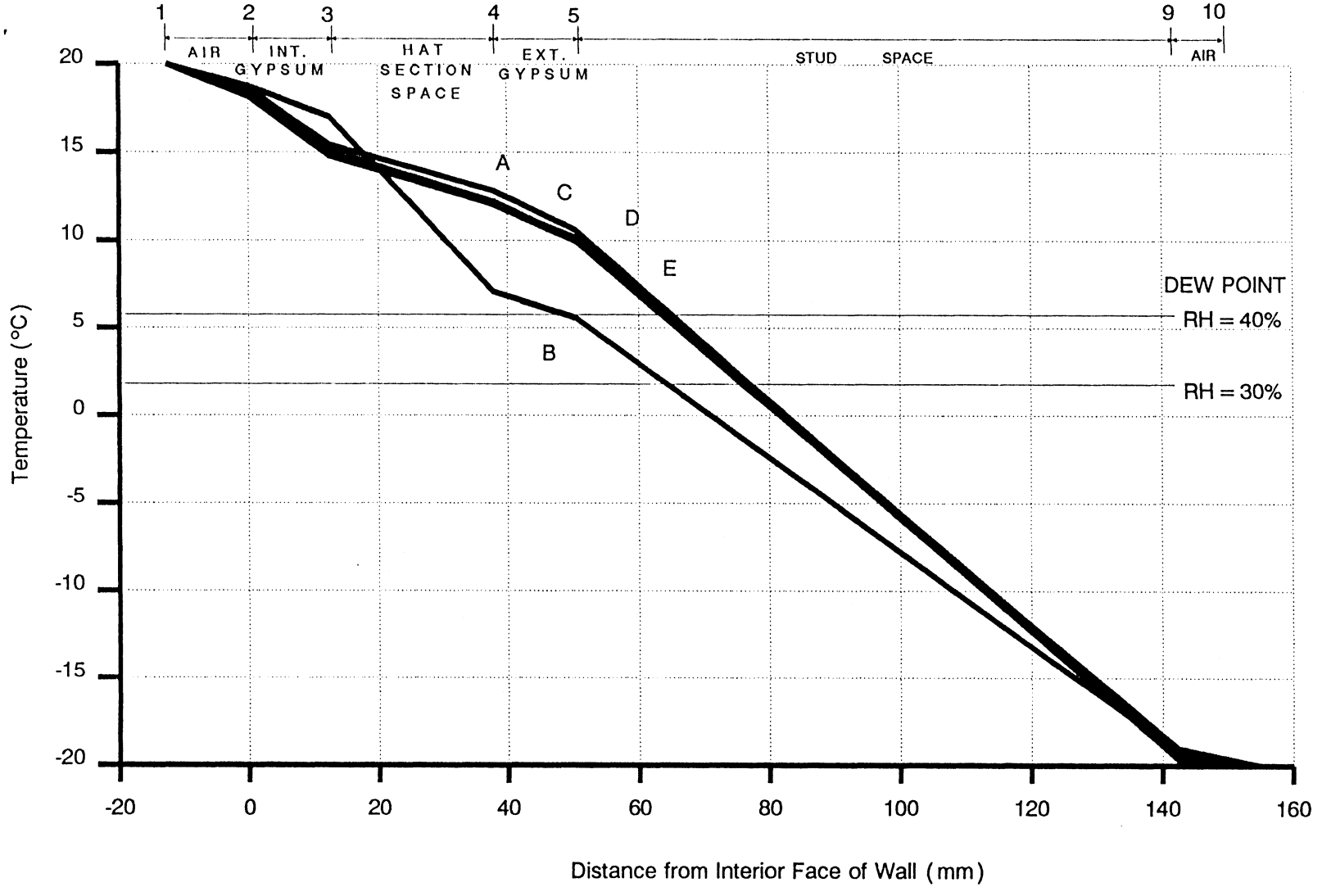

FIGURE 3.30(c) Through-the-Wall Thermal Profiles at Location S3 of Specimen 3

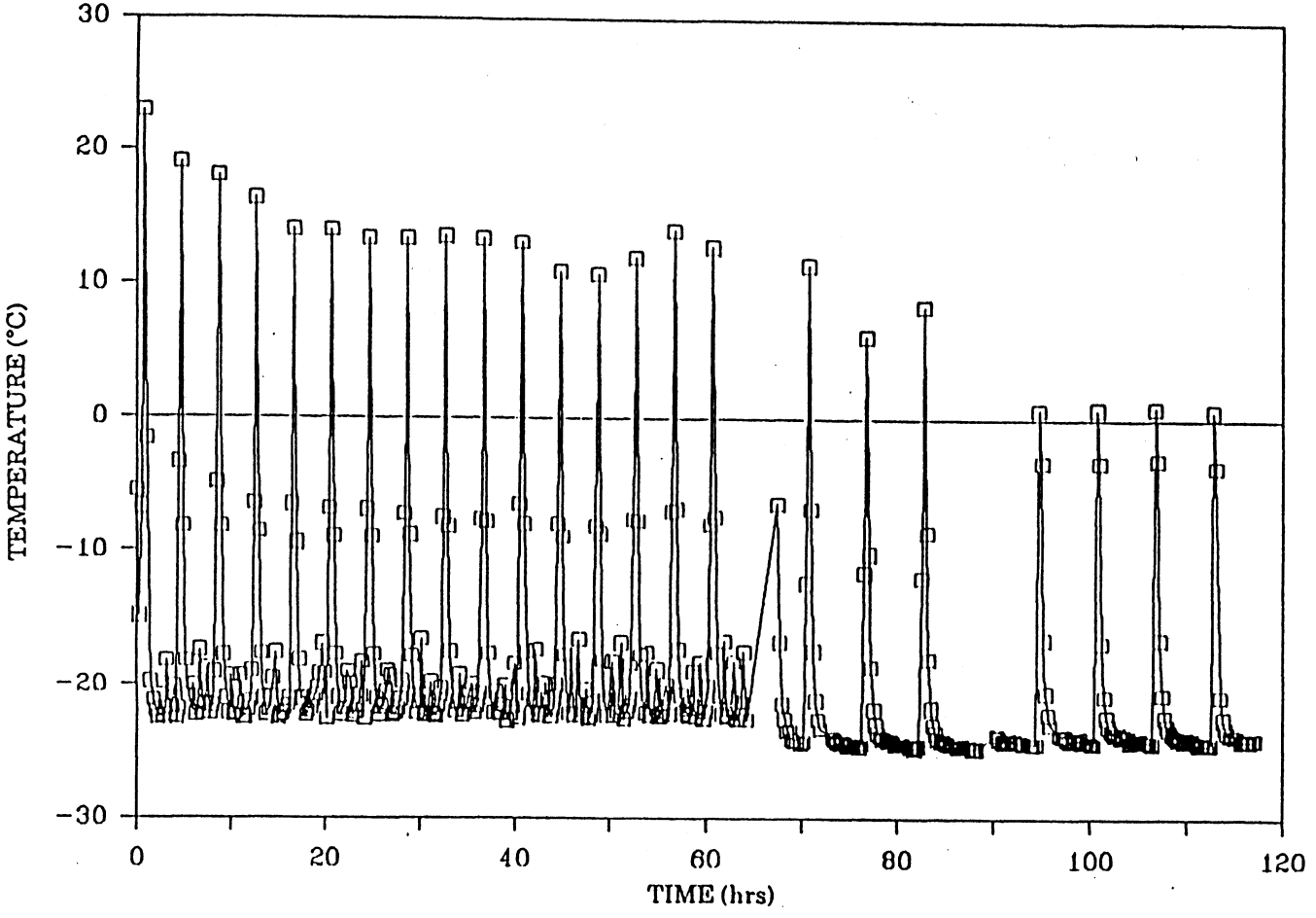

FIGURE 3.31 Cold Box Temperature Over Duration of Test - Specimen 3

both cases, after the wall went through a few initial cycles, equilibrium in the temperature profile was always achieved in the cooling part of the cycle.

Interior humidity was controlled within an average band of 39 to 44% RH. Air flow through the wall was set at 0.05 L/sm^2 for the first 65 hours and then increased to 0.15 L/sm^2 for the balance of the test.

At the end of the first 65 hours each of the 90 mm segments of rigid fibreglass insulation board were weighed. Board A, which was on one side of the centre studs, had gained a total of 6 grams of moisture while board B, on the other side, had gained 5 grams. Although moisture was not apparent on the board surfaces, the bottoms of the boards did feel wet in the middle portion. Figure 3.32 is a sketch showing the bottom of the board along with the wet area. This observation provided evidence that condensation tended to drain through the open fibres of the insulation toward the bottom. There was no condensation apparent on any steel components.

The air flow rate was tripled to 0.15 L/s.m^2 for a further 55 hours. When the test was completed, the insulation boards were again weighed. Board A did not gain weight while Board B gained a further 4 grams of moisture. In this case, small frost beads were apparent on the exterior surface of Board B.

Figure 3.33 contains the standardized plots of temperature profiles through location S3 (the mid point between studs). As can be seen,after 117 hours of operation the existence of moisture in the rigid fibreglass insulation resulted in a decrease in temperature along the temperature profile.

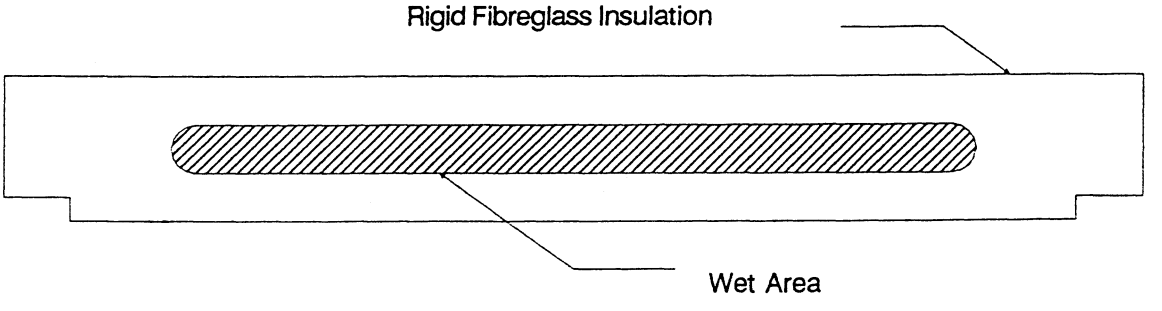

FIGURE 3.32 Moisture Pattern at Bottom of Insulation - Specimen 3

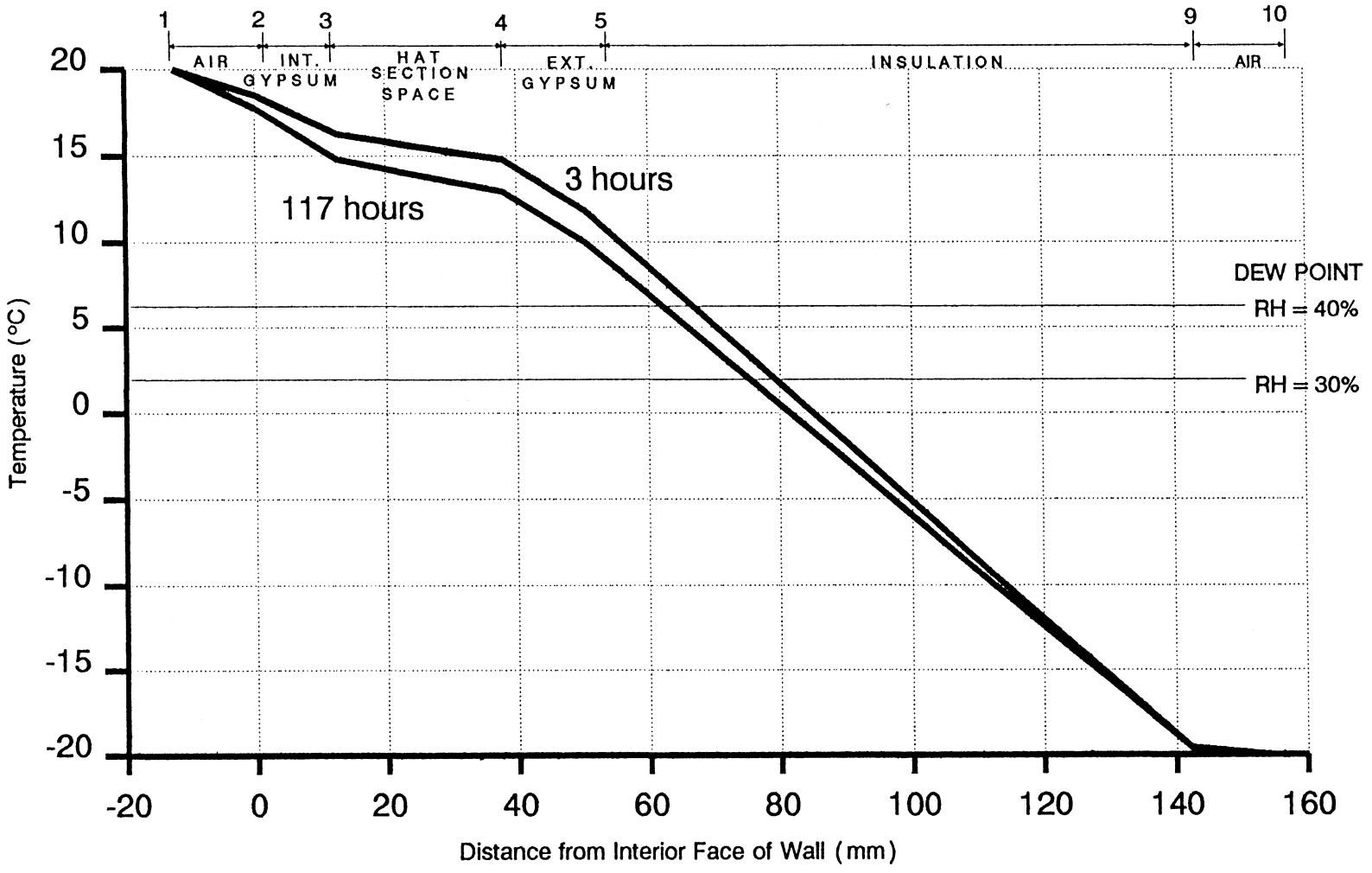

FIGURE 3.33 Effect of Condensation on Temperature Profile for Location S3 - Specimen 3

3.5 CLOSURE

The discussion of the experimental results presented in this chapter is presented in Chapter 5 while conclusions and recommendations are provided in Chapter 6. The main point that needs to be emphasized, however, is that condensation resulting from a relatively small amount of air leakage was seen to occur and to cause potential safety and serviceability problems. It is no small thing, for instance, that corrosion occurred around a screw fastener attaching a brick tie to a steel stud.

Since a small amount of air leakage in the range of 0.01 to 0.1 L/sm^2 can cause problems, wall designs incorporating even very well built air barriers should not be built without first assessing the impact of "incidental" or "construction related" air leakage on the environmental performance. This issue is taken up in the next chapter which primarily focuses on an analytical model which can be used to determine thermal profiles in steel stud framed wall systems to assess the wall for the potential for condensation related damage.

CHAPTER 4

ANALYTICAL CONSIDERATIONS

4.1 INTRODUCTION

As stated in the introduction to this thesis, this research is primarily concerned with the condensation of water vapour in wall systems. How this occurs was described in Chapter 1. That it occurs was documented in Chapter 3. This chapter contains information from an analytical model that was developed to predict temperature profiles in wall systems incorporating a steel stud framing system. The model is described, verified and then used to analyze several types of wall systems to provide a basis for assessing the vulnerability of the system to damage from condensation. Also, before looking at the model, an equation developed to calculate the dew point temperature from the interior temperature and relative humidity is presented.

4.2 ANALYTICAL DETERMINATION OF THE DEW POINT TEMPERATURE

In the many pieces of literature reviewed regarding this work, a recurring theme was the determination of the dew point temperature by consulting the Psychrometric Chart. As outlined in Chapter 1, this graphical method, based on prior knowledge of the interior temperature

and relative humidity, is both simple and illustrative; however, it lacks the potential that an analytical approach would have - especially in view of the use of computers to help solve engineering problems.

An analytical approach to the problem was developed in the course of this work by consultation with Mr Shiping Zhu[48] of the Chemical Engineering Department of McMaster University which resulted in the formulation of a semi-empirical equation to determine the dew point temperature given the interior temperature and relative humidity. The equation is based on a double application of the semi-empirical Antoine equation of 1888 (reference 28, pg 10-28) relating vapour pressure to temperature. This equation has the following form :

$$\text{Log}_e(P_S) = A - B/(T + C) \qquad \text{[Eq. 4.1}$$

where P_S = saturation vapour pressure, Pa

T = temperature, $^\circ C$

and A, B, & C are constants.

Since tables relating water vapour saturation pressures to air temperature for standard conditions are commonly available (eg. Hutcheon and Handegord[25], pg 60), the empirical coefficients can be determined by substitution of three temperature / pressure conditions into the equation to establish three equations with three unknowns over the desired range of temperatures. Based on this approach and for pressure units of pascals and temperature units of degrees celsius, the coefficients for the temperature range 0 to 30°C are as follows :

$A = 28.77$

$B = 6067$

$C = 271.4$

The equation is developed in the following manner. The saturation vapour pressure, P_S, for the interior air at temperature T_i, is found directly from Equation 4.1. The actual vapour pressure, P_V, of the interior air having a relative humidity, RH, is :

$$P_V = RH \times P_S \qquad \text{[Eq. 4.2}$$

This vapour pressure is equivalent to the vapour pressure at saturation after the air is cooled down to the dew point temperature, T_d, and therefore :

$$\text{Log}_e(RH \times P_S) = A - B/(T_d + C) \qquad \text{[Eq. 4.3}$$

By subtracting Equation 4.1 from 4.3 :

$$\text{Log}_e(RH) = -B/(T_d + C) + B/(T + C)$$

Which can be rearranged to obtain :

$$T_d = 1/\{1/(T + C) - (\text{Log}_e(RH)/B)\} - C \qquad \text{[Eq. 4.4}$$

Given the interior temperature and relative humidity, Equation 4.4 can be used to calculate the dew point temperature.

To verify the equation, Table 4.1 was prepared to compare the values obtained by interpolation of the Psychrometric Chart to those from calculation. Three interior temperatures, 18, 20 and 22°C, were chosen along with three humidity levels, 30, 40 and 50% RH.

It is evident from Table 4.1 that the equation gives consistently higher values than the chart. In every case the difference is less than 0.5°C with an average difference of 0.3°C. For a reference temperature of 0K or --273°C this represents an error of about 1%. Moreover, the equation results could be made to agree more closely with the chart values by simply increasing the value of C in the equation by 0.3. However, it is not likely that such an "accuracy" is necessary for most applications of the equation.

TABLE 4.1

Comparison of Interpolated to Calculated Dew Point Temperatures

Interior Air Conditions		Dew Point Temperature		
Temperature (Dry Bulb)	Relative Humidity	Psychrometric Chart*	Equation 4.4	Difference (T_{Eq}-T_{PC})
°C	%	°C	°C	°C
18	30	0.25	0.51	+0.26
	40	4.00	4.46	+0.46
	50	7.25	7.61	+0.36
20	30	2.00	2.23	+0.23
	40	6.00	6.24	+0.24
	50	9.25	9.45	+0.20
22	30	3.50	3.95	+0.40
	40	7.75	8.02	+0.27
	50	11.00	11.28	+0.28
			Avg.	+0.30

* Interpolated to nearest 0.25 °C.

In conclusion, it is clear that Equation 4.4 is a valuable tool for the analytical determination of the dew point temperature from the interior temperature and relative humidity.

4.3 HEAT FLOW MODEL

4.3.1 Introduction

It was noted in Chapter 1 that water vapour enters the wall by either diffusion or air flow and that air flow presents by far the most serious problem. Because of this, modern wall systems incorporate air barriers to minimize air flow on the basis that if air flow through the wall can be eliminated then there can be no condensation problem resulting from it. However, as discussed in Chapter 1, although the National Building Code of

Canada requires that wall systems have air barriers, and although it is a recognized fact that it would be an impossibility to build a wall system for any size building in such a way that it was perfectly air tight, there is as yet no standard specification stating the allowable amount of air flow. Numbers that have been discussed are in the range of 0.1 L/sm^2 yet it was in this very range that the experimental work of Chapter 3 was carried out and it was shown that, even with such a small leakage rate, appreciable condensation still occurs. This, of course, is logical and raises the question of whether the concept of "allowable leakage rates" is the proper direction to be taken by code writers.

The premise developed in this thesis is that a better approach to the problem is to evaluate the proposed wall system at the design stage to determine its suitability for the expected environmental conditions considering some likely degree of imperfection. To accomplish this, an analytical heat flow model to calculate temperature profiles is of interest because it permits the portions of the wall system below the dew point temperature to be identified. An assessment can then be made as to the vulnerability of the wall system to damage by condensation.

In the following section, a description of the heat flow model is given along with verification of its accuracy and general applicability. The model is then used to analyze several types of veneer wall systems incorporating steel studs in a standard framing configuration.

4.3.2 Description of Model

The analytical heat flow model developed in the course of this work can be used to analyze steady state, two dimensional heat flow problems

using pre-established values for the material conductivities. It is based on the Finite Difference approach were the problem can be viewed as a series of interconnected "resistors" much like an electrical circuit. This method was chosen for its intuitive nature and simplicity. It is especially well suited for the analysis of wall systems incorporating a thermal bridging component such as a steel stud.

The method involves considering the problem as a series of interconnected nodes where the connecting links are characterised by a thermal conductivity value. For the steady-state equilibrium condition, the sum of the heat flow from the connecting links at each node must be zero. Development of the equations can best be visualized by considering a particular node. In this regard, the grid network used in the subsequent verification process is shown in Figure 4.1. In this grid, node 34 is a particularly interesting node as it includes the thermal bridging steel stud.

In general terms, the equation for this node is:

$$Q = \frac{k_{34,11} A_{34,11}}{\ell_{34,11}} (T_{34} - T_{11}) + \frac{k_{34,33} A_{34,33}}{\ell_{34,33}} (T_{34} - T_{33})$$
$$+ \frac{k_{34,35} A_{34,35}}{\ell_{34,35}} (T_{34} - T_{35}) + \frac{k_{34,57} A_{34,57}}{\ell_{34,57}} (T_{34} - T_{57})$$

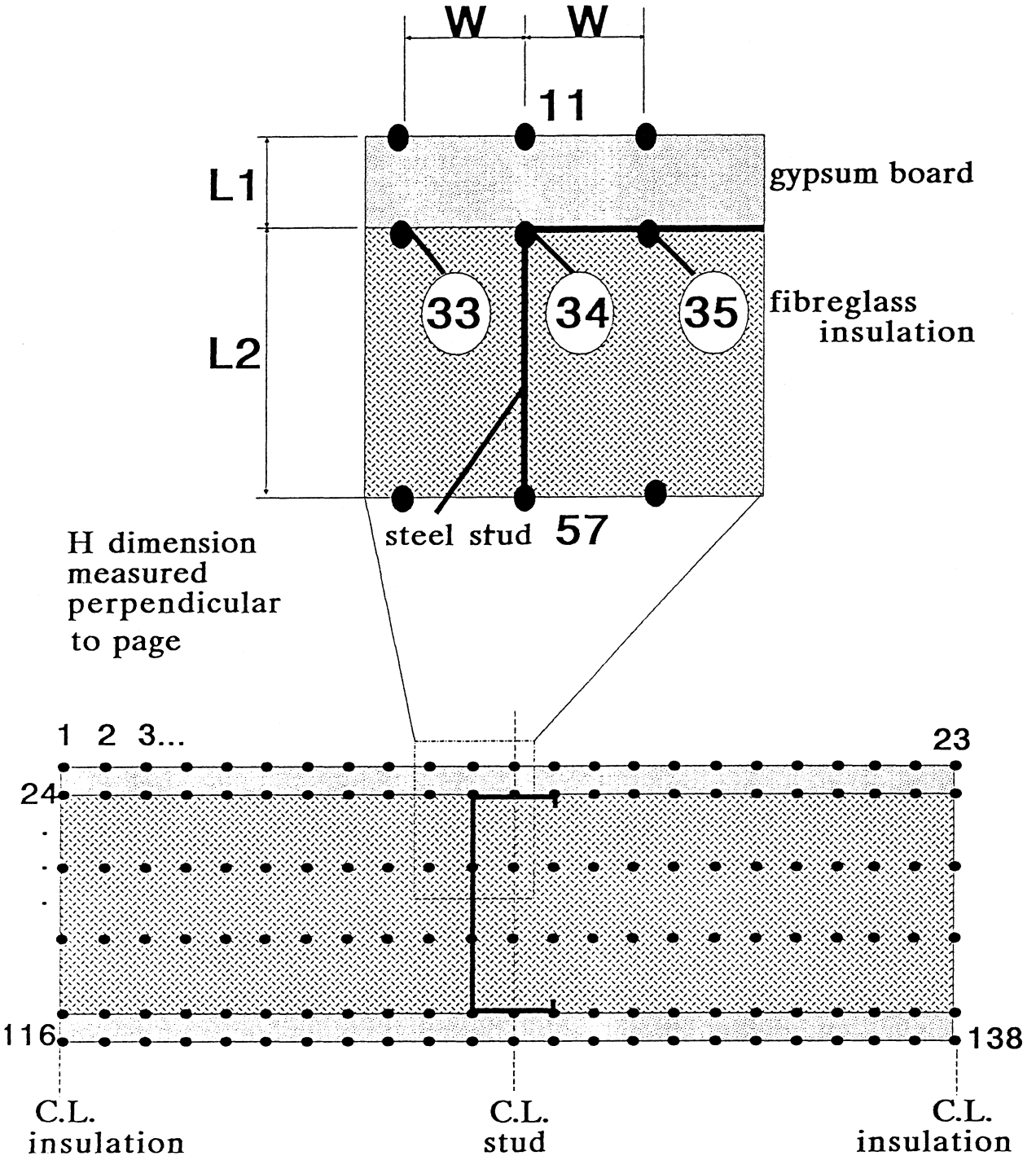

FIGURE 4.1 Grid Used in Analytical Model

By reference to Figure 4.1, expansion of the terms leads to :

$$\frac{k_{34,11} A_{34,11}}{\ell_{34,11}} = \frac{1}{R_{34,11}} = \frac{k_{gyp} \times W \times H}{L_1}$$

$$\frac{k_{34,33} A_{34,33}}{\ell_{34,33}} = \frac{1}{R_{34,33}} = \frac{1}{\frac{W}{k_{gyp} \times \frac{L_1}{2} \times H}} + \frac{1}{\frac{W}{k_{ins} \times \frac{L_2}{2} \times H}}$$

$$\frac{k_{34,35} A_{34,35}}{\ell_{34,35}} = \frac{1}{R_{34,35}} = \frac{1}{R_{34,33}} + \frac{1}{\frac{W}{k_{st} \times L_{st} \times H}}$$

$$\frac{k_{34,57} A_{34,57}}{\ell_{34,57}} = \frac{1}{R_{34,57}} = \frac{1}{\frac{L_2}{k_{ins} \times W \times H}} + \frac{1}{\frac{L_2}{k_{st} \times L_{st} \times H}}$$

where Q = heat flow (W); k = thermal conductivity (W/m°C); A = area (m^2); ℓ = distance between nodes (m); T_x = temperature at node x (°C); R = thermal resistance (C/W); k_{gyp} = conductivity of gypsum board; k_{ins} = conductivity of batt insulation; k_{st} = conductivity of steel; L_{st} = gauge of steel (0.91 mm); L_1, L_2, W and H are defined in Figure 4.1

From the above, it is seen that connecting links are taken to consist of half the width between nodes on either side of the line joining the nodes. For instance, the link between Node 34 and 35 has three parallel heat flow paths including $L_1/2$ of the gypsum board and $L_2/2$ of the fibreglass. The full width of the stud flange comprises the third heat flow path in this link.

The algorithm used for formulation of the equations is described in the program listing in Appendix C. A listing of the subroutines used to solve the equations is also found in Appendix C . In addition, data is prepared for the program by a preprocessor consisting of a spread sheet which can be used with programs such as Lotus 1-2-3™.

4.3.3 Verification of the Model

In order to have confidence in the results a two step verification process was undertaken. Firstly, the formulation and solution of the equations was verified by comparison to the analytical solution for two dimensional heat flow in a plate. The second part of the verification process involved comparison with experimental data described in Chapter 3.

Chapman[13] presented analytical solutions for steady-state conduction in rectangular plates. One of these cases involves "one edge at a uniform temperature, all other edges at constant temperature" (pg 103). The equation presented for this case, Chapman Equation 3.17, is based on a Fourier series. Although the heat flow program was developed for the analysis of wall sections having two boundaries as lines of symmetry and two boundaries at specified temperatures, it was a simple matter to adapt it for the case where all four boundaries or edges were at a specified temperature.

Figure 4.2 represents the solution as determined by the numerical model to a particular problem presented by Chapman. In this problem the plate has an assumed X dimension of 550 and a Y of 350. Three sides are held at 0°C while the fourth side is held at 100°C. Only half of the plate is shown as the results are symmetric about the center line, X=275. Table 4.2 contains a comparison of the results for 12 separate points in the plate. For the points detailed, all are in close agreement with the analytical solution.

The final stage of the verification process involved comparing experimental results to numerical results. In this regard, when comparing a

numerical solution to actual measured values, there can be some uncertainty regarding the selection of numerical values to be used for material conductivities and air film conductances. It would be theoretically possible to calibrate the model to the measured results by adjusting conductivity values. However, the approach taken in this work was to take values typically available to designers. The following values, taken from ASHRAE[2], were used in this study :

- Gypsum Board 0.156 W/mK
- Fibreglass 0.044 W/mK
- Polystyrene 0.029 W/mK
- Steel 45 W/mK

Two particular cases of steel stud wall assemblies were considered. These were the Type 1 and 2 walls detailed in Chapter 3 in which the thermally significant wall components were :

- interior air film
- 12.5 mm gypsum board
- 93 mm, 20 gauge (0.91 mm thick), steel stud with 35 mm flanges/glass fibre batt insulation, RSI 2.1
- exterior sheathing
- exterior air film

The exterior sheathing on Wall 1 was a 12.5 mm exterior grade gypsum board. Wall 2 had an exterior sheathing of 25.4 mm of polystyrene. The conductance value of the interior and exterior air films were taken as 8.3 W/m^2C. Since it is very difficult to know to what extent convection affects the thermal performance of the cavity, the analyses in this and subsequent sections are concerned with the temperatures in the wall between the

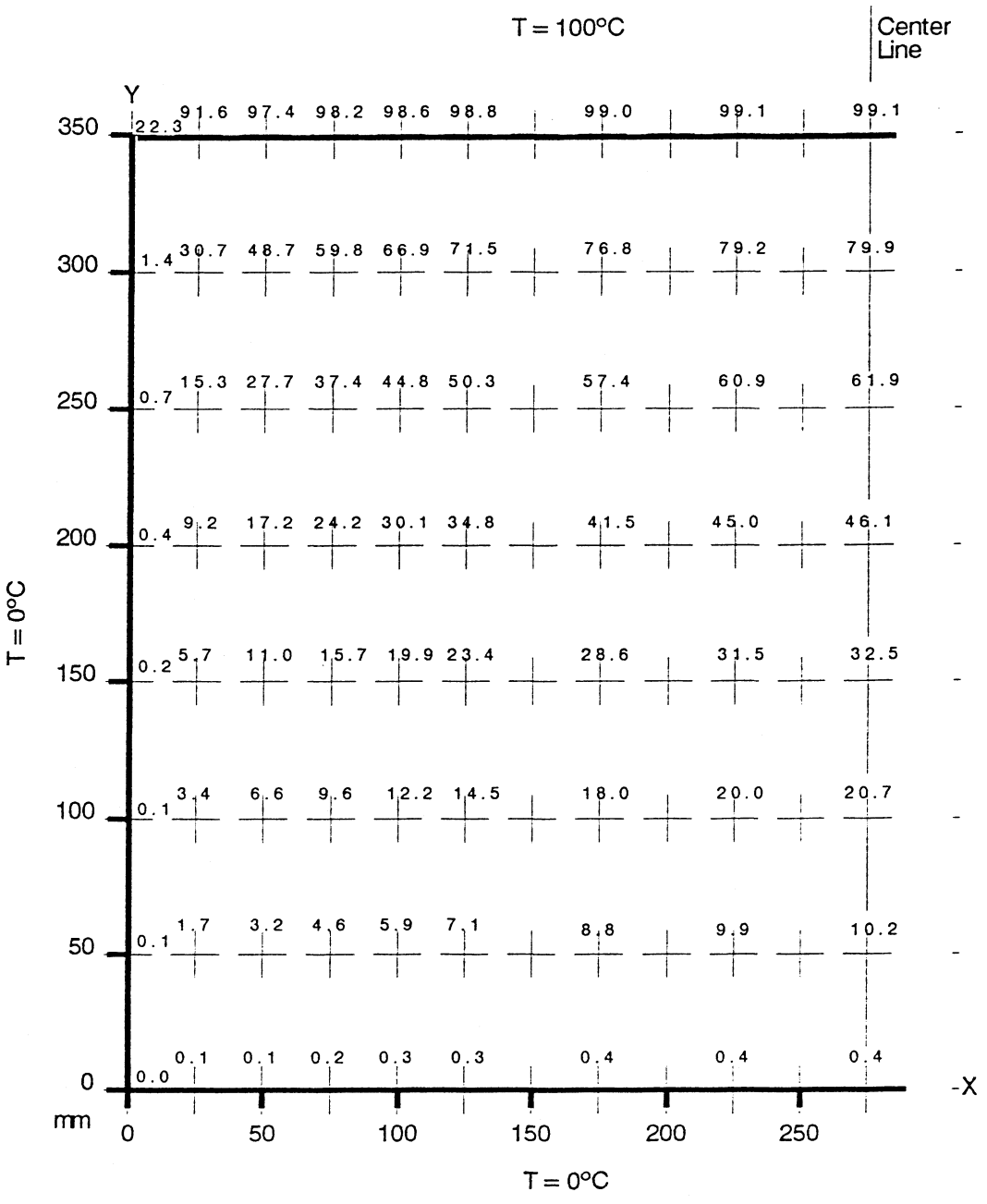

FIGURE 4.2 Temperature Distribution in a Rectangular Plate with One Edge at 100 °C, All Other Edges at 0 °C as Predicted by Numerical Heat Flow Model

TABLE 4.2

Comparison of Analytical to Numerical Solution for Heat Flow in a Rectangular Plate

X	Y	Analytical	Numerical
275	0	0.0	0.4
275	50	10.0	10.2
275	100	20.6	20.7
275	150	32.6	32.5
275	200	46.5	46.1
275	250	62.6	61.9
275	300	80.7	79.9
275	350	101.3	99.1
125	0	0.0	0.3
125	50	6.8	7.1
125	100	14.3	14.5
125	150	23.3	23.4
125	200	34.9	34.8
125	250	50.8	50.3
125	300	72.6	71.5
125	350	100.8	98.8

Note:X and Y as defined in Figure 4.2
Analytical solution represents iterations to n = 49 (see Chapman, pg 104)

interior air and cavity air. No attempt is made to model the cavity with an equivalent conduction value. In the model, the constant nodal spacing in the plane of the wall was taken as 17.5 mm which is half the 35 mm flange width.

The results of the verification process are listed in Table 4.3 where the experimental and the corresponding calculated temperature values at the stud and insulation centerlines are summarized for each of the two walls described above. The results are also presented in graphical form in Figures 4.3a) and b).

TABLE 4.3

Summary of Measured and Calculated Temperatures

Wall	Location	Centerline of Insulation Temperature(°C) Meas'd	Cal'd	%DIF*	Centerline of Stud Temperature(°C) Meas'd	Cal'd	%DIF*
1	Interior Air	22.6	22.6	-	21.1	21.1	-
	Air/Gypsum	22.0	20.9	3.1	17.5	14.3	9.4
	Gypsum/Ins. or Stud	20.5	19.8	2.0	10.0	9.7	0.9
	Ins. or Stud/Sheathing	-9.8	-10.0	0.6	1.7	-1.4	9.1
	Sheathing/Air	-11.9	-11.1	2.3	-9.4	-6.0	-10.0
	Exterior Air	-12.8	-12.8	-	-12.8	-12.8	-
2	Interior Air	21.3	21.3	-	21.3	21.3	-
	Air/Gypsum	21.3	20.4	3.6	19.7	18.7	4.0
	Gypsum/Ins. or Stud	20.3	19.8	2.0	16.5	17.0	-2.0
	Ins. or Stud/Sheathing	5.0	4.1	3.6	11.6	13.1	-6.0
	Sheathing/Air	-1.8	-2.6	3.2	-0.3	-1.5	4.8
	Exterior Air	-3.5	-3.5	-	-3.5	-3.5	-

* %DIF = (Measured-Calculated) / (Interior Air-Exterior Air)

In both cases, the difference between experimental and calculated values at the centerline of the insulation was less than 4%. At the stud centerline for Wall 1, a maximum difference of approximately plus or minus 10% existed at three of the four measured points. In this particular wall the

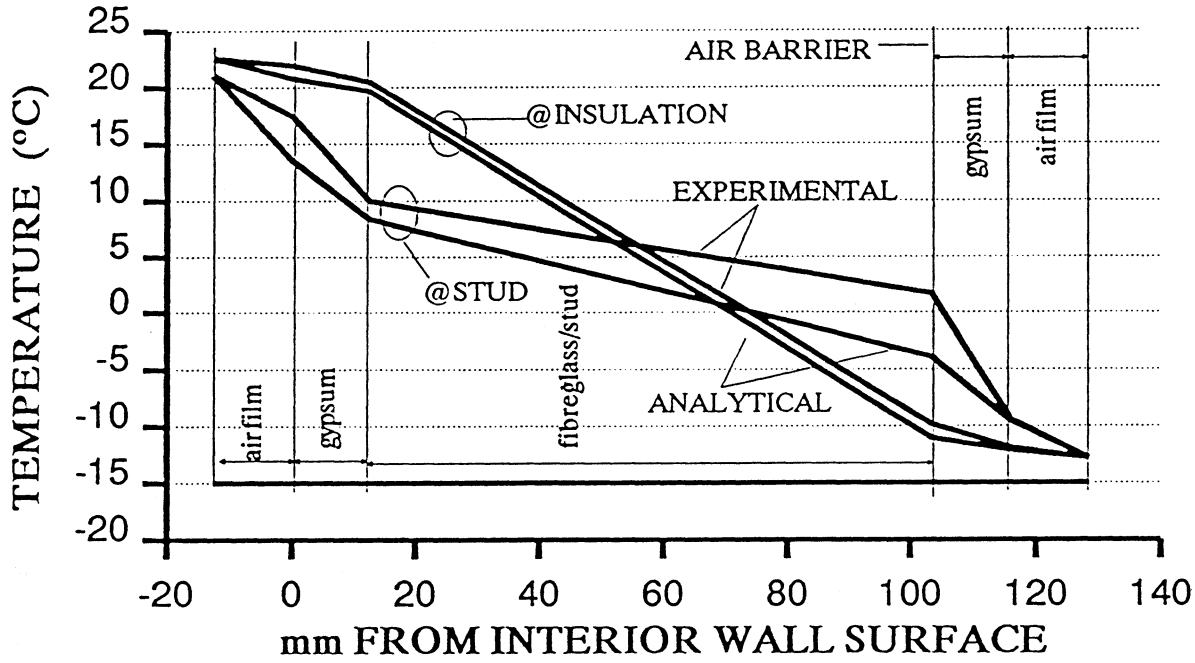

4.3(a) Type 1 Wall

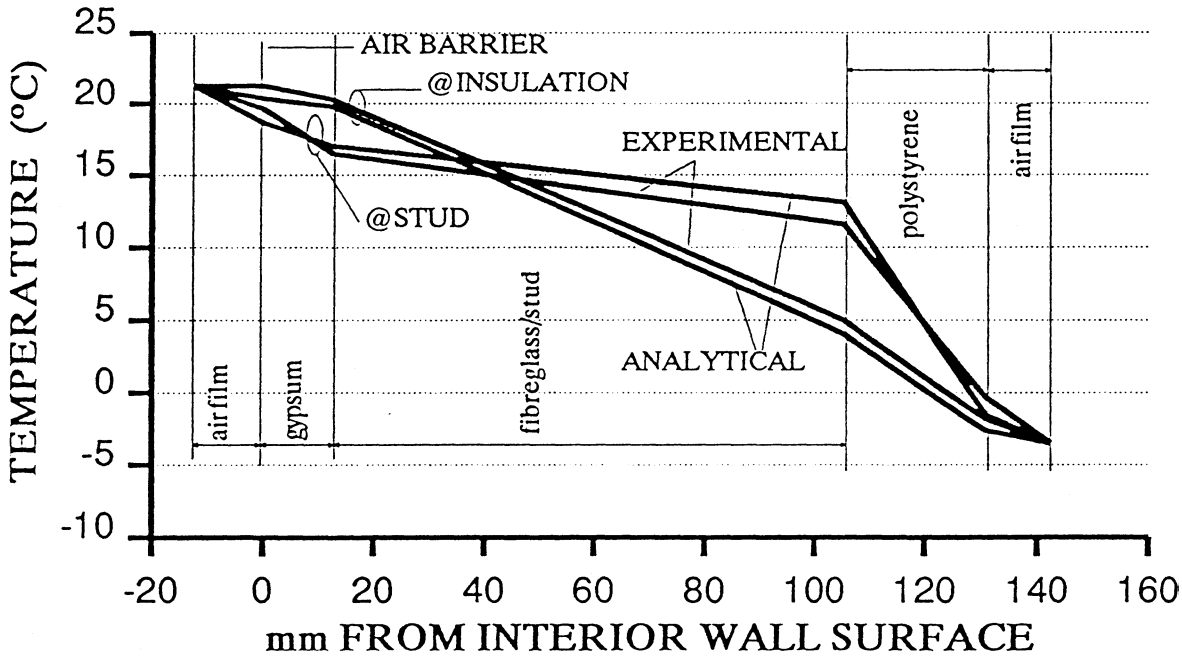

4.3(b) Type 2 Wall

FIGURE 4.3 Comparison of Analytical to Experimental Results

exterior gypsum board served as the air barrier. Since little effort was made to seal the interior gypsum board, it is thought that significant convection effects occurred between the interior air and the air barrier causing the stud to be warmer than expected on the outside flange. Air movement in the vicinity of the stud is aided by the fact that the returns on the stud flanges cause poor fitting of the batt insulation. In Wall 2, the air barrier was formed by the interior gypsum board. The maximum difference between experimental and calculated values at the stud centerline in this case is 6%.

On the basis of the above, it is suggested that the model adequately predicts one and two dimensional conduction effects with text book values for conductivities and is thus suitable to be used as a design aid. The caution that is raised is that the model cannot account for convection effects. Moreover, the model also ignores radiation effects. Since the analysis is performed between the inside air and the cavity air, radiation effects would be small for most circumstances.

4.3.4 Analysis and Results

The thermal analysis of steel stud wall systems was carried out in two parts. Part 1 deals with the 1 - Type 1 and 4 - Type 2 walls to look at the general trend of temperature profiles. In Part 2, six different alternatives are analyzed and compared.

Part 1 : In the first part of the analysis two basic configurations of walls were analyzed. Type 1 consists of an interior 12.5 mm gypsum board; a 93 mm 20 gauge steel stud with the stud space fully insulated with glass fibre

batt insulation; and an exterior sheathing of 12.5 mm gypsum board. This wall type is labelled GFG (gypsum - fibre glass - gypsum). Type 2 is identical to Type 1 except that the exterior gypsum sheathing is replaced with 25.4, 50.8, 76.2 and 101.6 mm thicknesses of polystyrene insulation. These correspond to GFP1, GFP2, GFP3 and GFP4 (gypsum - fibre glass - polystyrene).

The difference between Type 1 and Type 2 walls lies principally in the insulating value of the exterior sheathing material. For this reason, Type 1 is classified as having a non-insulating sheathing while Type 2 is classified as having an insulating sheathing.

For this study, the interior temperature was held at 20° C while exterior cavity temperatures of -10, -20 and -30° C were included as separate analyses. In addition, interior humidity levels of 30, 40 and 50% RH were considered. Three plots representing the temperature at the interior face of the sheathing for each of the five walls analysed are presented in Figure 4.4 corresponding to the three temperature profiles. On each plot, the dew point temperatures corresponding to the three humidity levels are also plotted. The dew point temperatures as obtained from a Psychrometric Chart are 2, 6 and 9° C corresponding respectively to humidity levels of 30, 40 and 50% RH and at a temperature of 20° C.

In Figure 4.4, the left and right extremities represent the center of the batt insulation between studs while the center of the plot is the center of the steel stud. Line A on the plot represents the location of the stud web and A-B represents the flange. In this study, the batt insulation was assumed to be coupled to the stud at all nodal points.

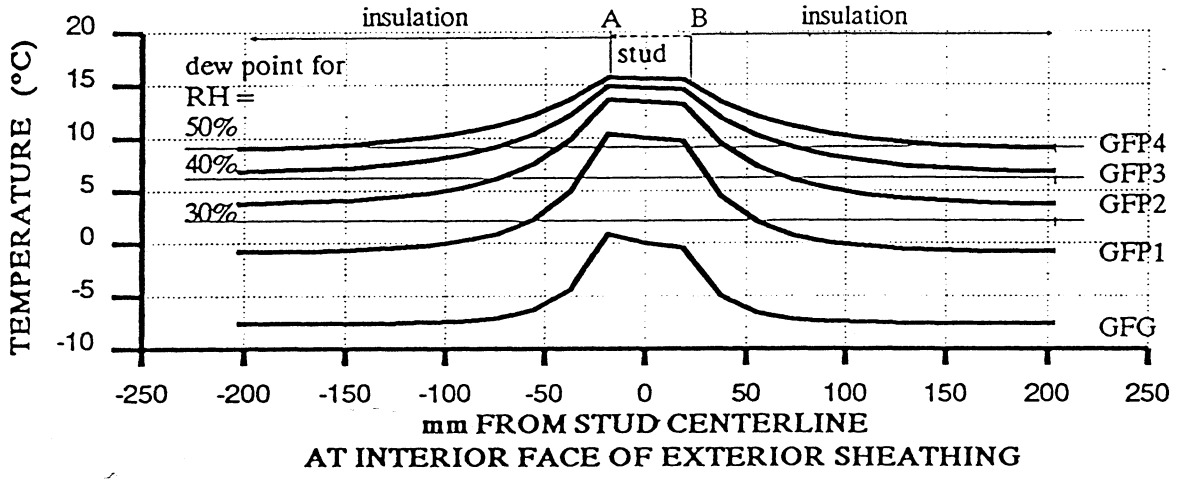

4.4(a) +20 to -10°C

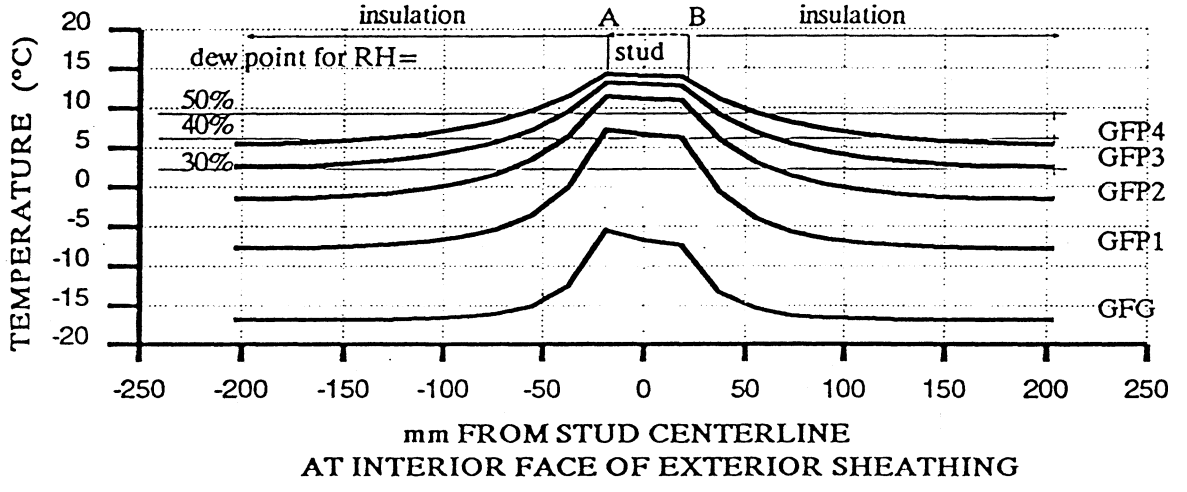

4.4(b) +20 to -20°C

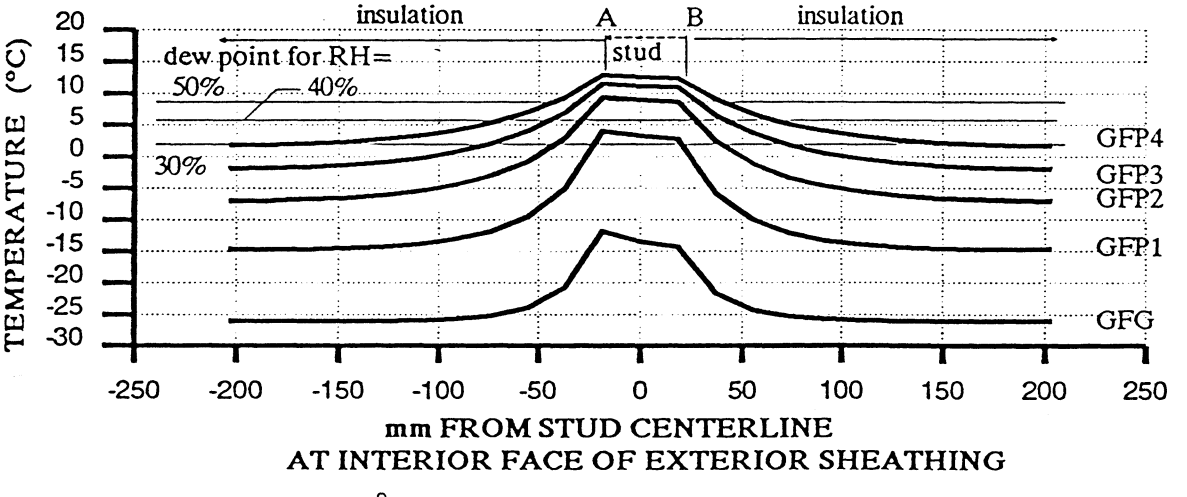

4.4(c) +20 to -30°C

FIGURE 4.4 Temperature Profiles for Type 1 and Type 2 Walls Along Interior Face of Exterior Sheathing

Part 2 : In the second part of the analysis, the basic wall types represented by GFG and GFP1 were compared to four alternate wall configurations. The first alternative, GFFG, was the GFG wall with an additional layer of fibre glass batt insulation (RSI = 0.8 m^2C/W) on the interior face of the stud. The second alternative, GFP1-18, was identical to GFP1 except that the 20 gauge stud (0.91 mm thick steel) was replaced with an 18 gauge stud (1.2 mm thick steel). The third alternative, GFP1stud, was identical to GFP1 except that the polystyrene sheathing was replaced with a 111 mm wide strip of 25.4 mm polystyrene centered on the stud. The fourth alternative, GAP3, was unique in that the space between studs was not insulated. The sheathing consisted of 76.2 mm of polystyrene and the air space between studs was modelled as having a k value of 0.575 W/mC. The results of the analysis are shown in Figure 4.5. The curve shapes follow the same pattern as noted in Part 1 of the analysis.

4.4 CLOSURE

The analytical model presented in this chapter was developed to assess the vulnerability of wall systems to damage by condensation. The Finite Difference approach taken was chosen for its simplicity and intuitive nature. It may be possible to obtain better results with a more powerful method such as the Finite Element Method although this questionable since only text book conductivity values are of any practical use to designers. A significant weak point of the model is the inability to incorporate convection effects, although, as seen in the verification process, convection tends to warm up the stud portion of the wall and thus the model gives a colder more conservative estimate of the stud

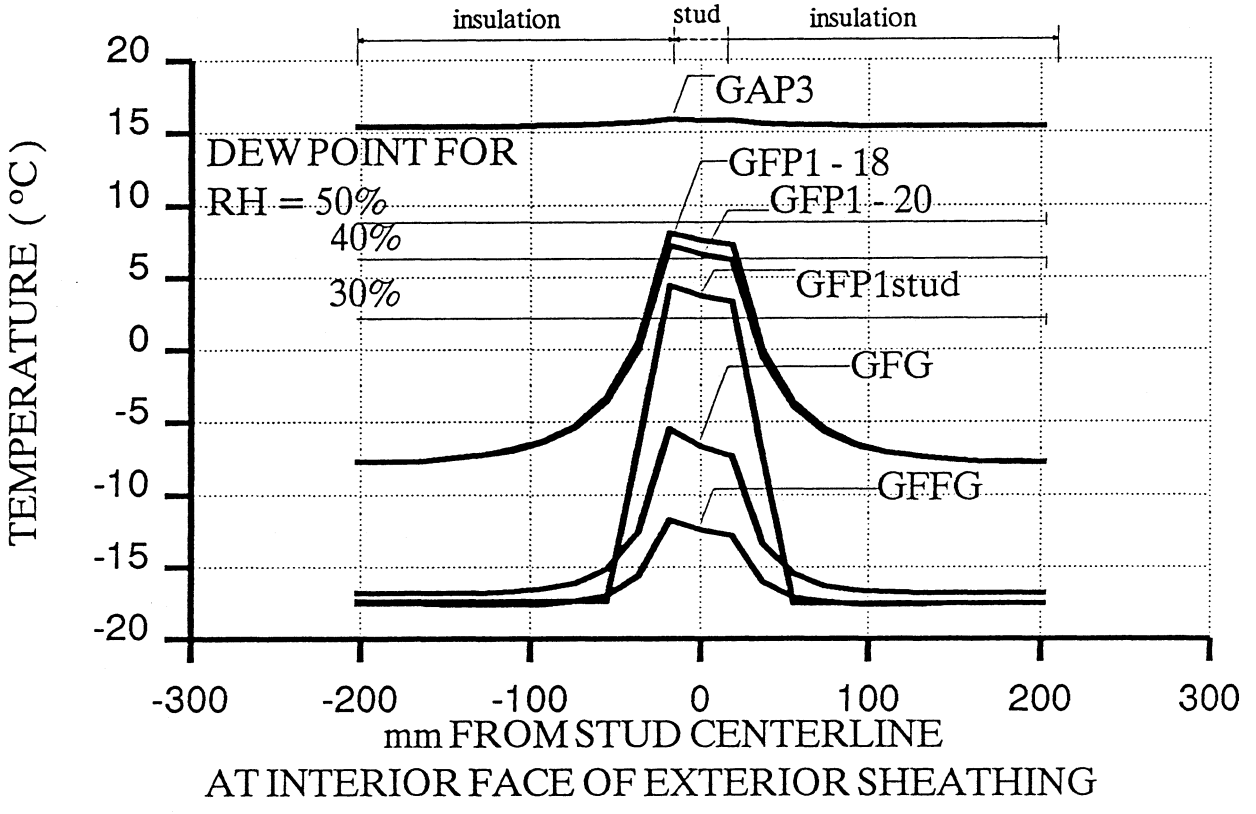

FIGURE 4.5 Temperature Profiles for Various Wall Configurations Along Interior Face of Exterior Sheathing

temperature. It is felt that radiation effects that may occur between inside air and cavity air would not have a significant effect in most wall systems. As noted in Section 1.4, latent heat of condensation is beyond the scope of this thesis but is acknowledged to exist and possibly be significant especially where large amounts of air flow occur along a path where the dew point temperature is passed.

A discussion of the results presented in this chapter is given in the next chapter.

CHAPTER 5

DISCUSSION OF TEST AND ANALYTICAL RESULTS

5.1 INTRODUCTION

The results of the tests performed on the five different wall specimens are given in Chapter 3. It was there noted that the test program consisted of three basic types of tests; ie, air leakage, thermal properties and moisture accumulation. In the present chapter, the test results will be discussed under these three headings for the five wall specimens involved. In addition, the results of the analyses presented in Chapter 4 are discussed in this chapter.

5.2 AIR LEAKAGE

5.2.1 Specimen 1A

The results of the air leakage tests of Specimen 1A are presented in Figures 3.12 (a) and (b), in which the results are plotted over the 0 to 100 Pa range of pressures. The resulting leakage is presented in L/sm^2. For discussion purposes, a range of suggested allowable leakage rates at 75 Pa is noted in Figure 3.12 (b).

In Figure 3.12 (a) the apparatus leakage is included in the plotted values and is itself plotted to illustrate its order of magnitude. As can be seen, apparatus leakage over the range of pressures tested was about equal

to the leakage through the 12 mm crack. At 75 Pa its value was about 0.019 L/sm^2. Although this is a relatively high leakage value it was difficult to obtain a lower value with ESTA 1. In Figure 3.12 (b) the results are presented with the apparatus leakage removed from the plotted leakage rates.

It is notable that at a pressure difference of 75 Pa the 12 and 120 mm cracks produced leakage rates at 75 Pa of 0.013 and 0.044 L/sm^2 - both of which are below even the minimum suggested rate of 0.05 L/sm^2. On the other hand, although the equipment could not supply enough air flow to produce 75 Pa across the wall for the 1200 mm crack, by extrapolation it is clear that the air flow rate would have been above the suggested 0.15 L/sm^2 maximum.

It is further of note that flow rates in these specimens were not directly proportional to crack size. That is, the flow through the 120 mm crack was not 10 times the flow through the 12 mm crack. This discrepancy is attributed to the fact that the gypsum board was not the only element resisting flow. The polyethylene vapour barrier, although made continuous only by lapping ends over a stud, was for the most part tightly held against the studs and therefore also offered some resistance. (In this specimen the exterior gypsum had an unsealed joint the full width of the wall and therefore offered little, if any resistance to air flow.)

5.2.2 Specimen 2B

Since sealing the drywall with a plastic sheet (Test 1) and painting the drywall with two coats of a latex paint (Test 6) gave the same results it must be concluded that paint can be an effective air barrier on interior gypsum

board. The fact that unpainted gypsum board is not air tight is of interest especially if such board is used as an air barrier. Also notable is that carefully drilled bugle head screws can seal up against the gypsum board in an air tight fashion although this should not be relied upon.

A polyethylene vapour barrier can serve as a partial air barrier (Test 2 - 4) although, if not supported, it will experience deflections and possible deterioration. It is also questionable whether polyethylene could be installed in an air tight fashion on the job site.

The flow rate through unpainted gypsum board was found to be linear over the measured pressure range (Test 5) and for the board tested is represented by the following equation:

$Q = 0.000584 * P$

Q = air flow rate (L/sm^2)

P = pressure (Pa)

At 75 Pa this gives a flow rate of 0.044 L/sm^2.

It is notable that an 8 mm hole through the gypsum board and the vapour barrier allowed 0.16 L/s of air to flow at 75 Pa of pressure. This value is greater than suggested values[10] and occurs with a relatively small hole.

Although it was found that an electrical box can be partially sealed up with polyethylene and tape (Test 9 and 10), it could not be made air tight. Moreover, job site conditions will inevitably lead to lower quality. It was, however, demonstrated that by providing a containment box for the electrical box and by sealing the containment box with a polyurethane foam made continuous with the painted drywall air barrier an air tight seal

around the electrical box was accomplished. The advantage of this approach is that wiring passing into the box are also positively sealed.

5.2.3 Specimen 3

Specimen 3 initially had very high leakage rates. Part of the problem was that, in general, insufficient caulking had been used. However, a specific problem was that the approximately 3 mm high heads of the screws used to fasten the hat sections to the steel studs kept the exterior layer of gypsum board from being screwed up tight to the hat section and stud in this area. While the use of more caulking would remedy this situation it is suggested that screws with lower profile heads would also reduce the potential for leakage.

In order to improve the effectiveness of the air barrier as well as provide an unbroken vapour barrier, it is suggested that consideration be given to placing a continuous polyethylene sheet over the inside faces of the stud after placing the rigid fibreglass insulation but before screwing on the hat and J sections. This sheet would be continuously supported between the insulation and the outside layer of gypsum board and would reduce the dependence on caulking for prevention of air leakage.

5.3 THERMAL PERFORMANCE

5.3.1 Specimen 1A

From the normalized profiles presented in Figure 3.14 (a), (b), and (c), it can be seen that the profiles measured at the top location (AT, IT, and BT) are consistently higher than those measured at the bottom (AB, IB and BB). This difference is highest in the cavity at about 7% (i.e. 2.8°C for

a 40°C temperature difference) and indicates the presence of convection currents causing warmer air to rise.

In Figure 3.14 (a)-(c), the dew points corresponding to the interior conditions of 20°C and 30 and 40% R.H. have been added. For both humidity conditions it is evident that the majority of the stud is below the temperature where dew will form and is therefore prone to some degree of moisture accumulation if interior air is allowed to pass through the wall. In the case of the temperature profile through the insulation, since condensation generally occurs at the first surface below the dew point, it is clear that the vulnerability of this wall system to moisture accumulation at the batt insulation/exterior gypsum board interface is quite high.

Under the +20 to -20°C condition, both frost and dew could form on the stud while only frost could form at the insulation/gypsum board interface. It is questionable whether the accumulation of such moisture at this point could be easily removed by drainage or drying.

In Figure 3.14 (c) the interior gypsum board portion of profile IB is shown as horizontal. This is attributed to faulty data as one dimensional heat flow is expected at this section and the slope should be the same as through the exterior gypsum board at the same section.

5.3.2 Specimen 1B

Results from Specimen 1B are similar to Specimen 1A in that the stud was below the dew points indicated. The in-plane temperature profile given in Figure 3.19 indicates that two dimensional heat flow effects around the studs are significant for about 50 to 100 mm either side of the stud centerline. Beyond that there is little effect seen.

5.3.3 Specimen 2A

5.3.3.1 General Thermal Performance

From Figures 3.21(a), (b) and (c), it is noted that the trend seen in Specimen 1A is also observed in Specimen 2A whereby the top profiles are warmer than the bottom profiles. Although in Specimen 2A the difference is not as great, the biggest difference again occurs in the cavity region. This is attributed to convection effects.

By comparing Figure 3.21(a) with 3.21 (b), it can been seen that Stud A is colder than Stud B by about 3°C. With a net difference of 40°C, this represents 7.5% and, as discussed in Section 3.3.3, is attributed to the use of more steel as connectors on Stud A than on Stud B.

Also on Figures 3.21(a)-(c) the dew points corresponding to interior air at 20°C and 30 and 40% R.H. have been plotted. In each case the stud temperature stayed above even the 40% R.H. dew point of 6°C with the only exception being on Stud A with the large amount of steel fasteners where the exterior face of the stud is just below 6°C. This is quite different from Specimen 1A and 1B where the stud temperature was for the most part below the dew points and demonstrates the benefit of a small amount of insulation on the exterior stud face (25 mm of polystyrene in this case). This 'insulation served as a thermal break and helped to keep the stud warm.

In the insulation temperature profile in Figure 3.21(c), it is seen that the interface between batt and polystyrene insulation is below the noted dew points and also below 0°C. It is evident from this that moisture can form at this point in the form of frost. Again a concern with this situation is whether this moisture can be removed before it damages wall components.

5.3.3.2 Localized Thermal Bridging Effects

From Figure 3.23(a) it can be seen that the fasteners which passed through the polystyrene insulation did not significantly change the stud temperature. At most, the effect was 5%. This minimal effect is also seen in Figure 3.23(b) where the heavy bayonette type tie attached to the lower portion of Stud B lowered its temperature by less than 5% from the upper temperature profile.

5.3.4 Specimen 3

Specimen 3 was instrumented at three locations S1, S2 and S3, as discussed earlier. For each of these three locations, the following includes a discussion of the merits of the various insulation configurations investigated. Again reference is made to interior air at 20°C and 30 and 40% R.H.

Location S1: The five thermal profiles at location S1 are plotted in Figure 3.30(a) for various insulation configurations. Commencing with Test A, it is seen that the entire stud is below both dew points. Furthermore, a portion of the exterior gypsum board which will be at about the same temperature as the stud/hat section overlap, is also below both dew points. In fact, at this section there could be conceivably one continuous line of steel extending from the interior gypsum board screw to the hat section, to the exposed stud. Local temperatures around the screw head would be very low and staining at the head would be likely. Although not specifically

addressed within the scope of this work, high heat loss would also occur at this section.

In Test B, the extra 25 mm of insulation on the warm side of the stud lowered the stud temperature even further although the insulation was not directly covering the stud at this section. This is evidence of the effect of two and three dimensional heat flow in this type of construction. At this location the temperature over the entire hat section is below both dew points.

In Test C, the 25 mm of insulation on the warm side was replaced by 25 mm strips of rigid polystyrene insulation on the cold side of the stud face. The increase in stud temperature is notable although, for the most part, it is still below the two dew points. Of interest is the dip in temperature at point 7. This is attributed to existence of a small gap between the insulation of the stud and the insulation in the stud space. This gap would allow air to circulate in and around the outer flange and web of the stud thus lowering it's temperature. Therefore it was noted that the channel shape of the polystyrene dimensioned to fit around the exterior flanges of the stud would need to totally eliminate any air circulation to the studs.

The fact that the temperature at the inside flange of the stud at point 4 is so much higher than along the web at point 5 is again an indication of multidimensional heat flow effects where heat from the inside maintains a nearly constant temperature over the depth of the hat section.

In Test D, the insulation on the outer face of the stud was removed and the interior of the hat section was insulated. Although this helped raise the stud temperature slightly above the profile obtained in Test A, the entire stud remained below the dew point.

The final test, Test E, was performed with the hat section and outer face of the stud insulated. In this test, the stud face insulation and the stud space insulation were mated tightly together. That is, there was no gap as in Test C. This better fit had a significant effect on the thermal profile by raising the stud temperature considerably. Part of this increase should be attributed of course to the hat section insulation as found in the comparison between Tests A and D. In this case the entire stud remained above the dew point temperature for 30% relative humidity but was below the 6°C dew point for the 40% relative humidity.

Location S2: The main differences between location S2 and S1 is that in S2 the hat section of S1 is replaced by a layer of gypsum board and an air space. From Figure 3.30(b) it can be seen that compared to the location with the steel hat section which drew in heat from the interior gypsum board, this section has more insulating value on the warm side of the stud. As a result, the wall is consistently colder at S2 from the exterior gypsum board outward and warmer inward from this point. Therefore, to raise the temperature of the steel stud above the dew point, it would be necessary to increase the thickness or RSI of the insulation over the exterior flanges of the studs.

Location S3: The thermal profile location S3 is different from the other two as there is no steel and it is thus the best insulated part of the wall. As is shown in Figure 3.30(c), all profiles are essentially the same except for Test B where the effects of the extra 25 mm of insulation are noticeable. The main observation drawn from this set of tests is that air leakage may

result in condensation within or on the outside surface of the 90 mm layer of rigid fibreglass insulation.

5.4 MOISTURE ACCUMULATION

5.4.1 Specimen 1A

The observation that corrosion products formed in Specimen 1A could have been predicted from the thermal performance as discussed under 5.3.2. At that point it was noted that the stud temperature was significantly below the dew point for the +20 to -20°C condition. The location of the corrosion, - on unplated fasteners, steel cuttings and steel burs - is of interest, since, although the fasteners can be richly plated and the stud can be heavily galvanized, the action of self-drilling a fastener into a stud invariably exposes unprotected steel as noted in Section 3.3.2.2. Bugle-shaped burs are of special significance since the deeper root, heavier gauge screws cause the biggest burs and thus expose the most steel. If corrosion begins to form at this point it could conceivably work its way in resulting in weakening of the screw/stud connection and possible failure.

The fact that the observed corrosion occurred in a period of 7 days with a very low flow rate of 0.015 L/sm^2, indicates that it may be difficult to support the concept of maximum allowable leakage values.

5.4.2 Specimen 1B

As in Specimen lA, air flowing through the wall specimen from interior to exterior resulted in the formation of corrosion products on unplated fasteners and on burs in fastener holes in the exterior stud face.

This second similar result tends to validate the observations of Specimen 1A for the test conditions.

The relatively high air flow rate of 0.15 L/sm^2 also resulted in moisture accumulation in gypsum board panels which indicates that exterior grade gypsum board can absorb condensation moisture on its back surface. This may be due to the fact that the glued paper joint in gypsum sheathing products can deteriorate with time and thus provide an entry point for water vapour or that the sheathing paper, although manufactured to strict water tightness guidelines, was itself water vapour permeable.

5.4.3 Specimen 2A

Parts 1 and 2 of the moisture accumulation test on Specimen 2A demonstrated that, as could be predicted from the thermal profiles, no moisture accumulation and therefore no corrosion occurred at the exterior stud face since the stud was kept above the dew point temperature of $6^{\circ}C$.

In Part 3, with the interior humidity level increased to 50 - 55%, the amount of moisture accumulation was significant although no moisture formed on the stud. It appears that the polystyrene may have acted as a partial barrier to air flow and thus caused the air flow to diffuse over its surface thus causing moisture to accumulate over a large area. Furthermore, the effect of the presence of the polystyrene may have been to hinder the drying out of the accumulated moisture although this aspect was not thoroughly investigated.

Part 4 is notable in that by giving an easy path for the exfiltrating air to flow past the polystyrene, the path became a point of major moisture accumulation. The same phenomena was seen in the upper brick vent holes

which also frosted shut. This would indicate that moisture tends to accumulate along the main airflow path. In Part 3 there was no single easy flow path and thus the pattern of accumulation was rather diffuse. The deduction of diffuse flow of air in Part 3 would be further supported by the finding in the subsequent testing of Specimen 2B showing that unpainted gypsum board is not air tight. Since the board of Specimen 2A was not painted, this would have been a source of diffuse air flow. On the other hand, in Part 4 the flow path was very distinct and was thus the main location for condensation. Furthermore, although there was an accumulation of moisture away from the hole as seen in Part 3, this may have been caused after the main leakage path had filled with frost.

5.4.4 Specimen 3

It has been stated that condensation tends to occur at the first surface below the dew point. In the moisture accumulation test of Specimen 3 this was not the case as indicated by the pattern of moisture on the bottom of the batt insulation (Figure 3.32). The fact that the inner part of the batt was wet does, however, substantiate the manufacturer's claim that this semi-rigid type fibreglass insulation is self draining. However, the claim that moisture in the batt does not affect thermal performance was brought into question by the test results as Figure 3.33 indicates that after 117 hours of air flow under the test conditions, the thermal profile through the insulation was lowered slightly.

5.5 DISCUSSION OF ANALYTICAL RESULTS

In Chapter 3 it was demonstrated in laboratory tests that condensation on the stud can lead to the formation of rust were screw type fasteners pierce the stud. This is a major reason why it is desirable to keep the stud temperature above the dew point. The formation of frost at the batt insulation / polystyrene interface was also documented. Significant amounts of rust, when caused to melt, can saturate the insulation and hence reduce the insulating value. Furthermore, the weight of accumulated moisture could pull batt insulation down and leave an uninsulated gap in the stud space above. With this in mind, it is apparent that there should be some concern regarding the performance of the GFG type wall. As shown in Figure 4.4, even in the least severe conditions (T_{ext} = -10°C, RH = 30%), the exterior stud face is below the dew point. Furthermore, the batt insulation being much colder yet, provides a large potential for condensation.

The results for walls GFP1-4 (Figure 4.4) indicate an improvement over the GFG wall due to the insulating value of the exterior sheathing providing a thermal break at the stud. With a cavity temperature of -30°C and an interior RH of 30%, this thermal break is sufficient, with only 25.4 mm of polystyrene, to maintain the stud temperature above the dew point. Although in most cases condensation can occur at the batt / polystyrene interface, the potential is less than in the GFG case. However, it is possible for the same conditions to choose a thickness of polystyrene that would force the dew point into the layer of rigid insulation which is itself relatively impermeable and therefore would result in condensation occurring at the exterior surface of the sheathing where it can be easily dealt with. For

instance, for a design temperature of -20°C and an interior humidity of 30% RH, 76.2 mm of polystyrene would ensure that no condensation occurs inboard of the polystyrene. The most severe case in this study is the case where T_{ext} = -30°C (Western Canada) and RH = 50% (e.g. hospital, museum). In this case, a minimum of 76 mm of polystyrene is required to maintain the stud above the dew point. The potential for condensation at the fibre glass / polystyrene interface cannot be eliminated in this situation.

In Part 2 of the analysis and with reference to Figure 4.5, the case of GFFG demonstrates clearly the disadvantage associated with insulating the warm side of the stud as the net result is to force the stud temperature even further below the GFG case. (In fact, as noted in Section 1.2.1, this is the opposite of what was recommended by Hutcheon[1] in 1960 when he suggested that by the use of heat, or in this case by keeping the stud warm, building elements can be kept above the dew point temperature.) By replacing the full width of polystyrene board, GFP1, with strips of polystyrene, GFP1stud, the temperature is lowered by about 10% at the stud and 24% at the fibre glass insulation centerline. This approach has the added possible weakness of providing the potential for convection to carry cold air in behind the polystyrene if the polystyrene / fibre glass joint is not tight. This would allow convection effects to lower the stud temperature. Switching from a 20 gauge stud to an 18 gauge stud raises the temperature of the stud by about 3% since more steel is present to conduct more heat.

Finally, the ultimate solution is seen in GAP3 where the stud and the interior face of the sheathing are always above the dew point. This is really no different than the recommended practice for concrete block / masonry veneer walls where the block is always kept warm by insulating on the

exterior block surface with some rigid board insulation[31]. The problem with this method is that to obtain an RSI value of 2.6 m^2C/W in the insulation, 76.2 mm of polystyrene must be placed on the exterior surface of the stud. The cost of floor space and practical problems associated with larger cavity spaces may prohibit this approach. (The use of phenolic foam insulation would reduce the required thickness). Otherwise, this type of wall system is ideal in terms of incidental air leakage causing condensation problems. With the dew point being always inside the rigid insulation, condensation would first occur at the exterior sheathing surface.

CHAPTER 6

CONCLUSIONS AND RECOMMENDATIONS

6.1 GENERAL

The conclusions of this thesis are organized under the two headings, Experimental Apparatus and BV/SS Wall Performance. Recommendations as to the design and construction of BV/SS wall systems are also presented.

6.2 EXPERIMENTAL APPARATUS

Development of the Environmental Simulation Test Apparatus has shown that a single compact test apparatus can be capable of evaluating the performance of wall systems under individually and simultaneously applied environmental loads. Although other types of test equipment have been developed over the years for the precise scientific evaluation of wall systems subject to individual environmental loads, the complexity of the problem of the interaction of several environmental loads has deterred the development of a single test apparatus to study this multi-dimensional problem. ESTA, while not designed to be a precise scientific tool, has nevertheless been demonstrated by this work to be a valuable tool for observing the effects of various environmental loads and thus allowing an assessment of the vulnerability of wall systems to such loads.

The cost advantage of testing small wall areas as opposed to full scale is also significant and allows many more combinations of wall types and wall details to be investigated for the same cost. With ESTA, the systematic environmental evaluation of wall systems is brought into the realm of affordability. This should allow new wall systems to be thoroughly tested before being marketed. Current wall systems as well as new systems can be tested to identify weaknesses and provide suggestions for improvement.

6.3 BV/SS WALL PERFORMANCE

6.3.1 Air Leakage

The following is a list of conclusions reached as a result of this work with particular reference to air leakage considerations.

- It has been demonstrated that even small openings in the air barrier can allow significant amounts of air leakage.
- Elements in the wall system other than the intended air barrier can act as partial barriers to air flow.
- Unpainted interior gypsum board is not air tight.
- Two coats of a latex paint on gypsum board is an efficient air barrier.
- Where an air tight seal is intended along any steel framing member, the heads of screws used to fasten the framing system together can introduce local air leakage paths.
- Electrical boxes can be made integral with an interior gypsum board air barrier.

- Even under laboratory conditions it was observed that air leakage paths can accidently occur in construction. Therefore design of air barriers should involve evaluation of the perfection required during construction and the ability to correct faults after construction.
- Many air barriers can also act as vapour barriers and where this results in a double set of vapour barriers, condensation from exfiltrating air can be trapped leading to potential problems of wetting of sheathing and insulation and corrosion of steel components.

6.3.2 Thermal Performance and Condensation

The following is a list of conclusions reached which pertain to thermal performance. Condensation is also considered since condensation effects are so closely related to thermal performance.

- Thermal bridges can result in cold spots along the inside surface of the wall.
- Air leakage paths around the insulation will allow cold exterior air to reduce the effectiveness of the insulation. This was particularly evident at stud locations where fit of the insulation was not always perfect.
- The steel framing portion of BV/SS wall systems can be kept above the dew point temperature for normal interior and climatic conditions.
- Many standard designs have parts of the wall below the dew point temperature of exfiltrating air.

- Two dimensional heat flow effects around studs spaced at 406 mm with the stud space insulated extended about 50 - 100 mm either side of the stud centerline.
- Large steel fasteners which passed through the insulating sheathing were shown to affect the local thermal profile by less than 5%.
- Any amount of air leakage can introduce the potential for moisture condensation at some point in the wall system.
- Even leakage rates as low as 0.03 L/sm^2 were shown to result in significant accumulations of water.
- Condensation was shown to wet exterior grade gypsum board, batt insulation, and hardware components relating to both, depending on the design and arrangement of components.
- Where rigid insulation on the exterior of the steel studs acts as a vapour barrier, a sufficient thickness of this insulation will prevent condensation within the stud cavity. Moisture will still condense along the leakage path (crack) through this insulation.
- Moisture accumulation due to vapour transmission was not measurable for the tests performed.
- The size and distribution of leakage paths can cause condensation patterns to be either localized or diffused.
- Unplated screws as well as burs in the steel stud caused by screw application are areas where corrosion can initiate if they are below the dew point temperature.
- Keeping any component above the dew point will ensure that moisture will not condense at that point.

6.3.3 Analytical Model

- Thermal performance of a wall system can be predicted with an appropriate analytical model
- The predicted temperature profiles can be used to determine the portion of the wall below the dew point temperature.
- An assessment can then be made of the wall system to assess its potential vulnerability to condensation related problems.
- The model presented predicts conduction effects with text book conductivities to an acceptable accuracy. Convection effects cannot be accurately modelled. Omission of such effects leads to a conservative solution. Radiation effects are small for winter conditions and are not included in the model.

6.4 RECOMMENDATIONS

Air barriers should be included in the design of wall systems. However, generally it should not be assumed that an air barrier can be constructed in a perfectly air tight fashion. Allowance should be made for incidental leakage by examining the wall system to determine where condensation can form. Then the formation of such condensation should be assessed to determine if it will be detrimental to the serviceability of the wall system. For this reason it is suggested that air barriers placed toward the outside of the wall system be carefully evaluated. Any violation of the air barrier will be the point of moisture accumulation since air leakage and low temperatures will exist at such a location. This condensation may

become trapped between the vapour barrier and the air barrier requiring a lengthy drying out period.

New designs of wall systems can be introduced to reduce the vulnerability of walls to effects of thermal bridges and condensation of moisture from exfiltrating air. It is recommended that designs be evaluated on the basis that some degree of imperfection will exist.

In the design of wall systems, including caulking, tape as well as major components, assessment of the long term performance of the wall should include provision for maintenance and repair. Air barriers placed in hard to access places, eg. on the exterior face of the backup wall, can be difficult to inspect during construction and are difficult to inspect after construction. Moreover, such systems are very costly to maintain and/or repair. It would be preferable to have a wall system design which would facilitate inspection of air and vapour barriers during and after construction. Maintenance of the various components would then be possible and, should problems arise with such a system in the service life of the building, the cost factor for repairs would be minimized.

REFERENCES

1. ACHENBACH, P. R. "Design of a Calibrated Hot Box for Measuring the Heat, Air and Moisture Transfer of Composite Building Walls: ASHRAE SP28, Dec. 1979

2 ASHRAE HANDBOOK OF FUNDAMENTALS, ASHRAE, New York, 1985.

3. ASSOCIATE COMMITTEE ON THE NATIONAL BUILDING CODE, "National Building Code of Canada", Ottawa 1985.

4. ASTM, "C236 Steady State Thermal Performance By Means of a Guarded Hot Box", Annual Book of ASTM Standards, Philadelphia, 1988.

5. ASTM "C976 Thermal Performance of Building Assemblages by Means of a Calibrated Hot Box", Annual Book of ASTM Standards, Philadelphia, 1988.

6. ASTM "E283 Rate of Air Leakage Through Exterior Windows, Curtain Walls, and Doors", Annual Book of ASTM Standards, Philadelphia, 1988.

7. ASTM "E331 Water Penetration of Exterior Windows, Curtain Walls and Doors by Uniform Static Air Pressure Difference", Annual Book of ASTM Standards, Philadelphia, 1988.

8. BOMBERG, M. and KUMARAN, M.K., "A Test Metod to Determine Air Flow Resistance of Exterior Membranes and Sheathings", DBR, NRCC, April 1985.

9. BROWN, W.C. and POIRIER, G.F., "Testing of Air Barrier Systems for Wood Frame Walls", DBR, NRCC.

10. Building Science Insight '86. Conference sponsored by DBR, NRCC. Proceedings not available.

11. BUMBARU, D., JUTRAS, R. and PATENAUDE, A., "Air Permeance of Building Materials", Air-Ins Inc., St Laurent, Quebec, June 1988.

12. BURN, K.N., "Concrete Block Wall Enclosures for Swimming Pools", Proceedings - Building Science Forum '82, DBR, NRCC, April 1983.

13. CHAPMAN, A.J., Fundamentals of Heat Transfer, MacMillan Publishing Comp., New York, 1987

14. Data Acquisition Handbook, Sciemetric Inc.,

15. ENVIRONMENT CANADA, "Principal Station Data" - provincial and territorial capitals.

16. GANGULI, U. and DALGLEISH, W.A., "Wind Pressures on Open Rain Screen Walls: Place Air Canada", Journal of Structural Engineering, Vol. 114, No 3, March 1988.

17. GARDEN, G.K., "Control of Air Leakage is Important", CBD 72, DBR, NRCC, December 1965.

18. GRIMM, C.T., "Brick Veneer: A Second Opinion", The Construction Specifier, Alexandria, Vt., April, 1984.

19. HANDEGORD, G.O.P., "The Need for Improved Air Tightness in Buildings", Building Research Note No. 151, DBR, NRCC, November 1979.

20. HANSEN, A.T., "Moisture Problems in Houses", CBD 231, DBR, NRCC, May 1984.

21. HICKS, G., personal communication, Sudbury, Ontario, 1981.

22. HUTCHEON, N.B., "Humidity in Canadian Buildings", CBD 1, DBR, NRC, Ottawa, January 1960, pp.4.

23. HUTCHEON, N.B., "Humidified Buildings", CBD 42, DBR, NRC, Ottawa, June 1963, pp 4.

24. HUTCHEON, N.B., "Requirements for Exterior Walls", CBD 48, DBR, NRCC, December 1963.

25. HUTCHEON, N.B., and HANDEGORD, G.O.P., Building Science for a Cold Climate, John Wily & Sons, Toronto, 1983, 440 pages.

26. KELLER, H., "Brick Veneer/Steel Stud Wall Design and Construction Practices in Canada: Results of a 1986 Survey", for Canada Mortgage and Housing Corporation, Ottawa, Ontario, March 1986.

27. KLUGE, A., and DRYSDALE, R.G., "Environmental Performance of Brick Veneer Curtain Walls - Background and Description of a Test Apparatus", Fourth North American Masonry Conference, Los Angeles, 1987.

28. LANGE'S HANDBOOK OF CHEMISTRY, 13th Edition, pg 10-28, McGraw Hill Book Comp., New York, 1985.

29. LATTA, J.K., "Vapour Barriers: What Are They? How Are They Effective?", CBD 175, DBR, NRCC, March 1976.

30. LSTIBUREK, J.W., "The Airtight Drywall Approach", report written for the Alberta Department of Housing, Innovative Housing Grants Program, 1984

31. MASONRY COUNCIL OF CANADA, "Guide to Energy Efficiency in Masonry and Concrete Buildings", 1982, 144 pages.

32. QUIROUETTE, R.L., "The Difference Between a Vapour Barrier and an Air Barrier", Building Practice Note No. 54, DBR/NRCC, July 1985

33. ROUSSEAU, J., "Rain Penetration and Moisture Damage in Residential Construction", Proceedings - Building Science Insight '83, DBR, NRCC, May 1984.

34. ROUSSEAU, M.Z., "Control of Surface and Concealed Condensation", Building Science Insight '83, DBR/NRCC, May 1984

35. SASAKI, J.R., "Thermal Performance of Exterior Steel Stud Frame Walls", NRCC Publication No. 2226, DBR, 1972.

36. SHAW, C.Y., "A Method for Predicting Air Infiltration for a Tall Building Surrounded by Lower Structures of Uniform Height", ASHRAE Transactions, Vol. 85, Part I, 1979.

37. SHAW, C.Y., "Air Leakage Tests on Polyethylene Membrane Installed in a Wood Frame Wall", DBR, NRCC, January 1985.

38. SHAW, C.Y. and TAMURA, G.T., "The Calculation of Air Infiltration Rates Caused by Wind and Stack Action for Tall Buildings", ASHRAE Transactions, Vol. 83, Part II, 1977.

39. SOLVASON, K.R., "Large-Scale Wall Heat-Flow Measuring Apparatus", ASHRAE Transactions, 65, 1959

40. TAMURA, G.T. and WILSON, A.G., "Air Leakage and Pressure Measurements on Two Occupied Houses", ASHRAE Transactions, Vol. 5, No 12, December 1963.

41. TAMURA, G.T. and WILSON, A.G., "Pressure Differences for a Nine-Storey Building as a Result of Chimney Effect and Ventilation System Operation", ASHRAE Transactions, Vol. 73, Part II, 1967.

42. TAMURA, G.T. and WILSON, A.G., "Pressure Differences Caused by Chimney Effect in Three High Buildings" ASHRAE Transactions, Vol. 73, Part II, 1967.

43. TAMURA, G.T. and SHAW, C.Y., "Studies on Exterior wall Air Tightness and Air Infiltration of Tall Buildings", ASHRAE Transactions, Vol. 82, Part I, 1976.

44. WILSON, A.G., and GARDEN, G.K., "Moisture Accumulation in Walls Due to Air Leakage", DBR Technical Paper No.227, NRCC, 1965

45. WILSON, A.G. and TAMURA, G.T., "Stack Effect in Buildings", Canadian Building Digest, No. 104, Building Research, National Research Council, Ottawa, 1968.

46. WILSON, A.G., "Air Leakage in Buildings", Canadian Building Digest No. 23, NRCC, 1961.

47. WILSON, A.G., and TAMURA, G.T., "Stack Effect and Building Design", CBD 107, DBR, NRCC, November 1968.

48. ZHU, S., private communication.

APPENDIX A

Rotameter Calibration Curves

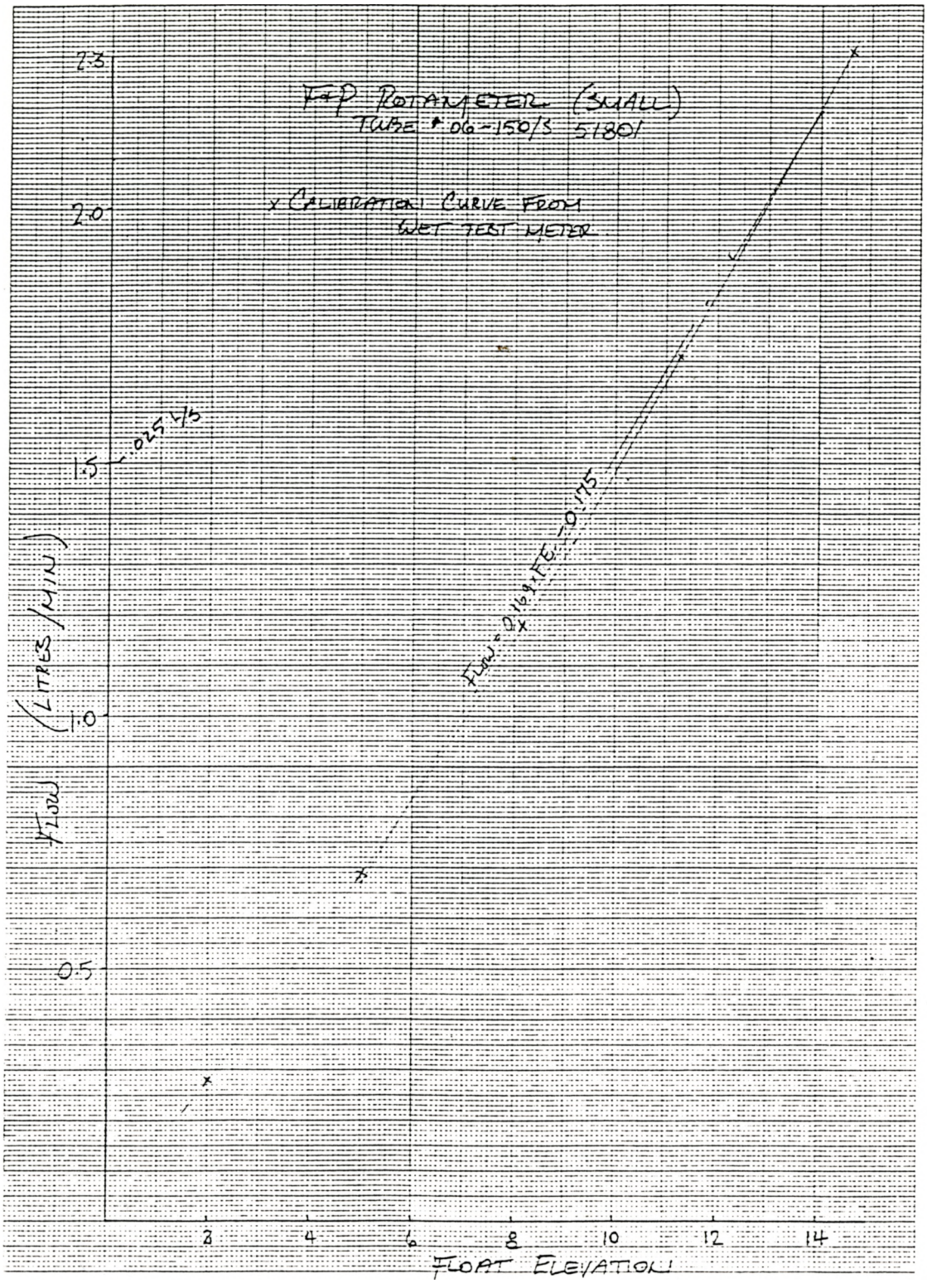
FAP ROTAMETER (SMALL)
TUBE # 06-150/5 5180I
x CALIBRATION CURVE FROM WET TEST METER
FLOW = 2.169 FE - 0.175
2.5
2.0
1.5
1.0
0.5
FLOW (LITRES/MIN)
.025 4/5
2
4
6
8
10
12
14
FLOAT ELEVATION

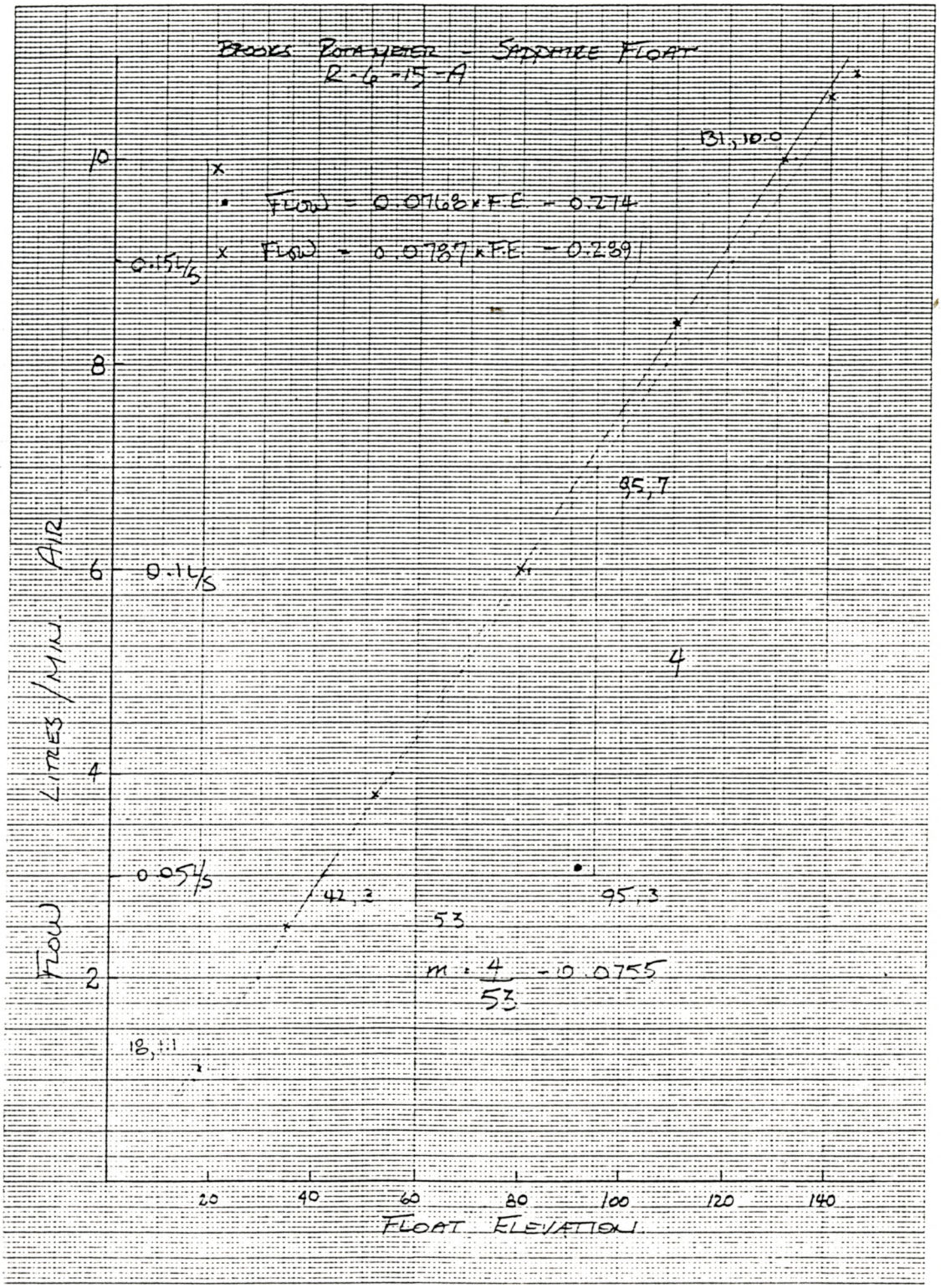
BROOKS ROTAMETER - SAPPHIRE FLOAT
R-6-15-A
FLOW = 0.0768 x F.E. - 0.274
FLOW = 0.0787 x F.E. - 0.289
0.15 l/s
0.1 l/s
0.05 l/s
131, 10.0
95, 7
95, 3
42, 3
18, 1
53
m = 4/53 = 0.0755
FLOW LITRES/MIN. AIR
FLOAT ELEVATION
10
8
6
4
2
20
40
60
80
100
120
140

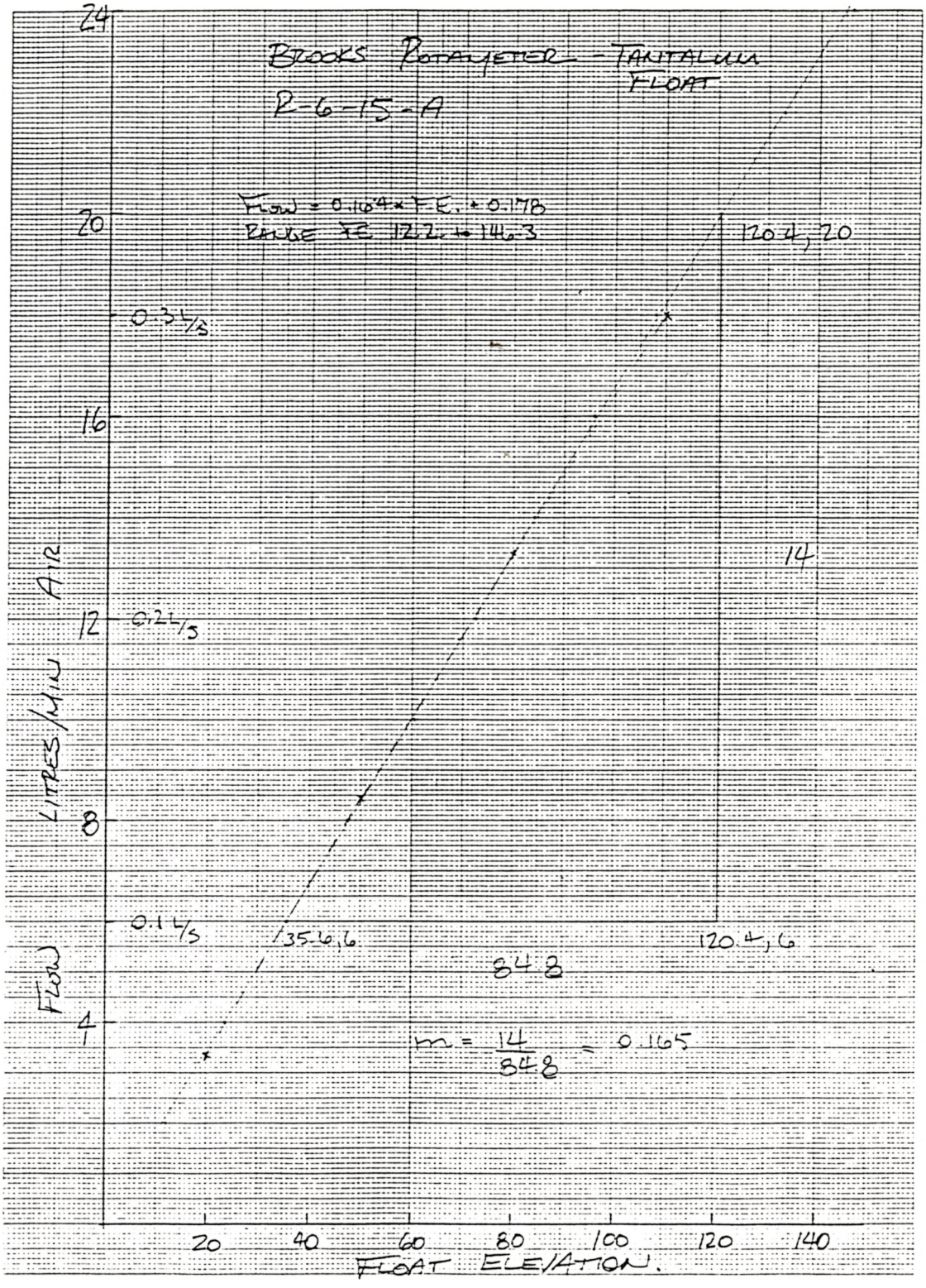
BROOKS ROTAMETER - TANTALUM FLOAT
R-6-15-A
FLOW = 0.164 × F.E. + 0.178
RANGE F.E. 122.2 → 146.3
120.4, 20
0.3 L/s
0.2 L/s
0.1 L/s
135.6, 6
120.4, 6
14
8 4 8
m = 14/848 = 0.165
FLOW LITRES/MIN AIR
24
20
16
12
8
4
20
40
60
80
100
120
140
FLOAT ELEVATION.

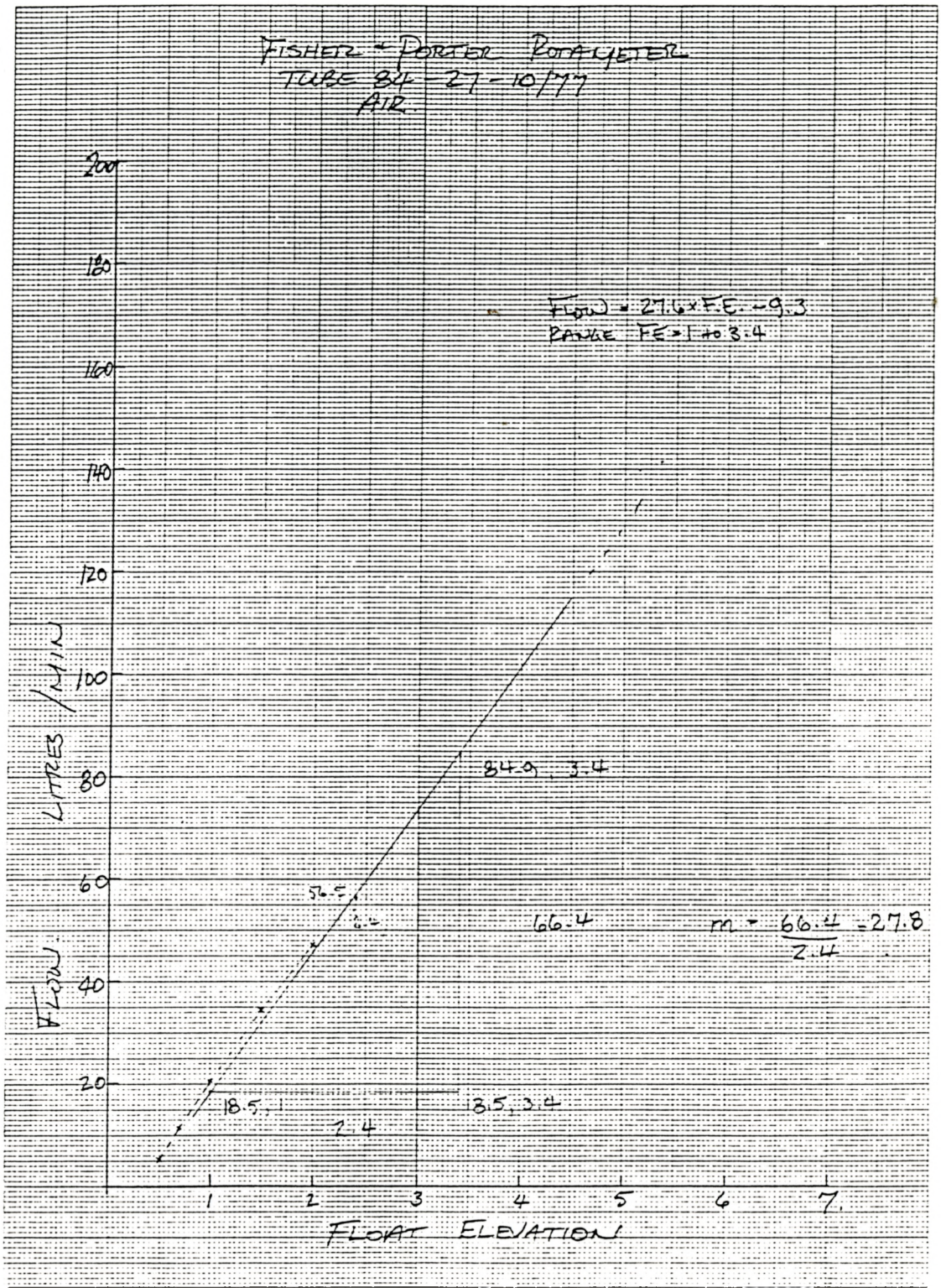
FISHER - PORTER ROTAMETER
TUBE 84 - 27 - 10/77
AIR
FLOW = 27.6 x F.E. - 9.3
RANGE F.E. = 1 TO 3.4
200
180
160
140
120
100
80
60
40
20
LITRES / MIN
FLOW
84.9 - 3.4
66.4
m = 66.4 / 2.4 = 27.8
18.5 - 1
2.4
18.5 - 3.4
1
2
3
4
5
6
7
FLOAT ELEVATION

APPENDIX B

Measured Temperatures

TABLE B1 Measured Temperatures, Specimen 1A

Location (1) . . . . . .

Name	I A	A/G	G/S,I	S,I/G	G/A	C A	A/B	B/A	E A
AT 1	22.9	20.5	15.9	11.2	9.2	5.2	4.9	0.8	0.5
2	18.5	17.5	13.0	9.3	7.4	4.5	3.7	1.0	0.4
3	21.2	19.2	11.5	4.4	1.7	-4.3	-4.0	-8.6	-9.6
4	21.0	19.2	13.9	8.4	5.9	1.5	1.4	-3.5	-3.8
5	20.7	18.9	13.6	8.2	5.8	1.5	1.4	-3.4	-3.3
6	19.6	17.9	12.8	7.7	4.8	0.8	0.6	-4.3	-4.1
IT 1	22.9	22.6	22.2	5.5	5.0	5.2	3.8	0.5	0.5
2	18.5	18.5	17.6	5.0	4.4	4.5	3.1	0.5	0.4
3	21.2	21.3	20.4	-3.7	-4.5	-4.3	-6.4	-9.4	-9.6
4	21.0	21.0	20.5	2.0	1.2	1.5	-0.6	-3.6	-3.8
5	20.7	20.8	20.2	2.0	1.2	1.5	-0.4	-2.9	-3.3
6	19.6	19.7	19.1	1.8	0.5	0.8	-1.1	-3.8	-4.1
BT 1	22.9	21.1	16.5	10.5	6.9	5.2	5.2	1.1	0.5
2	18.5	17.2	13.5	8.8	5.9	4.5	4.5	1.0	0.4
3	21.2	18.3	11.8	3.7	-2.4	-4.3	-4.3	-9.4	-9.6
4	21.0	18.8	14.2	7.7	3.4	1.5	1.3	-3.1	-3.8
5	20.7	18.7	14.0	7.8	3.6	1.5	1.6	-2.6	-3.3
6	19.6	17.6	13.1	6.8	2.7	0.8	0.8	-3.4	-4.1
AB 1	23.5	19.9	15.1	10.0	6.5	3.0	2.6	0.1	-0.2
2	18.4	16.7	11.6	7.7	4.8	2.3	2.2	-0.4	-0.6
3	22.8	17.7	10.1	2.6	-2.3	-7.0	-6.9	-10.1	-10.4
4	21.8	18.4	12.7	7.0	2.8	-0.8	-0.9	-4.3	-4.5
5	21.5	18.5	12.7	7.1	2.9	-0.6	-0.6	-4.0	-4.1
6	19.9	16.9	11.4	6.1	2.0	-1.4	-1.5	-4.8	-5.0
IB 1	23.5	19.9	15.1	10.0	6.5	3.0	2.6	*	-0.2
2	18.4	18.4	16.7	2.7	1.8	2.3	1.3	*	-0.6
3	22.8	24.1	25.6	-5.5	-7.3	-7.0	-8.2	-10.3	-10.4
4	21.8	22.3	22.8	0.0	-1.5	-0.8	-2.2	-4.3	-4.5
5	21.5	21.8	21.7	0.3	-1.1	-0.6	-1.9	-3.9	-4.1
6	19.9	20.4	20.5	-0.6	-2.1	-1.4	-2.9	-4.8	-5.0
BB 1	23.5	20.3	15.4	10.3	6.1	3.0	3.1	0.3	-0.2
2	18.4	16.2	11.6	7.6	4.4	2.3	2.7	-0.1	-0.6
3	22.8	18.1	10.7	2.9	-2.9	-7.0	-6.4	-10.2	-10.4
4	21.8	18.3	13.0	6.9	2.4	-0.8	-0.5	-4.2	-4.5
5	21.5	18.3	12.8	7.0	2.7	-0.6	0.0	-3.8	-4.1
6	19.9	16.8	11.6	5.9	1.5	-1.4	-1.0	-4.6	-5.0

* N/A

1 I A : interior air
A/G : interiorair / gypsum board
G/S,I : gypsum board / stud or insulation
S,I/G : stud or insulation / gypsum board
G/A : gypsum board / cavity air
C A : cavity air
A/B : cavity air / brick
B/A : brick / exterior air
E A :exterior air

TABLE B2 Measured Temperatures, Specimen 1B

Name	Day	No.	Location . . . . . I A	A/G	G/S,I	S,I/G	G/A	E A
STUD A	1	1	23.3	19.3	12.1	2.8	-9.5	-12.7
		2	22.6	17.9	10.7	2.1	-10.0	-13.1
		3	22.5	18.8	10.8	2.1	-10.3	-13.6
		4	23.4	18.8	11.2	2.1	-10.4	-13.4
		5	23.5	19.1	11.4	2.2	-10.4	-13.4
		6	23.2	19.0	11.5	2.3	-10.3	-13.3
		7	23.3	19.0	11.6	2.4	-10.1	-13.0
		8	23.2	19.0	11.7	2.5	-10.0	-12.7
		9	22.7	18.8	11.8	2.8	-9.8	-12.7
		10	22.2	19.2	11.9	2.9	-9.8	-12.8
	2	1	19.9	17.5	12.3	4.4	-8.2	-11.8
		2	19.9	17.5	12.3	4.4	-8.2	-11.8
		3	20.6	18.0	12.7	4.6	-8.0	-11.5
		4	20.5	17.8	12.5	4.3	-8.1	-11.5
		5	19.8	17.5	12.5	4.6	-8.0	-11.4
		6	19.9	17.5	12.3	4.4	-8.2	-11.8
		7	19.8	17.3	11.9	3.8	-8.3	-11.4
		8	20.6	18.0	12.7	4.6	-8.0	-11.5
		9	20.5	17.8	12.5	4.3	-8.1	-11.5
		10	20.3	17.7	12.3	4.1	-8.0	-11.2
	3	1	22.2	19.0	12.9	4.2	-8.6	-11.8
		2	19.9	17.1	11.0	3.0	-8.9	-12.0
		3	20.0	17.1	11.0	2.9	-9.0	-11.9
		4	22.2	19.0	12.9	4.2	-8.6	-11.8
		5	20.0	17.0	11.1	3.1	-8.5	-11.7
		6	19.9	17.1	11.0	3.0	-8.9	-12.0
		7	20.0	17.1	11.0	2.9	-9.0	-11.9
		8	22.2	19.0	12.9	4.2	-8.6	-11.8
		9	20.0	17.0	11.1	3.1	-8.5	-11.7
		10	19.9	17.1	11.0	3.0	-8.9	-12.0
	4	1	20.5	17.5	11.8	3.9	-7.5	-10.4
		2	20.6	17.5	11.8	3.8	-7.5	-10.5
		3	20.6	17.5	11.7	3.7	-7.6	-10.5
		4	20.5	17.5	11.8	4.0	-7.2	-10.3
		5	20.5	17.5	11.8	3.9	-7.5	-10.4
		6	20.6	17.5	11.8	3.8	-7.5	-10.5
		7	20.6	17.5	11.7	3.7	-7.6	-10.5
		8	20.5	17.5	11.8	4.0	-7.2	-10.3
		9	20.5	17.5	11.8	3.9	-7.5	-10.4
		10	20.6	17.5	11.8	3.8	-7.5	-10.5
	5	1	19.5	16.5	10.3	2.1	-9.8	-12.9
		2	19.5	16.3	10.3	1.9	-10.0	-12.8
		3	19.5	16.3	10.3	1.8	-10.1	-12.9
		4	19.6	16.5	10.2	1.9	-10.0	-12.7
		5	19.7	16.4	10.2	1.9	-10.0	-12.7
		6	19.5	16.3	10.2	1.8	-10.0	-12.8
		7	19.7	16.3	10.2	1.8	-9.9	-12.7
		8	19.8	16.4	10.2	1.8	-10.0	-12.8
		9	19.6	16.4	10.2	1.8	-10.0	-12.9

		10	20.1	16.8	10.6	2.2	-9.5	-12.6
	6	1	19.5	16.4	10.5	2.1	-10.0	-12.7
		2	19.6	16.4	10.4	1.9	-9.8	-12.7
		3	19.7	16.4	10.3	2.0	-9.7	-12.7
		4	19.7	16.4	10.3	2.0	-9.8	-12.6
		5	19.6	16.5	10.3	2.0	-9.9	-12.8
		6	19.9	16.5	10.3	1.9	-10.0	-12.7
		7	19.8	16.5	10.3	1.9	-10.0	-12.8
		8	19.5	16.4	10.5	2.1	-10.0	-12.7
		9	19.7	16.5	10.5	2.0	-9.9	-12.5
		10	19.6	16.4	10.4	1.9	-9.8	-12.7
	7	1	20.8	18.0	12.3	4.0	-8.5	-11.1
		2	20.8	17.9	12.1	3.8	-8.6	-11.2
		3	20.5	17.7	11.9	3.5	-8.9	-11.5
		4	20.5	17.6	11.8	3.3	-8.9	-11.4
		5	20.7	17.7	11.6	3.1	-9.0	-11.5
		6	20.6	17.6	11.5	3.0	-8.9	-11.1
		7	20.6	17.5	11.4	2.9	-8.9	-11.1
		8	20.4	17.7	12.1	3.9	-8.4	-11.3
		9	20.3	17.5	11.8	3.6	-8.7	-11.3
		10	20.2	17.4	11.7	3.3	-9.0	-11.4
	8	1	20.4	17.1	10.9	2.1	-10.2	-12.8
		2	20.0	16.9	10.7	1.8	-10.4	-12.9
		3	20.0	16.8	10.5	1.6	-10.4	-12.9
		4	20.5	17.5	11.6	3.1	-9.6	-12.6
		5	20.3	17.2	11.1	2.3	-10.1	-12.7
		6	20.4	17.1	10.9	2.1	-10.2	-12.8
		7	20.3	17.2	10.8	2.0	-10.3	-12.8
		8	20.0	16.9	10.7	1.8	-10.4	-12.9
		9	20.1	16.9	10.6	1.8	-10.4	-12.7
		10	20.0	16.8	10.5	1.6	-10.4	-12.9
STUD B	1	1	25.7	21.0	10.9	2.6	-8.6	-12.3
		2	24.9	19.8	9.8	2.5	-7.8	-13.6
		3	24.2	20.6	10.0	2.4	-8.0	-13.5
		4	25.9	20.8	10.4	2.6	-8.2	-13.7
		5	25.7	20.8	10.7	2.7	-8.2	-13.8
		6	25.5	21.0	10.9	2.9	-8.0	-13.3
		7	25.4	21.0	11.1	3.1	-7.8	-12.6
		8	25.3	20.9	11.2	3.1	-7.9	-13.3
		9	24.9	20.7	11.3	3.3	-7.5	-12.4
		10	23.6	20.7	11.3	3.3	-7.4	-12.3
	2	1	21.2	18.4	11.0	4.2	-5.9	-10.5
		2	21.2	18.4	11.0	4.2	-5.9	-10.5
		3	21.8	18.9	11.7	4.8	-5.0	-9.7
		4	21.8	18.9	11.5	4.6	-4.9	-8.9
		5	21.1	18.4	11.2	4.5	-5.1	-9.5
		6	21.2	18.4	11.0	4.2	-5.9	-10.5
		7	21.2	18.2	10.7	3.7	-6.0	-11.2
		8	21.8	18.9	11.7	4.8	-5.0	-9.7
		9	21.8	18.9	11.5	4.6	-4.9	-8.9
		10	21.6	18.7	11.3	4.4	-5.0	-9.2
	3	1	24.0	20.6	12.0	3.9	-7.1	-11.5
		2	21.2	18.1	9.8	2.4	-7.5	-11.7
		3	21.3	18.2	9.8	2.4	-7.4	-11.2

	4	24.0	20.6	12.0	3.9	-7.1	-11.5
	5	21.4	18.1	9.7	2.4	-7.3	-11.8
	6	21.2	18.1	9.8	2.4	-7.5	-11.7
	7	21.3	18.2	9.8	2.4	-7.4	-11.2
	8	24.0	20.6	12.0	3.9	-7.1	-11.5
	9	21.4	18.1	9.7	2.4	-7.3	-11.8
	10	21.2	18.1	9.8	2.4	-7.5	-11.7
4	1	22.2	18.9	10.6	3.4	-6.4	-10.1
	2	22.3	18.9	10.6	3.4	-6.3	-10.0
	3	22.3	19.0	10.6	3.3	-6.2	-9.7
	4	22.2	18.8	10.6	3.4	-6.3	-10.4
	5	22.2	18.9	10.6	3.4	-6.4	-10.1
	6	22.3	18.9	10.6	3.4	-6.3	-10.0
	7	22.3	19.0	10.6	3.3	-6.2	-9.7
	8	22.2	18.8	10.6	3.4	-6.3	-10.4
	9	22.2	18.9	10.6	3.4	-6.4	-10.1
	10	22.3	18.9	10.6	3.4	-6.3	-10.0
5	1	21.4	18.3	9.4	2.1	-7.7	-13.1
	2	21.4	17.9	9.4	2.0	-8.2	-12.8
	3	21.3	17.9	9.4	2.0	-7.9	-12.4
	4	21.5	18.4	9.4	2.0	-7.9	-12.5
	5	21.5	18.0	9.4	2.0	-7.7	-12.0
	6	21.5	17.8	9.4	2.1	-7.7	-12.1
	7	21.5	18.0	9.5	2.2	-7.5	-11.8
	8	21.6	18.1	9.6	2.4	-7.0	-11.5
	9	21.6	18.1	9.6	2.5	-6.7	-10.9
	10	22.0	18.4	9.7	2.1	-7.9	-12.5
6	1	21.3	17.9	9.2	1.4	-9.3	-14.0
	2	21.5	17.9	9.1	1.4	-9.1	-13.7
	3	21.5	17.9	9.2	1.8	-7.7	-11.3
	4	21.6	18.1	9.3	1.9	-7.7	-11.8
	5	21.7	18.1	9.4	2.0	-7.9	-12.2
	6	21.7	18.2	9.5	2.0	-7.6	-12.0
	7	21.8	18.3	9.5	2.2	-7.2	-11.3
	8	21.3	17.9	9.2	1.4	-9.3	-14.0
	9	21.5	17.8	9.2	1.4	-9.2	-13.7
	10	21.5	17.9	9.1	1.4	-9.1	-13.7
7	1	22.5	19.1	10.7	2.8	-8.3	-12.5
	2	22.3	19.1	10.5	2.5	-8.5	-12.7
	3	22.2	18.9	10.3	2.2	-8.7	-13.1
	4	22.1	18.8	10.1	2.1	-8.7	-12.9
	5	22.4	19.0	10.0	1.9	-8.7	-12.9
	6	22.4	18.9	9.9	1.8	-8.7	-13.0
	7	22.4	18.8	9.8	1.7	-8.7	-12.7
	8	22.1	18.8	10.6	2.7	-8.2	-12.5
	9	22.0	18.6	10.3	2.4	-8.5	-12.9
	10	21.8	18.5	10.0	2.1	-8.7	-13.0
8	1	22.1	18.4	9.2	0.9	-10.2	-14.4
	2	22.1	18.2	8.9	0.6	-10.4	-14.6
	3	21.9	18.2	8.7	0.4	-10.4	-14.5
	4	22.1	18.7	10.0	1.9	-9.6	-14.3
	5	22.1	18.6	9.3	1.0	-10.2	-14.4
	6	22.1	18.4	9.2	0.9	-10.2	-14.4
	7	22.1	18.5	9.1	0.7	-10.4	-14.8
	8	22.1	18.2	8.9	0.6	-10.4	-14.6
	9	21.9	18.1	8.8	0.5	-10.4	-14.6

		10	21.9	18.2	8.7	0.4	-10.4	-14.5
INS	1	1	25.5	24.1	22.1	-9.4	-11.6	-12.4
		2	24.6	22.7	20.4	-10.1	-12.4	-13.3
		3	24.5	23.2	20.7	-10.2	-12.5	-13.6
		4	25.5	23.7	21.3	-10.2	-12.5	-13.6
		5	25.7	24.0	21.7	-10.2	-12.5	-13.7
		6	25.6	24.1	22.0	-10.1	-12.4	-13.5
		7	25.5	24.2	22.2	-10.1	-12.2	-12.9
		8	25.4	24.2	22.3	-10.0	-11.9	-12.7
		9	25.2	24.2	22.5	-9.7	-11.6	-12.6
		10	24.3	24.0	22.5	-9.6	-11.6	-12.6
	2	1	21.7	21.3	20.1	-6.9	-9.9	-11.6
		2	21.7	21.3	20.1	-6.9	-9.9	-11.6
		3	22.4	22.0	20.7	-6.7	-9.4	-10.7
		4	22.3	21.9	20.7	-7.0	-9.4	-10.4
		5	21.6	21.3	20.0	-6.7	-9.6	-10.9
		6	21.7	21.3	20.1	-6.9	-9.9	-11.6
		7	21.6	21.3	20.0	-7.7	-10.2	-11.4
		8	22.4	22.0	20.7	-6.7	-9.4	-10.7
		9	22.3	21.9	20.7	-7.0	-9.4	-10.4
		10	22.2	21.9	20.6	-7.2	-9.4	-10.3
	3	1	24.7	24.2	23.0	-8.1	-10.5	-11.6
		2	21.9	21.6	20.2	-8.5	-10.6	-11.8
		3	22.1	21.6	20.3	-8.6	-10.7	-11.7
		4	24.7	24.2	23.0	-8.1	-10.5	-11.6
		5	22.0	21.6	20.2	-8.3	-10.5	-11.6
		6	21.9	21.6	20.2	-8.5	-10.6	-11.8
		7	22.1	21.6	20.3	-8.6	-10.7	-11.7
		8	24.7	24.2	23.0	-8.1	-10.5	-11.6
		9	22.0	21.6	20.2	-8.3	-10.5	-11.6
		10	21.9	21.6	20.2	-8.5	-10.6	-11.8
	4	1	22.6	22.1	20.7	-7.1	-9.3	-10.3
		2	22.7	22.1	20.6	-7.3	-9.3	-10.3
		3	22.8	22.2	20.6	-7.4	-9.2	-10.1
		4	22.6	22.1	20.6	-7.0	-9.1	-10.3
		5	22.6	22.1	20.7	-7.1	-9.3	-10.3
		6	22.7	22.1	20.6	-7.3	-9.3	-10.3
		7	22.8	22.2	20.6	-7.4	-9.2	-10.1
		8	22.6	22.1	20.6	-7.0	-9.1	-10.3
		9	22.6	22.1	20.7	-7.1	-9.3	-10.3
		10	22.7	22.1	20.6	-7.3	-9.3	-10.3
	5	1	21.5	21.1	19.7	-10.1	-12.3	-13.2
		2	21.8	21.2	19.7	-10.1	-11.9	-12.7
		3	21.8	21.2	19.7	-9.9	-11.9	-12.9
		4	21.7	21.2	19.7	-9.8	-11.8	-12.6
		5	22.0	21.2	19.7	-9.8	-11.7	-12.6
		6	21.8	21.2	19.7	-9.7	-11.7	-12.5
		7	21.8	21.2	19.7	-9.6	-11.5	-12.4
		8	22.0	21.3	19.7	-9.4	-11.5	-12.6
		9	21.9	21.3	19.7	-9.4	-11.5	-12.6
		10	22.3	21.7	20.2	-10.1	-12.3	-13.2
	6	1	21.9	21.3	19.9	-10.3	-12.3	-13.4
		2	22.0	21.4	19.9	-10.2	-12.2	-13.3
		3	21.9	21.4	19.9	-10.1	-12.1	-12.9

	4	22.1	21.4	19.9	-10.1	-12.0	-12.8
	5	22.1	21.4	19.9	-10.0	-11.9	-12.7
	6	22.1	21.5	19.9	-9.8	-11.7	-12.6
	7	22.2	21.5	20.0	-9.6	-11.5	-12.3
	8	21.9	21.3	19.9	-10.3	-12.3	-13.4
	9	22.1	21.4	19.9	-10.3	-12.2	-13.3
	10	22.0	21.4	19.9	-10.2	-12.2	-13.3
7	1	22.9	22.4	21.0	-7.8	-10.4	-11.5
	2	22.9	22.4	20.9	-8.2	-10.6	-11.8
	3	22.9	22.3	20.9	-8.5	-10.9	-12.2
	4	22.8	22.3	20.8	-8.8	-10.9	-12.1
	5	22.9	22.3	20.8	-8.9	-11.0	-12.2
	6	23.0	22.3	20.8	-9.0	-11.0	-11.9
	7	22.9	22.3	20.8	-9.1	-11.0	-11.8
	8	22.7	22.2	20.8	-7.8	-10.3	-11.7
	9	22.5	22.0	20.6	-8.1	-10.6	-12.0
	10	22.4	22.0	20.5	-8.5	-10.9	-12.0
8	1	22.7	22.0	20.5	-10.4	-12.5	-13.6
	2	22.7	22.0	20.5	-10.7	-12.8	-13.8
	3	22.5	22.0	20.4	-10.9	-12.8	-13.7
	4	22.7	22.1	20.6	-9.0	-11.7	-13.2
	5	22.4	22.0	20.5	-10.2	-12.5	-13.5
	6	22.7	22.0	20.5	-10.4	-12.5	-13.6
	7	22.7	22.1	20.5	-10.5	-12.7	-13.7
	8	22.7	22.0	20.5	-10.7	-12.8	-13.8
	9	22.6	22.0	20.5	-10.8	-12.8	-13.6
	10	22.5	22.0	20.4	-10.9	-12.8	-13.7

TABLE B3 Measured In-Plane Temperatures, Specimen 1B

	mm From STUD A (1)									Int.	Ext.
No.	0	50	100	150	200	250	300	350	406	Temp	Temp
1	2.8	-8.5	-9.0	-9.6	-9.4	-9.3	-9.4	-7.4	2.6	24.8	-12.5
	2.1	-8.9	-9.6	-10.2	-10.1	-9.7	-9.6	-7.1	2.5	24.0	-13.3
	2.1	-8.9	-9.6	-10.2	-10.2	-9.9	-9.8	-7.3	2.4	23.7	-13.6
	2.1	-8.9	-9.6	-10.3	-10.2	-9.9	-9.9	-7.5	2.6	24.9	-13.6
	2.2	-8.9	-9.6	-10.3	-10.2	-10.0	-10.0	-7.6	2.7	25.0	-13.6
	2.3	-8.9	-9.6	-10.3	-10.1	-10.0	-10.0	-7.6	2.9	24.8	-13.4
	2.4	-8.8	-9.5	-10.2	-10.1	-9.9	-9.9	-7.5	3.1	24.7	-12.8
	2.5	-8.7	-9.4	-10.0	-10.0	-9.8	-9.9	-7.4	3.1	24.6	-12.9
	2.8	-8.4	-9.1	-9.8	-9.7	-9.6	-9.7	-7.3	3.3	24.3	-12.6
	2.9	-8.2	-8.9	-9.6	-9.6	-9.4	-9.5	-7.2	3.3	23.4	-12.6
2	4.4	-6.1	-6.5	-7.1	-6.9	-6.4	-5.9	-4.0	4.2	20.9	-11.3
	4.4	-6.1	-6.5	-7.1	-6.9	-6.4	-5.9	-4.0	4.2	20.9	-11.3
	4.6	-5.7	-6.2	-6.8	-6.7	-6.4	-5.9	-3.7	4.8	21.6	-10.6
	4.3	-6.0	-6.6	-7.1	-7.0	-6.7	-6.2	-4.0	4.6	21.5	-10.3
	4.6	-5.7	-6.2	-6.8	-6.7	-6.4	-5.8	-3.6	4.5	20.8	-10.6
	4.4	-6.1	-6.5	-7.1	-6.9	-6.4	-5.9	-4.0	4.2	20.9	-11.3
	3.8	-6.7	-7.3	-7.9	-7.7	-7.3	-6.9	-4.8	3.7	20.9	-11.3
	4.6	-5.7	-6.2	-6.8	-6.7	-6.4	-5.9	-3.7	4.8	21.6	-10.6
	4.3	-6.0	-6.6	-7.1	-7.0	-6.7	-6.2	-4.0	4.6	21.5	-10.3
	4.1	-6.2	-6.8	-7.3	-7.2	-6.9	-6.4	-4.1	4.4	21.4	-10.2
3	4.2	-6.8	-7.5	-8.1	-8.1	-8.1	-8.3	-6.1	3.9	23.6	-11.6
	3.0	-7.3	-7.9	-8.5	-8.5	-8.4	-8.4	-6.5	2.4	21.0	-11.8
	2.9	-7.5	-8.1	-8.7	-8.6	-8.5	-8.6	-6.7	2.4	21.1	-11.6
	4.2	-6.8	-7.5	-8.1	-8.1	-8.1	-8.3	-6.1	3.9	23.6	-11.6
	3.1	-7.2	-7.8	-8.3	-8.3	-8.3	-8.3	-6.4	2.4	21.1	-11.7
	3.0	-7.3	-7.9	-8.5	-8.5	-8.4	-8.4	-6.5	2.4	21.0	-11.8
	2.9	-7.5	-8.1	-8.7	-8.6	-8.5	-8.6	-6.7	2.4	21.1	-11.6
	4.2	-6.8	-7.5	-8.1	-8.1	-8.1	-8.3	-6.1	3.9	23.6	-11.6
	3.1	-7.2	-7.8	-8.3	-8.3	-8.3	-8.3	-6.4	2.4	21.1	-11.7
	3.0	-7.3	-7.9	-8.5	-8.5	-8.4	-8.4	-6.5	2.4	21.0	-11.8
4	3.9	-6.0	-6.6	-7.1	-7.1	-7.1	-7.1	-5.4	3.4	21.8	-10.3
	3.8	-6.1	-6.7	-7.3	-7.3	-7.3	-7.4	-5.5	3.4	21.9	-10.3
	3.7	-6.1	-6.7	-7.3	-7.4	-7.4	-7.4	-5.5	3.3	21.9	-10.1
	4.0	-5.9	-6.5	-7.1	-7.0	-6.9	-7.0	-5.2	3.4	21.8	-10.3
	3.9	-6.0	-6.6	-7.1	-7.1	-7.1	-7.1	-5.4	3.4	21.8	-10.3
	3.8	-6.1	-6.7	-7.3	-7.3	-7.3	-7.4	-5.5	3.4	21.9	-10.3
	3.7	-6.1	-6.7	-7.3	-7.4	-7.4	-7.4	-5.5	3.3	21.9	-10.1
	4.0	-5.9	-6.5	-7.1	-7.0	-6.9	-7.0	-5.2	3.4	21.8	-10.3
	3.9	-6.0	-6.6	-7.1	-7.1	-7.1	-7.1	-5.4	3.4	21.8	-10.3
	3.8	-6.1	-6.7	-7.3	-7.3	-7.3	-7.4	-5.5	3.4	21.9	-10.3
5	2.1	-8.5	-9.3	-10.1	-10.1	-9.9	-10.0	-7.4	2.1	20.8	-13.1
	1.9	-8.5	-9.3	-10.0	-10.1	-9.9	-10.0	-7.6	2.0	20.9	-12.8
	1.8	-8.5	-9.2	-9.9	-9.9	-9.8	-9.9	-7.5	2.0	20.9	-12.7
	1.9	-8.4	-9.1	-9.8	-9.8	-9.7	-9.8	-7.5	2.0	20.9	-12.6
	1.9	-8.4	-9.0	-9.7	-9.8	-9.7	-9.8	-7.4	2.0	21.1	-12.4
	1.8	-8.4	-9.0	-9.7	-9.7	-9.6	-9.7	-7.3	2.1	20.9	-12.5
	1.8	-8.4	-9.0	-9.6	-9.6	-9.5	-9.6	-7.1	2.2	21.0	-12.3
	1.8	-8.2	-8.9	-9.4	-9.4	-9.3	-9.3	-6.8	2.4	21.1	-12.3
	1.8	-8.3	-8.9	-9.4	-9.4	-9.3	-9.3	-6.8	2.5	21.0	-12.1

	2.2	-8.5	-9.3	-10.0	-10.1	-10.0	-10.0	-7.6	2.1	21.5	-12.8
6	2.1	-9.2	-9.6	-10.2	-10.3	-10.1	-10.3	-8.0	1.4	20.9	-13.4
	1.9	-9.1	*	-10.2	-10.2	-10.1	-10.2	-8.0	1.4	21.0	-13.2
	2.0	-8.8	*	-10.1	-10.1	-9.9	-9.8	-7.4	1.8	21.0	-12.3
	2.0	-8.7	*	-10.0	-10.1	-9.9	-9.9	-7.4	1.9	21.1	-12.4
	2.0	-8.5	*	-10.0	-10.0	-9.8	-9.8	-7.4	2.0	21.1	-12.6
	1.9	-8.4	*	-9.7	-9.8	-9.6	-9.7	-7.3	2.0	21.2	-12.4
	1.9	-8.3	*	-9.6	-9.6	-9.5	-9.5	-7.1	2.2	21.3	-12.1
	2.1	-9.2	-9.6	-10.2	-10.3	-10.1	-10.3	-8.0	1.4	20.9	-13.4
	2.0	-9.1	-9.6	-10.2	-10.3	-10.1	-10.3	-8.0	1.4	21.1	-13.2
	1.9	-9.1	*	-10.2	-10.2	-10.1	-10.2	-8.0	1.4	21.0	-13.2
7	4.0	-6.9	-7.1	-7.8	-7.8	-7.8	-8.0	-6.4	2.8	22.1	-11.7
	3.8	-7.3	-7.5	-8.2	-8.2	-8.2	-8.4	-6.8	2.5	22.0	-11.9
	3.5	-7.6	-7.9	-8.5	-8.5	-8.5	-8.7	-7.0	2.2	21.9	-12.3
	3.3	-7.8	-8.1	-8.7	-8.8	-8.8	-9.0	-7.2	2.1	21.8	-12.1
	3.1	-8.0	-8.2	-8.9	-8.9	-8.9	-9.1	-7.3	1.9	22.0	-12.2
	3.0	-8.0	-8.4	-9.0	-9.0	-8.9	-9.2	-7.4	1.8	22.0	-12.0
	2.9	-8.1	-8.4	-9.0	-9.1	-9.0	-9.3	-7.5	1.7	22.0	-11.9
	3.9	-6.9	-7.2	-7.9	-7.8	-7.8	-8.0	-6.4	2.7	21.7	-11.8
	3.6	-7.2	-7.3	-8.1	-8.1	-8.1	-8.2	-6.6	2.4	21.6	-12.1
	3.3	-7.5	-7.8	-8.5	-8.5	-8.5	-8.7	-7.0	2.1	21.5	-12.1
8	2.1	-9.3	-9.7	-10.4	-10.4	-10.4	-10.5	-8.7	0.9	21.7	-13.6
	1.8	-9.6	*	-10.7	-10.7	-10.7	-10.8	-9.0	0.6	21.6	-13.8
	1.6	-9.8	-10.1	-10.8	-10.9	-10.8	-11.0	-9.1	0.4	21.5	-13.7
	3.1	-8.1	-8.2	-9.0	-9.0	-9.1	-9.2	-7.5	1.9	21.8	-13.4
	2.3	-9.1	-9.5	-10.1	-10.2	-10.2	-10.3	-8.6	1.0	21.6	-13.5
	2.1	-9.3	-9.7	-10.4	-10.4	-10.4	-10.5	-8.7	0.9	21.7	-13.6
	2.0	-9.5	*	-10.5	-10.5	-10.5	-10.6	-8.9	0.7	21.7	-13.8
	1.8	-9.6	*	-10.7	-10.7	-10.7	-10.8	-9.0	0.6	21.6	-13.8
	1.8	-9.7	-10.1	-10.8	-10.8	-10.8	-10.9	-9.0	0.5	21.5	-13.6
	1.6	-9.8	-10.1	-10.8	-10.9	-10.8	-11.0	-9.1	0.4	21.5	-13.7

(1) at interior face of exterior sheathing

* N/A

TABLE B4 Measured Temperatures, Specimen 2A

Location (I) . . . . . .

Name		I A	A/G	G/S,I	S,I/P	P/A	C A	A/B	B/A	E A
AT	1	20.4	18.8	15.3	10.0	0.4	-4.0	-5.7	-9.2	-9.5
	2	20.1	18.8	15.8	11.4	3.3	-0.6	-1.6	-4.4	-5.3
	3	20.6	19.1	15.4	9.9	-0.1	-5.0	-6.1	-8.9	-9.3
	4	20.0	18.5	15.3	10.6	1.8	-2.3	-3.5	-6.1	-6.6
	5	21.8	20.0	16.6	11.6	2.1	-2.3	-3.7	-6.0	-6.5
	6	22.7	20.9	17.4	12.4	3.2	-1.2	-2.4	-5.1	-5.4
IT	1	20.4	20.5	19.7	3.9	-3.9	-4.0	-5.9	-8.5	-9.5
	2	20.1	20.0	19.4	6.2	-0.4	-0.6	-1.9	-4.1	-5.3
	3	20.6	20.8	20.1	3.4	-4.9	-5.0	-6.8	-8.7	-9.3
	4	20.0	19.9	19.0	4.7	-2.1	-2.3	-3.7	-5.8	-6.6
	5	21.8	21.7	20.7	5.4	-2.1	-2.3	-3.9	-5.8	-6.5
	6	22.7	22.7	21.5	6.5	-0.9	-1.2	-2.7	-4.6	-5.4
BT	1	20.4	18.7	15.9	11.8	-2.9	-4.0	-5.2	-7.9	-9.5
	2	20.1	18.5	16.3	12.6	0.4	-0.6	-1.5	-3.9	-5.3
	3	20.6	18.8	16.0	11.5	-3.7	-5.0	-6.2	-8.5	-9.3
	4	20.0	18.4	15.9	12.0	-0.6	-2.3	-3.0	-5.5	-6.6
	5	21.8	20.2	17.5	13.4	-0.2	-2.3	-3.1	-5.5	-6.5
	6	22.7	20.8	18.1	14.2	0.7	-1.2	-1.9	-4.3	-5.4
AB	1	21.0	18.3	14.9	9.5	-1.0	-6.4	-7.2	-10.3	-10.7
	2	20.3	18.2	15.3	10.9	2.5	-2.3	-2.8	-5.9	-6.5
	3	21.3	18.6	14.9	9.4	-1.2	-7.0	-7.7	-10.1	-10.5
	4	19.8	17.9	14.8	9.8	0.7	-4.2	-4.8	-7.2	-7.4
	5	22.1	19.5	16.2	10.7	0.8	-4.4	-5.2	-7.1	-7.3
	6	23.5	20.5	17.3	11.8	2.2	-2.8	-3.5	-5.9	-6.4
IB	1	21.0	21.4	21.1	3.7	-6.0	-6.4	-8.3	-10.4	-10.7
	2	20.3	20.5	19.9	5.7	-1.9	-2.3	-3.7	-5.9	-6.5
	3	21.3	21.8	21.4	3.0	-6.7	-7.0	-8.8	-10.3	-10.5
	4	19.8	19.8	18.8	3.8	-4.0	-4.2	-5.8	-7.3	-7.4
	5	22.1	22.4	22.0	4.9	-4.1	-4.4	-6.0	-7.2	-7.3
	6	23.5	24.1	24.2	6.4	-2.6	-2.8	-4.5	-6.2	-6.4
BB	1	21.0	18.8	16.4	11.0	-5.0	-6.4	-7.9	-10.1	-10.7
	2	20.3	18.6	16.5	12.3	-1.0	-2.3	-3.3	-5.6	-6.5
	3	21.3	19.1	16.5	11.1	-5.5	-7.0	-8.3	-10.0	-10.5
	4	19.8	18.5	16.2	11.3	-2.8	-4.2	-5.2	-7.0	-7.4
	5	22.1	20.3	18.2	12.6	-2.7	-4.4	-5.4	-6.9	-7.3
	6	23.5	21.4	19.4	13.7	-1.3	-2.8	-3.8	-5.7	-6.4

I I A : interior air
A/G : interiorair / gypsum board
G/S,I : gypsum board / stud or insulation
S,I/P : stud or insulation / polystyrene board
P/A : polystyrene board / cavity air
C A : cavity air
A/B : cavity air / brick
B/A : brick / exterior air
E A : exterior air

TABLE B5 Measured Bridging Temperatures, Specimen 2A

		Location							
Name		I A	A/G	G/S	S/P	P/A	A/B	B/A	E A
AT	1	22.4	19.7	14.9	7.0	-6.2	-14.4	-19.8	-21.2
	2	22.6	19.9	14.9	6.7	-6.8	-15.0	-20.0	-21.4
	3	22.6	20.0	15.0	7.1	-6.0	-14.0	-19.7	-21.2
	4	22.2	19.6	14.9	6.8	-6.5	-14.7	-20.2	-21.5
	5	22.5	19.8	14.8	6.7	-6.8	-14.9	-20.3	-21.5
	6	22.8	20.0	15.0	7.0	-6.3	-14.5	-20.0	-21.4
	7	22.7	20.0	15.0	6.9	-6.6	-14.8	-20.2	-21.5
	8	22.8	20.0	14.9	6.8	-6.8	-15.1	-20.2	-21.4
	9	22.8	20.0	15.0	7.0	-6.3	-14.5	-20.1	-21.4
	10	22.8	20.0	14.9	6.8	-6.6	-14.9	-20.2	-21.5
	11	22.7	20.0	15.0	7.1	-6.0	-14.0	-19.9	-21.2
AB	1	22.1	19.2	15.4	6.9	-6.7	-14.8	-20.6	-21.4
	2	22.5	19.5	15.5	6.4	-7.4	-16.0	-21.3	-21.9
	3	22.5	19.6	15.6	6.7	-6.7	-15.1	-20.6	-21.1
	4	22.0	19.2	15.4	6.5	-7.1	-15.7	-21.0	-21.5
	5	22.4	19.3	15.4	6.4	-7.4	-15.9	-21.1	-21.6
	6	22.6	19.6	15.6	6.6	-7.0	-15.5	-20.8	-21.3
	7	22.4	19.5	15.5	6.5	-7.3	-15.9	-21.0	-21.5
	8	22.6	19.5	15.5	6.3	-7.5	-16.1	-20.9	-21.5
	9	22.5	19.6	15.6	6.6	-7.1	-15.5	-20.6	-21.2
	10	22.6	19.5	15.5	6.4	-7.3	-15.8	-20.9	-21.6
	11	22.4	19.4	15.5	6.7	-6.7	-15.1	-20.3	-21.0
BT	1	22.4	20.0	15.9	9.5	-10.7	-13.7	-19.5	-21.2
	2	22.6	20.3	16.1	9.4	-11.4	-14.3	-19.6	-21.4
	3	22.6	20.3	16.2	9.6	-10.6	-13.5	-19.4	-21.2
	4	22.2	20.1	16.1	9.5	-11.2	-14.1	-20.0	-21.5
	5	22.5	20.2	16.0	9.3	-11.4	-14.3	-20.0	-21.5
	6	22.8	20.6	16.3	9.6	-11.0	-13.9	-19.8	-21.4
	7	22.7	20.5	16.2	9.5	-11.3	-14.2	-20.0	-21.5
	8	22.8	20.6	16.2	9.4	-11.5	-14.5	-19.8	-21.4
	9	22.8	20.6	16.3	9.6	-11.0	-13.9	-19.9	-21.4
	10	22.8	20.6	16.2	9.4	-11.5	-14.3	-20.2	-21.5
	11	22.7	20.5	16.3	9.6	-10.6	-13.3	-19.3	-21.2
BB	1	22.1	19.5	14.6	8.1	-11.2	-14.2	-20.4	-21.4
	2	22.5	20.0	14.8	8.2	-11.0	-14.4	-20.9	-21.9
	3	22.5	19.9	14.9	8.5	-9.9	-13.4	-20.1	-21.1
	4	22.0	19.6	14.8	8.5	-10.3	-13.9	-20.6	-21.5
	5	22.4	20.0	14.8	8.3	-10.6	-14.1	-20.7	-21.6
	6	22.6	20.3	15.1	8.6	-10.2	-13.6	-20.4	-21.3
	7	22.4	20.2	15.0	8.5	-10.5	-14.0	-20.7	-21.5
	8	22.6	20.2	15.0	8.3	-10.7	-14.3	-20.6	-21.5
	9	22.5	20.2	15.0	8.6	-10.1	-13.6	-20.5	-21.2
	10	22.6	20.2	15.0	8.4	-10.4	-13.9	-20.9	-21.6
	11	22.4	20.1	14.8	8.1	-10.4	-13.7	-20.2	-21.0

TABLE B6 Measured Temperatures, Specimen 3

		Location									
Name		1	2	3	4	5	6	7	8	9	10
S1 A	1	23.0	18.4	11.0	11.3	5.3	-2.6	-4.3	-8.6	-11.2	-20.9
	2	22.9	18.2	10.5	11.0	4.7	-3.2	-4.9	-9.1	-11.8	-21.2
	3	23.1	18.1	10.1	10.5	4.3	-3.8	-5.5	-9.6	-12.2	-21.4
	4	23.1	16.5	7.1	7.2	1.2	-6.5	-7.9	-11.5	-13.5	-21.0
	5	23.1	16.5	7.1	7.2	1.1	-6.6	-8.0	-11.7	-13.7	-20.9
	6	23.2	16.5	7.0	7.1	1.1	-6.7	-8.1	-11.7	-13.7	-20.9
	7	23.1	16.4	6.9	7.0	1.0	-6.8	-8.2	-11.8	-13.7	-20.9
	8	23.2	16.3	6.9	7.0	0.9	-6.9	-8.3	-11.8	-13.8	-21.0
	9	23.1	16.3	6.8	6.9	0.8	-7.0	-8.3	-11.9	-13.9	-21.2
	10	23.3	16.4	6.7	6.7	0.7	-7.0	-8.4	-11.9	-13.9	-21.0
	11	23.1	16.3	6.6	6.7	0.6	-7.0	-8.4	-12.0	-14.0	-21.2
	12	23.1	16.4	6.7	6.7	0.6	-7.1	-8.4	-12.0	-13.9	-21.0
	13	23.1	16.3	6.6	6.6	0.5	-7.1	-8.5	-12.0	-14.0	-21.3
	14	22.9	16.1	6.4	6.4	0.3	-7.3	-8.6	-12.2	-14.2	-21.5
	15	22.9	16.0	6.3	6.2	0.2	-7.3	-8.7	-12.3	-14.3	-21.7
	16	22.8	15.9	6.2	6.2	0.2	-7.3	-8.7	-12.3	-14.2	-21.6
	17	22.8	16.0	6.2	6.1	0.2	-7.4	-8.7	-12.3	-14.4	-21.9
	18	22.8	15.9	6.2	6.1	0.1	-7.4	-8.7	-12.3	-14.3	-21.8
	19	23.3	17.1	8.3	8.4	2.5	-5.2	-6.5	-10.6	-11.6	-20.7
	20	23.2	17.0	8.1	8.2	2.3	-5.4	-6.8	-10.8	-11.8	-20.8
	21	23.3	16.9	8.0	8.0	2.0	-5.6	-7.0	-10.9	-12.0	-21.0
	22	23.2	16.8	7.8	7.9	1.9	-5.8	-7.1	-11.1	-12.2	-21.3
	23	23.3	16.8	7.7	7.7	1.7	-6.0	-7.3	-11.3	-12.4	-21.4
	24	23.2	16.6	7.6	7.6	1.6	-6.1	-7.5	-11.4	-12.4	-21.2
	25	23.2	16.6	7.5	7.5	1.5	-6.3	-7.6	-11.5	-12.6	-21.5
	26	23.2	16.5	7.3	7.3	1.3	-6.4	-7.7	-11.7	-12.7	-21.8
	27	23.3	16.5	7.3	7.2	1.2	-6.5	-7.8	-11.8	-12.8	-21.4
	28	23.3	16.5	7.2	7.2	1.1	-6.6	-7.9	-11.9	-13.0	-21.8
	29	23.3	16.3	6.8	6.8	0.7	-7.0	-8.3	-12.0	-13.1	-22.0
	30	23.2	16.3	6.8	6.8	0.7	-7.1	-8.4	-12.2	-13.4	-22.0
S2 A	1	23.0	21.2	17.4	10.4	1.3	-5.3	-6.3	-8.8	-14.9	-21.8
	2	22.9	21.1	17.1	9.8	0.6	-6.1	-7.1	-9.5	-15.6	-22.2
	3	23.1	21.0	16.8	9.4	-0.0	-6.7	-7.7	-10.1	-16.0	-22.4
	4	23.1	20.0	14.8	6.1	-3.2	-9.2	-9.8	-11.4	-16.2	-21.1
	5	23.1	19.9	14.8	5.9	-3.3	-9.3	-10.0	-11.6	-16.3	-21.1
	6	23.2	19.9	14.7	5.9	-3.4	-9.5	-10.1	-11.7	-16.4	-21.1
	7	23.1	19.8	14.7	5.8	-3.5	-9.6	-10.2	-11.8	-16.3	-21.0
	8	23.2	19.8	14.6	5.7	-3.6	-9.6	-10.3	-11.9	-16.5	-21.3
	9	23.1	19.8	14.6	5.6	-3.7	-9.7	-10.4	-11.9	-16.5	-21.4
	10	23.3	19.9	14.5	5.5	-3.8	-9.8	-10.4	-12.0	-16.4	-21.0
	11	23.1	19.7	14.5	5.4	-3.9	-9.8	-10.5	-12.0	-16.6	-21.3
	12	23.1	19.8	14.5	5.4	-3.9	-9.9	-10.5	-12.1	-16.5	-21.2
	13	23.1	19.7	14.4	5.3	-4.0	-10.0	-10.5	-12.1	-16.7	-21.4
	14	22.9	19.4	14.2	5.1	-4.2	-10.1	-10.7	-12.2	-16.7	-21.6
	15	22.9	19.3	14.1	5.0	-4.2	-10.2	-10.8	-12.4	-16.9	-21.8
	16	22.8	19.4	14.1	5.0	-4.3	-10.2	-10.9	-12.4	-16.9	-21.7
	17	22.8	19.4	14.0	4.9	-4.4	-10.3	-10.9	-12.5	-17.0	-21.9

	18	22.8	19.3	14.0	4.9	-4.4	-10.3	-11.0	-12.5	-17.0	-22.0
	19	23.3	20.4	15.4	7.4	-1.6	-7.5	-8.2	-10.0	-15.6	-20.7
	20	23.2	20.2	15.3	7.1	-1.8	-7.8	-8.5	-10.2	-15.9	-21.3
	21	23.3	20.2	15.2	7.0	-2.1	-8.1	-8.7	-10.5	-16.0	-21.2
	22	23.2	20.1	15.1	6.8	-2.3	-8.3	-9.0	-10.7	-16.4	-21.4
	23	23.3	20.1	15.1	6.6	-2.6	-8.6	-9.2	-10.9	-16.5	-21.5
	24	23.2	20.1	15.0	6.4	-2.7	-8.8	-9.4	-11.1	-16.6	-21.5
	25	23.2	20.0	14.9	6.3	-3.0	-9.0	-9.6	-11.3	-16.6	-21.4
	26	23.2	20.0	14.8	6.1	-3.1	-9.2	-9.8	-11.4	-16.8	-21.8
	27	23.3	20.0	14.8	6.0	-3.3	-9.3	-9.9	-11.6	-16.9	-21.5
	28	23.3	20.0	14.7	6.0	-3.4	-9.4	-10.0	-11.7	-17.1	-21.9
	29	23.3	19.9	14.5	5.6	-3.7	-9.8	-10.4	-12.2	-17.6	-22.1
	30	23.2	19.8	14.5	5.6	-3.8	-9.9	-10.4	-12.1	-17.6	-22.1
S3 A	1	23.0	22.0	19.7	17.8	16.0				-21.5	-22.8
	2	22.9	21.9	19.4	17.4	15.5				-21.8	-23.0
	3	23.1	21.9	19.2	17.0	15.1				-22.1	-23.3
	4	23.1	20.9	17.1	13.9	11.7				-20.9	-22.0
	5	23.1	20.9	17.0	13.8	11.6				-20.9	-22.0
	6	23.2	20.8	17.0	13.7	11.5				-21.1	-22.1
	7	23.1	20.8	16.9	13.6	11.4				-21.1	-22.1
	8	23.2	20.8	16.8	13.6	11.3				-21.1	-22.1
	9	23.1	20.8	16.8	13.5	11.2				-21.2	-22.3
	10	23.3	20.9	16.7	13.4	11.1				-21.0	-22.0
	11	23.1	20.7	16.7	13.3	11.1				-21.1	-22.2
	12	23.1	20.8	16.7	13.3	11.0				-21.2	-22.3
	13	23.1	20.7	16.7	13.2	10.9				-21.2	-22.1
	14	22.9	20.5	16.4	13.0	10.6				-21.4	-22.4
	15	22.9	20.3	16.3	12.9	10.6				-21.6	-22.7
	16	22.8	20.3	16.3	12.8	10.5				-21.6	-22.7
	17	22.8	20.4	16.2	12.8	10.5				-21.7	-22.8
	18	22.8	20.3	16.2	12.8	10.5				-21.7	-22.7
	19	23.3	21.4	17.7	14.9	12.8				-21.0	-22.2
	20	23.2	21.4	17.6	14.8	12.7				-21.1	-22.3
	21	23.3	21.4	17.5	14.6	12.5				-21.1	-22.3
	22	23.2	21.3	17.5	14.5	12.4				-21.2	-22.4
	23	23.3	21.4	17.4	14.4	12.3				-21.3	-22.5
	24	23.2	21.3	17.4	14.3	12.2				-21.4	-22.7
	25	23.2	21.3	17.3	14.2	12.1				-21.4	-22.6
	26	23.2	21.2	17.2	14.1	12.0				-21.6	-22.8
	27	23.3	21.2	17.1	14.0	11.8				-21.6	-22.8
	28	23.3	21.2	17.1	14.0	11.8				-21.6	-22.7
	29	23.3	21.2	16.9	13.6	11.4				-22.0	-23.1
	30	23.2	21.1	16.9	13.6	11.3				-21.9	-22.9
S1 B	1	22.7	16.8	9.8	2.2	-3.8	-10.9	-12.1	-15.6	-17.3	-24.4
	2	22.5	16.5	9.3	1.7	-4.5	-11.6	-12.7	-16.1	-17.8	-24.6
	3	22.6	16.4	9.1	1.4	-4.8	-12.0	-13.1	-16.5	-18.2	-24.6
	4	22.5	16.2	8.9	1.1	-5.1	-12.3	-13.4	-16.7	-18.4	-24.8
	5	22.6	16.2	8.7	1.0	-5.3	-12.5	-13.6	-17.0	-18.7	-24.9
	6	22.4	16.1	8.5	0.7	-5.4	-12.7	-13.8	-17.1	-18.7	-25.0
	7	22.4	16.1	8.3	0.7	-5.6	-12.9	-13.9	-17.2	-18.8	-25.0
	8	22.4	16.0	8.2	0.5	-5.8	-13.0	-14.1	-17.3	-19.0	-25.1
	9	22.3	15.9	8.0	0.3	-5.9	-13.1	-14.2	-17.4	-19.0	-25.0
	10	22.5	15.9	7.9	0.2	-6.0	-13.2	-14.2	-17.5	-19.0	-25.2
	11	22.3	15.9	7.8	0.1	-6.1	-13.3	-14.3	-17.6	-19.2	-25.1

	12	22.3	15.8	7.7	-0.0	-6.2	-13.4	-14.4	-17.6	-19.2	-25.0
	13	22.3	15.8	7.7	0.2	-5.9	-12.7	-13.6	-16.6	-18.0	-24.4
	14	22.2	16.2	8.9	1.5	-4.5	-11.5	-12.6	-15.9	-17.6	-24.5
	15	22.3	16.2	8.6	1.3	-4.9	-11.9	-12.9	-16.2	-17.8	-24.6
	16	22.2	16.0	8.5	1.0	-5.1	-12.1	-13.2	-16.5	-18.0	-24.9
	17	22.3	15.9	8.3	0.7	-5.4	-12.4	-13.3	-16.6	-18.2	-24.9
	18	22.2	15.9	8.1	0.6	-5.5	-12.6	-13.6	-16.8	-18.3	-25.0
	19	22.1	15.8	8.0	0.4	-5.7	-12.7	-13.7	-17.0	-18.4	-24.7
	20	22.1	15.7	7.9	0.3	-5.8	-12.8	-13.8	-17.0	-18.4	-24.9
	21	22.1	15.7	7.7	0.1	-6.0	-12.9	-13.9	-17.1	-18.6	-24.9
	22	22.0	15.6	7.6	0.1	-6.1	-13.1	-14.1	-17.3	-18.6	-25.0
	23	22.1	15.6	7.5	-0.0	-6.2	-13.2	-14.1	-17.4	-18.8	-25.1
	24	22.2	15.6	7.5	-0.2	-6.3	-13.2	-14.2	-17.4	-18.8	-25.0
	25	22.1	15.6	7.4	-0.2	-6.4	-13.3	-14.3	-17.4	-18.9	-25.1
	26	22.3	15.7	7.6	-0.0	-6.2	-13.1	-14.1	-17.1	-18.5	-24.6
	27	22.2	15.6	7.4	-0.2	-6.4	-13.4	-14.3	-17.3	-18.6	-24.7
	28	22.3	15.6	7.3	-0.3	-6.5	-13.4	-14.3	-17.3	-18.8	-25.1
	29	22.4	16.0	8.2	0.8	-5.3	-12.2	-13.2	-16.4	-17.8	-24.5
	30	22.3	15.9	8.1	0.6	-5.5	-12.4	-13.4	-16.5	-18.0	-24.6
S2 B	1	22.7	20.8	17.3	-4.9	-9.4	-13.3	-13.9	-15.4	-20.6	-24.7
	2	22.5	20.7	17.1	-5.7	-10.2	-14.1	-14.7	-16.1	-20.8	-24.7
	3	22.6	20.7	16.9	-6.2	-10.7	-14.5	-15.1	-16.5	-21.2	-25.0
	4	22.5	20.6	16.8	-6.6	-11.0	-14.9	-15.4	-16.8	-21.4	-25.1
	5	22.6	20.6	16.7	-6.8	-11.2	-15.1	-15.7	-17.0	-21.7	-25.2
	6	22.4	20.5	16.6	-7.1	-11.5	-15.3	-15.9	-17.2	-21.8	-25.3
	7	22.4	20.5	16.5	-7.3	-11.7	-15.5	-16.0	-17.4	-21.9	-25.4
	8	22.4	20.5	16.5	-7.5	-11.9	-15.7	-16.2	-17.5	-21.9	-25.4
	9	22.3	20.3	16.4	-7.7	-12.1	-15.8	-16.3	-17.6	-22.0	-25.4
	10	22.5	20.4	16.3	-7.9	-12.2	-15.9	-16.4	-17.7	-22.0	-25.4
	11	22.3	20.4	16.2	-8.0	-12.3	-15.9	-16.4	-17.8	-22.1	-25.3
	12	22.3	20.2	16.2	-8.0	-12.4	-16.0	-16.5	-17.8	-22.2	-25.4
	13	22.3	20.1	16.2	-7.6	-11.8	-15.2	-15.7	-17.0	-21.1	-24.9
	14	22.2	20.4	16.7	-5.7	-10.2	-13.8	-14.4	-15.8	-20.5	-24.6
	15	22.3	20.4	16.6	-6.1	-10.6	-14.2	-14.8	-16.2	-20.7	-24.9
	16	22.2	20.3	16.5	-6.5	-10.9	-14.6	-15.1	-16.5	-21.0	-24.9
	17	22.3	20.2	16.4	-6.8	-11.1	-14.8	-15.3	-16.7	-21.2	-25.0
	18	22.2	20.1	16.3	-7.1	-11.4	-15.0	-15.5	-16.9	-21.4	-25.2
	19	22.1	20.1	16.3	-7.3	-11.6	-15.2	-15.7	-17.1	-21.4	-25.0
	20	22.1	20.1	16.2	-7.5	-11.8	-15.3	-15.9	-17.2	-21.5	-25.1
	21	22.1	20.1	16.1	-7.7	-12.0	-15.5	-16.0	-17.3	-21.6	-25.2
	22	22.0	20.0	16.1	-7.8	-12.1	-15.6	-16.1	-17.4	-21.7	-25.2
	23	22.1	20.1	16.0	-7.9	-12.2	-15.7	-16.2	-17.5	-21.9	-25.4
	24	22.2	20.0	16.0	-8.1	-12.3	-15.8	-16.3	-17.6	-21.8	-25.4
	25	22.1	20.0	16.0	-8.1	-12.4	-15.9	-16.4	-17.6	-22.0	-25.4
	26	22.3	20.1	16.1	-7.6	-11.9	-15.3	-15.8	-17.2	-21.4	-25.0
	27	22.2	20.0	16.0	-7.9	-12.2	-15.5	-16.1	-17.4	-21.5	-25.2
	28	22.3	20.0	15.9	-8.0	-12.2	-15.6	-16.2	-17.5	-21.6	-25.2
	29	22.4	20.3	16.4	-6.8	-11.2	-14.8	-15.3	-16.7	-21.1	-25.1
	30	22.3	20.3	16.3	-7.1	-11.4	-15.0	-15.5	-16.9	-21.2	-24.9
S3 B	1	22.7	21.4	19.5	8.6	6.9				-24.0	-25.2
	2	22.5	21.3	19.4	8.1	6.4				-24.3	-25.5
	3	22.6	21.2	19.3	7.9	6.1				-24.4	-25.5
	4	22.5	21.2	19.2	7.7	5.9				-24.5	-25.6
	5	22.6	21.1	19.1	7.5	5.7				-24.6	-25.7

	6	22.4	21.1	19.0	7.3	5.5				-24.7	-25.8
	7	22.4	21.1	19.0	7.1	5.3				-24.7	-25.9
	8	22.4	21.0	19.0	7.0	5.2				-24.7	-25.9
	9	22.3	21.0	18.9	6.8	5.0				-24.8	-25.9
	10	22.5	21.0	18.8	6.7	4.9				-24.8	-26.0
	11	22.3	20.9	18.8	6.6	4.8				-24.8	-25.9
	12	22.3	20.9	18.7	6.5	4.7				-24.8	-25.9
	13	22.3	20.8	18.6	6.1	4.3				-24.8	-25.7
	14	22.2	20.9	18.8	7.5	5.7				-24.3	-25.4
	15	22.3	20.9	18.8	7.3	5.5				-24.6	-25.7
	16	22.2	20.8	18.8	7.1	5.3				-24.6	-25.7
	17	22.3	20.7	18.7	6.9	5.1				-24.7	-25.8
	18	22.2	20.7	18.7	6.7	5.0				-24.8	-25.8
	19	22.1	20.7	18.6	6.6	4.8				-24.8	-25.8
	20	22.1	20.7	18.6	6.5	4.7				-24.9	-25.9
	21	22.1	20.7	18.5	6.3	4.5				-24.9	-25.9
	22	22.0	20.7	18.5	6.2	4.4				-25.0	-26.0
	23	22.1	20.6	18.4	6.1	4.3				-25.0	-26.1
	24	22.2	20.7	18.4	6.0	4.2				-25.0	-26.0
	25	22.1	20.6	18.4	6.0	4.1				-25.0	-26.0
	26	22.3	20.6	18.4	5.9	4.0				-25.1	-26.1
	27	22.2	20.7	18.3	5.6	3.7				-25.1	-26.1
	28	22.3	20.7	18.3	5.5	3.6				-25.1	-26.0
	29	22.4	20.8	18.7	6.8	5.0				-24.9	-25.9
	30	22.3	20.8	18.6	6.6	4.8				-24.9	-25.8
SI C	1	21.6	17.3	11.6	6.8	6.0	-2.7	-2.8	-8.7	-5.8	-18.4
	2	21.2	16.3	11.8	7.3	6.5	-2.2	-2.4	-8.4	-5.5	-18.3
	3	21.3	16.1	12.1	7.6	6.8	-1.8	-1.9	-8.1	-5.2	-18.0
	4	21.1	16.1	12.3	7.8	7.1	-1.4	-1.5	-7.8	-4.8	-18.0
	5	21.2	16.3	12.5	8.1	7.3	-1.1	-1.2	-7.6	-4.6	-18.0
	6	21.5	17.4	14.4	10.5	9.8	2.0	1.9	-4.9	-1.6	-17.3
	7	21.2	17.3	14.1	10.2	9.4	0.9	0.9	-6.4	-2.8	-17.2
	8	21.4	17.2	14.2	10.2	9.5	1.2	1.1	-5.9	-2.5	-17.4
	9	21.4	17.2	14.1	10.1	9.3	1.1	1.0	-6.1	-2.6	-17.5
	10	21.3	17.1	14.0	10.0	9.2	1.0	0.9	-6.3	-2.7	-17.5
	11	21.3	17.1	14.0	9.9	9.2	0.9	0.8	-6.3	-2.8	-17.6
	12	21.4	17.0	13.9	9.9	9.1	0.9	0.8	-6.3	-2.8	-17.7
	13	21.3	17.1	13.9	9.8	9.1	0.8	0.7	-6.4	-2.9	-17.7
	14	21.2	17.2	13.9	9.8	9.0	0.7	0.7	-6.6	-3.0	-17.5
	15	21.3	17.6	14.7	11.0	10.3	2.2	2.1	-4.8	-1.4	-17.4
	16	21.2	17.7	14.6	10.8	10.1	2.0	1.9	-4.9	-1.6	-17.4
	17	21.2	17.5	14.5	10.6	9.9	1.8	1.8	-5.2	-1.8	-17.5
	18	21.1	17.4	14.4	10.6	9.9	1.7	1.6	-5.2	-1.9	-17.3
	19	21.2	17.4	14.2	10.3	9.6	1.5	1.4	-5.4	-2.1	-17.3
	20	21.1	17.4	14.1	10.1	9.4	1.3	1.2	-5.8	-2.3	-18.0
	21	21.1	17.2	14.0	9.9	9.2	1.1	1.0	-5.8	-2.5	-17.4
	22	21.2	17.2	14.0	9.8	9.1	1.1	1.0	-5.9	-2.5	-18.1
	23	21.3	17.7	14.8	10.9	10.2	2.3	2.1	-4.9	-1.5	-17.3
	24	21.3	17.6	14.6	10.7	10.0	2.0	1.9	-5.2	-1.7	-17.2
	25	21.2	17.5	14.4	10.3	9.5	1.4	1.3	-6.1	-2.3	-17.3
	26	21.3	17.4	14.3	10.2	9.4	1.3	1.2	-6.1	-2.4	-17.4
	27	21.2	17.4	14.2	10.1	9.3	1.2	1.1	-6.2	-2.5	-17.2
	28	21.3	17.3	14.2	10.0	9.2	1.1	1.0	-6.3	-2.6	-17.5
	29	21.2	17.3	14.2	9.9	9.1	1.0	0.9	-6.4	-2.7	-17.5
	30	21.2	17.3	14.1	9.9	9.1	0.9	0.9	-6.5	-2.8	-17.4

S2 C	1	21.6	20.3	14.8	4.4	-2.1	-5.7	-5.7	-6.4	-6.6 -20.8
	2	21.2	19.4	13.9	5.6	-1.0	-5.3	-5.4	-6.1	-6.4 -20.7
	3	21.3	19.1	13.7	6.1	-0.4	-4.9	-5.0	-5.7	-6.0 -20.7
	4	21.1	19.0	13.7	6.4	-0.0	-4.6	-4.7	-5.4	-5.8 -20.7
	5	21.2	19.1	13.7	6.6	0.3	-4.4	-4.4	-5.2	-5.5 -20.5
	6	21.5	19.8	15.2	9.1	3.3	-1.3	-1.3	-2.1	-2.5 -20.1
	7	21.2	19.8	14.9	8.3	2.2	-2.7	-2.7	-3.4	-3.7 -19.8
	8	21.4	19.6	14.9	8.6	2.5	-2.2	-2.2	-3.0	-3.3 -19.9
	9	21.4	19.7	14.9	8.5	2.4	-2.4	-2.4	-3.2	-3.5 -20.1
	10	21.3	19.5	14.8	8.4	2.3	-2.5	-2.5	-3.3	-3.6 -20.1
	11	21.3	19.5	14.7	8.3	2.2	-2.6	-2.6	-3.4	-3.7 -20.1
	12	21.4	19.5	14.7	8.3	2.2	-2.6	-2.6	-3.4	-3.7 -20.2
	13	21.3	19.5	14.7	8.2	2.1	-2.7	-2.7	-3.5	-3.8 -20.2
	14	21.2	19.6	14.7	8.2	2.0	-2.8	-2.8	-3.6	-3.8 -20.1
	15	21.3	20.0	15.4	9.4	3.6	-1.1	-1.1	-1.9	-2.3 -20.1
	16	21.2	20.0	15.3	9.3	3.4	-1.3	-1.3	-2.2	-2.5 -20.1
	17	21.2	19.9	15.2	9.1	3.2	-1.5	-1.5	-2.4	-2.7 -20.2
	18	21.1	19.8	15.2	9.0	3.0	-1.7	-1.7	-2.6	-2.9 -20.2
	19	21.2	19.8	15.1	8.8	2.7	-2.0	-2.0	-2.8	-3.1 -20.3
	20	21.1	19.8	15.0	8.6	2.6	-2.2	-2.2	-3.0	-3.3 -20.6
	21	21.1	19.6	14.9	8.5	2.4	-2.4	-2.3	-3.2	-3.5 -20.4
	22	21.2	19.8	14.9	8.5	2.4	-2.4	-2.4	-3.2	-3.5 -20.6
	23	21.3	20.1	15.5	9.5	3.7	-1.0	-1.0	-1.8	-2.2 -19.8
	24	21.3	20.0	15.4	9.4	3.4	-1.3	-1.3	-2.1	-2.4 -19.7
	25	21.2	19.9	15.1	8.8	2.7	-2.0	-2.0	-2.8	-3.1 -19.7
	26	21.3	19.8	15.1	8.7	2.6	-2.2	-2.2	-3.0	-3.2 -19.7
	27	21.2	19.9	15.1	8.6	2.5	-2.3	-2.3	-3.1	-3.4 -19.7
	28	21.3	19.8	15.0	8.6	2.4	-2.4	-2.4	-3.2	-3.4 -19.7
	29	21.2	19.8	15.0	8.5	2.3	-2.5	-2.5	-3.3	-3.5 -19.7
	30	21.2	19.7	15.0	8.5	2.3	-2.5	-2.6	-3.4	-3.6 -19.6

S3 C	1	21.6	20.3	15.6	9.8	6.4				-21.4 -22.0
	2	21.2	19.4	15.0	10.5	7.7				-21.3 -22.0
	3	21.3	19.1	14.8	10.9	8.3				-21.3 -22.0
	4	21.1	19.0	14.8	11.1	8.7				-21.4 -22.0
	5	21.2	19.1	15.0	11.4	9.0				-21.2 -21.9
	6	21.5	19.7	16.3	13.3	11.2				-20.8 -21.3
	7	21.2	19.5	16.1	13.1	11.0				-20.3 -20.8
	8	21.4	19.7	16.2	13.1	10.9				-20.6 -21.3
	9	21.4	19.7	16.1	13.0	10.8				-20.8 -21.5
	10	21.3	19.6	16.1	12.9	10.8				-20.8 -21.6
	11	21.3	19.5	16.0	12.9	10.7				-20.6 -21.6
	12	21.4	19.6	16.0	12.9	10.7				-20.9 -21.7
	13	21.3	19.6	16.0	12.9	10.7				-20.8 -21.7
	14	21.2	19.5	16.0	12.8	10.7				-20.9 -21.7
	15	21.3	19.7	16.5	13.6	11.4				-20.7 -21.2
	16	21.2	19.7	16.4	13.4	11.3				-20.7 -21.3
	17	21.2	19.7	16.3	13.3	11.1				-21.0 -21.5
	18	21.1	19.6	16.3	13.2	11.0				-20.7 -21.1
	19	21.2	19.6	16.1	13.0	10.9				-21.0 -21.4
	20	21.1	19.5	16.1	12.9	10.7				-21.5 -22.2
	21	21.1	19.5	16.0	12.8	10.6				-20.9 -21.5
	22	21.2	19.5	16.0	12.8	10.6				-21.5 -22.2
	23	21.3	19.9	16.6	13.7	11.6				-20.6 -21.2
	24	21.3	19.8	16.6	13.6	11.5				-20.5 -21.1
	25	21.2	19.7	16.4	13.3	11.3				-20.5 -21.4
	26	21.3	19.7	16.3	13.3	11.2				-20.5 -21.3
	27	21.2	19.7	16.3	13.2	11.1				-20.4 -21.2
	28	21.3	19.6	16.2	13.2	11.1				-20.3 -21.2
	29	21.2	19.6	16.2	13.2	11.1				-20.4 -21.4

	30	21.2	19.6	16.2	13.1	11.0				-20.2	-21.2
S1 D	1	23.1	18.8	16.9	10.8	1.0	-2.0	-3.5	-6.9	-10.0	-21.1
	2	23.1	18.6	16.2	10.0	0.0	-2.9	-4.3	-7.7	-10.9	-21.2
	3	23.1	18.2	15.6	9.4	-0.6	-3.6	-5.0	-8.4	-11.3	-21.5
	4	22.9	18.0	15.2	8.9	-1.2	-4.2	-5.5	-8.9	-11.7	-21.4
	5	23.0	17.8	14.8	8.5	-1.6	-4.5	-5.8	-9.2	-12.0	-21.4
	6	23.0	17.9	14.5	8.3	-1.9	-4.8	-6.1	-9.4	-12.2	-21.8
	7	22.9	17.6	14.3	8.0	-2.1	-5.0	-6.3	-9.6	-12.3	-21.6
	8	23.3	18.1	15.2	9.2	-0.7	-3.6	-4.9	-8.2	-11.9	-21.0
	9	23.3	17.9	14.8	8.6	-1.4	-4.3	-5.7	-8.9	-12.5	-21.2
	10	23.3	17.7	14.6	8.3	-1.8	-4.8	-6.1	-9.3	-12.6	-21.2
	11	23.3	17.6	14.3	8.0	-2.2	-5.1	-6.4	-9.7	-12.9	-21.4
	12	23.3	17.5	14.1	7.8	-2.4	-5.3	-6.7	-9.8	-13.0	-21.4
	13	23.2	17.4	14.0	7.7	-2.5	-5.4	-6.8	-10.0	-12.8	-21.4
	14	23.1	17.4	13.9	7.6	-2.7	-5.5	-6.9	-10.0	-12.9	-21.3
	15	23.0	17.6	13.8	7.5	-2.7	-5.6	-7.0	-10.2	-13.1	-21.5
	16	22.9	17.4	13.7	7.4	-2.8	-5.7	-7.0	-10.2	-13.2	-21.6
	17	23.0	17.3	13.7	7.4	-2.8	-5.8	-7.1	-10.2	-13.0	-21.5
	18	23.1	17.9	14.7	8.6	-1.5	-4.5	-5.9	-9.0	-12.5	-21.2
	19	23.0	17.6	14.4	8.2	-2.0	-4.9	-6.2	-9.4	-12.8	-21.2
	20	23.1	17.7	14.2	7.9	-2.2	-5.2	-6.5	-9.7	-13.1	-21.4
	21	23.1	17.7	14.0	7.7	-2.4	-5.4	-6.7	-9.9	-13.0	-21.3
	22	23.0	17.4	13.9	7.6	-2.6	-5.5	-6.8	-10.0	-13.2	-21.7
	23	23.0	17.3	13.8	7.5	-2.7	-5.6	-6.9	-10.0	-13.2	-21.5
	24	22.9	17.3	13.7	7.4	-2.8	-5.7	-7.1	-10.2	-13.4	-21.5
	25	23.0	17.4	13.6	7.4	-2.9	-5.8	-7.1	-10.3	-13.4	-22.0
	26	22.9	17.1	13.5	7.3	-3.0	-5.9	-7.2	-10.3	-13.3	-21.7
	27	23.0	17.8	14.7	8.6	-1.4	-4.3	-5.6	-8.9	-12.0	-21.0
	28	23.1	17.7	14.4	8.3	-1.8	-4.7	-6.0	-9.2	-12.2	-21.2
	29	23.1	17.6	14.2	8.1	-2.0	-4.9	-6.2	-9.4	-12.3	-21.1
	30	22.9	17.4	14.1	7.9	-2.2	-5.1	-6.4	-9.6	-12.6	-21.1
S2 D	1	23.1	21.9	17.3	10.2	1.5	-4.2	-5.1	-7.5	-14.2	-20.9
	2	23.1	22.0	16.8	9.2	0.3	-5.3	-6.2	-8.4	-14.7	-21.1
	3	23.1	21.5	16.4	8.5	-0.5	-6.2	-7.0	-9.2	-15.1	-21.3
	4	22.9	21.5	16.0	7.9	-1.2	-6.9	-7.7	-9.8	-15.5	-21.4
	5	23.0	21.4	15.7	7.4	-1.7	-7.4	-8.2	-10.2	-15.7	-21.4
	6	23.0	21.4	15.4	7.1	-2.1	-7.7	-8.5	-10.5	-16.1	-21.7
	7	22.9	21.2	15.3	6.8	-2.4	-8.0	-8.8	-10.7	-16.0	-21.6
	8	23.3	21.6	16.0	8.3	-0.7	-6.3	-7.2	-9.5	-15.6	-21.4
	9	23.3	21.5	15.8	7.7	-1.4	-7.1	-8.0	-10.3	-16.1	-21.6
	10	23.3	21.4	15.5	7.3	-2.0	-7.7	-8.5	-10.8	-16.3	-21.7
	11	23.3	21.4	15.4	6.9	-2.4	-8.1	-8.9	-11.1	-16.5	-21.8
	12	23.3	21.3	15.2	6.7	-2.6	-8.3	-9.1	-11.2	-16.5	-21.8
	13	23.2	21.3	15.1	6.5	-2.8	-8.5	-9.3	-11.3	-16.5	-21.7
	14	23.1	21.1	15.0	6.4	-3.0	-8.7	-9.4	-11.4	-16.4	-21.6
	15	23.0	21.4	14.9	6.3	-3.1	-8.8	-9.5	-11.5	-16.5	-21.8
	16	22.9	21.2	14.9	6.2	-3.2	-8.8	-9.6	-11.6	-16.8	-22.0
	17	23.0	21.1	14.8	6.1	-3.3	-8.9	-9.6	-11.6	-16.5	-21.8
	18	23.1	21.6	15.7	7.6	-1.5	-7.2	-8.1	-10.2	-15.8	-21.7
	19	23.0	21.3	15.4	7.2	-2.0	-7.7	-8.5	-10.7	-16.1	-21.6
	20	23.1	21.4	15.3	6.9	-2.4	-8.0	-8.9	-11.0	-16.4	-21.8
	21	23.1	21.4	15.1	6.6	-2.6	-8.3	-9.1	-11.2	-16.4	-21.8
	22	23.0	21.1	15.0	6.5	-2.8	-8.5	-9.3	-11.4	-16.5	-21.9
	23	23.0	21.1	14.9	6.3	-2.9	-8.6	-9.4	-11.5	-16.6	-21.7

	24	22.9	21.0	14.9	6.2	-3.1	-8.8	-9.6	-11.6	-16.8	-22.0
	25	23.0	21.3	14.8	6.1	-3.2	-8.9	-9.6	-11.7	-16.9	-22.1
	26	22.9	20.9	14.8	6.1	-3.2	-8.9	-9.7	-11.8	-16.8	-21.9
	27	23.0	21.4	15.7	7.6	-1.5	-7.0	-7.9	-10.0	-15.6	-21.3
	28	23.1	21.3	15.4	7.2	-2.0	-7.5	-8.3	-10.4	-15.9	-21.5
	29	23.1	21.2	15.3	6.9	-2.3	-7.9	-8.6	-10.7	-15.9	-21.3
	30	22.9	21.2	15.2	6.7	-2.5	-8.1	-8.9	-10.9	-16.0	-21.3
S3 D	1	23.1	22.5	19.7	17.6	15.5				-20.2	-21.3
	2	23.1	22.3	19.2	16.7	14.6				-20.5	-21.5
	3	23.1	22.1	18.7	16.1	13.9				-20.7	-21.6
	4	22.9	21.9	18.3	15.5	13.2				-20.9	-21.8
	5	23.0	21.7	18.0	15.1	12.7				-20.8	-21.8
	6	23.0	21.6	17.7	14.7	12.3				-21.1	-22.0
	7	22.9	21.5	17.5	14.4	11.9				-21.1	-22.0
	8	23.3	21.9	18.1	15.1	12.7				-21.2	-21.6
	9	23.3	21.8	17.8	14.7	12.2				-21.5	-21.8
	10	23.3	21.7	17.6	14.4	11.8				-21.4	-21.9
	11	23.3	21.7	17.5	14.1	11.5				-21.6	-21.9
	12	23.3	21.6	17.3	13.9	11.2				-21.5	-21.9
	13	23.2	21.5	17.2	13.8	11.1				-21.3	-21.8
	14	23.1	21.4	17.1	13.6	11.0				-21.3	-21.8
	15	23.0	21.3	17.0	13.5	10.9				-21.5	-21.9
	16	22.9	21.3	17.0	13.4	10.8				-21.7	-22.2
	17	23.0	21.2	16.9	13.4	10.7				-21.5	-21.9
	18	23.1	21.6	17.7	14.5	12.1				-21.2	-22.1
	19	23.0	21.5	17.4	14.2	11.7				-21.3	-21.9
	20	23.1	21.4	17.3	14.0	11.4				-21.4	-22.1
	21	23.1	21.4	17.2	13.8	11.2				-21.5	-22.2
	22	23.0	21.3	17.0	13.6	11.0				-21.5	-22.3
	23	23.0	21.2	17.0	13.5	10.9				-21.5	-21.9
	24	22.9	21.3	16.9	13.4	10.7				-21.6	-22.2
	25	23.0	21.2	16.9	13.3	10.7				-21.7	-22.4
	26	22.9	21.1	16.8	13.3	10.6				-21.7	-22.2
	27	23.0	21.6	17.7	14.5	12.1				-20.8	-21.5
	28	23.1	21.5	17.5	14.2	11.7				-20.9	-21.6
	29	23.1	21.3	17.3	14.0	11.5				-20.9	-21.5
	30	22.9	21.4	17.2	13.8	11.3				-20.9	-21.5
S1 E	1	23.7	20.4	17.5	14.3	8.9	7.1	6.8	4.5	3.9	-20.1
	2	23.7	20.3	17.3	14.2	8.7	6.9	6.6	4.4	3.7	-20.2
	3	24.0	20.7	18.1	15.1	10.1	8.5	8.1	6.0	5.3	-20.0
	4	24.1	20.6	17.8	14.8	9.5	7.8	7.5	5.3	4.7	-20.2
	5	24.0	20.5	17.7	14.7	9.4	7.6	7.3	5.1	4.4	-20.5
	6	24.1	20.4	17.7	14.5	9.2	7.4	7.1	4.9	4.3	-20.4
	7	23.9	20.4	17.6	14.4	9.0	7.3	6.9	4.7	4.1	-20.5
	8	23.9	20.5	17.6	14.4	8.9	7.2	6.8	4.6	3.9	-20.5
	9	23.8	20.4	17.5	14.3	8.8	7.1	6.7	4.5	3.8	-20.7
	10	23.7	20.3	17.4	14.2	8.8	7.0	6.6	4.4	3.8	-20.8
	11	23.7	20.3	17.4	14.2	8.7	6.9	6.6	4.3	3.7	-20.8
	12	23.8	20.9	18.3	15.4	10.5	8.8	8.5	6.4	5.8	-20.1
	13	23.7	20.7	18.1	15.2	10.1	8.4	8.1	5.9	5.3	-20.3
	14	23.8	20.7	18.0	15.0	9.8	8.1	7.8	5.5	4.9	-20.2
	15	23.7	20.6	17.9	14.8	9.5	7.8	7.4	5.2	4.6	-20.4
	16	23.8	20.5	17.7	14.6	9.3	7.5	7.2	4.9	4.3	-20.4
	17	23.7	20.4	17.7	14.5	9.1	7.3	7.0	4.7	4.1	-20.6

	18	23.7	20.4	17.6	14.4	8.9	7.2	6.8	4.5	3.9	-20.7
	19	23.8	20.4	17.5	14.3	8.8	7.0	6.7	4.4	3.8	-20.7
	20	23.7	20.3	17.4	14.2	8.7	6.9	6.5	4.2	3.7	-20.7
	21	23.7	20.2	17.4	14.1	8.6	6.8	6.4	4.1	3.5	-20.7
	22	23.6	20.2	17.3	14.1	8.5	6.7	6.3	4.0	3.4	-20.8
	23	23.7	20.8	18.1	15.2	10.1	8.4	8.1	5.9	5.3	-20.0
	24	23.8	20.6	17.8	14.8	9.6	7.8	7.5	5.2	4.6	-20.1
	25	23.7	20.5	17.8	14.7	9.3	7.6	7.3	5.0	4.4	-20.1
	26	23.7	20.5	17.6	14.5	9.1	7.4	7.0	4.7	4.1	-20.3
	27	23.7	20.4	17.5	14.4	9.0	7.2	6.9	4.6	4.0	-20.4
	28	23.9	20.4	17.5	14.3	8.9	7.1	6.7	4.5	3.8	-20.3
	29	23.9	20.3	17.4	14.2	8.8	7.0	6.6	4.4	3.7	-20.4
	30	24.0	20.2	17.4	14.2	8.7	6.9	6.5	4.2	3.6	-20.4
S2 E	1	23.7	22.7	17.7	12.4	6.6	2.7	2.7	2.0	0.6	-20.0
	2	23.7	22.4	17.6	12.2	6.4	2.5	2.5	1.8	0.4	-20.0
	3	24.0	22.8	18.3	13.5	8.1	4.5	4.5	3.7	2.1	-20.1
	4	24.1	22.7	18.0	13.0	7.4	3.6	3.6	2.9	1.4	-20.3
	5	24.0	22.6	17.9	12.7	7.2	3.3	3.3	2.6	1.1	-20.4
	6	24.1	22.6	17.8	12.6	7.0	3.1	3.1	2.3	0.8	-20.4
	7	23.9	22.6	17.7	12.5	6.8	2.9	2.8	2.1	0.7	-20.6
	8	23.9	22.7	17.7	12.4	6.7	2.7	2.7	1.9	0.5	-20.6
	9	23.8	22.6	17.7	12.3	6.5	2.6	2.6	1.8	0.4	-20.7
	10	23.7	22.5	17.6	12.2	6.5	2.5	2.5	1.7	0.3	-20.8
	11	23.7	22.5	17.5	12.1	6.4	2.4	2.3	1.6	0.2	-20.8
	12	23.8	22.8	18.5	13.8	8.6	5.1	5.0	4.3	2.7	-20.0
	13	23.7	22.8	18.3	13.5	8.2	4.4	4.4	3.7	2.1	-20.2
	14	23.8	22.8	18.1	13.2	7.8	4.0	3.9	3.2	1.7	-20.1
	15	23.7	22.7	18.0	12.9	7.4	3.5	3.5	2.8	1.3	-20.4
	16	23.8	22.6	17.9	12.7	7.1	3.2	3.2	2.5	1.0	-20.4
	17	23.7	22.6	17.7	12.5	6.9	3.0	2.9	2.2	0.8	-20.6
	18	23.7	22.6	17.7	12.4	6.6	2.7	2.7	2.0	0.6	-20.6
	19	23.8	22.6	17.6	12.3	6.5	2.5	2.5	1.8	0.4	-20.8
	20	23.7	22.5	17.6	12.1	6.4	2.4	2.4	1.7	0.3	-20.6
	21	23.7	22.6	17.5	12.1	6.3	2.3	2.3	1.5	0.1	-20.7
	22	23.6	22.4	17.5	12.0	6.1	2.2	2.2	1.4	0.0	-20.7
	23	23.7	22.7	18.3	13.4	8.1	4.5	4.4	3.7	2.2	-19.6
	24	23.8	22.7	18.0	12.9	7.4	3.6	3.6	2.8	1.4	-19.9
	25	23.7	22.7	17.9	12.7	7.1	3.3	3.3	2.5	1.2	-20.0
	26	23.7	22.6	17.8	12.6	6.9	3.0	3.0	2.3	0.9	-20.0
	27	23.7	22.5	17.7	12.4	6.7	2.8	2.8	2.1	0.7	-20.1
	28	23.9	22.5	17.6	12.3	6.5	2.6	2.6	1.9	0.6	-20.1
	29	23.9	22.4	17.5	12.2	6.4	2.5	2.5	1.8	0.5	-20.1
	30	24.0	22.4	17.5	12.1	6.3	2.4	2.4	1.6	0.3	-20.0
S3 E	1	23.7	22.3	18.6	15.7	13.1				-20.9	-21.3
	2	23.7	22.1	18.5	15.6	13.0				-20.9	-21.4
	3	24.0	22.6	19.2	16.5	14.0				-21.0	-21.3
	4	24.1	22.5	18.9	16.0	13.4				-21.1	-21.4
	5	24.0	22.4	18.8	15.9	13.2				-21.5	-21.8
	6	24.1	22.5	18.7	15.7	13.1				-21.3	-21.9
	7	23.9	22.4	18.6	15.6	12.9				-21.5	-22.0
	8	23.9	22.3	18.5	15.5	12.8				-21.6	-22.2
	9	23.8	22.2	18.5	15.4	12.7				-21.5	-22.2
	10	23.7	22.2	18.4	15.3	12.6				-21.7	-22.2

11	23.7	22.1	18.3	15.2	12.6	-21.7	-22.2
12	23.8	22.5	19.2	16.6	14.2	-21.0	-21.5
13	23.7	22.4	19.0	16.3	13.8	-21.0	-21.4
14	23.8	22.4	18.9	16.1	13.5	-20.9	-21.3
15	23.7	22.4	18.7	15.8	13.3	-21.1	-21.3
16	23.8	22.3	18.7	15.7	13.1	-21.2	-21.5
17	23.7	22.3	18.5	15.6	13.0	-21.4	-21.7
18	23.7	22.2	18.5	15.4	12.9	-21.4	-21.7
19	23.8	22.2	18.4	15.4	12.8	-21.5	-21.8
20	23.7	22.2	18.4	15.3	12.7	-21.4	-21.8
21	23.7	22.1	18.3	15.3	12.7	-21.4	-21.8
22	23.6	22.2	18.3	15.2	12.6	-21.5	-21.8
23	23.7	22.5	19.1	16.3	14.0	-20.6	-21.1
24	23.8	22.4	18.8	15.9	13.4	-20.9	-21.4
25	23.7	22.3	18.7	15.8	13.3	-20.9	-21.3
26	23.7	22.2	18.6	15.6	13.1	-21.0	-21.4
27	23.7	22.3	18.5	15.5	13.0	-21.0	-21.5
28	23.9	22.3	18.5	15.5	12.9	-21.1	-21.5
29	23.9	22.3	18.4	15.4	12.8	-21.0	-21.5
30	24.0	22.3	18.4	15.4	12.8	-20.9	-21.5

APPENDIX C

Fortran Listing of Heat Flow Program

```
**************************************************************************
      PROGRAM TWOWAY
*
*       Two dimensional heat flow program developed at McMaster University
*       during the period Sept 1986 to August 1987 to compliment
*       a Masters of Engineering thesis by Andrew Kluge.
*
*       Program uses resistor analogy to develop simultaneous equations
*       describing heat flow.
*
*       Program most appropriate for solving problems involving flow of
*       heat between two parallel planes through multiple layers
*       of various conductivities (i.e. a wall section) which also include
*       in-plane discontinuities in material conductivites (e.g. a steel
*       stud).
*
*       The equations are developed by first considering the parallel
*       layers without any discontinuities (e.g. without a stud section)
*       In this regard:
*               Perpendicular to the wall section nodes are spaced at material
*               interfaces as well as between for thicker materials.
*               In the plane of the wall section the node spacing is constant.
*       To these equations which describe one dimensional heat flow
*       is then added the element causing two dimensional heat flow
*       to the center of the wall section.
*
*       The matrix of equations thus developed is then arranged in
*       symetrical form and solved using a standard LDL solving routine
*       for any number of interior and exterior temperature combinations.
*
*       List of input variables
*       general nodes:
*               NPL     number of nodes in the plane of the wall
*               NL      number of nodes perpindicular to the wall
*               N       total number of nodes (NPL*NL)
*               W       width between nodes in the plane of the wall
*               H       height in vertical plane of wall (1)
*               RK()    layer conductivity
*               S()     layer thickness
*       at a discontinuity node:
*               NSP     node number with a discontinuity
*               NM      number of materials in parallel
*               RKAS()  conductivity, width and lenght of heat flow path
*                       for each material
*       temperature:
*               TI      interior temperature
*               TE      exterior temperature
*
*       Description of matrices
*               IB()    nodal connectivity
*               C()     nodal heat flow balance
*               T()     interior and exterior temperature conditions
*               GT()    global heat flow balance
*               ST()    nodal temperatures
*
      IMPLICIT REAL*8 (A-H,O-Z)
      DIMENSION GT(184,184),IB(184,4),C(184,4),ST(184),T(46),RK(9),S(9)
      OPEN(5,FILE='DATA.DAT',STATUS='OLD')
      OPEN(6,FILE='OUTPUT',STATUS='NEW')
      FLAG=0
      WRITE(6,1)
```

```
1   FORMAT(' ***TWO DIMENSIONAL HEAT FLOW ANALYSIS***'///)
*
    CALL INIT(NPL,NL,N,W,RK,S,H)
    CALL GENC(NPL,NL,N,C,RK,S,W,H)
    CALL GENIB(NPL,NL,N,IB)
100  CALL GENT(NPL,T,FLAG)
        IF(FLAG)11,10,11
10   CALL GENGAS(N,C,IB,GT,ST,T)
    CALL SOLVER(GT,ST,N)
    CALL PRINT(NPL,NL,N,ST,T)
    GOTO 100
11   CLOSE(5)
    CLOSE(6)
    STOP
    END
*
*************************************************************************
    SUBROUTINE INIT(NPL,NL,N,W,RK,S,H)
*
    IMPLICIT REAL*8 (A-H,O-Z)
    DIMENSION RK(9),S(9)
    READ(5,*)NPL,NL,W,H,(RK(I),I=1,NL+1),(S(I),I=1,NL+1)
    N=NPL*NL
    WRITE(6,1)NPL,NL,N,W,H
1   FORMAT('      NODES PER LAYER :',I4,/,
   *     '         NODAL LAYERS :',I4,/,
   *     ' TOTAL NUMBER OF NODES :',I4,/,
   *     '  WIDTH BETWEEN NODES :',F6.4/,
   *     '        LAYER HEIGHT :',F6.4/)
    WRITE(6,'(A35/)')' LAYER         K            S'
    DO 3 IJ=1,NL+1
3   WRITE(6,'(3X,I2,8X,E9.3,6X,E9.3)')IJ,RK(IJ),S(IJ)
    RETURN
    END
*
*************************************************************************
    SUBROUTINE GENC(NPL,NL,N,C,RK,S,W,H)
*
    IMPLICIT REAL*8 (A-H,O-Z)
    DIMENSION C(184,4),R(4),RK(9),S(9)
    DO 90 JKK=1,N
    DO 90 JJ=1,4
90   C(JKK,JJ)=0
    WRITE(6,55)
55   FORMAT(//'              NODE RESISTANCE '/
   *' GENERAL NODES'/
   *' LEVEL   DIR 1     DIR 2     DIR 3     DIR 4')
    DO 9 J=1,NL
      R(1)=S(J)/(RK(J)*W*H)
        RK1=RK(J)
        RK2=RK(J+1)
        IF(J.EQ.1)RK1=0.
        IF(J.EQ.NL)RK2=0.
      R(2)=W/(RK1*S(J)*H/2+RK2*S(J+1)*H/2)
      R(3)=R(2)
      R(4)=S(J+1)/(RK(J+1)*W*H)
      DO 10 IJ=1,4
        DO 11 IK=NPL*(J-1)+1,NPL*J
11          C(IK,IJ)=R(IJ)
10        CONTINUE
      WRITE(6,'(I5,3X,4E12.3)')J,(C(NPL*(J-1)+1,IJ),IJ=1,4)
```

```
9     CONTINUE
      WRITE(6,'(/)')
      WRITE(6,*)'THERMAL BRIDGE NODES '
      WRITE(6,*) 'NODE    DIR 1     DIR 2     DIR 3     DIR 4'
91    READ(5,*)NSP
      IF(NSP.EQ.0) GOTO 101
      DO 12 IJ=1,4
        CALL RESIST(RS,H)
12      C(NSP,IJ)=RS
      WRITE(6,'(I5,3X,4E12.3)')NSP,(C(NSP,IJ),IJ=1,4)
      GOTO 91
101   CONTINUE
      RETURN
      END
*
*************************************************************************
      SUBROUTINE GENT(NPL,T,FLAG)
*
      IMPLICIT REAL*8 (A-H,O-Z)
      DIMENSION T(46)
      DO 90 JJ=1,5
90    T(JJ)=0
      READ(5,*)TI,TE
      IF(TI.NE.0.AND.TE.NE.0)GOTO 11
10    FLAG=1
      GOTO 12
11    DO 17 I=1,NPL
17      T(I)=TI
      DO 18 I=NPL+1,2*NPL
18      T(I)=TE
      WRITE(6,1)TI,TE
1     FORMAT(/' INSIDE TEMPERATURE = ',F5.1,/
     *' OUTSIDE TEMPERATURE = ',F5.1/)
12    RETURN
      END
*
*************************************************************************
      SUBROUTINE GENIB(NPL,NL,N,IB)
*
      IMPLICIT REAL*8 (A-H,O-Z)
      DIMENSION IB(184,4)
      DO 90 KK=1,N
      DO 90 JJ=1,4
90    IB(KK,JJ)=0
      J=1
      DO 13 I=NPL+1,N
        IB(I,1)=J
13      J=J+1
      J=0
      DO 14 I=1,N
        IB(I,2)=J
        IB(I,3)=J+2
14      J=J+1
      J=NPL+1
      DO 15 I=1,N-NPL
        IB(I,4)=J
15      J=J+1
      DO 16 I=1,N-NPL+1,NPL
        IB(I,2)=IB(I,3)
16      IB(I+NPL-1,3)=IB(I+NPL-1,2)
*     DO 5 I=1,N
```

```
*5   WRITE(6,'(4I8)')(IB(I,K),K = 1,4)
     RETURN
     END
*
*************************************************************************
     SUBROUTINE GENGAS(N,C,IB,GT,ST,T)
*
     IMPLICIT REAL*8 (A-H,O-Z)
     DIMENSION C(184,4),IB(184,4),GT(184,184),ST(184),T(46)
     DO 90 KK = 1,N
     DO 90 JJ = 1,N
90   GT(KK,JJ) = 0
     DO 91 JJ = 1,N
91   ST(JJ) = 0
     J = 1
     DO 19 I = 1,N
       DO 20 II = 1,4
         IF(IB(I,II))200,18,200
18          ST(I) = T(J)/C(I,II)
         J = J + 1
         GOTO 20
200        GT(I,IB(I,II)) = GT(I,IB(I,II))-1/C(I,II)
20       CONTINUE
300    SUM = 0
       DO 21 II = 1,4
21       SUM = SUM + 1/C(I,II)
19     GT(I,I) = SUM
*    WRITE(6,'(23E10.3)')(ST(KI),KI = 1,N)
*    DO 34 KI = 1,N
*34   WRITE(6,'(23E10.3)')(GT(KI,KK),KK = 1,N)
     DO 50 I = 1,N-1
     IF (GT(I,I + 1).EQ.0.)GOTO 50
     RATIO = GT(I,I + 1)/GT(I + 1,I)
     DO 51 II = 1,N
51     GT(I + 1,II) = GT(I + 1,II)*RATIO
     ST(I + 1) = ST(I + 1)*RATIO
50   CONTINUE
     RETURN
     END
*
*************************************************************************
      SUBROUTINE RESIST(RS,H)
*
      IMPLICIT REAL*8 (A-H,O-Z)
      DIMENSION RKAS(9)
      READ(5,*)NM,(RKAS(I),I = 1,3*NM)
      SUM = 0
*      WRITE(*,'(I6,9F7.4)')NM,(RKAS(IK),IK = 1,3*NM)
      DO 2 I = 1,3*NM,3
2        SUM = SUM + RKAS(I)*RKAS(I + 1)*H/RKAS(I + 2)
      RS = 1/SUM
      RETURN
      END
*
*************************************************************************
     SUBROUTINE PRINT(NPL,NL,N,ST,T)
*
     IMPLICIT REAL*8 (A-H,O-Z)
     DIMENSION ST(184),T(46)
     WRITE(*,1)
1    FORMAT('1',' TEMPERATURE PROFILE '/)
```

```
      DO 25 I = 1,NPL
      WRITE(*,30)I,T(I),(ST(J),J = I,N,NPL),T(I + NPL)
30    FORMAT(/I4,10F7.1)
25    CONTINUE
      WRITE(6,2)
2     FORMAT('1',' TEMPERATURE PROFILE ')
      DO 26 I = 1,NPL
      WRITE(6,31)I,T(I),(ST(J),J = I,N,NPL),T(I + NPL)
31    FORMAT(/I4,10F7.1)
26    CONTINUE
      RETURN
      END
*********************************************************************
→
```

```
C ***********************************************************
C
      SUBROUTINE SOLVER(S,V,N)
C
C  STORES AN ORDINARY SYMMETRIC MATRIX IN COMPACT
C  SUBROUTINE COLSOL SOLVES THE SET OF EQUATIONS
C
C ***********************************************************
C
C
      IMPLICIT REAL*8 (A-H,O-Z)
      DIMENSION S(184,184),MAXA(185),A(5000),V(184)
C
      A(1)=S(1,1)
      MAXA(1)=1
      NWK=2
C
      DO 10 J=2,N
       MI=1
 20    IF(S(MI,J).NE.0.) GOTO 30
       MI=MI+1
       GOTO 20
 30    CONTINUE
      MAXA(J)=NWK
C
      DO 40 I=J,MI,-1
       A(NWK)=S(I,J)
       NWK=NWK+1
*       WRITE(*,*)NWK
 40    CONTINUE
C
 10   CONTINUE
C
      NWK=NWK-1
      NNM=N+1
      MAXA(NNM)=NWK+1
C
*     WRITE(*,*) NWK
C     WRITE(*,*) (A(I), I=1,NWK)
C     WRITE(*,*) (MAXA(I),I=1,NNM)
C
      CALL COLSOL(A,V,MAXA,N,NWK,NNM,1,6)
C
C     WRITE(*,*) (A(I), I=1,NWK)
C
      CALL COLSOL(A,V,MAXA,N,NWK,NNM,2,6)
C
C     WRITE(*,*) (V(I), I=1,N)
C
      RETURN
      END
***********************************************************************
    SUBROUTINE COLSOL(A,V,MAXA,NN,NWK,NNM,KKK,IOUT)
C ..................................................
C
C PROGRAM: COLSOL.FOR
C       TO PERFORM LDL DECOMPOSITION FOR A MATRIX A
C       STORE IN COMPACT FORM
C
C ---INPUT---
C A(NWK)    = SYMMETRIC STIFFNESS STORED IN COMPACT FORM
```

```
C V(NN)     = LOAD VECTOR
C MAXA(NNN)  = VECTOR CONTAINING ADDRESS OF DIAGONAL ELEMENT
C           OF MATRIX A
C NN        = # OF EQUATION
C NWK       = TOTAL NUMBER OF ELEMENT BELOW SKYLINE OF A
C NNM       = NN+1
C KKK
C   EQ 1    = TRIANGULARIZATION OF A
C   EQ 2    = REDUCTION AND  BACK SUBSTITUTION OF LOAD VECTOR
C IOUT      = OUTPUT DEVICE #
C
C ---OUTPUT---
C A(NWK)    = D AND L FACTOR OF STIFFNESS MATRIX
C V(NN)     = DISAPLCEMENT VECTOR
C
C .....................................................................
      IMPLICIT REAL*8(A-H,O-Z)
C
      DIMENSION A(NWK),V(184),MAXA(185)
C
C
C PERFORM L*D*L(T) FACTORIZATION OF STIFFNESS MATRIX
C
      IF(KKK-2) 40,150,150
C
 40   DO 140 N=1,NN
      WRITE(*,1234)N
1234   FORMAT(' +',I6)
       KN=MAXA(N)
       KL=KN+1
       KU=MAXA(N+1)-1
       KH=KU-KL
C
       IF (KH) 110,90,50
C
 50    K=N-KH
       IC=0
       KLT=KU
C
       DO 80 J=1,KH
        IC=IC+1
        KLT=KLT-1
        KI=MAXA(K)
        ND=MAXA(K+1)-KI-1
C
        IF (ND) 80,80,60
C
 60     KK=MIN0(IC,ND)
        C=0.D0
C
        DO 70 L=1,KK
         C=C+A(KI+L)*A(KLT+L)
 70      CONTINUE
C
        A(KLT)=A(KLT)-C
C
        K=K+1
 80    CONTINUE
C
 90    K=N
       B=0.D0
```

```
C
      DO 100 KK = KL,KU
       K = K-1
       KI = MAXA(K)
       C = A(KK)/A(KI)
       B = B + C*A(KK)
       A(KK) = C
 100   CONTINUE
C
      A(KN) = A(KN)-B
C
 110   IF (A(KN)) 120,120,140
C
 120   WRITE(*,2000) N,A(KN)
C
C      STOP
C
 140  CONTINUE
C
C
C     STOP
     RETURN
C
C
C REDUCE RIGHT  HANDSIDE LOAD VECTOR
C
 150  DO 180 N = 1,NN
      WRITE(*,1234)N
      KL = MAXA(N) + 1
      KU = MAXA(N + 1)-1
C
      IF (KU-KL) 180,160,160
C
 160   K = N
      C = 0.D0
C
      DO 170 KK = KL,KU
       K = K-1
       C = C + A(KK)*V(K)
 170   CONTINUE
C
      V(N) = V(N)-C
 180  CONTINUE
C
C      WRITE(*,*) (V(I), I = 1,NN)
C  BACK-SUBSTITUTION
C
     DO 200 N = 1,NN
      K = MAXA(N)
      V(N) = V(N)/A(K)
 200  CONTINUE
C
C
     IF (NN.EQ.1) RETURN
     N = NN
C
     DO 230 L = 2,NN
      KL = MAXA(N) + 1
      KU = MAXA(N + 1)-1
C
      IF (KU-KL) 230,210,210
```

```
C
 210   K=N
C
      DO 220 KK=KL,KU
       K=K-1
       V(K)=V(K)-A(KK)*V(N)
 220   CONTINUE
C
 230   N=N-1
C
    RETURN
C
C
 2000 FORMAT(//,' STOP - STIFFNESS MATRIX NOT POSITIVE DEFINITE ',
   1 //,' NON-POSITIVE PIVOT FOR EQUATION ',I4,
   2 //,' PIVOT = ', E20.12 )
    END
*
```